Fibre reinforced concrete column-supported flat slabs: from material and structural characterization to design and economic optimization

DOCTORAL THESIS

Thesis by publications

Doctoral Thesis by:
Stanislav Aidarov

Directed by:
Albert de la Fuente Antequera
Nikola Tošić

Barcelona, March 2022

Universitat Politècnica de Catalunya
Departament d'Enginyeria Civil i Ambiental

Acta de calificación de tesis doctoral

Curso académico: 2021 - 2022

Nombre y apellidos	STANISLAV AIDAROV
Programa de doctorado	INGENIERÍA DE LA CONSTRUCCIÓN
Unidad estructural responsable del programa	DEPARTAMENTO DE INGENIERÍA CIVIL Y AMBIENTAL

Resolución del Tribunal

Reunido el Tribunal designado a tal efecto, el doctorando / la doctoranda expone el tema de su tesis doctoral titulada

"Fibre reinforced concrete column-supported flat slabs: from material and structural characterization to design and economic optimization".

Acabada la lectura y después de dar respuesta a las cuestiones formuladas por los miembros titulares del tribunal, éste otorga la calificación:

☐ NO APTO ☐ APROBADO ☐ NOTABLE ☐ SOBRESALIENTE

(Nombre, apellidos y firma) Presidente/a	(Nombre, apellidos y firma) Secretario/a	
(Nombre, apellidos y firma) Vocal	(Nombre, apellidos y firma) Vocal	(Nombre, apellidos y firma) Vocal

_____, _____ de _____ de _____.

El resultado del escrutinio de los votos emitidos por los miembros titulares del tribunal, efectuado por la Escuela de Doctorado, a instancia de la Comisión de Doctorado de la UPC, otorga la MENCIÓN CUM LAUDE:

☐ SÍ ☐ NO

(Nombre, apellidos y firma) Presidente de la Comisión Permanente de la Escuela de Doctorado	(Nombre, apellidos y firma) Secretario de la Comisión Permanente de la Escuela de Doctorado

Barcelona a _____ de _____ de _____.

“Roxsmæ, fæsevæd, tunʒetæ,

Roxsmæ cæwyetæ ængom,

Nifs, lægʒinadæ warzetæ,

Skæntæ muggagmæ stur nom …”

G. Maliti (1886-1942)

ACKNOWLEDGMENTS

During the writing of these lines, I found myself thinking that I was undeservedly fortunate to meet people without whom this doctoral dissertation would never be developed.

First of all, I would like to express my sincere gratitude to both my supervisors, Albert de la Fuente and Nikola Tošić. With their support, guidance, and trust, I could maintain a positive approach towards any challenge that should have been overtaken during this journey. I have learnt a lot from them, not only about engineering, but also about attitude and character.

Furthermore, I would like to acknowledge el *Plan de Doctorados Industriales de la Secretaría de Universidades e Investigación del Departamento de Empresa y Conocimiento de la Generalitat de Cataluña* for providing support through the PhD Industrial Fellowship (2018 DI 77) in collaboration with Smart Engineering Ltd. (UPC's Spin-Off).

I extend my gratitude to Tomàs Garcia, Jordi Cabrerizo, Robert Mc-Aloon, Carlos Hurtado, and Jordi Lafuente for all the support they have provided me with the experimental programme that was carried out in the Laboratory of Technology of Structures and Materials "Lluis Agulló".

I am also thankful to my "PhD comrade", Álex, for having been a good friend – hopefully, I will able to call him Dr. Alejandro Nogales at the moment of presenting this dissertation. Likewise, I feel lucky to have been able to share these four years in the Universitat Politècnica de Catalunya with the amazing people: Edu, Fran, Tai, Debora, Janill, Nirvan, Pablo, Behnam, Francesco, Philip, Lara, and Sara.

Moreover, I would like to mention friends with whom I managed to make "my first academic step" in Spain, receiving a MS in Structural and Construction Engineering from Universitat Politècnica de Catalunya: Oscar, Arantxa, Liam, Katy, Gabriel G., Gabriel C., Nadia, Daniel, Ena, Sara, and Soraya. Thank you for your amiability, friendliness and for facilitating my adaptation in a foreign country with a completely new culture/language.

Despite the fact that I have already been living for six years in Spain, I would never be close to achieve my goals without my relatives and friends from the native land. Thus, I would like to extend my sincerest thanks to Boris, Zaur, Totraz, Batraz, Marat, Rustam, Georgiy, Dzerassa, Zarina, Fatima, Irene, and Milana for "being around me", although there were more than 5000 km between us.

Finally, I would like to thank my family; in fact, there are not enough words to express what they mean to me. They are primary support in my life and everything that I have achieved up to now is their merit. Hopefully, I am/always be a son, brother, husband, and father that they can be proud of.

SUMMARY

Fibre reinforced concrete (FRC) has proven to be a suitable material for statically indeterminate elements. The FRC column-supported flat slabs with partial or even total substitution of reinforcing steel bars constructed within the scope of this thesis, provided the positive outcomes from both technical and sustainability perspectives, being a supporting evidence for this statement. Despite the successful experiences of FRC slab construction, the widespread use of this technology is still hindered because of a number of factors related to the general comprehension of the material's properties, design procedure, and accurate assessment of both technological and economic aspects.

In this context, further research is required to complement the current scope of knowledge, providing to practitioners and researchers a clear example of structural capacity of FRC column-supported flat slabs. Moreover, straightforward procedures focused on the design and following evaluation of the potential technological and economic benefits due to use of FRC should be derived. Therefore, a rather comprehensive doctoral thesis that covers the majority of the above-mentioned topics is proposed herein.

The first part of the study focuses on the material characterization and analysis of the flexural behaviour of FRC column-supported flat slab. A full-scale FRC slab was constructed and tested under different load magnitudes, assessing the structural response at both ultimate and serviceability limit states. The results derived proved the sufficient flexural strength at ultimate conditions along with the capacity of moment redistribution and the ductility of the system. Furthermore, the studied FRC slab evidenced the acceptable performance in terms of cracking and deflections.

Subsequently, the straightforward design-oriented method is proposed to estimate the structural response of FRC column-supported flat slabs in terms of flexural strength, cracking control, and instantaneous deformations. The results derived were compared with a nonlinear analysis, highlighting a suitable accuracy and precision of the proposed approach.

Finally, an industrial-oriented study was carried out with the main objective of elaborating a simplified method for the preliminary comparison of traditional and FRC solutions for column-supported flat slabs in terms of economic benefits. The results reflected an increment of direct costs for both fibre and hybrid (combination of steel reinforcing bars and fibres) solutions; however, these increments can be compensated by the reduction of the construction period and, as a consequence, time-dependent costs (i.e. preliminaries, equipment costs, overheads, and finance costs).

RESUMEN

El hormigón reforzado con fibras (HRF) ha demostrado ser un material adecuado para elementos sujetos a condiciones de contorno que conducen a hiperestaticidad. La construcción de forjados de HRF soportados por pilares ha proporcionado resultados positivos tanto desde el punto de vista técnico como de la sostenibilidad. A pesar de las experiencias de éxito en la sustitución parcial o incluso total del refuerzo tradicional (barras de acero) por fibras, el uso de esta tecnología todavía sigue siendo limitada debido a una serie de factores relacionados con la compresión general de las propiedades de HRF, los métodos de diseño junto con el análisis de los aspectos tecnológicos y económicos.

En este contexto, se hace necesario continuar investigando el comportamiento de las losas bidireccionales de HRF con el objeto de complementar el marco actual de conocimiento, proporcionando a los profesionales evidencias de la capacidad estructural de este tipo de elementos. Además, la industria requiere los métodos de diseño prácticos junto con herramientas para llevar a cabo el análisis comparativo de diferentes soluciones en términos de beneficios tecnológicos y económicos. Por este motivo, se plantea una tesis doctoral generalista que abarca la mayoría de los temas mencionados en el ámbito de la tecnología de los forjados de losa maciza de hormigón reforzado con fibras.

La primera parte del estudio se enfoca en la caracterización del material y posterior análisis del comportamiento a flexión de un forjado de HRF soportado por pilares. Para ello, se ha construido y ensayado una losa a escala real bajo diferentes magnitudes de carga, evaluando la respuesta estructural del elemento en estado límite de servicio y último. Los resultados obtenidos han mostrado la suficiente resistencia a flexión bajo las cargas últimas junto con una elevada ductilidad y capacidad de redistribuir los esfuerzos en el sistema hiperestático. Asimismo, la losa de HRF analizada ha cumplido con los requisitos del estado límite de fisuración y de deformaciones.

Posteriormente, se propone un método de diseño analítico para estimar la respuesta estructural de las losas de HRF soportadas por pilares en términos de resistencia a flexión, control de fisuración y de deformaciones instantáneas. Los resultados derivados se compararon con un análisis no lineal mediante el método de los elementos finitos, destacando una precisión adecuada desde el punto de vista ingenieril del método propuesto.

En la última parte se presenta un método simplificado para llevar a cabo un análisis comparativo de soluciones tradicionales y de HRF para las losas apoyadas sobre pilares en términos económicos. Los resultados del estudio comparativo demostraron un incremento de los costes directos para las soluciones con fibra (sustitución parcial o total del refuerzo tradicional); sin embargo, este incremento de los costes puede compensarse debido a la reducción del periodo de construcción y, como consecuencia, reducción de los costes indirectos (e.g. costes de maquinaria y herramientas, gastos de administración y dirección técnica, costes financieros).

TABLE OF CONTENTS

1. INTRODUCTION

This chapter provides relevant information on fibre reinforced concrete (FRC), emphasising properties of the material and its application in both structural and non-structural purposes. Thereafter, the use of FRC for column-supported flat slabs is described, highlighting the previous experiences, research contributions to this topic, and aspects that require further study. Based on this information, general and specific objectives of the thesis are formulated. Finally, the list of publications derived during the elaboration of the thesis is presented and the structure of the document is discussed.

Contents

1.1. BACKGROUND

In recent decades, fibre reinforced concrete (FRC) has emerged as one of the most promising types of concrete in the construction sector. The incorporation of fibres (primarily steel or synthetic) in cement-based composites can have a positive effect on the fracture energy of the matrix [1], crack control [2–6], fire resistance [7–9], fatigue [10,11], redistribution capacity [12–15], and impact resistance [16–18]. As a result, the reinforcing steel bars can be partially or totally substituted by fibres without jeopardising the reliability of the structure. In fact, this substitution is capable of guaranteeing more sustainable solutions for certain structural and non-structural elements in accordance with the recent studies [19–22].

Despite the potential enhancement of above-listed material properties, FRC has been primarily used in elements subjected to relatively low tensile stresses and/or in those whose consequences of failure are minor. Ground-supported slabs [23–25], precast tunnel segments [26–29], pavements [30], pipe sewer lines [31,32] are the examples of the most frequent fields of FRC application.

Nevertheless, the ongoing research and considerable scientific efforts have proven that this material can also be a viable alternative to traditional solutions (e.g. those based in steel bars for reinforcing concrete) in elements with high structural responsibility. In this regard, FRC slabs in statically indeterminate configurations gained a considerable interest among researchers. Laboratory tests and experimental programmes evidenced proper flexural response of FRC slabs under different boundary and load conditions in terms of crack control [13,33,34], load redistribution [13,35,36], ductility [37–39], and bearing capacity [39–42]. Moreover, the presence of fibres in the concrete mix provided a sufficient punching strength in accordance with [43–49].

The gained experience is having a certain impact on the industry, this resulting in the construction of a dozen buildings with FRC flat slabs. The reported results confirmed the positive outcomes with respect to the optimization of resources and reduction of construction time. The analysis of traditional reinforcement substitution by fibres in Ditton Nams shopping mall and Triangle office building concluded in considerable economic savings [41], whereas the 9 week time-saving effect along with the reduction of the required machinery were acknowledged during the construction of 16-floor Rocca Al-Mare office tower [50]. A more detailed comparison between potential alternatives was carried out by Orellana [51] – 12% reduction of total costs was achieved through using a FRC solution for the construction of the LKS office building in Spain (Figure 1).

Fig. 1. Pioneer experience in Spain: construction of LKS office building with FRC flat slabs [51]

1.2. MOTIVATIONS

The successful experiences of FRC column-supported slab construction should already have boosted the implementation of this technology. However, a number of factors still hinder its widespread use in the construction sector. Primarily, the limited knowledge of FRC properties generates concerns related to the distribution and orientation of fibres within the hardened matrix – resulting in the overall lack of confidence in the bearing capacity of FRC.

Furthermore, structural designers face certain challenges concerning the design procedures for FRC elevated slabs due to insufficiently detailed descriptions on how to cover both serviceability and ultimate limit states. In fact, the majority of provisions are focused on the assessment of flexural and punching strength at ultimate conditions and/or evaluation of the structural behaviour of FRC slabs by means of nonlinear finite element models. Nonetheless, the implementation of such models is infrequent among practitioners since the appropriate software to conduct these analyses are not meant for day-to-day design procedures.

Moreover, there is a lack of simplified tools for the construction planners to carry out the comparative analysis of traditional and FRC solutions from both technological and economic points of view. The comprehensive study of the above-presented aspects might lead to overcome both technical and psychological barriers and become a source of inspiration for construction industry to consider the possibility of using FRC in column-supported flat slabs (CSFS), i.e. elements with high structural responsibility.

1.3. OBJECTIVES

Considering the motivations presented in the previous section, the objectives of the thesis can be divided into three main blocks:

(1) to evidence the potential of FRC CSFSs s in terms of construction procedure, cracking and deflection control, redistribution capacity, and overall structural integrity;

(2) to provide design-oriented recommendations based on the accepted limit state format for dealing with both serviceability and ultimate limit states, and

(3) to elaborate a straightforward approach to compare FRC and traditional solutions for CSFSs in terms of mechanical and economic aspects.

To fulfil these goals, specific objectives are to be defined for each of the main blocks addressed in this thesis:

BLOCK 1: REAL-SCALE TESTING OF FRC CSFS

1.1 Characterize material properties of FRC in the fresh and hardened states, varying fibre type and content.

1.2 Assess the flexural response of the constructed real-scale FRC CSFS in terms of cracking, deflections, and overall bearing capacity.

1.3 Identify and characterize fibre distribution and fibre orientation in the studied FRC slab.

1.4 Monitor the structural effects of time-dependent phenomena (i.e. shrinkage and creep) on the pilot FRC CSFS during the experimental programme period

1.5 Analyse the adequacy of the current constitutive models to evaluate the flexural response of the FRC CSFS by means of analytical and nonlinear approaches.

BLOCK 2: DESIGN OF FRC CSFS

2.1 Develop a simplified approach to estimate the flexural capacity of FRC and hybrid reinforced concrete (fibres and reinforcing steel bars, HFRC) CSFS.

2.2 Propose an approach for the indirect control of cracking for FRC/HFRC CSFS.

2.3 Adapt the approach to calculate deflections by means of crossing beam analogy to (1) assess the instantaneous deflections and (2) to check the required ductility in bending of FRC/HFRC CSFS.

2.4 Validate the proposed limit state design approach through comparison with results derived from a nonlinear finite element analysis.

BLOCK 3: COST-ORIENTED ANALYSIS OF FRC CSFS CONSTRUCTION

3.1 Propose a straightforward method to assess the reduction of the reinforcing steel bars due to use of FRC for CSFS.

3.2 Analyse the technological aspects affected by the use of FRC for CSFS.

3.3 Study the economic factors that should be taken into account within the comparative analysis of the traditional and FRC solutions for CSFS.

1.4. METHODOLOGY AND STRUCTURE OF THE THESIS

Taking into consideration that the majority of topics covered during this research programme are industrial-oriented and the efficient spreading of the results will increase the impact of those, an article-based doctoral thesis has been elaborated for better diffusion of the achieved results in accordance with the academic regulations of Universitat Politècnica de Catalunya.

In this regard, the main core of the thesis (Chapter 2) is comprised of journal publications listed below. The specific objectives achieved by each publication are specified in brackets. Furthermore, based on the results derived, Chapter 3 presents both general and specific conclusions related to the main blocks addressed in the thesis: real-scale testing of FRC CSFS, design of FRC CSFS, and cost-oriented analysis of FRC CSFS construction.

Finally, an additional journal publication along with two research contributions are presented in the Annex in order to complement the analysis of certain aspects discussed in the thesis (Figure 2).

MAIN CORE: JOURNAL PAPERS

JOURNAL PAPER I (*Block 1: Specific objectives 1.1-1.5*): Stanislav Aidarov, Francisco Mena, and Albert de la Fuente. “Structural response of a fibre reinforced concrete pile-

supported flat slab: full-scale test". Engineering Structures 239 (2021): 112292. Impact factor 4.47, Q1. DOI: 10.1016/j.engstruct.2021.112292

JOURNAL PAPER II *(Block 2: Specific objectives 2.1-2.4)*: Stanislav Aidarov, Nikola Tošić, and Albert de la Fuente, "A limit state design approach for hybrid reinforced concrete column-supported flat slabs". Structural Concrete, 2021, Impact Factor: 2.72, Q1. DOI: 10.1002/suco.202100785.

JOURNAL PAPER III *(Block 3: Specific objectives 3.1-3.3)*: Stanislav Aidarov, Ana Nadaždi, Evgeniy Pugach, Nikola Tošić, and Albert de la Fuente. "Cost-oriented analysis of fibre reinforced concrete column-supported flat slabs construction". Journal of Building Engineering (2022): 104205. Impact Factor: 5.32, Q1. DOI: 10.1016/j.jobe.2022.104205.

ANNEX: JOURNAL PAPER AND RESEARCH CONTRIBUTIONS

RESEARCH CONTRIBUTION I (*Block 1: Specific objective 1.1*): Stanislav Aidarov, Francisco Mena, and Albert de la Fuente. "Self-compacting steel fibre reinforced concrete: material characterization and real scale test up to failure of a pile supported flat slab". In RILEM-fib International Symposium on Fibre Reinforced Concrete, pp. 702-713. Springer, Cham, 2021. DOI: 10.1007/978-3-030-83719-8_60.

JOURNAL PAPER *(Block 1: Specific objective 1.4)*: Nikola Tošić, Stanislav Aidarov, and Albert de la Fuente. "Systematic review on the creep of fiber-reinforced concrete". Materials 13, no. 22 (2020): 5098. Impact Factor: 3.6. DOI: 10.3390/ma13225098.

RESEARCH CONTRIBUTION II *(Block 2: Specific objective 2.5)*: Stanislav Aidarov, Nikola Tošić, and Albert de la Fuente. Steel fibre reinforced concrete two-way slab: evaluation of structural response under uniformly distributed load. In: Proceedings of the fib Symposium 2021, Lisbon (Portugal), 2021.

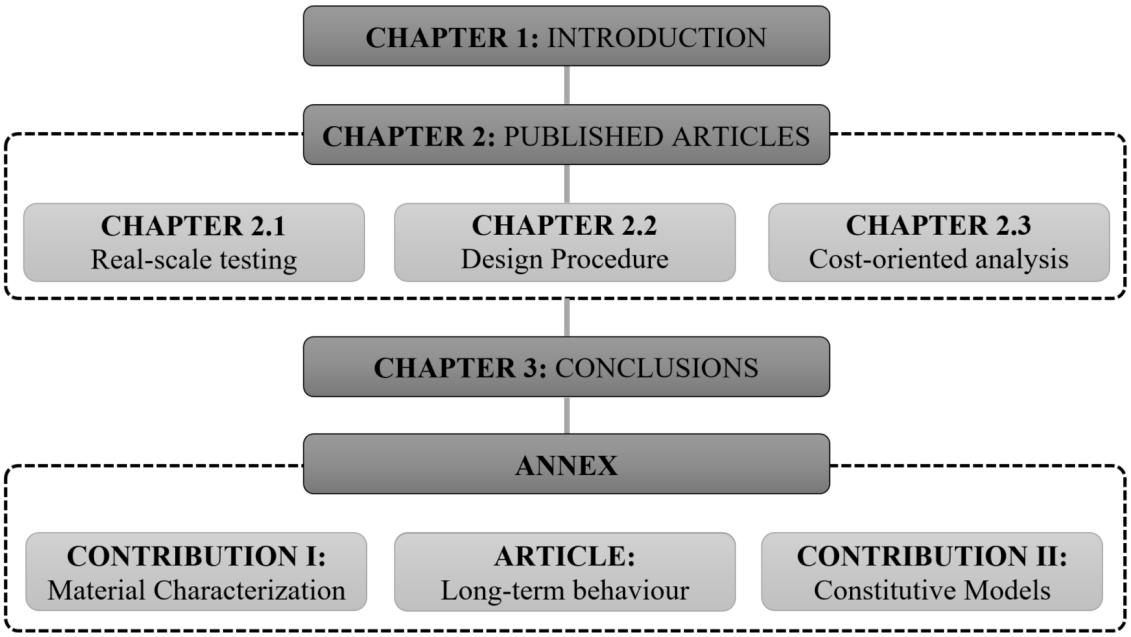

Fig. 2. Outline of the thesis

REFERENCES

[1] Zollo RF. Fiber-reinforced Concrete : an Overview after 30 Years of Development. Cem Concr Compos 1997;19:107–22.

[2] Tiberti G, Minelli F, Plizzari G. Cracking behavior in reinforced concrete members with steel fibers: A comprehensive experimental study. Cem Concr Res 2015;68:24–34. https://doi.org/10.1016/j.cemconres.2014.10.011.

[3] Pujadas P, Blanco A, de la Fuente A, Aguado A. Cracking behavior of FRC slabs with traditional reinforcement. Mater Struct Constr 2012;45:707–25. https://doi.org/10.1617/s11527-011-9791-0.

[4] McMahon JA, Birely AC. Service performance of steel fiber reinforced concrete (SFRC) slabs. Eng Struct 2018;168:58–68. https://doi.org/10.1016/j.engstruct.2018.04.067.

[5] Groli G, Caldentey AP. Improving cracking behaviour with recycled steel fibres targeting specific applications – analysis according to fib Model Code 2010. Struct Concr 2017;18:29–39. https://doi.org/10.1002/suco.201500170.

[6] Amin A, Gilbert RI. Instantaneous crack width calculation for steel fiber-reinforced concrete flexural members. ACI Struct J 2018;115:535–43. https://doi.org/10.14359/51701116.

[7] Lau A, Anson M. Effect of high temperatures on high performance steel fibre reinforced concrete. Cem Concr Res 2006;36:1698–707. https://doi.org/10.1016/j.cemconres.2006.03.024.

[8] Wu H, Lin X, Zhou A. A review of mechanical properties of fibre reinforced concrete at elevated temperatures. Cem Concr Res 2020;135:106117. https://doi.org/10.1016/j.cemconres.2020.106117.

[9] Khaliq W, Kodur V, Asce F. Effectiveness of Polypropylene and Steel Fibers in Enhancing Fire Resistance of High-Strength Concrete Columns. J Struct Eng 2018;144:1–12. https://doi.org/10.1061/(ASCE)ST.1943-541X.0001981.

[10] Germano F, Tiberti G. Post-peak fatigue performance of steel fiber reinforced concrete under flexure. Mater Struct 2015. https://doi.org/10.1617/s11527-015-0783-3.

[11] Carlesso DM, de la Fuente A, Cavalaro SHP. Fatigue of cracked high performance fiber reinforced concrete subjected to bending. Constr Build Mater 2019;220:444–55. https://doi.org/10.1016/j.conbuildmat.2019.06.038.

[12] di Prisco M, Martinelli P, Dozio D. The structural redistribution coefficient KRd: A numerical approach to its evaluation. 2016. https://doi.org/10.1002/suco.201500118.

[13] Fall D, Shu J, Rempling R, Lundgren K, Zandi K. Two-way slabs: Experimental investigation of load redistributions in steel fibre reinforced concrete. 2014. https://doi.org/10.1016/j.engstruct.2014.08.033.

[14] Mahmood SMF, Agarwal A, Foster SJ, Valipour H. Flexural performance of steel fibre reinforced concrete beams designed for moment redistribution. Eng Struct 2018;177:695–706. https://doi.org/10.1016/j.engstruct.2018.10.007.

[15] Colombo M, Martinelli P, di Prisco M. On the evaluation of the structural redistribution factor in FRC design: a yield line approach. Mater Struct 2017;50:1–18. https://doi.org/10.1617/s11527-016-0969-3.

[16] Jin L, Zhang R, Dou G, Du X. Fire resistance of steel fiber reinforced concrete beams after low-velocity impact loading. Fire Saf J 2018;98:24–37. https://doi.org/10.1016/j.firesaf.2018.04.003.

[17] Li W, Xu J. Mechanical properties of basalt fiber reinforced geopolymeric concrete under impact loading. Mater Sci Eng A 2009;505:178–86. https://doi.org/10.1016/j.msea.2008.11.063.

[18] Nili M, Afroughsabet V. Combined effect of silica fume and steel fibers on the impact resistance and mechanical properties of concrete. Int J Impact Eng 2010;37:879–86. https://doi.org/10.1016/j.ijimpeng.2010.03.004.

[19] de la Fuente A, Blanco A, Armengou J, Aguado A. Sustainability based-approach to determine the concrete type and reinforcement configuration of TBM tunnels linings. Case study: Extension line to Barcelona Airport T1. Tunn Undergr Sp Technol 2017;61:179–88. https://doi.org/10.1016/j.tust.2016.10.008.

[20] de la Fuente A, Casanovas-Rubio MDM, Pons O, Armengou J. Sustainability of Column-Supported RC Slabs: Fiber Reinforcement as an Alternative. J Constr Eng Manag 2019;145:1–12. https://doi.org/10.1061/(ASCE)CO.1943-7862.0001667.

[21] Josa I, Fuente A De, Casanovas-Rubio MM, Armengou J, Aguado A. Sustainability-Oriented Model to Decide on Concrete Pipeline Reinforcement. Sustainability 2021.

[22] Josa I, Tošić N, Marinković S, de la Fuente A, Aguado A. Sustainability-Oriented Multi-Criteria Analysis of Different Continuous Flight Auger Piles. Sustainability 2021;13:1–16. https://doi.org/https://doi.org/10.3390/su13147552.

[23] Alani AM, Beckett D. Mechanical properties of a large scale synthetic fibre reinforced concrete ground slab. Constr Build Mater 2013;41:335–44. https://doi.org/10.1016/j.conbuildmat.2012.11.043.

[24] Meda A, Plizzari GA. New design approach for steel fiber-reinforced concrete slabs-on-ground based on fracture mechanics. ACI Struct J 2004;101:298–303. https://doi.org/10.14359/13089.

[25] Meda A, Plizzari GA, Riva P. Fracture behavior of SFRC slabs on grade. Mater Struct Constr 2004;37:405–11. https://doi.org/10.1617/14093.

[26] Chiaia B, Fantilli AP, Vallini P. Combining fiber-reinforced concrete with traditional reinforcement in tunnel linings. Eng Struct 2009;31:1600–6. https://doi.org/10.1016/j.engstruct.2009.02.037.

[27] de la Fuente A, Pujadas P, Blanco A, Aguado A. Experiences in Barcelona with the use of fibres in segmental linings. Tunn Undergr Sp Technol 2012;27:60–71. https://doi.org/10.1016/j.tust.2011.07.001.

[28] Jamshidi M, Hoseini A, Vahdani S, Santos C De, De A. Seismic fragility curves for vulnerability assessment of steel fiber reinforced concrete segmental tunnel linings. Tunn Undergr Sp Technol 2018;78:259–74. https://doi.org/10.1016/j.tust.2018.04.032.

[29] Liao L, de la Fuente A, Cavalaro S, Aguado A. Design of FRC tunnel segments considering the ductility requirements of the Model Code 2010. Tunn Undergr Sp Technol Inc Trenchless Technol Res 2015;47:200–10. https://doi.org/10.1016/j.tust.2015.01.006.

[30] Belletti B, Cerioni R, Meda A, Plizzari G. Design Aspects on Steel Fiber-Reinforced Concrete Pavements 2009;20:599–607. https://doi.org/10.1061/(ASCE)0899-1561(2008)20.

[31] de la Fuente A, Escariz RC, De Figueiredo AD, Molins C, Aguado A. A new design method for steel fibre reinforced concrete pipes. Constr Build Mater 2012;30:547–55. https://doi.org/10.1016/j.conbuildmat.2011.12.015.

[32] de la Fuente A, Escariz RC, de Figueiredo AD, Aguado A. Design of macro-synthetic fibre reinforced concrete pipes. Constr Build Mater 2013;43:523–32. https://doi.org/10.1016/j.conbuildmat.2013.02.036.

[33] Blanco A, Pujadas P, de la Fuente A, Cavalaro SHP, Aguado A. Influence of the type of fiber on the structural response and design of FRC slabs. J Struct Eng (United States) 2016;142:1–11. https://doi.org/10.1061/(ASCE)ST.1943-541X.0001515.

[34] di Prisco M, Colombo M, Pourzarabi A. Biaxial bending of SFRC slabs: Is conventional reinforcement necessary? Mater Struct Constr 2019;52:1–15. https://doi.org/10.1617/s11527-018-1302-0.

[35] di Prisco M, Martinelli P, Parmentier B. On the reliability of the design approach for FRC structures according to fib Model Code 2010: the case of elevated slabs. Struct Concr 2016;17:588–602. https://doi.org/10.1002/suco.201500151.

[36] Di Prisco M, Martinelli P. A numerical approach for the evaluation of the structural redistribution coefficient KRd. Comput Model Concr Struct - Proc EURO-C 2014 2014;1:503–12. https://doi.org/10.1201/b16645-56.

[37] Facconi L, Minelli F, Plizzari G. Steel fiber reinforced self-compacting concrete thin slabs – Experimental study and verification against Model Code 2010 provisions. Eng Struct 2016;122:226–37. https://doi.org/10.1016/j.engstruct.2016.04.030.

[38] Michels J, Waldmann D, Maas S, Zürbes A. Steel fibers as only reinforcement for flat slab construction - Experimental investigation and design. Constr Build Mater 2012;26:145–55. https://doi.org/10.1016/j.conbuildmat.2011.06.004.

[39] Aidarov S, Mena F, de la Fuente A. Structural response of a fibre reinforced concrete pile-supported flat slab: full-scale test. Eng Struct 2021;239. https://doi.org/10.1016/J.ENGSTRUCT.2021.112292.

[40] Gossla U. Development of SFRC Free Suspended Elevated Flat Slabs. Aachen: 2005.

[41] Mandl J. Flat Slabs Made of Steel Fiber Reinforced Concrete (SFRC). CPI Worldw., 2008.

[42] Parmentier B, Itterbeeck P Van, Skowron A. The flexural behaviour of SFRC flat slabs : the Limelette full- scale experiments for supporting design model codes. Proc. FRC, 2014.

[43] Barros JAO, Teixeira MDE, Cuhna V, Morais Neto BN, Ventura-Gouveia A. Numerical Modelling of the Punching Behaviour of Steel Fibre Reinforced Self- Compacting Concrete Flat Slabs 2013:1–15.

[44] Cheng M-Y, Parra-Montesinos G. Evaluation of Steel Fiber Reinforcement for Punching Shear Resistance in Slab-Column Connections— Part I: Monotonically Increased Load 1991:166–85.

[45] Choi KK, Reda Taha MM, Park HG, Maji AK. Punching shear strength of interior concrete slab-column connections reinforced with steel fibers. Cem Concr Compos 2007;29:409–20. https://doi.org/10.1016/j.cemconcomp.2006.12.003.

[46] Gouveia ND, Fernandes NAG, Faria DMV, Ramos AMP, Lúcio VJG. SFRC flat slabs punching behaviour - Experimental research. Compos Part B Eng 2014;63:161–71. https://doi.org/10.1016/j.compositesb.2014.04.005.

[47] Maya LF, Fernández Ruiz M, Muttoni A, Foster SJ. Punching shear strength of steel fibre reinforced concrete slabs. Eng Struct 2012;40:83–94. https://doi.org/10.1016/j.engstruct.2012.02.009.

[48] Nguyen-Minh L, Rovňák M, Tran-Quoc T, Nguyen-Kim K. Punching shear resistance of steel fiber reinforced concrete flat slabs. Procedia Eng 2011;14:1830–7. https://doi.org/10.1016/j.proeng.2011.07.230.

[49] Tan KH, Venkateshwaran A. Punching shear in steel fiber-reinforced concrete slabs with or without traditional reinforcement. ACI Struct J 2019;116:107–18. https://doi.org/10.14359/51713291.

[50] Karv C. Shear and punching resistance of steel fibre reinforced concrete slabs. Aalto University, 2017.

[51] Maturana Orellana A. Estudio teórico-experimental de la aplicabilidad del hormigón reforzado con fibras de acero a losas de forjado multidireccionales. 2013. https://doi.org/10.1174/021435502753511268.

2. PUBLICATIONS: JOURNAL PAPERS

This chapter, being a main core of the thesis, reproduces the published journal papers derived from the conducted research programme. Each paper follows its own numbering of sections, figures, equations and references.

Contents

2.1. JOURNAL PAPER I. STRUCTURAL RESPONSE OF A FIBRE REINFORCED CONCRETE PILE-SUPPORTED FLAT SLAB: FULL-SCALE TEST

Published in Engineering Structures 239 (2021) 105-116.

Stanislav Aidarov [a, b, *], Francisco Mena [b], Albert de la Fuente [b]

[a] Smart Engineering Ltd., UPC Spin-Off, Jordi Girona 1-3, 08034 Barcelona, Spain

[b] Civil and Environmental Engineering Department, Universitat Politècnica de Catalunya (UPC), Jordi Girona 1-3, 08034 Barcelona, Spain

* Corresponding author: Tel.: +34 633 634 207; Full Postal address: 08034, Barcelona, Jordi Girona 1; Email address: stanislav.aydarov@smartengineeringbcn.com ; stanislav.aidarov@upc.edu

Abstract

The total substitution of traditional reinforcement in the form of steel bars by fibres can be mainly found in elements with favourable boundary conditions and subjected to low-moderate load levels. However, the rigorous study of fibre reinforced concrete (FRC) and its potential fields of application over the last decades permitted this material to face structural application with greater responsibility in terms of structural integrity and mechanical capacity – construction of FRC flat slabs. This promising technology was used in a dozen buildings with recognition of positive outcomes with respect to the optimization of resources, reduction of execution time, and environmental impacts. Despite these achievements, the application of FRC in flat slabs is still limited in the building sector because of certain concerns of the material capacities, and existence of some aspects related both to service and ultimate limit states, which are still unclear. With this in mind, an extensive experimental programme was carried out and focused on the construction of a full-scale FRC flat slab and its loading protocol in order to analyse both crack and deflection patterns. Likewise, the structure was led to failure, which also allowed assessing both the bearing and deformability capacities as well as the fibre distribution and orientation. The results derived from this experimental program are expected to increase the confidence of designers and practitioners on the use of FRC as structural material for column-supported flat slabs.

Keywords: elevated slab, two-way slab, fibre reinforced concrete, FRC, ultimate behaviour, serviceability behaviour, full-scale test

1. INTRODUCTION

The incorporation of fibres in cement-based composites allows increasing the fracture energy of the matrix [1] by providing post-cracking strength and, hence, improving the ductility [2], cracking control [3–5], and fatigue [6,7]; fire and impact resistance can also be enhanced depending on the type of fibres used [8–10]. These improvements enable the possibility of a partial or even total substitution of the traditional steel bars by structural fibres [11].

Over the last decades, a significant number of researchers has been investigating the FRC technology and noticeable advances were achieved, even the acceptance of FRC as structural material in the *fib* MC 2010 [11]. Nevertheless, so far, the FRC has been primarily used in elements for which the applied bending moments during transient and service loading situations are relatively low (usually below the cracking bending moment) and/or for those whose consequences of failure are minor. For instance: slabs on grade [12–14], precast tunnel segments [15–17], reinforced earth-retaining walls [18], and sewerage pipes [19]. The gained experience along with ongoing research have expanded the knowledge base related to FRC and, consequently, this is increasing its applicability in elements with higher structural responsibility.

One of the most complex challenges within this topic became the construction of FRC elevated slabs for residential buildings with total substitution of traditional reinforcement because of the occurrence of high tensile stresses during the service life of the structure. The first full-scale tests proved that FRC with steel macrofibre content of 100 kg/m^3 (volume fraction 1.3%) could provide the required structural integrity even under the loads that considerably exceeded the standard magnitudes for residential flat slabs at ultimate limit state (ULS) [20,21]. Other experimental results pointed out: the remarkable redistribution capacity of FRC statically redundant systems [22–24]; economically promising results of hybrid solutions (fibres + steel bars) [25, 26]; improvement of punching strength [27–29], and a sufficiently even distribution of fibres in the concrete mix to consider the material as homogenous [30,31].

Steel fibre reinforced concrete (SFRC) technology in construction of residential flat slabs was also applied in real projects: the Ditton Nams shopping mall (Latvia), the Triangle office building (Estonia), the Rocca Al-Mare office tower (Estonia), and the LKS office building (Spain) are representative examples. Each of these projects highlighted technical advantages of using SFRC: (1) the analysis of traditional reinforcement substitution by SFRC in Ditton Nams shopping mall and Triangle office building acknowledged economic savings [32]; (2) the 9 week time-saving effect along with reduction of the required machinery were mainly denoted during the construction of 16-floor Rocca Al-Mare office tower [33].

In case of the LKS office building, a more detailed comparative study was presented in [34]. This research presented three different alternatives to be analysed: (1) steel bar reinforced concrete (original design), (2) self-compacting SFRC with complementary use of steel bars in specific areas of the slab plus anti-progressive collapse reinforcement (APC), (3) self-compacting SFRC with complementary use of steel bars in specific areas of the slabs. Both SFRC solutions provided economic benefits: 12% and 16% reduction of total costs in comparison with the original design was reported for SFRC + APC and SFRC, respectively. Despite the fact that APC reinforcement is, basically, a redundant reinforcement to prevent

local failures [35] which could lead to the collapse of the entire structure, the alternative with APC reinforcement was selected for the LKS office building since this represented a pioneer experience in Spain and, as a consequence, an additional safety margin was provided.

The achieved results in both experimental and real projects gathered in Table 1 could have already turned SFRC technology into a competitive alternative for two-way slab construction. However, a number of constraining factors that require further development are compromising the widespread use of the SFRC for column-supported flat slabs. General comprehension of SFRC in terms of fibre distribution and orientation [36,37], ULS capacity of SFRC in statically redundant structural configurations [38,39], and the effect of long-term loads in terms of deformation and cracking [40,41] are found to be those more relevant. Also, the potential reduction of fibre content along with precise tools for thorough comparison with other alternatives [42] and established criteria for quality control [43,44] demand further detailed investigation.

Table 1. Cases of SFRC application in two-way slabs

Author	Type	C_f [kg/m3]	$L_{max/h}$ [m/m]	Steel Bars	l_f / $Ø_f$ / R_m - type
di Prisco et al. [22]	SSLT	35	13	Yes/None	60/0.9/1500 – DHE
Blanco et al. [45]	SSLT	40	15	None	50/0.62/1270 – SHE
Fall et al. [46]	SSLT	35	28	Yes/None	60/0.9/2300 – DHE
Facconi et al. [25]	SSLT	20/25	32	None	32/0.4/2200 – SHE
Facconi et al. [25]	SSLT	25	32	None	60/0.9/2200 – DHE
Barros et al. [47]	FSFT	90	16	Yes*	37/0.5/1100 – SHE
Salehian et. al [34]	FSFT	90	16	Yes*	37/0.5/1100 – SHE
Destreé et al. [21]	FSFT	45	19	No	50/1.3/850 – C
Hedebratt et al. [26]	FSFT	40/80	23	Yes/None	60/0.9/1160 – SHE
Døssland [31]	FSFT	62	23	Yes/None	60/0.9/1000 – SHE
Destreé et al. [21]	FSFT	100	28	Yes*	50/1.3/850 – C
Parmentier et al. [30]	FSFT	70	30	Yes*	60/1.0/1450 – SHE
Gossla [20]	FSFT	100	30	Yes*	50/1.3/900 – C
Ošlejs [48]	RB	100	24	Yes*	50/1.3/900 – C
Maturana [34]	RB	100	27	Yes	50/1.3/900 – C
Present study	FSFT	70	30	Yes*	60/0.9/2300 - DHE

NB: C_f – fibre content; Lmax – maximum span; h – depth of the slab; l_f – fibre length in mm; $Ø_f$ – fibre diameter in mm; R_m – fibre tensile strength in MPa; SSLT – small scale laboratory test; FSFT – full scale field test; RB – real building; DHE – double hooked-end; SHE – single hooked end; C – crimped; Yes* – only presence of APC steel bars.

To shed light on some aspects of abovementioned factors, an extensive experimental program was carried out in this study by following these steps: (1) characterization of several self-compacting SFRC mixes with different fibre content and type; (2) construction of SFRC slabs of different dimensions maintaining the same slenderness; (3) testing these slabs under

various boundary and load conditions. This paper focuses on the construction of a four-panel column-supported SFRC flat slab and its sequential loading protocol aimed at characterizing the structural response of the structure for load levels representative of both service and ultimate limit states. To this end, increasing uniformly distributed load (UDL) was applied onto the structure, in contrast to previous experiences in which point loads were mainly used, especially for simulation of ULS conditions (Table 2). After failure, 32 samples were cored from the tested SFRC slab to examine fibre distribution both throughout the element and over the slab depth. Additionally, fibre orientation was evaluated by means of an inductive test with the aim of assessing the contribution of fibres in the direction of the three main axes, which could be valuable information for further studies related to design procedures.

Table 2. Parameters studied within previous research programmes

Author	$C_{f,real}$	C_i	SLS		ULS		Cracking		
			UDL	G_UDL	PL	UDL	W	P	E
di Prisco et al. [22]					●		●	●	
Blanco et al. [45]		●			●			●	
Fall et al. [46]					●			●	
Facconi et al. [25]					●		●	●	
Facconi et al. [25]					●		●	●	
Barros et al. [47]					●				
Salehian et. al [34]		●		●	●			●	●
Destreé et al. [21]					●				
Hedebratt et al. [26]					●			●	
Døssland [31]	●				●			●	
Destreé et al. [21]					●				
Parmentier et al. [30]	●		●		●		●	●	
Gossla [20]					●		●	●	
Ošlejs [48]			●						
Maturana [34]	●		●						
Present study	●	●		●		●	●	●	●

NB: $C_{f,real}$ – real fibre distribution in the element; C_i – relative contribution of fibres in three main axes; G_UDL – gradual uniformly distributed loading; PL – point loading; W – crack opening; P – crack pattern; E – crack evolution

2. EXPERIMENTAL PROGRAMME

2.1. GEOMETRY OF SFRC SLAB

A 12.0 × 10.0 × 0.2 m^3 SFRC slab supported by nine columns with square cross section of 0.25 m was tested. These columns were supported on 1.85 × 1.85 × 0.7 m^3 concrete footings and formed four panels of 6.0 x 5.0 m^2 each. Figure 1 presents the geometry of superstructure along with the detailed description of the established reinforcement for concrete columns and footings. The geometry was selected to reproduce common dimensions of slab panels that could be used in office and residential buildings. Additionally, previous experiences were

considered and the achieved span-to-depth ratio (30) corresponded to the upper limit of those already constructed (Table 1).

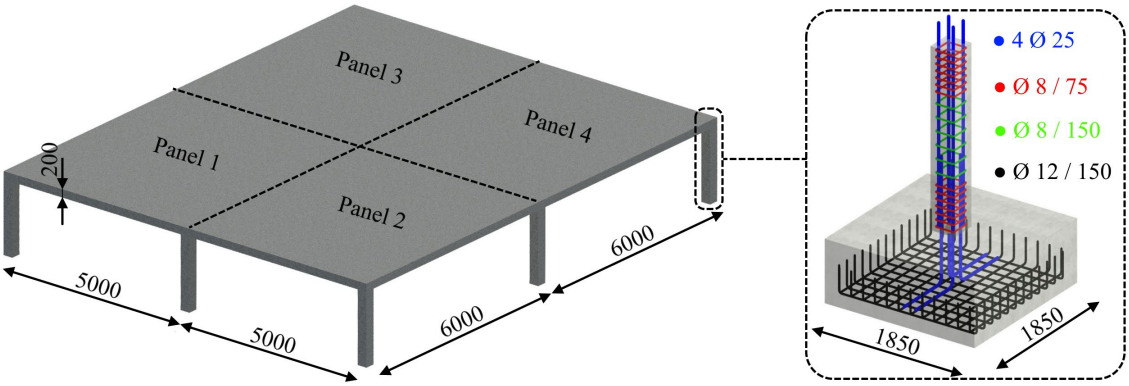

Fig. 1. Geometry of the SFRC prototype (units in [mm])

2.2. MATERIAL PROPERTIES

The experimental investigation presented herein was carried out by using a self-compacting SFRC with a steel fibre content of 70 kg/m^3 (volume fraction 0.9%) – the lower limit, to best authors' knowledge, reported in the scientific literature related to the erection and testing of full-scale SFRC two-way slabs of this slenderness. The used fibre was characterised by a high tensile strength (2300 MPa), double hooked-end shape and an aspect ratio of 65. Despite the relatively high content of fibres, the material was required to guarantee sufficient workability to avoid the concrete vibration. The absence of vibrating minimized the external influence on the distribution and orientation of fibres. Table 3 summarizes the details of the used concrete mix.

Table 3. Concrete mixture

Cement CEM II/A-L 45,2R (kg/m^3)	425
Coarse aggregate 10/20 (kg/m^3)	250
Coarse aggregate 4/10 (kg/m^3)	150
Fine aggregate 0/4 (kg/m^3)	725
Fine aggregate 0/2 (kg/m^3)	600
Limestone filler (kg/m^3)	25
Water-cement ratio	0.47
Additives (% on cement content)	2.77
Steel fibres (kg/m^3)	70

Four concrete trucks were required for the construction of the SFRC prototype slab and each of the batches was tested to evaluate the properties of the material. Mean values at 28 days for the modulus of elasticity (E_{cm}), compressive strength (f_{cm}) and residual flexural strengths ($f_{Rm,i}$) are gathered in Table 4. The presented properties at the hardened state were obtained in accordance with standards EN 12390-13 [49], EN 12390-3 [50], and EN 14651 [51], respectively. Three specimens per batch were tested to obtain E_{cm} and f_{cm}; whereas four 150 × 150 × 600 mm^3 notched prisms for $f_{Rm,i}$.

Table 4. Characterization of SFRC at 28 days

	Batch 1		Batch 2		Batch 3		Batch 4		Overall	
	Average (MPa)	CV (%)	Average (MPa)	CV (%)	Average (MPa)	CV (%)	Average (MPa)	CV (%)	Average (MPa)	CV (%)
E_c	25840	0.5	25030	1.4	26270	2.0	28080	3.1	26310	4.9
f_c	42.2	0.9	39.5	1.2	42.3	1.5	47.5	6.3	42.9	7.8
f_{LOP}	3.9	12.6	4.4	4.1	4.4	11.6	4.5	6.4	4.4	12.4
f_{R1}	5.8	30.0	7.8	9.1	5.3	51.5	10.0	10.2	7.2	35.3
f_{R2}	6.9	31.7	8.6	19.2	7.3	32.5	9.6	15.8	8.1	26.0
f_{R3}	6.7	25.7	8.4	21.6	6.9	33.4	9.0	13.4	7.7	24.7
f_{R4}	6.5	21.9	8.0	20.0	6.4	30.9	8.6	9.4	7.3	22.7

All tested batches had similar mechanical properties in terms of compressive strength and modulus of elasticity. The relatively low values of the modulus of elasticity can be explained by increased binder content that might have led to the reduction (<20%) of E_{cm} compared with conventional concrete with equivalent f_{cm} [11]. The obtained results of $f_{R,i}$ had a higher scatter in comparison with the expected values (especially for the given fibre content) [52,53]. This phenomenon led to considerable reduction of the characteristic values of residual flexural strengths $f_{Rk,i}$, the SFRC resulting in a 3e strength class according to the *fib* MC-2010 classification, whereas the obtained mean values corresponded to the 7c strength class [11]. However, taking into account that high density of cracks were expected, the mean $f_{R,i}$ was found to be representative of the post-cracking response of the material in the structure as the intrinsic scatter decreases due to the statistical scale effect reported in [54].

Additionally, the significant scatter observed in residual tensile strength reinforces the necessity of carrying out a rigorous control of FRC elaboration in order to keep the properties of the material in line with those obtained in the laboratory. To this end, the mixing procedure [34,55,56], transportation [34], and pouring approach [55–57] should be taken into account.

2.3. TEST CONFIGURATION AND PROCEDURE

The loads specified in the Spanish Building Code for residential buildings [58] were considered as reference for designing the loading protocol. In this regard, in addition to the 4.8 kN/m^2 due to the self-weight (q_{SW}), a dead load (q_G) and variable load (q_Q) of 2.0 and 3.0 kN/m^2, respectively, were considered. Load partial safety factors γ_G=1.35 and γ_Q=1.50 were assumed for computing the design load $q_{Sd} = \gamma_G \cdot (q_{SW} + q_G) + \gamma_G \cdot q_Q = 13.7 \approx 14.0$ kN/m^2 (for safe-side purposes).

The load was applied gradually in different time-steps in order to evaluate the response of the structure in terms of cracking and deformation. For this purpose, the load was provided by means of concrete cubes of 0.5 × 0.5 × 0.6 m^3 (≈ 350 kg each), dividing the process into four steps (Figure 2). Time-spans between loading phases (Table 5) depended on the structural response, i.e. the next phase could only be started if the total deflection increment, measured in the centres of each panel, during successive 10 days was less than 1

mm. The cracking evolution was also taken into account – stability of cracking in terms of maximum width and length within the mentioned period (10 days) was an essential factor to consider the load phase completed.

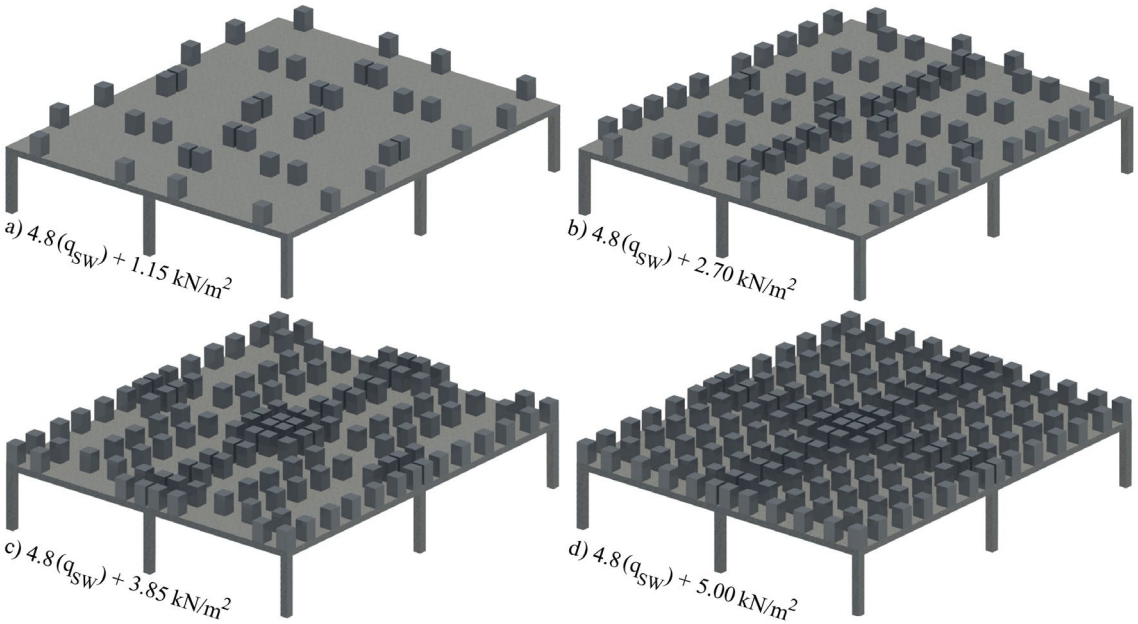

Fig. 2. Load phases: a) I b) II c) III and d) IV

The deflections of the structure were monitored by means of eight prisms and topography (Figure 3). These prism targets were installed, firstly, on the top surface of the slab and, once the formwork was removed and the structure stabilised under the self-weight, those were moved to the bottom surface in order to permit the loading protocol to start. As a result, the deflections were measured continuously during the testing procedure: the instantaneous component was quantified before and after every load step, whereas the time-dependent portion of deflections was assessed three times per week.

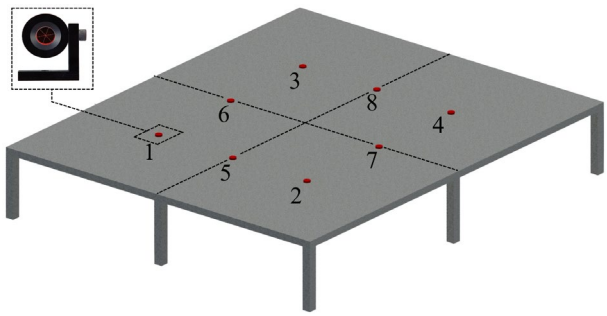

Fig. 3. Position of installed prisms

Table 5. Time-span between load phases

Phases	UDL (kN/m²)	Duration (days)
q_{SW} – I	4.8	14
I – II	6.0	14
II – III	7.5	14
III – IV	8.7	22
IV – ULS_I	9.8	140

Each loading step was complemented by a characterization of the bottom slab crack pattern evolution. Multiple high-resolution pictures were taken from underneath the structure one day before and two days after each load phase to evaluate the crack propagation. This procedure permitted to distinguish the cracks produced by load increments from those caused by other time-dependent imposed deformations (i.e., shrinkage, creep and temperature gradients).

Since the fourth loading phase was applied, the preparation for load increment up to ULS conditions was started. Firstly, acknowledging the significant load magnitude of the fourth phase (9.8 kN/m^2), the duration of the stabilization period was increased (Table 5): the phase was considered finished once the deflections measured by means of the prisms did not vary (with an accuracy of 1 mm) for two months. Afterwards, water tanks were placed onto first and second panels of the SFRC slab above the concrete cubes according to Figure 4a-b. The presented configuration provided the possibility of increasing the load up to 16 kN/m^2, i.e. a certain margin was left in comparison with the q_{Sd} of 14 kN/m^2.

Fig. 4. SFRC flat slab under ULS conditions: a-b) ULS_I: loading of the first half of the slab (3D model and real picture); c-d) ULS_II: loading of the rest of the slab (3D model and real picture)

Each panel was loaded increasing the water level by steps of 300 mm (2 kN/m^2 per step); the rate of filling was controlled by the inspection of the structural response of the SFRC prototype. The loading initiated by filling the tanks on the first and second panels, successively. The analysis of the SFRC slab behaviour under the first phase of ULS loading (ULS_I) was followed by water tank structure shifting from the already tested half of the element to the third and fourth panels (Figure 4c-d). The loading procedure (ULS_II) was repeated on the other part of the structure in a week.

After these two phases of loading, the analysis of both upper and lower surfaces (once the tanks and cubes were removed from the structure) was carried out. The bottom crack pattern surface was measured in accordance with the previously described method, whereas the top face of the SFRC prototype was studied by means of a photogrammetry technique for better precision.

The analysis of fibre distribution and fibre orientation was conducted (Figure 5) after the evaluation of structural capacity of SFRC two-way slab by means of a non-destructive magnetic method [59–61]. The method consists of measuring the alterations produced in a magnetic field due to the presence of an SFRC specimen in the coil by means of the device

SmartFibreC®. Such alterations are to be assessed in the direction of the three main axes of the studied specimen. The difference among these measurements indicate the alignment of the fibres in each direction, whereas the sum of those has a linear relation with the fibre content regardless of fibre distribution as was shown in numerous experimental investigations [43,62,63].

Cylindrical and cubic specimens are suitable for the described method; therefore, 32 cylindrical cores of 200 mm of height (slab depth) and 100 mm of diameter were drilled out the slab. The evaluation of cracking patterns during the entire loading process permitted the extraction of specimens close to both negative and positive yield lines which were developed in compliance with Johansen's theory [64,65]. The drilled cores were cut in half (Figure 5) for the sake of more detailed analysis: the evaluation of fibre content and fibre orientation was carried out for both lower and upper parts of the specimens to explore the variation of these parameters over the slab thickness.

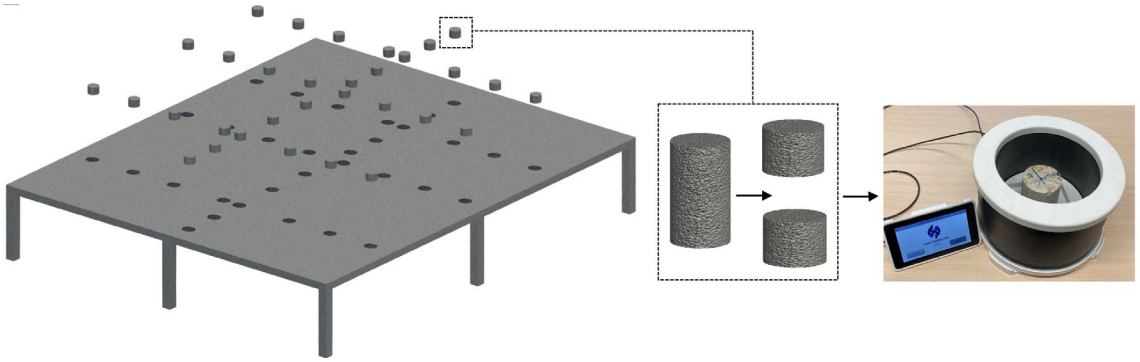

Fig. 5. Extraction of specimens with following inductive analysis

3. EXPERIMENTAL RESULTS AND DISCUSSION

3.1. CONSTRUCTION OF THE SFRC PROTOTYPE

The formwork installation was followed by the placement of APC reinforcement in the bottom of the slab with posterior casting of the SFRC prototype (Figure 6). The reinforcement consisted of 3 Ø12 conventional bars (Figure 6a) which were installed along the columns in both directions according to the North American Standards [66,67].

During the casting process, no fibre-balling was detected and the rheological properties of the material did not differ significantly with those achieved throughout the preliminary laboratory studies. In this regard, the slump flows measured in accordance with EN 12350-8 [68] ranged between 570 and 650 mm for all batches. Therefore, the vibration during the concrete placement was avoided because of self-compactability of the SFRC and the only external influence (negligible) on fibre orientation was due to the levelling of top surface of the slab.

After the construction and during the curing period, the effect of climatic conditions (with temperatures below 0ºC and snow in Barcelona two days after the concrete pouring) coupled with autogenous shrinkage of concrete led to a visible cracking of the upper surface of the prototype. However, the observed cracks presented a width controlled by the presence of fibres and had no influence on structural capacity of SFRC element. The inspection of the

slab was followed by formwork removal 14 days after casting in order to start analysing the behaviour of the structure under self-weight and various load magnitudes in terms of deformations, cracking, and bearing capacity.

Fig. 6. Construction of the SFRC prototype: a) Installed APC steel bars; b) SFRC pumping; c) executed SFRC flat slab in the fresh state; d) SFRC flat slab after formwork removal

3.2. STRUCTURAL ANALYSIS

Table 6 shows the instantaneous deflections of each panel that were produced under various load magnitudes. These deflections were calculated as $\Delta\delta_{i\text{-}j} = \Delta\delta_j - \Delta\delta_i$, where $\Delta\delta_i$ was the deflection measured after the stabilization of SFRC slab under load phase "*i*" and right before the load increment up to phase "*j*", $\Delta\delta_j$ being the deflection measured by means of installed prisms (Figure 3) eight hours after the application of load phase "*j*". It is remarkable that the deflections measured in each panel range between 9 and 10 mm and, thus, it can be stated that the slab presented a homogeneous response in each load step although a high variability of the post-cracking strength of the SFRC was observed (see Table 4).

The above described approach permitted to distinguish the instantaneous deflections from those produced due to sustained loads along with external factors, such as direct sunlight, heavy rains and high temperatures (up to 40°C). These external factors certainly increased the total deflections within seven months of testing and, therefore, only the instantaneous portion of deformations should be compared with the permitted values by structural codes [11,57,69].

These codes suggest using the quasi-permanent load combination $q_{k,\psi_2} = q_{sw} + q_G + \sum_{i\geq 1}(\psi_{2,i} \cdot q_{Q,i})$; $\psi_2 = 0.3$ for residential and office buildings in order to evaluate the structural behaviour in terms of deformations and crack control. In the present study, this load combination results in a UDL of 7.7 kN/m^2, i.e. a load slightly superior the one of phase II (7.5 kN/m^2, Figure 2b). The total load introduced in the phase II provoked a total

instantaneous deflection of 7 mm in two panels. Further investigation of long-term behaviour at this and previous loading stages (q_{SW}, I, II) was disregarded owing to the almost total absence of cracking (see Section 3.3) and, as a consequence, negligible difference in structural response comparing with the steel rebar reinforced concrete solution. In fact, previous researches state that the addition of less than 1% of steel fibres (≈ 80 kg/m^3) does not induce an effect on compressive creep and free shrinkage [70] or even these phenomena tends to decrease with the fibre content increase [71–75], i.e. the barely cracked SFRC pile-supported slab would exhibit at least similar performance in terms of long-term deformations.

Table 6. Instantaneous deflections under various load magnitudes

Installed Prisms	Instantaneous deflections (mm)					
	$\Delta\delta_{0\text{-}qSW}$	$\Delta\delta_{qSW\text{-}I}$	$\Delta\delta_{I\text{-}II}$	$\Delta\delta_{II\text{-}III}$	$\Delta\delta_{III\text{-}IV}$	$\Delta\delta_{total}$
1	4	2	1	1	2	10
2	4	1	1	1	2	9
3	4	1	1	1	2	9
4	4	1	2	1	2	10

Therefore, omitting a more comprehensive analysis and taking into account the registered values of the instantaneous deflections, the total deflections (including the time-dependent portion), could be computed as (1) two times the instantaneous deformation [34,76] or (2), conservatively, assuming the time-dependent deflection (λ_Δ) resulting from creep and shrinkage to be as per Expression 1, where ρ' is the compression reinforcement (equal to 0 in the presented case) and ξ is the factor for sustained loads ranged from 1.0 to 2.0 depending on the duration of the applied load [57,77]; although Tan et al. suggested to reduce this factor in order to better capture the effect of steel fibre reinforcement, multiplying the latter by the coefficient $\alpha = 1 - 0.069 \cdot V_f$ (for $V_f \leq 1.5\%$), where V_f is the steel fibre content in percentage [78,79]. As a result, the total deflection results to be (1) 14 mm or (2) 21 mm. These theoretical values can be expressed as the relation of diagonal span between columns across the panel (L = 7800 mm) to certain number, i.e. (1) $L/560$ and (2) $L/370$ – which is considerably smaller than the traditionally established limit of $L/250$. Hence, based on these results, it can be concluded that the slab designed had a suitable performance in terms of deflections and stiffness.

$$\lambda_\Delta = \frac{\xi}{1 + 50 \cdot \rho'} \quad (1)$$

Further increment of UDL up to 9.8 kN/m^2 (Figure 2c-d) did not reveal any significant difference in structural behaviour of the SFRC prototype in terms of instantaneous deformations. It is important to note that even at a load level corresponding to the characteristic load combination ($q_{k,\psi_0} = q_{sw} + q_G + q_Q$ = 9.8 kN/m^2), the structure achieved stabilization of deformations despite the external factors which were described previously – no measurable increment in deflections or cracking was observed within almost three months before starting ULS testing. Although the load of this magnitude is not representative to evaluate the structural behaviour in terms of produced deformations, the next observation can be pointed out: the tensile creep along with fibre-concrete bond showed not to have a

governing effect on the structural behaviour of the slab, even this being subjected to permanent 70% of the ultimate design load.

The next step was to assess ductility, flexural and punching strength of the slab under a ULS condition in accordance with described procedure in previous sections. Figure 7 depicts the time-load history; it is important to note that the produced deformations are represented from a relative zero, disregarding the deflections caused by previous load phases in order to highlight the total deformations at ULS loading. Firstly, panel 1 was loaded up to 14.0 kN/m^2; the structure showed almost no signs of pre-failure damage, along with evident deformation capacity, therefore, the loading process continued until reaching the load of 16.0 kN/m^2 – the maximum possible UDL for the established test configuration. The panel 2 was loaded up to the same load magnitude and even under these conditions no loss of integrity or deflections that would have led to predict an imminent failure were observed. Therefore, the slab was left fully loaded until the next day and the structure proved to have a significant strength and ductility capacity – in 25 h the maximum deflection increment of first and second panels was respectively equal to 7 and 10 mm (Figure 7a).

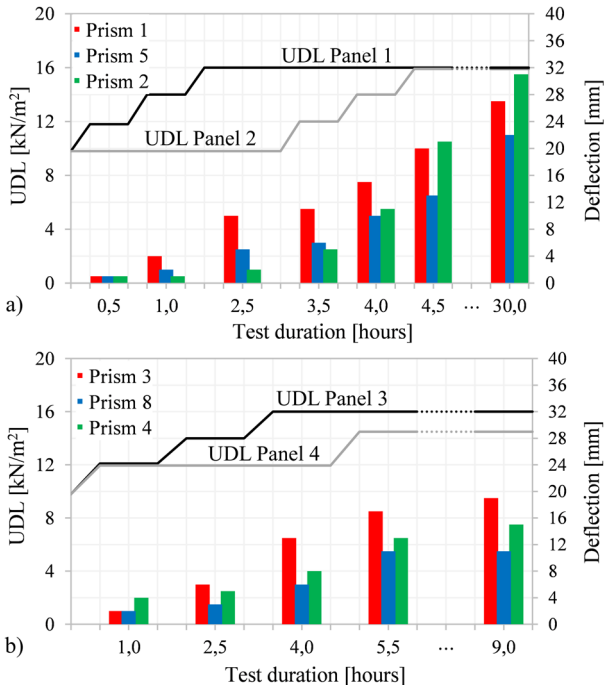

Fig. 7. Load protocol for UDL and deflections registered for: (a) panels 1 and 2 and (b) panels 3 and 4

At this point, the water tanks were emptied and shifted to other half of the SFRC slab. The ULS_II started with loading of the panel 3 up to 16.0 kN/m^2 based on the previously obtained results despite panels 1-2 were already damaged. Finally, panel 4 over-fulfilled the established q_{Sd} of 14 kN/m^2 – the load of 14.5 kN/m^2 was reached; further testing of this panel was stopped due to propagation of considerable shear cracks around the corner column, although the prototype maintained its structural integrity. Finally, as the maximum possible load of the chosen test configuration was not capable of producing the structure's failure, the bases of columns were shattered by the demolition excavator (Figure 8a) and, afterwards, the horizontal force was applied by means of the same machine (Figure 8b).

Based on the experimental results, it can be remarked that the bearing capacity was clearly superior to q_{Sd}. In this sense, taking into consideration the yield line theory [64,65] and the ACI report [80] related to the design of SFRC elevated slabs, the produced bending moment along the yield lines based on the achieved UDL can be calculated. For this purpose, the collapse mechanism compatible with the boundary conditions is to be postulated to assess the "ultimate load–produced moment" ratio by means of the method of virtual works. However, considering that the yield line pattern / collapse mechanism of the slab (Section 3.3) fully corresponded to the standard global failure mode for this type of structures subjected to UDL (Figure 9), the following expression can be used to evaluate the required ratio:

$$M_{Py}^{+/-} = \frac{UDL \cdot L_{rx}^2}{2 \cdot (\sqrt{(1 + \varnothing_h)} + 1)^2} \quad (2)$$

Fig. 8. a) Shattering the column base b) Demolition of the SFRC prototype

The ratio of negative to positive flexural capacities of the prototype cross sections ($\varnothing_h$) is to be considered as 1.0 for the sake of simplicity, although this assumption could be controversial in terms of real fibre distribution along the depth of a SFRC element. The distance of 5.65 m between the negative yield line and the slab edge (L_{ry}) for the established geometry of the slab was adopted; hence, the developed bending moment under the UDL of 16.0 kN/m^2 is equal to 43.8 kNm/m.

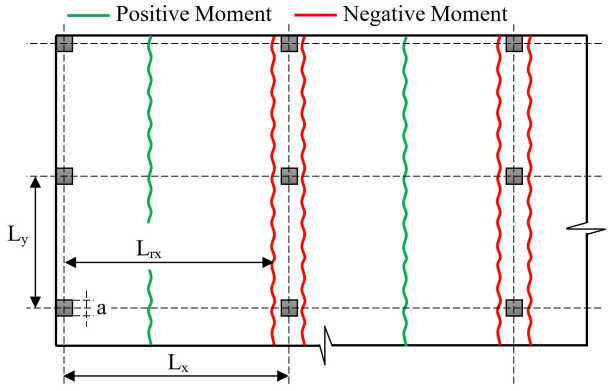

Fig. 9. Yield line pattern for global failure mode in Y direction

The conservative estimation of the design flexural capacity of SFRC flat slabs can be emphasized, based on presented above results. Currently, the majority of codes [11,57,81] propose the simplified rigid plastic model for the assessment of the ULS behaviour of FRC in tension which is identified by a unique value of $f_{Ftu,d}$. This value only depends on the characteristic residual tensile strength at the crack mouth opening displacement (CMOD) of

2.5 mm (f_{R3k}) in accordance with EN 14651 [51] and can be calculated as $f_{Ftu,d} = f_{R3k} / (3 \cdot \gamma_F)$, where $\gamma_F = 1.50$ is the partial safety factor in tension for FRC.

Taking into account the above described model, MC 2010 [11] suggests the expression $M_{Rd} = 0.5 \cdot f_{Ftu,d} \cdot h^2 \cdot b$ to evaluate the design resisting moment of FRC, where h and b are the depth and width of the cross section, respectively (Figure 10). This expression contains a certain simplification, permitting to concentrate the whole compressive force in the top fibre of the section, disregarding the traditionally adopted compressive block. However, this assumption insignificantly affects the magnitude of M_{Rd} since in a FRC section (as it happens in very low reinforced concrete section) the depth of the compression block at ULS is less than 10% of the cross-section thickness; i.e. the failure occurs due to excess of ultimate strain in tension ($\varepsilon_{Ftu} = 20‰$) whereas the maximum compressive strain is far from reaching its ultimate value ($\varepsilon_{cu} = 3.5‰$).

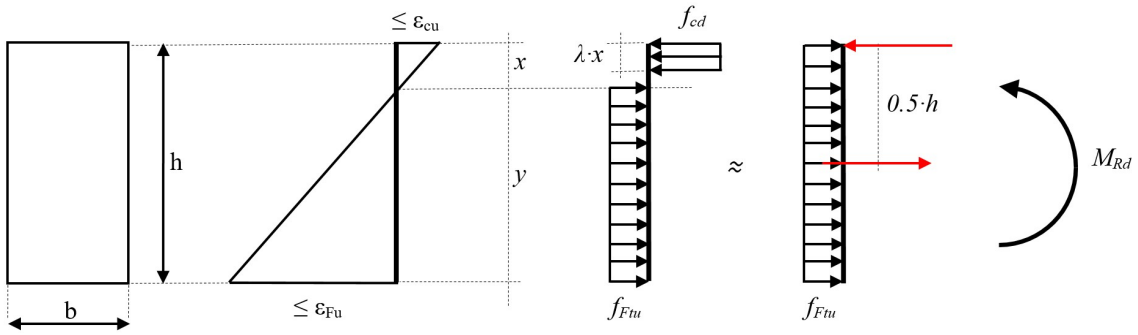

Fig. 10. Sectional model to assess flexural strength of FRC

The characteristic value of f_{R3k} of the SFRC used for constructing the slab was 4.57 MPa, therefore, based on the aforementioned expression, M_{Rd} is 20.3 kNm/m. The obtained value would provide the maximum UDL of 7.4 kN/m^2 using the yield-line theory (Eq. 1). Considering the significant redistribution capacity of elevated flat slabs [39,82], the upper limit of redistribution factor $K_{Rd} = 1.40$ could be assumed in accordance with MC 2010 [11]. As a result, an UDL of 10.3 kN/m^2 is derived from considering these assumptions and Equation 1, which is 36% below the experimental UDL (16 kN/m^2).

Alternatively, considering $f_{R3m} = 7.7$ MPa as representative for simulating the post-cracking response of the FRC at the yielding line and considering $\gamma_F = 1.00$, the ultimate resisting moment (M_R) of the yielding line results to be 51.3 kNm/m, which leads to a UDL of 18.8 kN/m^2. The test was stopped when a 16 kN/m^2 was reached; however, further load increment was possible since the prototype did not evidence signs of upcoming bending failure. Thus, the analytical estimation of the load bearing capacity of the prototype by using mean values of the mechanical parameters proved to provide a reasonable forecast.

The real-scale test emphasised that the flexural strength assessment was a governing criterion in design of SFRC pile-supported flat slabs, as in similar studies, punching failure is unlikely to occur [20,28,30]. This was verified using the mechanical model suggested by the *fib* Model Code 2010 [11] to evaluate the punching strength considering the first level approximation – the level which provides the safest and most conservative prediction of punching strength magnitude. This model, based on the Critical Shear Crack Theory [83,84], permits to estimate the punching shear behaviour of FRC by taking into account the

contribution of the matrix (concrete in tension and aggregate interlock, $V_{Rd,c}$) and fibres ($V_{Rd,f}$), i.e. $V_{Rd} = V_{Rd,c} + V_{Rd,f}$ [85].

The design shear resistance attributed to concrete ($V_{Rd,c}$) should be adopted as per Equations 3-6 [11], where b_0 is a basic control perimeter, d_v is the effective depth of the slab, k_{dg} is the parameter which takes into account the maximum size of the aggregate (d_g), and k_ψ is the parameter which depends on the rotation (ψ) of the slab. The contribution of fibres ($V_{Rd,f}$), in turn, may be computed in accordance with Equations 7-9, where f_{R1k} is the characteristic residual tensile strength at CMOD of 0.5 mm and w_u is the ultimate crack opening of 1.5 mm.

For comparing with experimental values, the safety coefficients in Equations 3 and 7 were removed and mean values of mechanical properties were used. Based on the obtained values of residual strength (Table 4) along with geometry of the structure (Figure 1), the punching strength of the FRC slab (V_R) was found to be 1155 kN whereas the reaction force in the centre column under the q_{Sd} = 14 kN/m^2 results to be 604 kN, i.e. even with a safe estimation of the rotation at failure ("Level I Approximation" pursuant to the fib Model Code 2010 [11]), the computed punching strength of the implemented material is significantly greater than design value of the applied shear force.

$$V_{Rd,c} = k_\psi \cdot \frac{\sqrt{f_{ck}}}{\gamma_c} \cdot b_0 \cdot d_v \tag{3}$$

$$k_\psi = \frac{1}{1.5 + 0.9 \cdot k_{dg} \cdot \psi \cdot d} \leq 0.6 \tag{4}$$

$$k_{dg} = \frac{32}{16 + d_g} \geq 0.75 \tag{5}$$

$$\psi = 1.5 \cdot \frac{r_s}{d} \cdot \frac{f_{yd}}{E_s} \tag{6}$$

$$V_{Rd,f} = \frac{f_{Ftuk}}{\gamma_F} \cdot b_0 \cdot d_v \tag{7}$$

$$f_{Ftuk} = f_{Ftsk} - \frac{w_u}{2.5} \cdot (f_{Ftsk} - 0.5 \cdot f_{R3k} + 0.2 \cdot f_{R1k}) \tag{8}$$

$$f_{Ftsk} = 0.45 \cdot f_{R1k} \tag{9}$$

3.3. CRACK PATTERNS

The first crack appeared at the vicinity of the central column after the formwork removal. This crack was in line with the nonlinear simulations [86] that were carried out before the construction of the SFRC prototype. The inspection of the lower surface presented no crack formation under the self-weight of the structure; no visible cracks appeared after the second load phase (Figure 2b), which roughly corresponded to the quasi-permanent combination ($q_{k,\psi 2}$ = 7.7 kN/m^2) of load as it was described in the Section 3.2. The absence of cracking at this loading stage can be beneficial in terms of serviceability performance and this is owed to the selected concrete mix (Table 3), i.e. the required self-compacting behaviour of the mix was achieved by augmenting the content of cement and fine aggregates along with the used

additives (to reduce the water-cement ratio) but, additionally, these modifications led to the increment of the material tensile strength.

Cracking occurred once the third phase was carried out (Figure 11a), i.e. once a UDL of 8.7 kN/m^2 was applied (Figure 2c). This magnitude of UDL was superior in 13% with respect to the quasi-permanent combination ($q_{k,\psi 2}$ = 7.7 kN/m^2). Nevertheless, the SFRC flat slab resulted to prove significant cracking control under this load level: after the application of the load and stabilization process, none of the observed cracks at this loading stage exceeded the width of 0.3 mm – the generally established limit of crack widths (w_{max}) for several exposure classes under quasi-permanent load combination of actions [11,57,87].

Further increment of the load during phase IV provoked the appearance of new cracks (Figure 11b) – the previously propagated cracks (Figure 11a) are depicted in grey in Figure 11b, whereas those that appeared posteriorly are highlighted in red for better visualisation; the similar approach is provided in Figure 11c. At this stage, several cracks did exceed the width of 0.3 mm, what was expected because of the considerable UDL of 9.8 kN/m^2. This magnitude of the sustained load along with the thermo-hygral phenomena (i.e., shrinkage and creep) led to bending moment and stresses redistribution – Figure 11c shows the evolution of the crack pattern under the same load of 9.8 kN/m^2 in comparison with the one presented by Figure 11b. This evolution of cracks can be also observed in Table 7 which presents the number of observed cracks and the total length of those for each load phase.

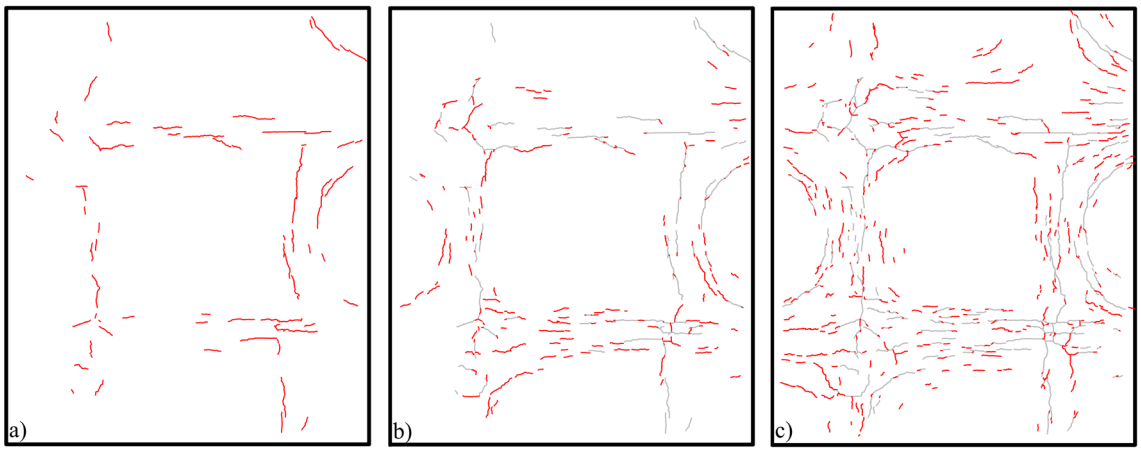

Fig. 11. Crack patterns of the lower surface: a) after the load phase III; b) after the load phase IV; c) before ultimate limit loading

Table 7. Number/total lengths of produced cracks under different load phases

Installed Prisms	Number / Total length (m) of cracks						w_{max} (mm)
	Panel 1	Panel 2	Panel 3	Panel 4	Average	CV (%)	
Phases I-II	0 / 0	0 / 0	0 / 0	0 / 0	0 / 0	0 / 0	0
Phase III	14 / 5.9	19 / 12.0	13 / 6.8	12 / 13.3	14.5 / 9.5	21.4 / 38.9	< 0.3
Phase IVa	54 / 21.3	45 / 24.9	34 / 15.3	30 / 18.0	40.8 / 19.9	26.7 / 20.9	> 0.3
Phase IVb	96 / 43.1	74 / 41.1	71 / 34.3	69 / 37.9	77.5 / 39.1	16.1 / 9.8	> 0.3
ULS I-II	123 / 82.8	101 / 78.5	135 / 70.7	126 / 77.4	121.3 / 77.4	11.9 / 6.5	> 0.3

Achieving ULS conditions by filling the water tanks triggered a significant increase of both the width and crack density (Figure 12a); the total crack lengths of all panels increased two times in comparison with the values of phase IVb. Figure 12b confirms the presence of cracks on the top surface of the prototype. The locations of these cracks are in total compliance with Johanssen´s theory [64,65] – along the column lines where the negative yield lines were formed. In addition, the effect of combined local flexural and shear stresses can be observed on Figure 12b by presence of cracking near corner and edge columns. Figure 13 presents the crack patterns of the lateral surfaces of SFRC slab to provide detailed information related to these cracks. The lateral surfaces are presented in accordance with corresponding panel for the sake of better scaling and, as a consequence, easier comprehension.

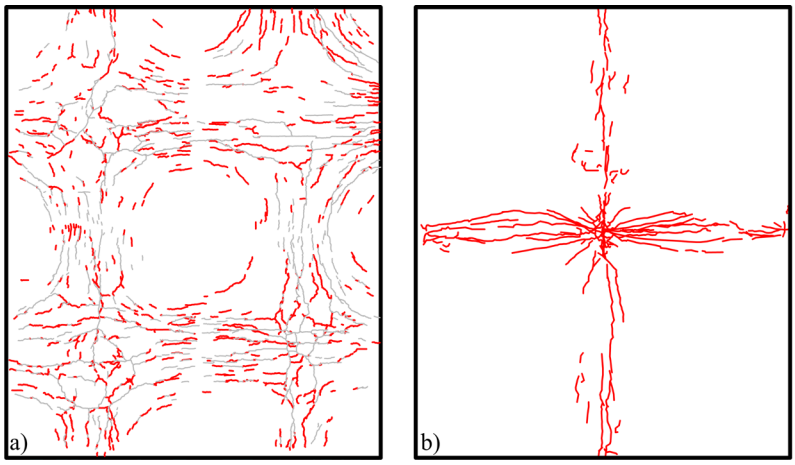

Fig. 12. Crack patterns after the test

3.4. FIBRE DISTRIBUTION

The structure maintained its integrity after the demolition process (Figure 8); hence, the cores were drilled in accordance with the pattern established in Figure 14b. The height of extracted specimens was measured to evaluate the real depth of the slab – an essential parameter for further studies in terms of both analytical and nonlinear analyses, including uncertainties and tolerances. The obtained mean thickness of 207.2 mm was slightly higher in comparison with the design value (200 mm). This depth may serve as a reference value in following design procedures due to similar measurements of slab thickness throughout the structure with a small coefficient of variation (3.1%).

Figure 15 depicts the distribution of fibres in the drilled cores. The average content of fibres along the principal yield lines resulted to be 67.4 kg/m^3 with a CV of 14.8%. This mean fibre content and CV allows confirming that the fibre distribution is homogenous from the design point of view, especially for this type of structures. However, the lack of homogeneity over the slab depth should be pointed out: the average fibre content of the upper halves of drilled specimens (Figure 5) was 44.9 kg/m^3, whereas the lower halves presented 89.5 kg/m^3 in average – almost more than twice the above value.

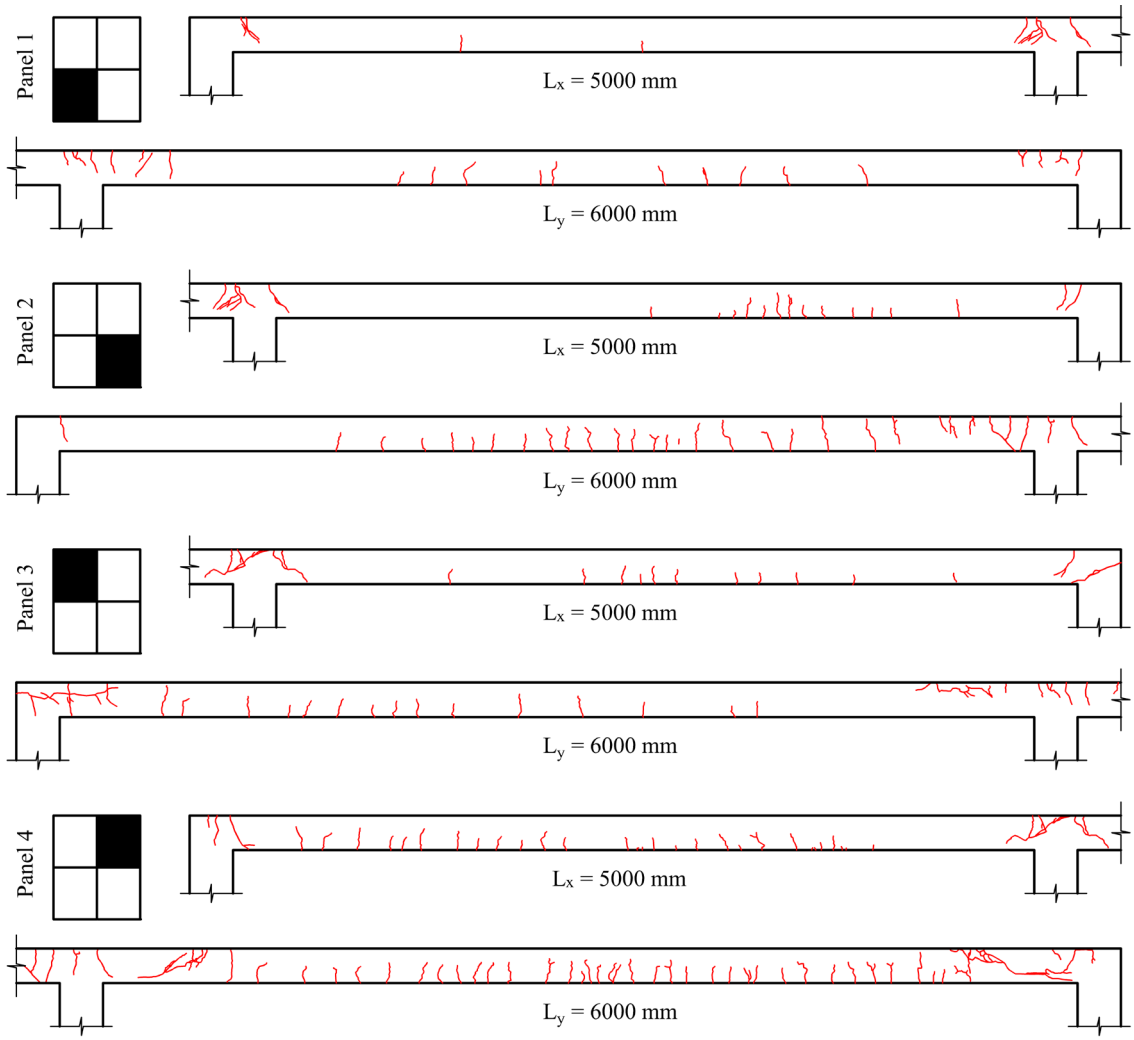

Fig. 13. Lateral crack patterns after the test

Fig. 14. a) Extraction of cores; b) Numeration of extracted specimens

The tendency for an increase of fibre percentage from the top to the bottom of SFRC slab due to presence of vibration was depicted in previous studies [47]. Nevertheless, in this experimental programme no vibration was applied and a considerable variation of fibre content over depth was also observed. This phenomenon may lead to development of insufficiently controlled cracks in the zones with significant negative moments; therefore, the

hybrid solutions with certain amount of conventional reinforcement and correspondently reduced fibre content could be an attractive alternative for this type of structures in terms of SLS requirements.

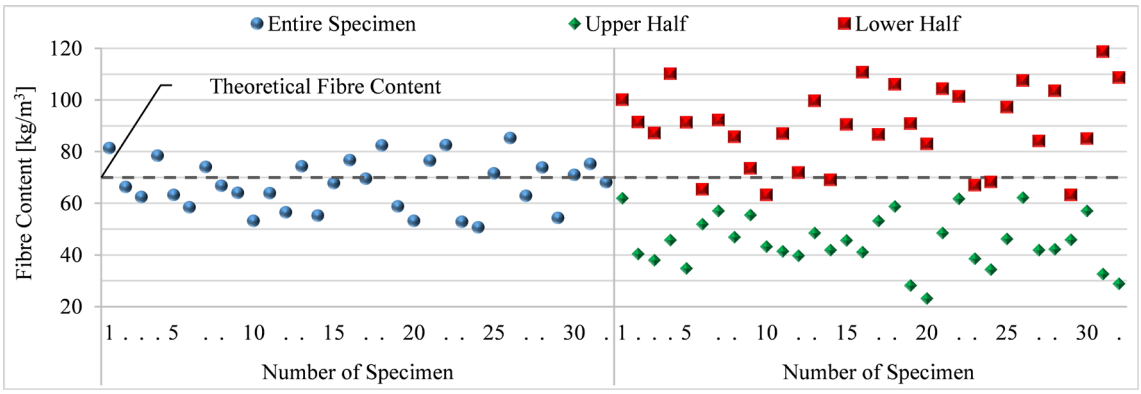

Fig. 15. Fibre distribution in extracted specimens

Evaluating the contribution of fibres along the direction of the main axes, a general trend for this type of structural elements was acknowledged: the preferential fibre orientation was perpendicular to the casting direction (Z axis) due to unrestricted radial flow of concrete along with the absence of vibration during the casting process. Moreover, the concrete flowability affected the tendency of fibres to orientate within the horizontal plane. Prove of that was the average fibre contribution of 76.8% detected by means of the inductive test orientated into this plane, i.e. more than three-quarters of total length of the fibres were oriented in the horizontal plane, once fibres are projected onto it [88,89]. Hence, this considerable percentage of fibres enhanced the post-cracking flexural strength of SFRC prototype – the essential factor for elevated flat slabs.

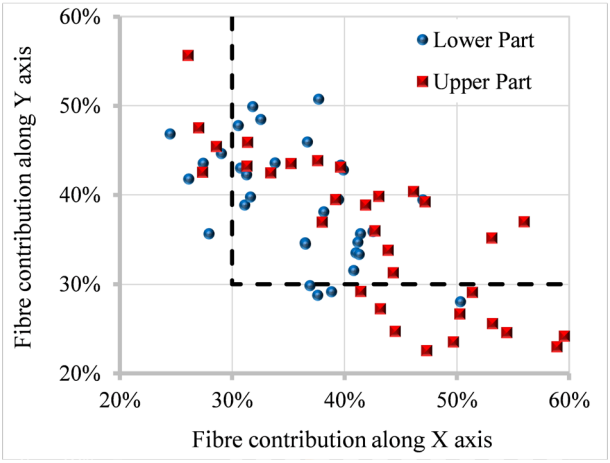

Fig. 16. Fibre contribution in the horizontal plane

Figure 16 shows that both main directions represent at least 30% of fibre contribution in most of the extracted cores (62.5%) and, therefore, no preferential orientation of the fibres along the slab axis can be confirmed. A preferential orientation could be more noticeable nearby the formworks due to geometrical boundary condition that those imposed to the concrete flow during the pouring.

4. CONCLUSIONS

In this paper, the structural response of a full-scale column-supported SFRC flat slab was described and analysed in terms of structural integrity, cracking and deflections. Five different uniformly-distributed load phases were applied in contrast to the previous experiences, in which point loading was mainly used. Thereafter, 32 cores were drilled from the tested SFRC flat slab in order to assess both fibre content and orientation. The following conclusions may be derived from the obtained results:

- A SFRC with f_{R1m} = 7.2 N/mm^2 (CoV = 35.3%) and f_{R3m} = 7.7 N/mm^2 (CoV = 24.7%) proved to be sufficient to guarantee a suitable structural response for loads representative of residential buildings in a column-supported slab with a span-to-depth ratio of 30.
- A load increase from the characteristic load combination (q_k = 9.8 kN/m^2) to 16.0 kN/m^2 (14% superior to the design load combination, q_{Sd} = 14.0 kN/m^2) led to an increment of deflections of 31 mm ($L/250$), without evidencing signs of failure; this proving both the moment redistribution capacity and the ductility of the system.
- The performance in terms of cracking and deflections resulted to be acceptable even when the structural system was subjected to loads (q = 8.7 KN/m^2) superior in 13% with respect to the quasi-permanent load combination ($q_{k,\psi 2}$ = 7.7 kN/m^2) for residential buildings.
- The results derived from performing the inductive test (non-destructive test oriented to characterize distribution and amount of steel fibres) on drilled cores confirmed that a 76.8% were favourably oriented along the slab in-plane axis.
- A higher amount of fibres (double in average) was detected in the middle-bottom part of the slab height respect to the upper half (even without vibration). Although this issue did not compromise the structural response of the slab, a steel mesh placed at the top side of the slab at the vicinities of the columns is recommendable.

The results obtained in this experimental program represent a new evidence of the structural suitability of the SFRC in elevated flat slabs, even with total substitution of the longitudinal steel bars. Nevertheless, as any incipient technology (or considerable change in the design and safety implications), certain aspects are still to be addressed for the acceptance of structural fibres as unique concrete reinforcement in elevated flat slabs, and its effective implementation. In this regard, casting and curing procedures for practical applications and systematic concrete production, monitoring time-dependent deformations for larger periods than that considered in this experimental program, the structural effect of induced holes into the slab, the hybrid use of fibres and steel mesh for optimization purposes are topics that should be further investigated.

ACKNOWLEDGMENTS

The authors wish to express their gratitude to the Spanish Ministry of Economy, Industry and Competitiveness (MINECO) for the financial support in the scope of the project eFIB (reference: RTC-2016-5263-5) which was carried out along with SACYR Ingeniería e

Infraestructura. The authors also appreciate valuable input of Nikola Tošić into the manuscript. The first author, personally, thanks the Department of Enterprise and Education of Catalan Government for providing support through the PhD Industrial Fellowship (2018 DI 77) in collaboration with Smart Engineering Ltd. (UPC's Spin-Off).

REFERENCES

[1] Zollo RF. Fiber-reinforced Concrete : an Overview after 30 Years of Development. Cem Concr Compos 1997;19:107–22.

[2] Liao L, de la Fuente A, Cavalaro S, Aguado A. Design of FRC tunnel segments considering the ductility requirements of the Model Code 2010. Tunn Undergr Sp Technol Inc Trenchless Technol Res 2015;47:200–10. https://doi.org/10.1016/j.tust.2015.01.006.

[3] Pujadas P, Blanco A, de la Fuente A, Aguado A. Cracking behavior of FRC slabs with traditional reinforcement. Mater Struct Constr 2012;45:707–25. https://doi.org/10.1617/s11527-011-9791-0.

[4] Groli G, Pérez A, Marchetto F, Aríñez F. Serviceability performance of FRC columns under imposed displacements : An experimental study. Eng Struct 2015;101:450–64. https://doi.org/10.1016/j.engstruct.2015.07.035.

[5] Vasanelli E, Micelli F, Aiello MA, Plizzari G. Crack width prediction of FRC beams in short and long term bending condition. Mater Struct Constr 2014;47:39–54. https://doi.org/10.1617/s11527-013-0043-3.

[6] Cachim PB, Figueiras JA, Pereira PAA. Fatigue behavior of fiber-reinforced concrete in compression 2002;24:211–7.

[7] Carlesso DM, de la Fuente A, Cavalaro SHP. Fatigue of cracked high performance fiber reinforced concrete subjected to bending. Constr Build Mater 2019;220:444–55. https://doi.org/10.1016/j.conbuildmat.2019.06.038.

[8] Nia AA, Hedayatian M, Nili M, Sabet VA. International Journal of Impact Engineering An experimental and numerical study on how steel and polypropylene fibers affect the impact resistance in fiber-reinforced concrete. Int J Impact Eng 2012;46:62–73. https://doi.org/10.1016/j.ijimpeng.2012.01.009.

[9] Teng T, Chu Y-A, Chang F-A, Shen B-C, Cheng D-S. Development and validation of numerical model of steel fiber reinforced concrete for high-velocity impact. Comput Mater Sci 2008;42:90–9. https://doi.org/10.1016/j.commatsci.2007.06.013.

[10] Serrano R, Cobo A, Prieto MI, De M, González N. Analysis of fire resistance of concrete with polypropylene or steel fibers 2016;122:302–9. https://doi.org/10.1016/j.conbuildmat.2016.06.055.

[11] fib. fib Model Code for Concrete Structures 2010. 2010.

[12] Belletti B, Cerioni R, Meda A, Plizzari G. Design Aspects on Steel Fiber-Reinforced Concrete Pavements 2009;20:599–607. https://doi.org/10.1061/(ASCE)0899-1561(2008)20.

[13] Alani AM, Beckett D. Mechanical properties of a large scale synthetic fibre reinforced concrete ground slab. Constr Build Mater 2013;41:335–44. https://doi.org/10.1016/j.conbuildmat.2012.11.043.

[14] Meda A, Plizzari GA, Riva P. Fracture behavior of SFRC slabs on grade. Mater Struct Constr 2004;37:405–11. https://doi.org/10.1617/14093.

[15] Jamshidi M, Hoseini A, Vahdani S, Santos C De, De A. Seismic fragility curves for vulnerability assessment of steel fiber reinforced concrete segmental tunnel linings. Tunn Undergr Sp Technol 2018;78:259–74. https://doi.org/10.1016/j.tust.2018.04.032.

[16] de la Fuente A, Pujadas P, Blanco A, Aguado A. Experiences in Barcelona with the use of fibres in segmental linings. Tunn Undergr Sp Technol 2012;27:60–71. https://doi.org/10.1016/j.tust.2011.07.001.

[17] Chiaia B, Fantilli AP, Vallini P. Combining fiber-reinforced concrete with traditional reinforcement in tunnel linings. Eng Struct 2009;31:1600–6. https://doi.org/10.1016/j.engstruct.2009.02.037.

[18] de la Fuente A, Aguado A, Molins C, Armengou J. Innovations on components and testing for precast panels to be used in reinforced earth retaining walls. Constr Build Mater 2011;25:2198–205. https://doi.org/10.1016/j.conbuildmat.2010.11.003.

[19] de la Fuente A, Escariz RC, de Figueiredo AD, Aguado A. Design of macro-synthetic fibre reinforced concrete pipes. Constr Build Mater 2013;43:523–32. https://doi.org/10.1016/j.conbuildmat.2013.02.036.

[20] Gossla U. Development of SFRC Free Suspended Elevated Flat Slabs 2005.

[21] Destrée X, Mandl J. Steel fibre only reinforced concrete in free suspended elevated slabs: Case studies, design assisted by testing route, comparison to the latest SFRC standard documents. Tailor Made Concr Struct 2008:437–43.

[22] di Prisco M, Colombo M, Pourzarabi A. Biaxial bending of SFRC slabs: Is conventional reinforcement necessary? Mater Struct Constr 2019;52:1–15. https://doi.org/10.1617/s11527-018-1302-0.

[23] Fall D, Shu J, Rempling R, Lundgren K. Two-way slabs : Experimental investigation of load redistributions in steel fibre reinforced concrete 2014. https://doi.org/10.1016/j.engstruct.2014.08.033.

[24] Pujadas P, Blanco A, Cavalaro S, Aguado A. Plastic fibres as the only reinforcement for flat suspended slabs: Experimental investigation and numerical simulation. Constr Build Mater 2014;57:92–104. https://doi.org/10.1016/j.conbuildmat.2014.01.082.

[25] Facconi L, Minelli F, Plizzari G. Steel fiber reinforced self-compacting concrete thin slabs – Experimental study and verification against Model Code 2010 provisions. Eng Struct 2016;122:226–37. https://doi.org/10.1016/j.engstruct.2016.04.030.

[26] Hedebratt J, Silfwerbrand J. Full-scale test of a pile supported steel fibre concrete slab. Mater Struct Constr 2014;47:647–66. https://doi.org/10.1617/s11527-013-0086-5.

[27] Tan KH, Venkateshwaran A. Punching shear in steel fiber-reinforced concrete slabs with or without traditional reinforcement. ACI Struct J 2019;116:107–18. https://doi.org/10.14359/51713291.

[28] Michels J, Waldmann D, Maas S, Zürbes A. Steel fibers as only reinforcement for flat slab construction - Experimental investigation and design. Constr Build Mater 2012;26:145–55. https://doi.org/10.1016/j.conbuildmat.2011.06.004.

[29] Gouveia ND, Lapi M, Orlando M, Faria DM V. Experimental and theoretical evaluation of punching strength of steel fiber reinforced concrete slabs 2017:13.

[30] Parmentier B, Itterbeeck P Van. The flexural behaviour of SFRC flat slabs : the Limelette full- scale experiments for supporting design model codes 2015.

[31] Døssland ÅL. Fibre Reinforcement in Load Carrying Concrete Structures. 2008.

[32] Mandl J. Flat Slabs Made of Steel Fiber Reinforced Concrete (SFRC) 2008.

[33] Karv C. Shear and punching resistance of steel fibre reinforced concrete slabs. Aalto University, 2017.

[34] Maturana Orellana A. Estudio teórico-experimental de la aplicabilidad del hormigón reforzado con fibras de acero a losas de forjado multidireccionales. 2013. https://doi.org/10.1174/021435502753511268.

[35] Mitchell D, Cook WD. Preventing Progressive Collapse of Slab Structures. J Struct Eng 1984;110:1513–32. https://doi.org/10.1061/(ASCE)0733-9445(1984)110:7(1513).

[36] Blanco A, Pujadas P, Fuente A De, Cavalaro SHP, Aguado A. Assessment of the fibre orientation factor in SFRC slabs. Compos PART B 2015;68:343–54. https://doi.org/10.1016/j.compositesb.2014.09.001.

[37] Mudadu A, Tiberti G, Germano F, Plizzari GA, Morbi A. The effect of fiber orientation on the post-cracking behavior of steel fiber reinforced concrete under bending and uniaxial tensile tests. Cem Concr Compos 2018;93:274–88. https://doi.org/10.1016/j.cemconcomp.2018.07.012.

[38] di Prisco M, Martinelli P, Dozio D. The structural redistribution coefficient KRd: A numerical approach to its evaluation. 2016. https://doi.org/10.1002/suco.201500118.

[39] Colombo M, Martinelli P, di Prisco M. On the evaluation of the structural redistribution factor in FRC design: a yield line approach. Mater Struct 2017;50:1–18. https://doi.org/10.1617/s11527-016-0969-3.

[40] Tan H, Saha MK. Ten-Year Study on Steel Fiber-Reinforced Concrete Beams Under Sustained Loads 2006.

[41] Monetti DH, Llano-torre A, Torrijos MC, Giaccio G, Zerbino R, Martí-vargas JR, et al. Long-term behavior of cracked fiber reinforced concrete under service conditions. Constr Build Mater 2019;196:649–58. https://doi.org/10.1016/j.conbuildmat.2018.10.230.

[42] de la Fuente A, Casanovas-Rubio MDM, Pons O, Armengou J. Sustainability of Column-Supported RC Slabs: Fiber Reinforcement as an Alternative. J Constr Eng Manag 2019;145:1–12. https://doi.org/10.1061/(ASCE)CO.1943-7862.0001667.

[43] Galeote E, Blanco A, Cavalaro SHP, de la Fuente A. Correlation between the Barcelona test and the bending test in fibre reinforced concrete. Constr Build Mater 2017;152:529–38. https://doi.org/10.1016/j.conbuildmat.2017.07.028.

[44] Pujadas P, Blanco A, Cavalaro SHP, de la Fuente A, Aguado A. Multidirectional double punch test to assess the post-cracking behaviour and fibre orientation of FRC. Constr Build Mater 2014;58:214–24. https://doi.org/10.1016/j.conbuildmat.2014.02.023.

[45] Blanco A, Pujadas P, de la Fuente A, Cavalaro SHP, Aguado A. Influence of the type of fiber on the structural response and design of FRC slabs. J Struct Eng (United States) 2016;142:1–11. https://doi.org/10.1061/(ASCE)ST.1943-541X.0001515.

[46] Fall D, Shu J, Rempling R, Lundgren K, Zandi K. Two-way slabs: Experimental investigation of load redistributions in steel fibre reinforced concrete. 2014. https://doi.org/10.1016/j.engstruct.2014.08.033.

[47] Barros J, Salehian H, Pires M, Gonçalves D. Design and testing elevated steel fibre reinforced self-compacting concrete slabs. Fibre Reinf Concr 2012:1–12.

[48] Ošlejs J. New Frontiers for Steel Concrete. Concr Int 2008;3:45–50.

[49] CEN. EN 12390-13:2013. Testing hardened concrete. Determination of secant modulus of elasticity in compression. 2013.

[50] CEN. EN 12390-3:2019. Testing hardened concrete. Compressive strength of test specimens. 2019.

[51] CEN. EN 14651:2007. Test method for metallic fibre concrete. Measuring the flexural tensile strength (limit of proportionality (LOP), residual). 2007.

[52] Molins C, Aguado A, Saludes S. Double punch test to control the energy dissipation in tension of FRC (Barcelona test). Mater Struct 2009;42:415–25. https://doi.org/10.1617/s11527-008-9391-9.

[53] Parmentier B, De Grove E, Vandewalle L, Van Rickstal F. Dispersion of the mechanical properties of FRC investigated by different bending tests. Proc Int FIB Symp 2008 - Tailor Made Concr Struct New Solut Our Soc 2008:123. https://doi.org/10.1201/9781439828410.ch84.

[54] Cavalaro SHP, Aguado A. Intrinsic scatter of FRC: an alternative philosophy to estimate characteristic values. Mater Struct Constr 2015;48:3537–55. https://doi.org/10.1617/s11527-014-0420-6.

[55] Grunewald S. Performance-based design of self-compacting fibre reinforced concrete. 2004.

[56] THE CONCRETE SOCIETY. Guidance of the Design of Steel-Fibre-Reinforced Concrete. 2007.

[57] Ministerio de Fomento. Instrucción de Hormigón Estructural (EHE-08). 2008. https://doi.org/10.1017/CBO9781107415324.004.

[58] Gobierno de España. Código Técnico de la Edificación (CTE) Documento básico: Seguridad estructural. Apartado de “Acciones en la Edificación” 2009.

[59] Torrents JM, Blanco A, Pujadas P, Aguado A, Juan-García P, Sánchez-Moragues MÁ. Inductive method for assessing the amount and orientation of steel fibers in concrete. Mater Struct Constr 2012;45:1577–92. https://doi.org/10.1617/s11527-012-9858-6.

[60] Cavalaro SHP, López-Carreño R, Torrents JM, Aguado A, Juan-García P. Assessment of fibre content and 3D profile in cylindrical SFRC specimens. Mater Struct Constr 2016;49:577–95. https://doi.org/10.1617/s11527-014-0521-2.

[61] Cavalaro SHP, López R, Torrents JM, Aguado A. Improved assessment of fibre content and orientation with inductive method in SFRC. Mater Struct Constr 2015;48:1859–73. https://doi.org/10.1617/s11527-014-0279-6.

[62] Orbe A, Cuadrado J, Losada R, Rojí E. Framework for the design and analysis of steel fiber reinforced self-compacting concrete structures. Constr Build Mater 2012;35:676–86. https://doi.org/10.1016/j.conbuildmat.2012.04.135.

[63] Orbe A, Rojí E, Losada R, Cuadrado J. Calibration patterns for predicting residual strengths of steel fibre reinforced concrete (SFRC). Compos Part B Eng 2014;58:408–17. https://doi.org/10.1016/j.compositesb.2013.10.086.

[64] Johansen KW. Yield-line theory. Cement and Concrete Association; 1962.

[65] Johansen KW. Yield-line formulae for slabs. Cement and Concrete Association; 1972.

[66] Canadian Standards Association. Design of Concrete Structures CSA A23.3-04. 2004.

[67] ACI Committee 544. Report on Design and Construction of Steel Fiber-Reinforced Concrete Elevated Slabs. 2004.

[68] CEN. EN 12350-8:2019. Testing fresh concrete. Self-compacting concrete. Slump-flow test. 2019.

[69] CEN. Eurocode - basis of structural design. vol. 1. Brussels: 2002.

[70] ACI Committee 544. Report on Fiber Reinforced Concrete. Farmington Hills, MI, USA: 2002. https://doi.org/10.14359/2355.

[71] Tošić N, Aidarov S, de la Fuente A. Systematic Review on the Creep of Fiber-Reinforced Concrete. Materials (Basel) 2020;13:5098. https://doi.org/10.3390/ma13225098.

[72] Bazant ZP, Baweja S. Creep and shrinkage prediction model for analysis and design of concrete structures - model B3. Mater Constr 1995;28:357–65. https://doi.org/10.1007/bf02486204.

[73] Nakov D, Markovski G, Arangjelovski T, Mark P. Experimental and analytical analysis of creep of steel fibre reinforced concrete. Period Polytech Civ Eng 2018. https://doi.org/10.3311/PPci.11184.

[74] Chern JC, Young CH. Compressive creep and shrinkage of steel fibre reinforced concrete. Int J Cem Compos Light Concr 1989;11:205–14. https://doi.org/10.1016/0262-5075(89)90100-0.

[75] Afroughsabet V, Teng S. Experiments on drying shrinkage and creep of high performance hybrid-fiber-reinforced concrete. Cem Concr Compos 2020;106:103481. https://doi.org/10.1016/j.cemconcomp.2019.103481.

[76] Calavera Ruiz J, Garcia Dutari L. Cálculo de flechas en estructuras de hormigon armado : forjados, losas, vigas de canto, vigas planas. 1992.

[77] ACI. 318-14 - Building Code Requirements for Structural Concrete and Commentary. 2014.

[78] Tan KH, Paramasivam P, Tan KC. Instantaneous and long-term deflections of steel fiber reinforced concrete beams. ACI Struct J 1994;91:384–93.

[79] Tan KH, Saha MK. Ten-year study on steel fiber-reinforced concrete beams under sustained loads. ACI Struct J 2005;102:472–80. https://doi.org/10.14359/14419.

[80] Committee A. ACI 544.6R-15: Report on Design and Construction of Steel Fiber-Reinforced Concrete Elevated Slabs 2015.

[81] Italian National Research Council. CNR. CNR-DT 204 /2006 Guide for the Design and Construction of Fiber-Reinforced Concrete Structures. Rome: 2006.

[82] di Prisco M, Martinelli P, Parmentier B. On the reliability of the design approach for FRC structures according to fib Model Code 2010: the case of elevated slabs. Struct Concr 2016;17:588–602. https://doi.org/10.1002/suco.201500151.

[83] Muttoni A. Punching Shear Strength of Reinforced Concrete Slabs without Transverse Reinforcement. ACI Struct J 2008;105:440–50.

[84] Muttoni A, Fernández RM, Bentz EC, Foster SJ, Sigrist V. Background to the Model Code 2010 Shear Provisions - Part II Punching Shear. Struct Concr 2013. https://doi.org/10.1002/suco.201200064.Submitted.

[85] Muttoni A, Ruiz M. The critical shear crack theory as mechanical model for punching shear design and its application to code provisions. Fédération Int. du Béton, Bull. 57, 2010.

[86] Nogales A, de la Fuente A. Numerical-aided flexural-based design of fibre reinforced concrete column-supported flat slabs. Eng Struct 2021;232:1–24. https://doi.org/10.1016/j.engstruct.2020.111745.

[87] EN 1992-1-1. Eurocode 2: Design of concrete structures: General rules and rules for buildings. Brussels: CEN; 2004. https://doi.org/[Authority: The European Union Per Regulation 305/2011, Directive 98/34/EC, Directive 2004/18/EC].

[88] Laranjeira F, Aguado A, Molins C, Grünewald S, Walraven J, Cavalaro S. Framework to predict the orientation of fibers in FRC: A novel philosophy. Cem Concr Res 2012;42:752–68. https://doi.org/10.1016/j.cemconres.2012.02.013.

[89] Laranjeira F, Grünewald S, Walraven J, Blom C, Molins C, Aguado A. Characterization of the orientation profile of steel fiber reinforced concrete. Mater Struct Constr 2011;44:1093–111. https://doi.org/10.1617/s11527-010-9686-5.

2.2. JOURNAL PAPER II. A LIMIT STATE DESIGN APPROACH FOR HYBRID REINFORCED CONCRETE COLUMN-SUPPORTED FLAT SLABS

Published in Structural Concrete (2022).

Stanislav Aidarov [a, b, *], Nikola Tošić [b], Albert de la Fuente [b]

[a] Smart Engineering Ltd., UPC Spin-Off, Jordi Girona 1-3, 08034 Barcelona, Spain

[b] Civil and Environmental Engineering Department, Universitat Politècnica de Catalunya (UPC), Jordi Girona 1-3, 08034 Barcelona, Spain

* Corresponding author. Tel.: +34 633 634 207; Full Postal address: 08034, Barcelona, Jordi Girona 1; Email address: stanislav.aidarov@upc.edu ; stanislav.aydarov@smartengineeringbcn.com

Abstract

Hybrid reinforced technology (combination of steel reinforcing bars and fibres) can be considered as a competitive alternative to the already existing solutions for the construction of column-supported flat slabs. Constructed hybrid-reinforced buildings prove that hybrid solutions have sufficient bearing capacity to maintain structural integrity despite being exposed to high stress levels, thereby providing a beneficial solution in terms of toughness, ductility, and sustainability performance. However, the lack of design-oriented recommendations based on the accepted limit state format for dealing with both serviceability and ultimate limit states slows down the wider implementation of this technology. Considering the above-mentioned, this paper presents a simplified design-oriented method that covers the evaluation of the structural response of hybrid reinforced concrete column-supported flat slabs in terms of flexural strength, cracking, and instantaneous deformations. Two hybrid reinforced alternatives for a given flat slab are studied by means of the proposed approach. Furthermore, a nonlinear finite element analysis is carried out in order to evaluate the effectiveness of the developed simplified method. Based on the achieved results, its suitable accuracy and precision can be pointed out. This outcome may motivate current practitioners to consider hybrid reinforced concrete solutions as a possible alternative during the design of residential and office buildings.

Keywords: elevated slab, two-way slab, fibre reinforced concrete, FRC, ultimate behaviour, flexure, serviceability behaviour, cracking control, deflection

Nomenclature

List of symbols

$A_{c,ef}$	effective area of concrete in tension
A_s	area of reinforcement
b	section width
c	concrete cover
$CMOD$	crack mouth opening displacement
d	section depth
E_c	modulus of elasticity of concrete
E	action–effect
E_s	modulus of elasticity of reinforcing steel
f_c	cylinder compressive strength of concrete
f_{ct}	axial tensile strength of concrete
f_{Fts}	serviceability residual strength for FRC
f_{Ftu}	ultimate residual strength for FRC
$f_{R,i}$	residual flexural tensile strength of FRC corresponding to CMODi
f_y	yield strength of reinforcing steel in tension
f_t	tensile strength of reinforcing steel
h	overall depth of member
L	length
L_n	length of clear span
$L_{rx/y}$	distance between two adjacent negative yield lines in a panel parallel to the x/y direction
$L_{x/y}$	length of span in x/y direction
l_{cs}	characteristic length
$l_{s,max}$	length over which the slip between steel and concrete occurs
m_E	value of applied moment
m_{cr}	cracking moment
m_R	value of resistant moment
q	uniformly distributed load
q_G	permanent load
q_Q	variable load
q_S	Combination of acting loads
q_{SW}	self–weight load
R	value of resistance
V_R	coefficient of variation of resistance
w	crack width
w_u	ultimate crack opening
x	depth of compression zone
α_e	modular ratio (Es/Ec)
α_R	sensitivity factor
β	reliability index
γ_c	partial safety factor for concrete properties
γ_F	partial safety factor for FRC
γ_G	partial safety factor for permanent actions
γ_Q	partial safety factor for variable actions
γ_R	global resistance safety factor
γ_{Rd}	model uncertainty factor
γ_s	partial safety factor for reinforcing steel properties
δ	displacement
δ_{tot}	displacement at the centre of the panel
ε_{cm}	average concrete strain
ε_{cs}	shrinkage strain at concrete
ε_{sm}	mean steel strain
η_r	coefficient to consider the shrinkage contribution
ρ_s	ratio of tensile reinforcement
$\rho_{s,ef}$	effective reinforcement ratio
σ_s	steel stress
σ_{sr}	steel stress in the crack under cracking load
τ_{bm}	mean bond strength between steel and concrete
χ	curvature
$Ø_s$	nominal diameter of bar

General subscripts

m	mean value of the variable
k	characteristic value of the variable
d	design value of the variable
FRC	fibre reinforced concrete
HRC	hybrid reinforced concrete
YL	yield line

1. INTRODUCTION

During the last two decades, considerable scientific efforts have been made to identify and quantify the full potential of fibre reinforced concrete (FRC) and hybrid reinforced concrete (combination of steel reinforcing bars and fibres, HRC) slabs in statically redundant structures. Numerous laboratory tests were carried out, varying the fibre/rebar content, slab geometry, boundary and load conditions [1–7]. The obtained results highlighted the enhanced structural response in terms of ductility [4–6], cracking control [1–3], and load redistribution [1,3,4].

Real-scale testing of elevated flat slabs confirmed the possibility of even total substitution of traditional reinforcement through using fibres in the concrete mix, this providing sufficient and even enhanced flexural and punching strength [8–13]. The promising capability of FRC technology was also confirmed in real projects: significant benefits in terms of construction time and costs were highlighted during the construction of the Ditton Nams shopping mall (Latvia), the Triangle office building (Estonia), the Rocca Al-Mare office tower (Estonia), and the LKS office building (Spain) [14–16].

Despite the successful experiences of FRC slab construction, a number of shortcomings were revealed under special structural and/or construction conditions. The total substitution of traditional reinforcement by FRC can be inefficient if the bending and shear stresses magnitudes differ significantly throughout the slab. This variation requires different residual tensile strength (f_R) of the FRC and, as a consequence, different amount of fibres in different areas of the slab. In this sense, FRC has to be designed for guaranteeing the most demanding f_R requirement; this strategy will provide over-reinforced areas and uncompetitive solutions.

Another drawback of FRC is the slight material heterogeneity within the depth of the element [8]; the tendency of an increase in the fibre content towards the lower layers of the slab [9,17] can lead to insufficiently controlled cracks in the zones with high negative bending moments (in the vicinity of the columns). Considering these aspects, hybrid solutions might be even more attractive from technical and economic points of view since moderate values of f_R can be imposed while most demanding bending and punching forces can be resisted by the combination of fibres and steel bars – enhancing also the workability of the concrete due to reduction of the fibre content in the mix.

Although the use of FRC and HRC in elevated flat slabs evidenced encouraging results, these alternatives are barely considered by engineers within the design process of residential and office buildings despite the acceptance of using FRC in structural elements by national and international codes along with specific guidelines [18–23]. One of the main reasons, apart from general concerns regarding the material capacity, is the lack of a detailed description on how to cover all the limit states for FRC/HRC flat slab design. Even scientific literature do not cover all required design aspects for this type of structural elements. In this regard, Table 1 shows that the majority of works are focused on the behaviour of FRC/HRC elevated slabs at the ultimate limit state (ULS), providing the analytical and numerical approaches to assess the flexural and/or punching strength of the studied structural element.

Table 1. Mechanical properties and prices of the selected fibres

Reference	Analytical or Numerical Approaches				NLFEA
	Flexural Strength	Punching Strength	Cracking	Instant Deformations	
[2,5,10,24,25]	•				
[26–33]		•			
[34,35]	•	•			
[36–40]					•
[9,17,41]	•				•
Present Study	•		•	•	•

In this context, the frequent questions of design engineers, which are hindering the widespread use of FRC/HRC in column-supported flat slabs, can be summarized as the following:

- How should the cracking behaviour of FRC/HRC elevated flat slab be estimated at the serviceability limit state (SLS)?
- What is the most appropriate way to assess the deformations of FRC/HRC flat slabs?
- Does the FRC/HRC approach provide adequate results with respect to long-term behaviour?
- What is a suitable method to carry out a comparison between traditional and FRC/HRC solutions?

Most of the questions can actually be answered by means of nonlinear finite element analysis (NLFEA). The existing scientific literature (Table 1) evidences the capacity to properly predict the structural response of two-way slabs using nonlinear finite element models [39,41,42]. Moreover, a NLFE parametric studies were carried out in order to analyse the structural response of the different FRC/HRC alternatives [40]. However, the application of these models is infrequent among structural designers since: (1) appropriate software to perform these analyses are not meant for day-to-day design procedures and (2) the lack of thoroughly described approaches for nonlinear analysis in current codes and guidelines for this specific purpose.

Taking this into account, this paper presents a simplified method for the design of FRC/HRC elevated slabs which responds to the majority of above-presented questions. This method permits the evaluation of the flexural capacity of the structural elements at ULS and the analysis of their response in terms of cracking and instantaneous deformations at SLS. Moreover, the developed approach allows checking the required ductility of FRC/HRC column-supported flats slabs. Based on the proposed design procedure, HRC solutions were analysed for the given structure and the obtained results were compared with those obtained by NLFEA.

2. PROPOSED DESIGN APPROACH

2.1. FLEXURAL ULS BEARING CAPACITY

2.1.1. Basis of the Yield Line Method

The Yield Line Method (YLM) is being frequently suggested to evaluate the flexural load-carrying capacity of FRC flat slabs owing to its representativeness and the ease of application (very few restrictions) [23]. These restrictions, that exist for elasticity-based methods, are related to the boundary conditions, opening dimensions and load types along with the possibility of taking into account the ductility/rotation capacity of FRC – the essential parameter to use the plastic analysis methods. YLM is also a suitable analytical approach to design RC slabs, as long as the required ductility can be proven by limiting the area of tensile reinforcement so that the following limits are fulfilled: $x/d \leq 0.25$ and $x/d \leq 0.15$ for concrete strength classes ≤ C50/60 and ≥ C55/67, respectively [19,43]. Taking into account that flat slabs typically have low ratios of tensile reinforcement ($\rho_s = A_s/(b \cdot d)$), the abovementioned restrictions are to be generally fulfilled.

YLM is based on Johansen's theory [44–46] and claims that the ultimate load of a slab can be obtained by postulating a collapse mechanism (generated by yield lines) that is compatible with boundary conditions. The selection of the collapse mechanism is of paramount importance considering that its wrong estimation will lead to the theoretically unsafe results since the presented method gives upper bound solutions. However, yield line patterns have been developed and thoroughly studied for common geometries (Figure 1). Additionally, the standard formulae are already developed for these geometries in order to directly calculate the relation between applied load and produced moments per unit length ($m^{+}_{Ed,YL}, m^{-}_{Ed,YL}$); otherwise, such ratios can be found by means of segmental equilibrium or method of virtual work [23,45,47].

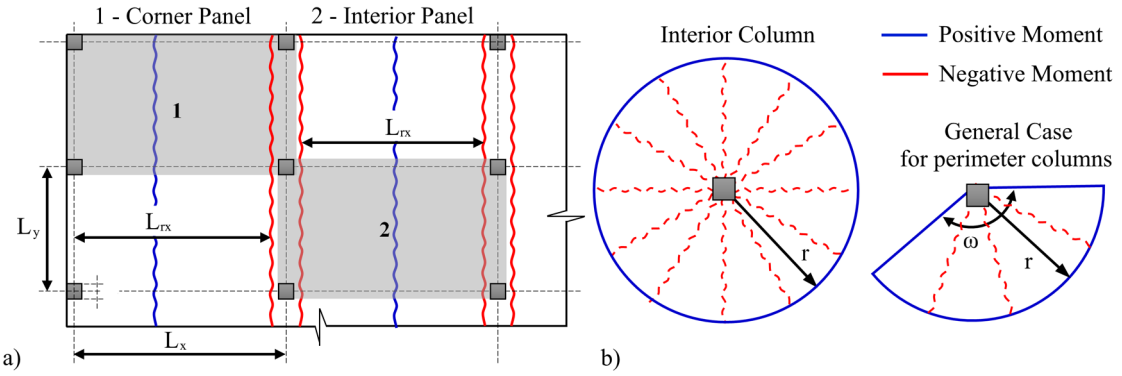

Fig. 1. Yield line patterns for elevated flat slabs: global and local failures

In case of a column-supported flat slabs with a common column grid which is subjected to uniformly distributed load (UDL), three "applied load–produced design moment" relationships are to be assessed by means of standard formulae. Two of these refer to, so-called, global failure of internal (Eq. 1) and corner (Eq. 2) panels of the slab (Figure 1a), whereas the third case concerns local failure (Figure 1b) – the situation where the ultimate load is transferred to the column from the slab tributary area [23]. Equation 3 presents

"concentrated load–produced design moment" relationship for the internal column, whereas Eq. 4 covers the general case for the perimeter columns with an unknown angle (ω, in [rad]) [47-49] which is equal to π or $\pi/2$ for edge and corner columns, respectively. Importantly, these equations permit to vary the ratio of support to mid span moments ($\varnothing_h$, Eq. 5) as long as the ductility requirement is respected.

$$m^{+}_{Ed,YL} = \frac{q_d \cdot L^2_{rx}}{8 \cdot (1 + \varnothing_h)} \quad (1)$$

$$m^{+}_{Ed,YL} = \frac{q_d \cdot L^2_{ry(x)}}{2 \cdot (\sqrt{(1 + \varnothing_h)} + 1)^2} \quad (2)$$

$$m^{+}_{Ed,YL} = \left. P \cdot \left(1 - \sqrt[3]{\frac{q_d \cdot A}{P}}\right) \right/ 2\pi \cdot (1 + \varnothing_h) \quad (3)$$

$$m^{+}_{Ed,YL} = \left. P \cdot \left(1 - \sqrt[3]{\frac{q_d \cdot A}{P}}\right) \right/ (\omega \cdot (1 + \varnothing_h) - 1.14 \cdot \varnothing_h) \quad (4)$$

$$m^{-}_{Ed,YL} = \varnothing_h \cdot m^{+}_{Ed,YL} \quad (5)$$

2.1.2. Flexural strength of HRC: sectional model

Currently, the majority of codes [18–20] suggest the simplified rigid plastic model for the assessment of the ULS behaviour of FRC in tension which is identified by a unique value of f_{Ftud}. This can be based on the characteristic residual tensile strength at the crack mouth opening displacement (*CMOD*) of 2.5 mm (f_{R3k}) according to EN 14651 [50] and can be calculated as $f_{Ftu,d} = f_{R3k} / (3 \cdot \gamma_F)$, where $\gamma_F = 1.50$ is the partial safety factor in tension for FRC. Taking into account this model, the *fib* MC 2010 [19] suggests to evaluate the design resisting moment of FRC ($m_{Rd,FRC}$) by concentrating the whole compressive force in the top fibre of the section, disregarding the traditionally adopted compressive block. However, considering the appearance of relatively high stresses in certain zones of column-supported slabs, the neutral axis may be fixed at 10% of the element thickness for all studied sections in order to provide a safer design procedure; thus, $m_{Rd,FRC} = 0.45 \cdot f_{Ftu,d} \cdot h^2$ [14].

The design resisting moment of HRC ($m_{Rd,HRC}$) could be evaluated complementing the above described sectional analysis by the presence of additional force provided by steel reinforcing bars ($A_s \cdot f_{yd}$). However, the more convenient way is to estimate $m_{Rd,HRC}$ as depicted in Figure 2, i.e. the total flexural strength corresponds to the sum of separately calculated $m_{Rd,FRC}$ and $m_{Rd,RC}$ where the latter is the design resisting moment of traditionally reinforced concrete [51]. This approach permits to compute the maximum design moments (m_{Ed}) in the critical areas (section 2.1.3.) and after calculating the contribution of fibres ($m_{Rd,FRC}$), assess the requirement of reinforcing bars as if it were traditionally reinforced concrete in every section which satisfies the following condition: $m_{Rd,RC} = m_{Ed} - m_{Rd,FRC} \geq 0$.

Nevertheless, the neutral axis can be found below 10% of the element thickness which will lead to an overestimation of the flexural strength of the section using the simplified sectional model (Figure 2). Therefore, for the cases where more accurate results are

demanded, the essential sectional parameters for both FRC and HRC can be computed by imposing sectional force equilibrium and deformation compatibility conditions in accordance with models presented in Figure 3. These parameters permit to assess the bearing capacity of the two-way system (providing more accurate outcomes in comparison with the previously suggested approach, Figure 2) based on the procedure described in the section 2.1.3.

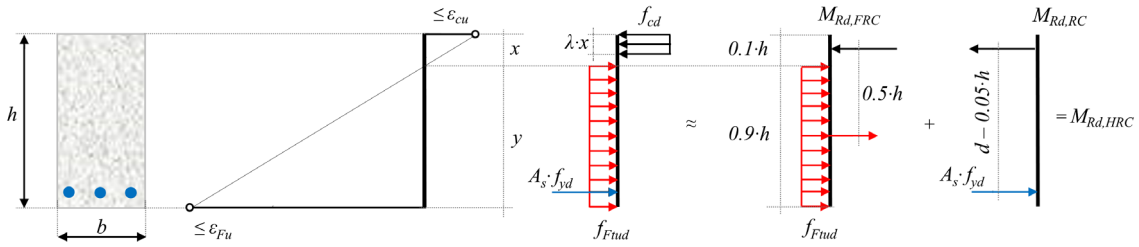

Fig. 2. Simplified sectional model to assess flexural strength of HRC

The above-described models are currently used within the analytical design procedure of FRC two-way slabs. However, the recent studies revealed that the implementation of these could be complemented by the introduction of the structural redistribution factor [52,53] and/or orientation factor [54–56] in order to ensure the more accurate evaluation of the structural response in flexure. The magnitude of the former (up to 1.4) depends on the redistribution capacity of the studied element, whereas the latter takes into account the orientation of fibres which, in turn, is influenced by the rheological properties of concrete, casting method, and the geometry of the element in question [57].

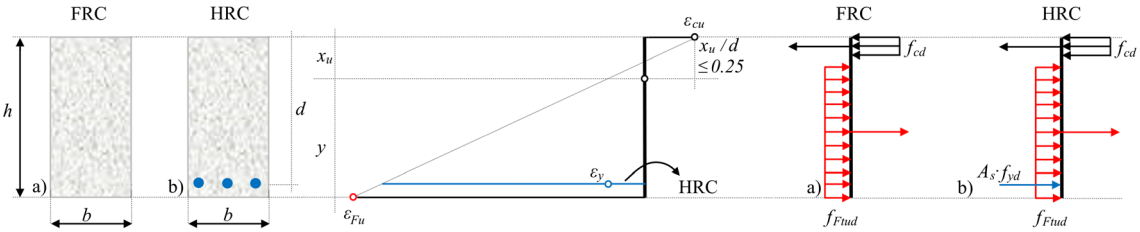

Fig. 3. Sectional models to assess flexural strength of a) FRC; b) HRC

2.1.3. YLM for HRC flat slabs

The difference between FRC and HRC column-supported flat slab design by means of YLM consists of certain challenges in the correct proportioning of the stresses along the yield lines in the latter case, taking into account the possible variety in reinforcement layouts [41]. However, drawing an analogy to the design of RC flat slabs by YLM, the procedure does not differ significantly. Once the geometry, reinforcement layout, and load conditions are established, the ratio of support to mid span moments ($\varnothing_h$) is to be chosen to calculate maximum design moments per unit length for the global failure mode.

The slight difference arises in the following step, when the required traditional reinforcement shall be computed in accordance with (1) considered layout and (2) maximum design moments along the yield lines. Firstly, the required amount of the reinforcing bars can be calculated for the bottom reinforcement. Taking into account that, in accordance with YLM, the curtailment is not advisable for the latter, the procedure is straightforward: the simplified approach (Figure 2) or accurate sectional analysis (Figure 3) can be applied. In

turn, the top reinforcement is frequently found curtailed; therefore, the need of design moment proportioning should be considered.

In case of RC flat slabs (Figure 4), the task can be performed by means of Eq. 6: multiplying the calculated moment (Eqs. 1 and 2) by the length of the yield line (LYL) and dividing the obtained value by the length along the same yield line which is covered by the top reinforcement. [47]. The presence of fibres in the concrete mix modifies the above described procedure; Eq. 7 provides the consideration of its contribution to the flexural strength and, as a consequence, the design bending moment which shall be resisted by reinforcing bars in accordance with the simplified model presented in Figure 2. The more accurate procedure demands to find the resisting moment of the FRC section (Figure 3a) with following proportioning of the design bending moment to the HRC zones by means of Eq. 8 (Figure 4). The obtained magnitude of this moment permits to compute the required amount of the reinforcing bars using the sectional model presented in Figure 3b. Finally, the verification of the sufficient flexural strength against local flexural failure modes shall be performed for both cases in order to complete the analysis (the detailed description of the method implementation is provided in the Supporting Information available with the online version of the article).

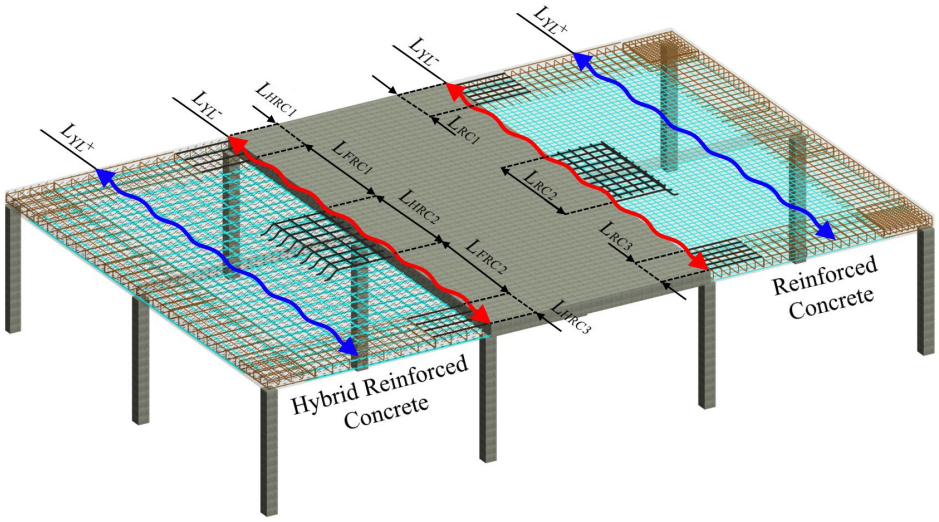

Fig. 4. Yield line pattern for the global failure mode: HRC and RC solutions

$$m^{-}_{Ed} = \frac{m^{-}_{Ed,YL} \cdot L_{YL^-}}{\sum L_{RC_i^-}} \tag{6}$$

$$m^{-}_{Ed,RC} = \frac{(m^{-}_{Ed,YL} - m_{Rd,FRC}) \cdot L_{YL^-}}{\sum L_{HRC_i^-}} \tag{7}$$

$$m^{-}_{Ed,HRC} = \frac{m^{-}_{Ed,YL} \cdot L_{YL^-} - m_{Rd,FRC} \cdot \sum L_{FRC_i^-}}{\sum L_{HRC_i^-}} \tag{8}$$

2.2. STRUCTURAL RESPONSE OF HRC FLAT SLABS AT SLS

2.2.1. Internal forces and reinforcement distribution

In already constructed HRC flat slabs, generally, the absence of cracking under quasi-permanent load combinations was pointed out which permitted to evaluate the produced deformations as for an isotropic linear elastic material [15,25]. However, the presence of cracks in this type of elements is expectable – in accordance with ACI 421.3R-15, microcraking in two-way concrete slabs starts at an early level of approximately 10% of the service load, whereas the pattern of potential yield lines is almost fully developed at 30% of the same load [58].

Therefore, straightforward analytical methods are required to evaluate the response of HRC in terms of cracking and deformations. This is not a trivial task considering that even the behaviour of RC two-way slabs at SLS still demands further studies and seems to be significantly more complex than the cases related to beams and/or one-way plates. Additionally, the proposed methods should be correlated with the current codes and guidelines in order to be used by practitioners. With this in mind, the approach based on the analogy with RC flat slabs design is presented herein; the overarching goal is to prove that HRC solutions comply with minimum requirements described in the *fib* MC 2010 [19] and Eurocode 2 (EC2) [43] for traditionally reinforced alternative.

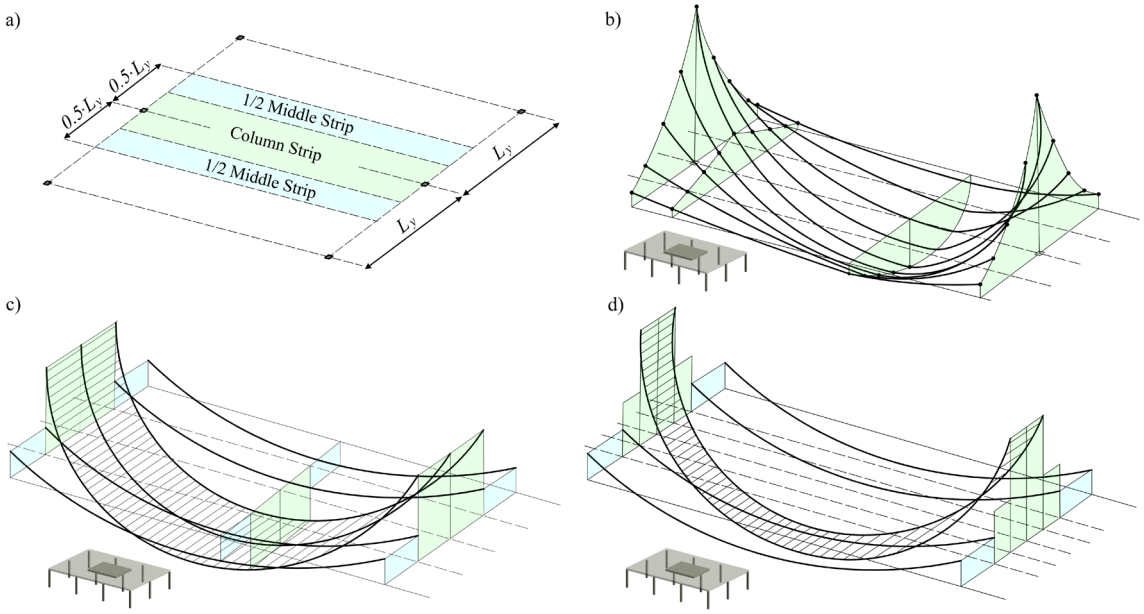

Fig. 5. a) Division of flat slab into column and middle strips b) Typical elastic moment distribution under UDL c) Moment distribution according to DDM/EFM d) Adjustments of moment distribution to meet SLS requirements (Adapted from [59])

To this end, several additional steps, which are not directly dealing with the HRC flat slab design process, are to be carried out: (1) divide the given structure into column and middle strips (Figure 5a) pursuant to current regulations [18,23,43] and (2) simplify the regular elastic distribution of moments (Figure 5b) at ULS by means of the Direct Design Method (DDM) or Equivalent Frame Method (EFM, Figure 5c). The same procedure can be performed by finite element analysis, averaging the moments within each strip in order to obtain constant moments in critical sections (in the vicinity of columns and at mid-spans).

The obtained information will serve as a basis for further design assumptions which are described in sections 2.2.2 and 2.2.3.

2.2.2. Cracking control

Generally, the indirect control of cracking is widely applied for RC slabs subjected to bending without significant axial tension, i.e. respecting the established values of maximum permitted steel stresses and reinforcing bar diameter/spacing [19]. In case of RC flat slabs, specific suggestions regarding the detailing of the reinforcement can be found in different studies and regulations. For instance, EC2 [43] states that at internal columns, 50% of the reinforcement, which is required to resist the full negative moment from the sum of the two half panels each side of the column, should be placed in a width equal to the sum of 0.125 times the panel width on either side of the column. Similarly, the works of Jofriet [60] and Brotchie et al. [61] propose the division of the negative column strip into two strips of equal length. Further, the inner negative column strip is to be designed for two-thirds of the total negative column strip moment in order to meet SLS requirements.

The demand for more rigorous calculations can be accompanied with a number of constraints. ACI Codes [58,62,63], for instance, consider that crack control equations for beams underestimate the crack widths developed in two-way slabs, drawing on the scientific works developed, mainly, by Nawy [64,65]. However, the development of this expression was formulated for cracks produced mainly in positive-moment regions, i.e. the regions with clear two-way bending. In turn, cracks tend to appear in the vicinity of columns under the quasi-permanent combination of actions in column-supported flat slabs [66], therefore, it might be important to note that the one-way bending is predominant at faces of the columns.

Referring the above described information to HRC flat slabs, it is evident that further experimental tests along with the validation of existing models are necessary for the accurate assessment of maximum crack widths in column-supported flat slabs. Therefore, being conservative, the methods related to indirect control of cracking in RC column-supported flat slabs can be adapted to HRC solutions, assuring that the latter is not inferior to the RC alternative.

For that purpose, firstly, the maximum design moment above the columns computed by DDT / EFM (Figure 5c) is to be modified in accordance with EC2 [43] (Figure 5d). In fact, EC2 [43] provides this re-proportioning in terms of required top reinforcement area; however, the same relationship can be presented in terms of ultimate flexural moments for the sake of more direct design procedure (with minor difference in the overall result). Based on the modified moment, the required amount of the reinforcement for RC solution is to be assessed – the obtained result permits to omit the subsequent verification of the structure at limit state of cracking according to EC2 [43]. Eventually, the steel stresses can be evaluated in the RC section above the columns as for a continuous beam with a unit width (1,000 mm) and the depth equal to the thickness of the slab (h).

A similar procedure should be repeated for HRC solution. Basing on the FRC properties along with the reinforcement layout, the required amount of steel bars is to be found by means of YLM (section 2.1). Thereafter, the steel stresses in the critical sections should be estimated, considering the same dimensions ($h \times 1000$ mm). For more detailed

analysis of FRC contribution to the structural response of the HRC section at SLS, the multilinear constitutive model in tension (Figure 6) shall be applied [19]. The majority of variables for this model depend on the mean residual tensile strengths at *CMOD*s of 0.5 mm (f_{R1m}), 2.5 mm (f_{R3m}) according to EN 14651 [29] and can be computed as follows: (1) $f_{ct} = 0.30 \cdot (f_{ck})^{2/3}$; (2) $f_{Ftsm} = 0.45 \cdot f_{R1m}$; (3) $f_{Ftum} = f_{Ftsm} - (w_u/CMOD_3) \cdot (f_{Ftsm} - 0.5 \cdot f_{R3m} + 0.2 \cdot f_{R1m})$; (4) $\varepsilon_{SLS} = \mathrm{CMOD}_1/l_{cs}$; (5) $\varepsilon_{ULS} = w_u/l_{cs} = \min(\varepsilon_{Fu}, 2.5/l_{cs} = 2.5/y)$; (6) $\varepsilon_{Fu} = 20‰$ (considering variable strain distribution along the cross section).

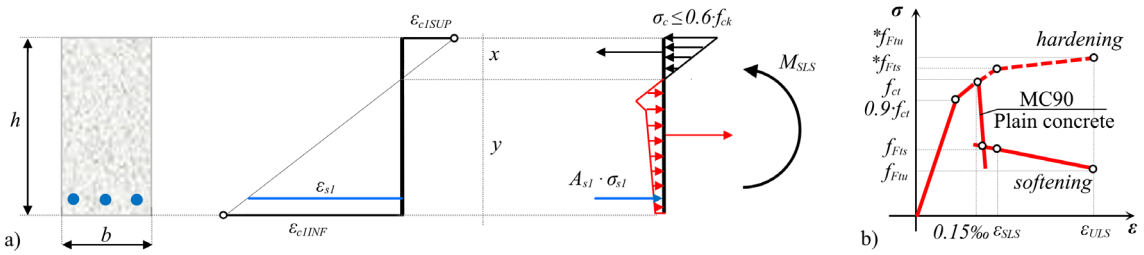

Fig. 6. Sectional model to assess steel stresses in cracked sections (Adapted from [67])

The computed sectional parameters for both RC and HRC should be used to check the sufficient cracking control of the latter by means of two approaches: (1) comparing the achieved stresses (more conservative method) or (2) computing the crack widths as for one-way elements. Conservatively, the steel stresses in each section should be compared and, in case of $\sigma_{s,HRC} \leq \sigma_{s,RC}$, HRC solution presents at least the same performance in terms of cracking control in comparison with RC alternative owing to the fact that the presence of fibres in the material enhances the bond between steel bars and concrete. This phenomenon leads to the reduction of the bond transfer length and, as a result, crack spacing [68–70]. The reduction of crack spacing will ensure a minor crack width in the HRC alternative for the same magnitudes of steel stresses (strains).

Otherwise ($\sigma_{s,HRC} \geq \sigma_{s,RC}$), the chosen reinforcement layout for ULS (YLM) can be unevenly distributed within the column strip pursuant to EC2 [43] in order to reduce the steel stresses up to the required magnitude. However, it is important to consider the necessity to keep the required flexural strength in the column strip outside the mentioned area (Figure 5d). The described case is not likely to occur in the HRC solution with moderate fibre content since YLM allows to concentrate the rebar layout in the vicinity of columns (Figure 4) and, as a consequence, lead to considerable values of negative moments in these zones. [47]. Nevertheless, by increasing the fibre content, the negative moments along the yield line will be more uniformly distributed, i.e. less traditional reinforcement in the form of steel bars is required. Therefore, the verification of sufficient crack control might be necessary and can be assured even by placement of the additional steel bars in the centre part of the column strip.

Alternatively, the crack widths can be assessed in the critical sections as for one-way elements [66]. The design crack width for the RC solution can be evaluated by means of Eq. 9–13 in accordance with the *fib* MC 2010 (Clause 7.6.4.4) [19]. The same equations are valid for the analysis of HRC – for that purpose, provided f_{ctm} is to be substituted by $f_{ctm} - f_{Ftsm}$ in Eq. 10 and 12, taking into account the effect of fibres on the transfer length. Thereafter, the comparative procedure is identical with the one related to the analysis of the produced steel stresses. Summarising, Figure 7 highlights the essential steps to justify the appropriate

structural response of HRC column-supported flats slabs at limit states of cracking for both approaches.

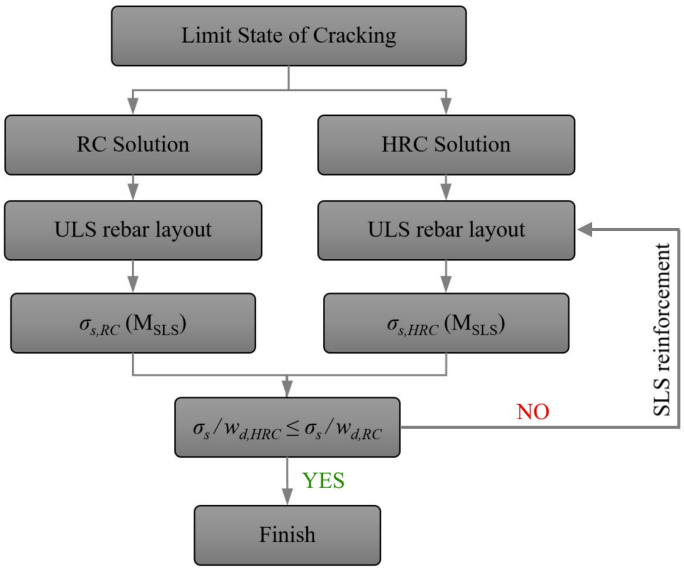

Fig. 7. Flowchart to present the sufficient crack control of HRC solutions in column-supported flat slabs

$$w_d = 2 \cdot l_{s,max} \cdot (\varepsilon_{sm} - \varepsilon_{cm} - \varepsilon_{cs}) \tag{9}$$

$$l_{s,max} = k \cdot c + \frac{1}{4} \cdot \frac{f_{ctm}}{\tau_{bms}} \cdot \frac{\emptyset_s}{\rho_{s,ef}} \tag{10}$$

$$\varepsilon_{sm} - \varepsilon_{cm} - \varepsilon_{cs} = \frac{\sigma_s - \beta \cdot \sigma_{sr}}{E_s} - \eta_r \cdot \varepsilon_{sh} \tag{11}$$

$$\sigma_{sr} = \frac{f_{ctm}}{\rho_{s,ef}} \cdot (1 + \alpha_e \cdot \rho_{s,ef}) \tag{12}$$

$$\rho_{s,ef} = \frac{A_s}{A_{c,ef}} \tag{13}$$

2.2.3. Instantaneous deformations

The design of elevated slabs is typically governed by the deflection control [71] and the correct evaluation of this aspect is of a paramount importance given that this structural element constitute 80–90% of the total cost of a concrete frame [72]. Moreover, it is also important to highlight that the flexural strength for the studied case is to be assessed by means of YLM – approach that provides suitable results for ULS, but does not provide information for serviceability design [66].

With this in mind, simplified analysis methods for RC solutions are adapted herein in order to evaluate the magnitude of deflections in HRC column-supported flats slabs (Figure 8 [73]). Several methods were studied [73–78] and the approach to calculate deflections by

means of crossing beam analogy was chosen as this providing: (1) relatively simple design procedure and (2) significant correlation with experimental data [72,76,77]. Importantly, the presence of fibres as reinforcing material concrete is compatible with this design procedure. Moreover, that has a potential to be extended in order to assess the long-term response of the FRC structural elements – the aspect of the paramount importance that still requires further research [79] and is beyond the scope of this paper.

Having calculated a distribution of moments (Figure 5c), the total instantaneous deflection at the centre of certain panel (δ_{tot}) can be computed as the sum of the average deflection of two parallel column strips and the deflection of the middle strip spanning at right angle to the column strips (Figure 8b or Figure 8c). Among the possible approaches to assess the deflections of these strips, the procedure proposed by Ghali et al. [73,80] was found to be convenient for HRC solutions owing to the assumption that the variation of curvature follows a second degree parabola for the continuous straight members and, therefore, can be easily defined as per Figure 8d. As a result, this method is based on defining between six and nine curvatures depending on the symmetry of the bay considered.

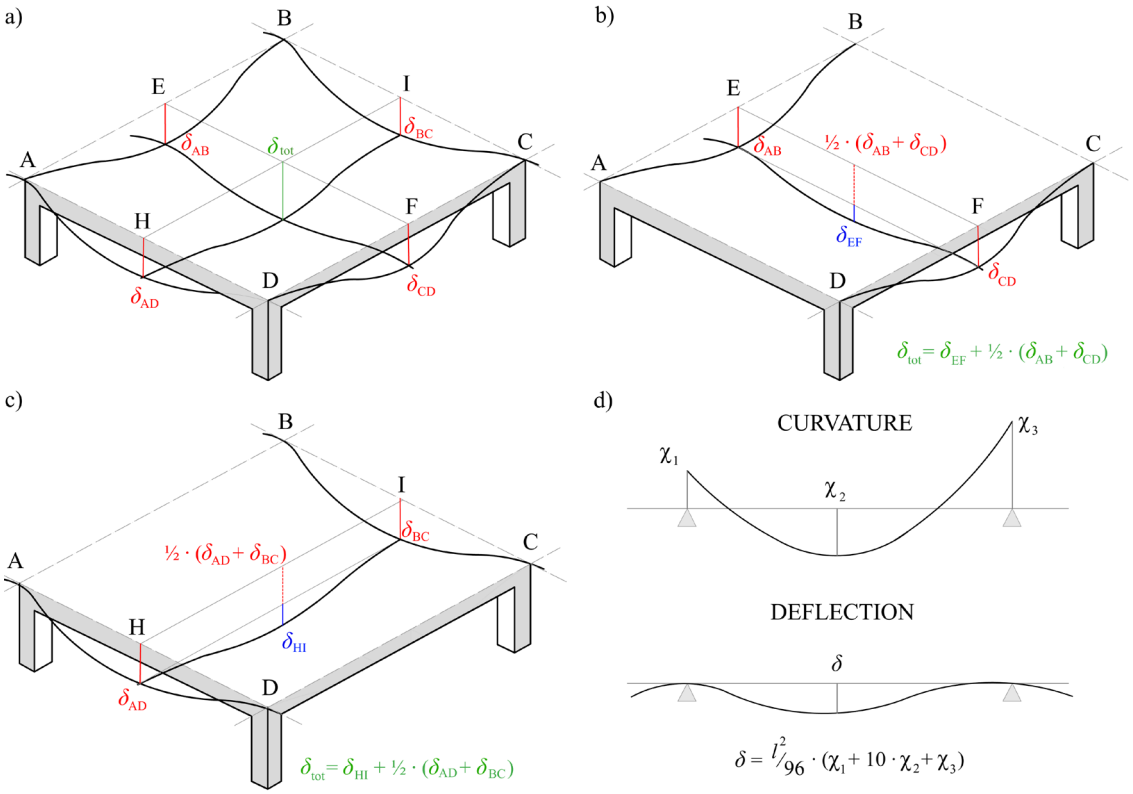

Fig. 8. a) Deflected shape of column-supported flat slab; b-c) Deflection at the centre of a rectangular panel; d) Deflection-curvature relationship for column and middle strips (Adapted from [73])

Moreover, the mid-span sections can be referred to as the "determinant" sections (representing the stiffness of the zone exposed to positive bending moments and having the largest overall effect on deflections), the simplified approach permits [73,80] to evaluate the influence of cracking on the produced curvatures only in these sections, i.e. curvatures at the end sections can be studied as per homogenous material with established properties (moment of inertia and modulus of elasticity). In case of RC solutions, the curvatures of "determinant"

sections can be computed considering two extreme states: the uncracked condition in which concrete and steel are assumed to behave elastically and exhibit compatible deformations, and the fully cracked condition with the concrete in tension ignored [80]. Thereafter, the mean value of curvatures is to be obtained by means of interpolation. Adapting this approach to HRC solution, the section model described previously (Figure 6) along with the multi-layer sectional approach (inverse analysis) [81] may be applied to estimate the curvatures at the governing sections subjected to the given bending moments with further evaluation of the produced deflections in accordance with Figure 8d.

3. DETAILS OF CASE STUDY

3.1. GEOMETRY AND REINFORCEMENT LAYOUT

The selection of the geometry for the case study was oriented to reproduce common dimensions of slab panels that could be representative for office and residential buildings. Additionally, the number of three successive panels in each direction was chosen in order to involve into the analysis both corner and internal panels. Moreover, the FRC slabs of nine panels had been previously tested, which permitted carrying out a numerical validation of the model for the structure of the same geometry (Section 5.1). As a result, an 18.3 × 18.3 × 0.2 m slab supported by 16 columns with square cross sections of 0.3 m was analysed. The uniform column grid (Figure 9a) formed nine panels of 6.0 x 6.0 m each.

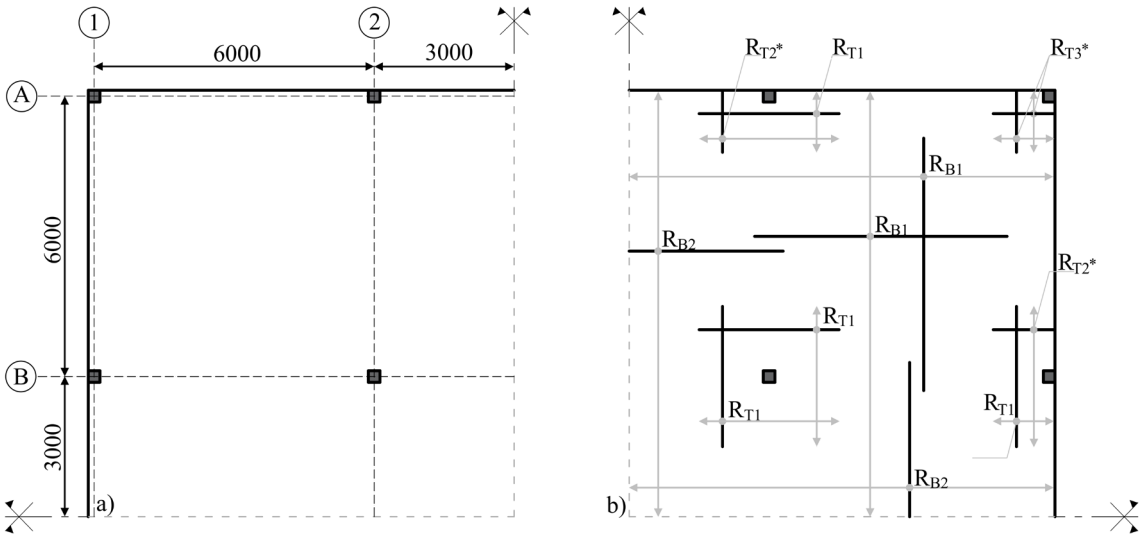

Fig. 9. Analysed HRC flat slab: a) Geometry; b) Reinforcement layout

The reinforcement layout (Figure 9b) was adopted taking into consideration the advantages of using YLM for flat slabs: the bottom reinforcement (R_{B1}, R_{B2}) may be placed across whole bays, generally without curtailment. The top reinforcement (R_{T1}, R_{T2*}, and R_{T3*}, Figure 9b) was concentrated in the vicinity of columns in order to enhance the structural response at service loads in accordance with following ratios: the areas of $0.5 \cdot L_x \times 0.5 \cdot L_y$, $0.5 \cdot L_{x/y} \times (0.2 \cdot L_{y/x} + \text{E.D.})$, and $(0.2 \cdot L_x + \text{E.D.}) \times (0.2 \cdot L_x + \text{E.D.})$ were respectively placed over the internal, edge, and corner columns – E.D. in the presented expressions was equal to the distance between the centreline of column to edge of the slab, i.e. edge distance. Additionally, the selected types of reinforcement R_{T2*} and R_{T3*} should be explained: YLM suggests to provide similar positive and negative bending capacities to sections at the vicinity

of columns once the possible local failures are to be analysed; therefore, the "U" bars were provided in these zones.

The top reinforcement between concentrations over column heads is omitted – this approach can be applied even for RC solution [47], even though cracking can develop in these areas (with minor effect on the structural performance). In case of HRC solutions, the possibility of cracking is significantly reduced due to presence of fibres. However, when necessary, the need of cracking-control mesh in the above discussed zones can be assessed: the minimum reinforcement for the crack control may be estimated in accordance with the Clause 7.7.4.3 of the *fib* MC 2010 [19].

3.2. DESIGN ACTIONS

The loads specified in the Spanish Building Code for residential buildings [82] were considered as a reference to compute load combinations for both ULS and SLS. Apart from the self-weight (q_{SW}) of 4.8 kN/m^2, a dead load (q_G) and variable load (q_Q) of 2.0 and 3.0 kN/m2, respectively, were assumed. Load partial safety factors $\gamma_G = 1.35$ and $\gamma_Q = 1.50$ were assumed to evaluate the design load at ULS: $q_{Sd} = \gamma_G \cdot (q_{SW} + q_G) + \gamma_Q \cdot q_Q = 13.7$ kN/m^2. The quasi-permanent load combination ($q_{k,\psi 2} = q_{SW} + q_G + \psi_2 \cdot q_Q$; $\psi_2 = 0.3$) for residential and office buildings was adopted for deflection and crack control checks. In the present study, this load combination resulted in a UDL of 7.7 kN/m^2.

3.3. MATERIAL PROPERTIES

Two different types of FRC were analysed in the presented study for a more comprehensive analysis. FRC of 3c and 4d strength classes were selected – both types of concrete fulfilled the established requirements to be capable of substituting conventional reinforcement at ULS in accordance with the *fib* MC 2010: $f_{R1k} / f_{Lk} > 0.4$ and $f_{R3k} / f_{R1k} > 0.5$ [19]. Table 2 gathers all mechanical properties of the selected materials which were considered in both analytical and numerical design procedures.

Table 2. Mechanical properties and prices of the selected fibres

	E_c (MPa)	f_{ck} (MPa)	f_{cm} (MPa)	f_{ct} (MPa)	f_{R1k} (MPa)	f_{R3k} (MPa)	f_{R1m} (MPa)	f_{R3m} (MPa)
FRC3c	32700	50.0	58.0	4.1	3.0	3.0	5.1	5.1
FRC4d	32700	50.0	58.0	4.1	4.0	4.7	6.0	7.0

The magnitudes of the compressive strength and modulus of elasticity were adopted based on the experimental campaign which involved the analysis of 15 self-compacting FRC mixes with fibre content up to 120 kg/m^3 in order to establish suitable material for the construction of full-scale SFRC flat slab [83]. The mean values of the residual tensile strengths (f_{R1m}, f_{R3m}) were established by (1) assuming the normal distribution of f_R and (2) imposing values of the coefficient of variation (CV_{fR}) for the latter. In this regard, taking into consideration the extensive experimental programme [84] and values of CV_{fR} derived from a numerical study on the intrinsic scatter of FRC [85], CV_{fR} of 25.0% and 20.0% were assumed for FRC3c and FRC4d, respectively.

The presented residual tensile strengths were not sufficient to provide the required bearing capacity of the structure in question. Therefore, the reinforcing steel B500C (classification was taken from the *fib* MC 2010 [19], Clause 5.2) was assumed for the reinforcing bars (Table 3). The numerical analysis also demands the mean yield/tensile strengths of steel to compute the global safety factor (section 6.1); for this purpose, the established characteristic values were increased by 10% in conformity with the *fib* MC 2010 and EC2 [19,86].

Table 3. Mechanical properties and prices of the selected fibres

	E_s (GPa)	f_{yk} (MPa)	f_{tk} (MPa)	f_{ym} (MPa)	f_{tm} (MPa)	ε_{yk} (‰)	ε_{ym} (‰)	$\varepsilon_{uk} = \varepsilon_{um}$ (%)
B500C	210	500	575	550	632	2.4	2.6	10

4. IMPLEMENTATION OF THE PROPOSED METHOD

4.1. REQUIRED FLEXURAL CAPACITY

Based on YLM along with the established design UDL at ULS and selected geometry, the maximum design bending moments can be computed for both corner and internal panels by means of Eq. 1 and 2. For this purpose, the ratio of negative to positive flexural capacities ($\oslash_h$) was considered as 1.0. Additionally, the distance between the negative yield line and the centreline of external columns was adopted as 5.85 m for the corner panels and spacing between two negative yield lines for the internal panels (Figure 1) was assumed to be 5.70 m.

As a result, $m^{+}_{Ed,YL} = m^{-}_{Ed,YL} = 40.2$ and 27.8 kNm/m for corner and internal panels, respectively (the detailed calculations can be found in the Supporting Information available with the online version of the article). Thereafter, the flexural strengths of FRC 3c and FRC 4d were calculated by using the sectional model presented in Figure 3 followed by (1) distribution of the negative moments (Equation 7) and (2) assessment of the required amount of reinforcement in order to provide the sufficient bearing capacity demanded by the global failure mode. Finally, the local failure mode was analysed; for this purpose, the loads transferred to each column from the slab tributary areas (under UDL of 13.7 kN/m^2) were calculated (Table 4), this permitting to check the already computed reinforcement and to estimate the reinforcement for the edge and corner columns by Equation 3.

Table 4. Loads transferred to columns

Columns	A1	B1, A2	B2
Load (kN)	95	221	573

Table 5 presents the required amount of reinforcing steel bars for both FRC 3c and FRC 4d in accordance with the reinforcement layout depicted in Figure 9b; the rebar detailing was not provided and the same amount of reinforcement per meter was used in the nonlinear analysis (section 5.2) in order to carry out a more accurate comparison.

Table 5. Required amount of reinforcement

Reinforcement Type	$A_{s,req}$ (mm^2 / m)	
	FRC 3c	FRC 4d
R_{B1}	382	283
R_{B2}	206	106
R_{T1}	804	592
R_{T2*}	331	233
R_{T3*}	328	230

4.2. CRACK CONTROL AT SLS

Firstly, the simplified elastic distribution of moments at ULS was evaluated by means of DDT (Figure 10). Table 6 reports the coefficients assumed to distribute the total static moment ($M_0 = q_u \cdot L_y \cdot L_n^2/8$) to supports and mid-span for negative moments and positive moments, respectively. Table 7 gathers the information regarding the distribution of the negative and positive moments transversely to the column and middle strips.

Table 6. Distribution of total static moment in design sections

Flat slab	Negative Moment		Positive Moment
	External Support	Internal Support	Mid-span
Without edge beams	26%	70%	52%
Exterior edge is restrained	65%	65%	35%

Table 7. Distribution of design moments between strips

Strips	Negative Moment		Positive Moment
	External Support	Internal Support	Mid-span
Column	100%	75%	60%
Middle	0%	25%	40%

Additionally, the obtained values should be modified in accordance with EC2 [43] to indirectly guarantee the cracking control (Figure 5d, Section 2.2.1) – the internal column B2 is taken as reference: 50% of the full negative moment from the sum of the two half panels (118.5 kNm) should be established in a width equal to the sum of 0.125 times the panel width on either side of the column (1.5 m), resulting in the overall bending moment of 79 kNm/m. Considering the material properties reported in Tables 2 and 3, the RC section of 200 × 1,000 mm requires 1,117 mm^2 in order to provide the adequate flexural strength under the moment of this magnitude (taking into account the traditionally adopted partial factors at ULS; γ_s = 1.15, γ_c = 1.5).

Finally, the structural response of three section alternatives should be studied at SLS in terms of the stresses to which the most demanded steel rebars are subjected under the quasi-

permanent load combination. These sections of 200 × 1000 mm differ only in the type of reinforcement: (1) RC section with 1,117 mm^2 of steel reinforcing bars, (2) FRC 3c with 804 mm^2, and (3) FRC 4d with 592 mm^2 (Table 5).

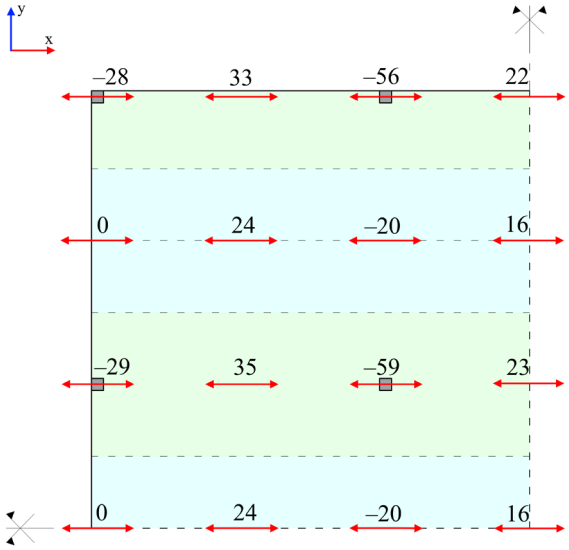

Fig. 10. Bending moments (M_x) in design sections at ULS; values are presented in kNm/m

The moment-steel stress relationship (Figure 11) was computed for the sections in question in order to provide better visualization of the structural response of the studied alternatives. The material properties gathered in Tables 2 and 3 (represented by mean values) along with the constitutive models depicted in Figure 6 were taken into consideration for the sectional analysis. As a result, the influence of the bending moment on the steel stresses was estimated by varying the magnitude of the bending moment from 30 kNm/m to 90 kNm/m.

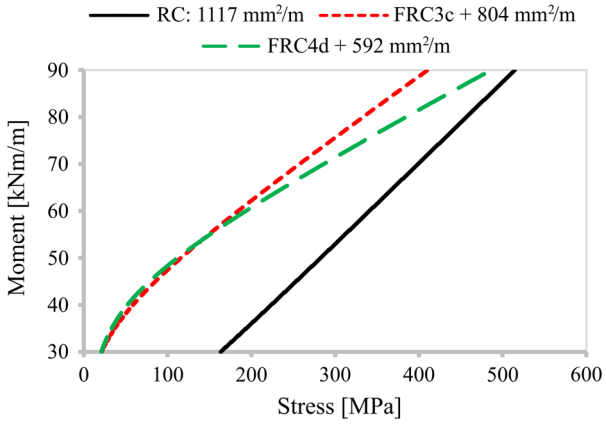

Fig. 11. Moment–steel stress relationship of the studied sections

The structural response of the RC section can be a reference for the evaluation of HRC solutions as it should ensure the sufficient cracking control of the studied two-way slab subjected to the previously described loads according to EC2 [43]. The better performance of FRC 3c + 804 mm^2/m in comparison with the FRC 4d + 592 mm^2/m was expected because the relatively moderate post-cracking residual flexural strength of FRC 3c permitted to concentrate negative moments in the vicinity of columns for the established top reinforcement layout, whereas FRC 4d tended to distribute the produced moments more evenly along the negative yield lines.

However, both solutions proved an enhanced behaviour in terms of cracking control at SLS in comparison with the reference RC solution – the computed steel stresses (the factor of a significant effect on the crack width) were lower within the presented range of moments. Moreover, the steel stresses of FRC 3c + 804 mm^2/m and FRC 4d + 592 mm^2/m were lower to those of the RC solution (1,117 mm^2/m) up to the yielding of the reinforcing steel bars. This fact guarantees the better performance of the HRC alternatives in terms of the required cracking control.

4.3. INSTANTANEOUS DEFLECTIONS AT SLS

The quasi-permanent load combination resulted in a UDL of 7.7 kN/m^2. The flexural moments in column and middle strip under this magnitude of UDL can be estimated by reducing (proportionally) those computed for ULS (Figure 10). Figure 12 presents the magnitudes of the bending moments to evaluate the instantaneous deformation in the centre of the corner panel. For this purpose, the deflections of two column strips in X direction (AB, CD) and the deflection of the middle strip at right angle to the column strips (EF) are to be calculated.

It is important to remark that only two of the bending moment presented in Figure 12 exceeded the cracking moment ($m_{cr} = f_{ct} \cdot b \cdot h^2/6 = 27.1$ kNm/m) – this is owed to the selected concrete mix, i.e. the required self-compacting behaviour of FRC demands the increased content of cement and fine aggregates along with the additives (to reduce the water–cement ratio) as it was evidenced in [8,83]. These modifications lead to the increment of the material tensile strength which, in turn, can be beneficial in terms of serviceability performance; especially, considering that RC solutions for the flat slabs are usually designed/constructed with concrete classes C25–C30 (classification was taken from the *fib* MC 2010 [19], Clause 5.1.2).

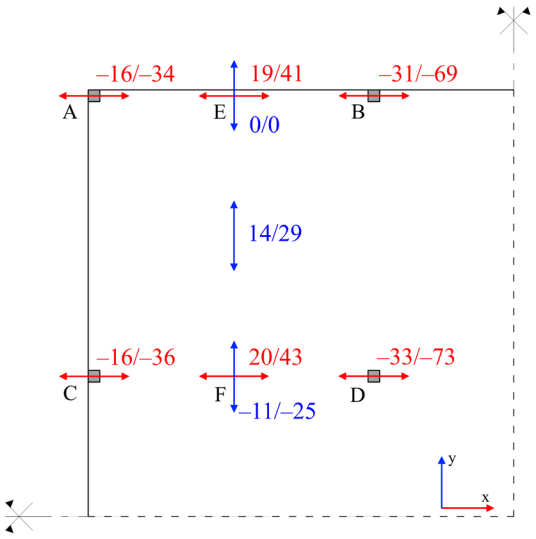

Fig. 12. Bending moments (M_x, M_y) in design sections at a) 7.7 kN/m^2 / b) 17.0 kN/m^2; values are presented in kNm/m

From a design perspective, the increased concrete tensile strength favours the use of a simplified approach to calculate the produced deformations – less cracking tends to keep at a certain degree the elastic distribution of moments, i.e. cracking of the slab would lead to

moment redistribution and, thereby, it would have an effect on deflections. Therefore, a traditional linear elastic analysis will produce a minor error.

Taking this into account, the elastic analysis was also carried out and compared with the results obtained by means of the adopted simplified method and NLFEA (section 5.2). Realizing that the produced deformations should not differ significantly for a UDL of 7.7 kN/m^2, it was decided to extend the study and estimate the instantaneous deformations up to a UDL of 17 kN/m^2 (Figure 12) by means of the elastic analysis and the proposed method in order to: (1) compare in more detail the computed output with the NLFEA and (2) to prove the possibility of evaluating the required ductility in bending of FRC / HRC column-supported flat slabs by the proposed method.

The abovementioned requirement, in accordance with the *fib* MC 2010 [19], must satisfy at least one of the following conditions: (1) $\delta_u \geq 20 \cdot \delta_{SLS}$ and (2) $\delta_{peak} \geq 5 \cdot \delta_{SLS}$, where δ_u is the displacement corresponding to the ultimate capacity (P_u), δ_{peak} is the deflection at the maximum load (P_{max}), and δ_{SLS} is the displacement at SLS computed by performing a linear elastic analysis with the assumption of uncracked concrete. The assessment of δ_u by considering the elastic distribution of moments is excessively conservative due to the significant redistribution capacity of two-way HRC elements. However, it is possible to prove that the structure does not reach the maximum load at the displacement of $5 \cdot \delta_{SLS}$, augmenting the UDL and computing the produced deformations up to the required value ($5 \cdot \delta_{SLS}$) relying on the estimated curvatures.

As a result, the UDL-displacement relationship was estimated by means of elastic analysis (the software SAP2000 [87] was used) and proposed method for both HRC solutions (Figure 13) varying the load from 0 to 17 kN/m^2. The produced displacement in the centre of the corner panel at SLS (UDL of 7.7 kN/m^2) is 3.2 and 4.2 mm according to the elastic analysis and proposed method, respectively – these values are to be compared with the NLFEA output in the following sections. Additionally, it is important to remark that the proposed method evidenced sufficient ductility of the structural system: the displacement under the UDL of 17 kN/m^2 (with the capability of further load increment) was found to respectively be 19.7 and 17.0 mm for HRC 3c (FRC 3c + reinforcing bars) and HRC 4d (FRC 4d + reinforcing bars), whereas $5 \cdot \delta_{SLS} = 16$ mm.

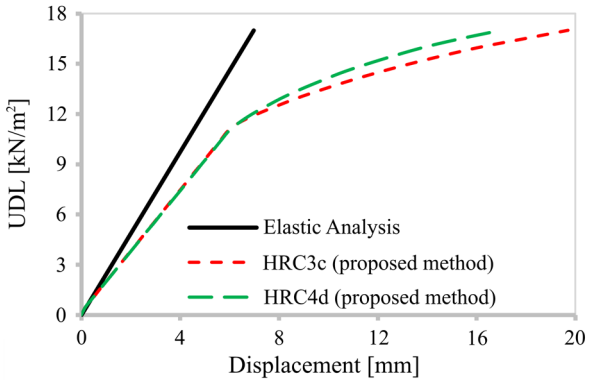

Fig. 13. Structural response of studied HRC slab: UDL–displacement relationship

5. NUMERICAL MODELLING

5.1. MODEL VALIDATION

The finite element software ATENA 5.7.0 [88] was used to model the structure under study, considering both hybrid alternatives. The structural response of FRC in tension was reproduced by means of the multi-linear constitutive diagram depicted in Figure 6 which was based on the mechanical properties of the selected materials (Table 2). The compressive behaviour of concrete was modelled using the stress-strain relationship for short-term loading in accordance with the Clause 5.1.8.1 of the *fib* MC 2010 [19]. The behaviour of steel was represented by the bilinear constitutive diagram following the Clause 3.2.7 of EC2 [43] and taking into account the mechanical properties of reinforcing steel (Table 3).

The geometry of the HRC column-supported flat slab was modelled by means of 3D shell and solid elements – almost the entire structure was comprised of 3D shell elements considering that the analysed element was mainly subjected to bending stresses; only the zones near the column-slab connections were modelled by solid 3D elements. Additionally, only a quarter of the studied element was modelled due to a double symmetry resulting in a total of 13,300 hexahedral elements (Figure 14). This approach required to impose the displacements in both symmetry planes. The column supports were reproduced by the rigid constraints in vertical direction – it is important to remark that the post-cracking tensile strength was increased in the regions above the columns (where vertical displacements were actually restricted) in order to properly reproduce the column-slab connection, avoiding the tensile local failures of these zones.

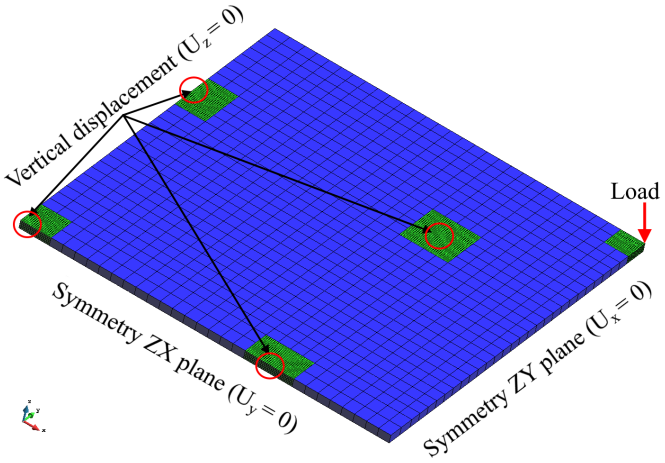

Fig. 14. Considered finite element meshed model

Before the verification of the proposed simplified method by means of NLFEA, the numerical model was validated by simulating two experimental tests [11,13] on full-scale column-supported flat slabs of the same geometry as that of the case study (Figure 9a). The first test was reported by Gossla [11], which consisted in evaluating the structural response of the FRC slab (fibre content of 100 kg/m^3) up to failure. The ultimate bearing capacity of the structure (named Bissen slab) was estimated by means of the point load which was gradually applied in the centre of the element.

Prior to the full-scale test, the material characterization of the FRC considered was performed by means of four point bending test, square panel and round panel tests. The

experimental outcome obtained by testing the round panels permitted to estimate the post-cracking behaviour of FRC using the inverse analysis [38]. These properties (f_{ct} = 2.5 MPa, f_1 = 1.75 MPa, f_2 = 1.06 MPa, f_3 = 0 MPa and w_{ct} = 0 mm, w_1 = 0.25 mm, w_2 = 1.25 mm, w_3 = 2 mm), along with the information related to the measured compressive strength (f_{cm} = 35 MPa) and modulus of elasticity (E_{cm} = 32,300 MPa) were used in the simulation of the Bissen slab with minor modifications: ATENA permits to modify the pre- and post-cracking tensile models by means of stress–strain constitutive diagrams and, therefore, the presented crack widths were transformed to corresponding strains in accordance with the crack band method and the smeared crack approach [89].

The second FRC full-scale test (fibre content of 70 kg/m^3, named Limelette slab) was tested under the same conditions up to failure – applying the point load at the centre of the slab. Therefore, only the material properties were reintroduced according to the information presented in the previous studies [41,52]. Post-cracking behaviour was modelled considering the following tensile and residual tensile strengths at established crack widths: f_{ct} = 2.2 MPa, f_1 = 1.2 MPa, f_2 = 1.2 MPa, f_3 = 0 MPa and w_{ct} = 0 mm, w_1 = 0.05 mm, w_2 = 1.5 mm, w_3 = 6 mm, whereas the compressive strength and modulus of elasticity were adopted as 35 and 29,000 MPa, respectively. In both cases, the self-weight was imposed and then the point load was applied at a circular steel plate of 20 mm of diameter by means of displacement control to guarantee the numerical convergence.

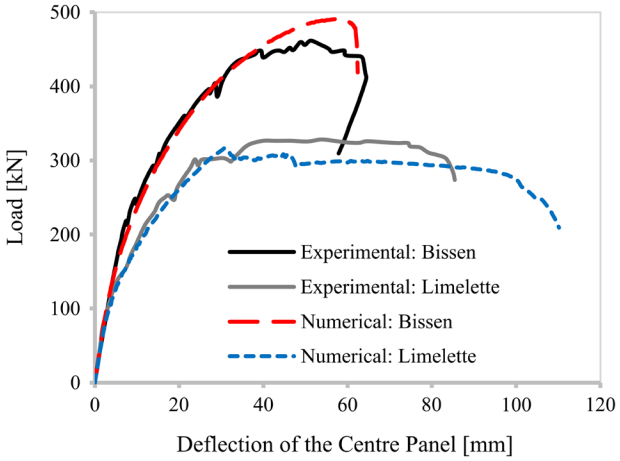

Fig. 15. Experimental and numerical structural response of Bissen [11] and Limilette [13] full-scale tests

As a result, both simulations of the full-scale tests showed an accurate prediction of the structural behaviour of FRC flat slabs tested experimentally (Figure 15). The computed maximum loads differed from those observed during the real testing by 6.3 and 3.6% in case of Bissen and Limellette slabs, respectively. Moreover, the simulations led to almost identical structural response up to deflections of 27 and 38 mm for the abovementioned FRC slabs – this aspect being of a paramount importance from the perspective of further analysis of the hybrid solutions at SLS. Additionally, the estimation of the developed cracks should be pointed out – considering that the crack patterns in both cases were similar, Figure 16 only presents the comparison of the produced cracks during the experimental test of the Limelette slab [13,52] with those predicted by the numerical simulation. Consequently, based on the obtained results, it can be stated that the numerical model was capable of predicting the structural response of the HRC solutions from low to high levels of applied loads.

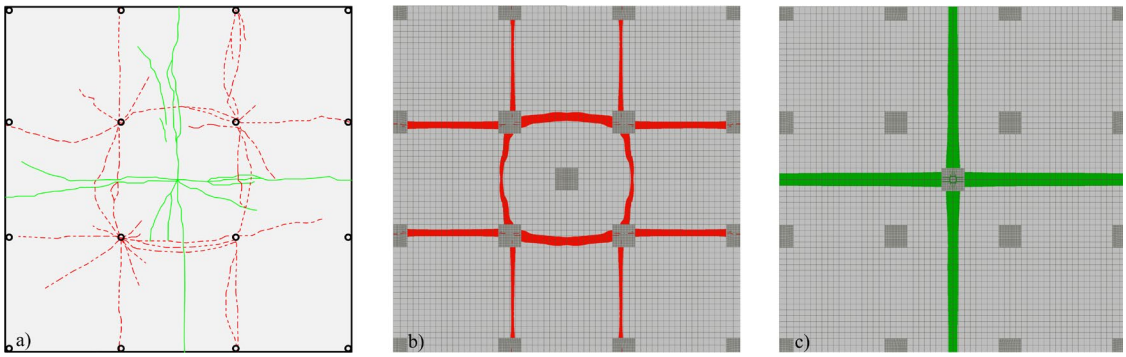

Fig. 16. Produced crack patterns at ULS (red and green lines/areas indicate cracks at the top and bottom of the slab, respectively): a) experimental test (Adapted from [69]);b-c) numerical prediction (the areas depict only the zones with wd > 1 mm)

5.2. MODELLING OF HRC CASE STUDIES

The geometry of Bissen and Limelette slabs was the same as that of the case study. Therefore, the previously described model (Figure 14) was used in order to analyse numerically the HRC alternatives with minor modifications – the one-dimensional reinforcing steel bars with a perfect bond were introduced to this model in accordance with (1) the established material properties (Table 3), (2) reinforcement layout (Figure 9), and analytical design output (Table 5). Additionally, the loading of the model was updated – the structure was subjected to the gradually increased UDL up to a failure. The failure criterion was related to the flexural response of the analysed HRC column-supported flat slabs in terms of the produced deflections – further increment of UDL of 0.1 kN/m^2 should not have led to disproportionate deformations at the corner panel.

Figure 17 presents similar UDL-deflection relationship for studied HRC solutions using both mean and characteristic values of material properties, despite the differences of both residual tensile strengths and reinforcing steel bars amounts. Therefore, it can be concluded that, varying the residual tensile strength, the proposed simplified approach based on the YLM permits to compute the required amount of the reinforcing steel bars, assuring almost identical structural response in flexure of HRC alternatives.

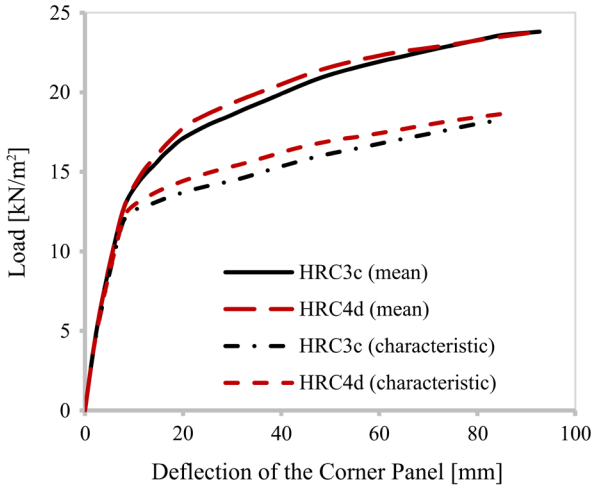

Fig. 17. UDL (self-weight included)–deflection relationship for both HRC alternatives

However, the next question that may arise is "Does this approach provide safe solutions in terms of design resistance?" To answer this question, the design global resistance of the structure was calculated in accordance with the *fib* MC 2010 [19] (Clause 4.6.2.2) and compared with the initially established q_{Sd} = 13.7 kN/m^2.

6. VALIDATION OF THE PROPOSED DESIGN METHOD

6.1. GLOBAL RESISTANCE OF THE STUDIED CASES

The structural response of both HRC solutions was predicted (Figure 17) by nonlinear analysis using the mean values of selected material properties (Tables 2-3). Nonetheless, the global safety factor should be quantified by complying with the design condition (Eq. 13). For this purpose, the method of estimation of a coefficient of variation of resistance (ECOV) was adopted.

In this simplified probabilistic approach, the underlying assumption states that the coefficient of variation of resistance (V_R) can be assumed as lognormally distributed and can be expressed by means of Equation 14, i.e. may be estimated based on the mean (R_m) and characteristic (R_k) values of global resistance [90]. The computed coefficient of variation provides the possibility of evaluating the global safety factor (γ_R) using the Equation 15, which also takes into account the sensitivity factor (α_R) for the reliability of resistance and the reliability index (β). These two values (α_R, β) can be considered to be respectively 0.8 and 3.8 (for a service life of 50 years). Finally, the model uncertainty factor (γ_{Rd}) should be taken into account – the magnitude of the latter can be assumed to be 1.0, 1.06 and 1.1 for the models with no uncertainties, with low uncertainties and high uncertainties, respectively [19]. In the current study, the typically adopted value of 1.06 was assumed.

$$E_d \leq R_d = \frac{R_m}{\gamma_R \cdot \gamma_{Rd}} \tag{13}$$

$$V_R = \frac{1}{1.65} \ln \cdot \left(\frac{R_m}{R_k}\right) \tag{14}$$

$$\gamma_R = \exp(\alpha_R \cdot \beta \cdot V_R) \tag{15}$$

Table 8. Distribution of total static moment in design sections

Material	NLFEA					E_d [kN/m^2]
	R_m [kN/m^2]	R_k [kN/m^2]	γ_R	γ_{Rd}	R_d [kN/m^2]	
FRC 3c	23.8	18.4	1.62	1.06	13.9	13.7
FRC 4d	23.8	18.7	1.56	1.06	14.4	13.7

Applying the abovementioned approach, the global design resistance for the HRC alternatives was evaluated (Table 8). The design values of the global strength (R_d) are 1.4 and

4.8% higher than the required global resistance (E_d) for the alternatives FRC 3c and FRC 4d, respectively, i.e. the required flexural capacity was achieved by means of the proposed simplified method.

6.2. STRUCTURAL RESPONSE OF STUDIED CASES AT SLS

The instantaneous deflections were computed by means of the developed approach (Figure 13). The numerical analysis, which was posteriorly conducted, permits to evaluate the accuracy of this approach. Figure 18 corroborates the precision of the proposed method – the estimated deflections at 7.7 kN/m^2 (quasi-permanent load combination) differ from those obtained numerically by 0.1 mm (2.4%). Moreover, the analytically assessed deflections were also in line with those calculated numerically up to the UDL which exceeded the established magnitude at ULS (13.7 kN/m^2).

Based on the abovementioned, the proposed method can be considered as suitable for verifying the ductility requirements in bending of the HRC alternatives. It must be highlighted that the numerical outcomes also allow confirming the viability of indirect method to guarantee the sufficient crack control since the maximum crack width at SLS is inferior to 0.3 mm, which is the value generally established as a maximum crack width (w_{max}) for several exposure classes under quasi-permanent load combination of actions [18,19,43].

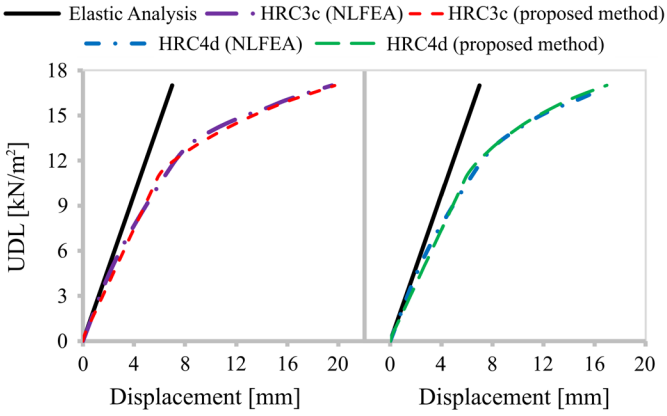

Fig. 18. UDL – Displacement relationship: NLFEA and proposed method

7. CONCLUSIONS

In this paper, a design-oriented approach to evaluate the flexural capacity along with the estimation of instantaneous deflections and crack-width governing parameters is proposed for HRC column-supported flat slabs. Two HRC alternatives were studied by means of the proposed approach for a given geometry and boundary conditions. Additionally, a NLFE analysis was conducted in order to compare and validate the results obtained with the analytical approach. From this analysis, the following conclusions may be derived:

- The Yield Line Method permits to evaluate the overall flexural capacity of the HRC flat slabs with a possibility of distributing moments while accounting for the presence of FRC and HRC sections along the same yield line. Based on nonlinear analyses, the analytical approach provides a reliable results in terms of overall bearing capacity in flexure in case of the given structure subjected to UDL.

- The proposed approach, based on the crossing beam analogy along with indirect control of cracking for RC flat slabs, proved to be promising for dealing with the design at both SLS (crack width control and instantaneous deflection control).
- Additionally, the proposed method permits to check the ductility requirements for bending ($\delta_{peak} \geq 5 \cdot \delta_{SLS}$) by evaluating the expected deflections at ULS.

Even though the numerical analyses showed a considerable accuracy and precision of the proposed design-oriented approach, certain aspects are still to be studied for the consideration of this technological alternative (partial substitution of reinforcing steel bars by fibres in HRC flat slabs) by practitioners in the design phase. In this regard, the potential modification of the current FRC constitutive models for two-way elements, the estimation of the long-term behaviour of FRC/HRC flat slabs, and the structural effect of induced holes into the slab are among the topics that should be further investigated. Furthermore, the parametric study which involves the variation of geometry, load type (UDL, point load) and magnitude of the latter can complement the presented investigation.

SUPPORTING INFORMATION

IMPLEMENTATION OF THE METHOD (WORKED EXAMPLE)

This Supporting Information presents a detailed calculation of the overall flexural capacity at ULS (13.7 kN/m^2) along with the estimation of the structural response at SLS (7.7 kN/m^2) in terms of instantaneous deflections and cracking control. Moreover, the verification of the ductility requirement is to be provided. The step-by-step design procedure is shown for the case study described in the section 3 of the manuscript – bearing in mind that the procedure does not differ for both hybrid alternatives, only the solution with FRC 3c was considered for this example. Finally, the algorithm of the proposed method is concisely presented by means of a flowchart.

REQUIRED FLEXURAL CAPACITY

The relation between applied load and produced moments per unit length (considering the global failure, Figure 1) for internal and corner panels can be found by means of Eq. 1 and Eq. 2 (section 2.2.1). Importantly, the ratio of support to mid-span moments ($\varnothing_h$) has been chosen to equal unity – this is generally satisfactory for flat slabs unless there is a significant difference in the length of adjacent spans [28].

Corner Panel:

$$m_{Ed,YL}^{+} = \frac{q_d \cdot L_{ry(x)}^2}{2 \cdot (\sqrt{(1+\varnothing_h)}+1)^2}$$

$$m_{Ed,YL}^{+} = \frac{13.7 \cdot 5.85^2}{2 \cdot (\sqrt{(1+1)}+1)^2} = 40.2 \text{ kNm/m}$$

Interior Panel:

$$m^{+}_{Ed,YL} = \frac{q_d \cdot L^2_{rx}}{8 \cdot (1 + \varnothing_h)}$$

$$m^{+}_{Ed,YL} = \frac{13.7 \cdot 5.7^2}{8 \cdot (1+1)} = 27.8 \text{ kNm/m}$$

Based on the established material properties of FRC 3c (Table 2) and reinforcing steel (Table 3), the required amount of bottom reinforcement can be calculated by means of the sectional model presented in Figure 3. For this purpose, the presented below system of equations should be solved for both magnitudes of bending moments. As a result, the required amount of bottom reinforcement is **382 mm²/m** and **206 mm²/m** for corner and interior panels, respectively.

$$\begin{cases} x = \dfrac{f_{Ftu,d} \cdot h \cdot b + A_s \cdot f_{yd}}{\left(0.8 \cdot f_{cd} + f_{Ftu,d}\right) \cdot b} \\ m^{+}_{Ed,YL} = 0.48 \cdot f_{cd} \cdot x^2 \cdot b + f_{Ftu,d} \cdot \dfrac{(h-x)^2}{2} \cdot b + A_s \cdot f_{yd} \cdot (d-x) \end{cases}$$

In case of negative design bending moments, the top reinforcement is found curtailed (Figure 10) and, therefore, the design resisting moment of FRC is to be initially found by means of the same system of equations with a minor modification – there is no additional force provided by steel reinforcing bars ($A_s = 0$). Once the design resisting moment of FRC section is calculated (***$m_{Rd,FRC}$* = 13.2 kNm/m**), the design moment along the yield line should be distributed in accordance with Eq. 8:

$$m^{-}_{Ed,HRC} = \frac{m^{-}_{Ed,YL} \cdot L_{YL^-} - m_{Rd,FRC} \cdot \sum L_{FRC_i^-}}{\sum L_{HRC_i^-}}$$

$$m^{-}_{Ed,HRC} = \frac{40.2 \cdot 9.125 - 13.2 \cdot 4.725}{4.4} = 69.3 \text{ kNm/m}$$

The computed design moment must be resisted by the HRC sections along the analysed yield line. Solving the presented above system of equations, the amount of top reinforcement results in **804 mm²/m**. Finally, the local failure mode is to be studied in order to (1) check that provided amount of reinforcement to fulfil the requirements of global failure mode is sufficient to prevent local failure (Eq.3) and (2) determine the adequate amount of reinforcement for corner columns (R_{T3}, Figure 9) and edge columns in one direction (R_{T2}, Figure 9) by means of Eq.4.

Interior Panel:

$$m^{+}_{Ed,YL} + m^{-}_{Ed,YL} = \frac{P}{2\pi} \cdot \left(1 - \sqrt[3]{\frac{q_d \cdot A}{P}}\right)$$

$$m^{+}_{Ed,YL} + m^{-}_{Ed,YL} = \frac{573}{2\pi} \cdot \left(1 - \sqrt[3]{\frac{13.7 \cdot 0.09}{573}}\right) = 79.4 \text{ kNm/m}$$

The average flexural capacity of bottom reinforcement ($m^{+}_{Ed,YL}$) near the internal column is (see the evaluation of global failure mode for corner and interior panels):

$$\frac{40.2 + 27.8}{2} = 34 \text{ kNm/m}$$

Therefore,

$$m^{+}_{Ed,YL} + m^{-}_{Ed,YL} = 79.4 \text{ kNm/m}$$

$$m^{-}_{Ed,YL} = 79.4 - 34 = 45.4 \text{ kNm/m}$$

Taking into account that the top reinforcement in the vicinity of internal column was designed to resist the bending moment of 69.3 kNm/m, the local mode failure is not critical.

Edge Panel:

$$5.14 \cdot m^{+}_{Ed,YL} = P \cdot \left(1 - \sqrt[3]{\frac{q_d \cdot A}{P}}\right)$$

$$5.14 \cdot m^{+}_{Ed,YL} = 221 \cdot \left(1 - \sqrt[3]{\frac{13.7 \cdot 0.09}{221}}\right)$$

$$m^{+}_{Ed,YL} = m^{-}_{Ed,YL} = 35.4 \text{ kNm/m}$$

Although, 313 mm^2/m is sufficient to provide the required flexural strength under the bending moment of 35.4 kNm/m (solving the system of equations), the amount of reinforcing steel bars should be increased up to 331 mm^2/m in order to guarantee the adequacy of the bottom reinforcement (in average) within this local failure pattern (see Figure 9b):

$$A_{s,average} = \frac{1.4 \cdot 382 + 1.4 \cdot 206 + 3.0 \cdot 331}{1.4 + 1.4 + 3.0} = 313.1 \text{ mm}^2\text{/m}$$

Corner Panel:

Finally, the amount of the reinforcement is to be assessed for the corner columns by means of Eq.4 (considering ω = 90°, i.e. π/2) and adopting $m^{+}_{Ed,YL} = m^{-}_{Ed,YL}$:

$$2 \cdot m^{+}_{Ed,YL} = P \cdot \left(1 - \sqrt[3]{\frac{q_d \cdot A}{P}}\right)$$

$$2 \cdot m^{+}_{Ed,YL} = 95 \cdot \left(1 - \sqrt[3]{\frac{13.7 \cdot 0.09}{95}}\right)$$

$$m^{+}_{Ed,YL} = m^{-}_{Ed,YL} = 36.4 \text{ kNm/m}$$

$$\boldsymbol{A_s = 328 \text{ mm}^2\text{/m}}$$

The obtained results are gathered in the Table 5 of the manuscript.

CRACK CONTROL AT SLS

The procedure to evidence that the HRC solutions provides at least the same performance in terms of cracking control in comparison with the RC alternative (according to EC2 [25]) was thoroughly described in the section 2.2.2 and summarized by the flowchart (Figure 7). The only aspect that could be additionally highlighted is: once the reference RC and HRC sections are computed (section 4.2), the nonlinear sectional analysis (Figure 6) should be performed in order to obtain steel strain under the given bending moment in order to analyse the alternatives. For this purpose, a multi-layer sectional approach may be used which is presented in [59].

INSTANTANEOUS DEFLECTIONS AT SLS

Once the bending moments in the required sections are calculated (Figure 12) the procedure explained in section 2.2.3 is to be carried out, i.e. up to nine curvatures should be computed in order to estimate the deflection in the centre of the panel. Firstly, the deflection in the centre of the corner panel is calculated under the UDL of 7.7 kN/m^2 (quasi-permanent load combination of the case study):

$$E_{cm} = 32700 \text{ N/mm}^2$$

$$I_g = \frac{b \cdot h^3}{12} = \frac{1000 \cdot 200^3}{12} = 6.67 \cdot 10^8 \text{ N/mm}^2$$

Column Strip AB (Figure 12)

$$\chi_1 = \frac{M}{E \cdot I} = \frac{-16 \cdot 10^6}{32700 \cdot 6.67 \cdot 10^8} = -7.34 \cdot 10^{-7} \text{mm}^{-1}$$

$$\chi_2 = \frac{M}{E \cdot I} = \frac{19 \cdot 10^6}{32700 \cdot 6.67 \cdot 10^8} = 8.72 \cdot 10^{-7} \text{mm}^{-1}$$

$$\chi_3 = \frac{M}{E \cdot I} = \frac{-31 \cdot 10^6}{32700 \cdot 6.67 \cdot 10^8} = -1.42 \cdot 10^{-6} \text{mm}^{-1}$$

$$\delta_{AB} = \frac{l^2}{96} \cdot (\chi_1 + 10 \cdot \chi_2 + \chi_3)$$

$$\delta_{AB} = \frac{5700^2}{96} \cdot (-7.34 \cdot 10^{-7} + 10 \cdot 8.72 \cdot 10^{-7} - 1.42 \cdot 10^{-6}) = 2.22 \text{ mm}$$

Column Strip CD (Figure 12)

$$\chi_1 = \frac{M}{E \cdot I} = \frac{-16 \cdot 10^6}{32700 \cdot 6.67 \cdot 10^8} = -7.34 \cdot 10^{-7} \text{mm}^{-1}$$

$$\chi_2 = \frac{M}{E \cdot I} = \frac{20 \cdot 10^6}{32700 \cdot 6.67 \cdot 10^8} = 9.17 \cdot 10^{-7}\text{mm}^{-1}$$

$$\chi_3 = \frac{M}{E \cdot I} = \frac{-33 \cdot 10^6}{32700 \cdot 6.67 \cdot 10^8} = -1.51 \cdot 10^{-6}\text{mm}^{-1}$$

$$\delta_{CD} = \frac{5700^2}{96} \cdot (-7.34 \cdot 10^{-7} + 10 \cdot 9.17 \cdot 10^{-7} - 1.51 \cdot 10^{-6}) = 2.34 \text{ mm}$$

Middle Strip EF (Figure 12)

$$\chi_1 = \frac{M}{E \cdot I} = \frac{0 \cdot 10^6}{32700 \cdot 6.67 \cdot 10^8} = 0 \text{ mm}^{-1}$$

$$\chi_2 = \frac{M}{E \cdot I} = \frac{14 \cdot 10^6}{32700 \cdot 6.67 \cdot 10^8} = 6.42 \cdot 10^{-7}\text{mm}^{-1}$$

$$\chi_3 = \frac{M}{E \cdot I} = \frac{-11 \cdot 10^6}{32700 \cdot 6.67 \cdot 10^8} = -5.05 \cdot 10^{-7}\text{mm}^{-1}$$

$$\delta_{EF} = \frac{6000^2}{96} \cdot (0 + 10 \cdot 6.42 \cdot 10^{-7} - 5.05 \cdot 10^{-7}) = 2.22 \text{ mm}$$

Total deflection

$$\delta_{tot} = \frac{2.22 + 2.34}{2} + 2.22 = \mathbf{4.5\ mm}$$

NB: Section 4.3 states that the deflection in the centre of the corner panel is 4.2 mm. The difference arises due to rounding the magnitudes of the bending moments in the worked example.

VERIFICATION OF DUCTILITY REQUIREMENT

The UDL of 7.7 kN/m^2 does not lead to cracking of the "determinant" sections (in accordance with the adopted moment distribution). However, verifying the ductility requirement ($\delta_{peak} \geq 5 \cdot \delta_{SLS}$), the cracking of the mid-span sections must be taken into account (section 2.2.3). For this purpose, the nonlinear sectional analysis was carried out in order to obtain curvatures under the given bending moments provoked by the UDL of 17 kN/m^2 (Figure 13, Figure 14). Apart from that, the design calculations are identical with those explained in the section related to the estimation of the instantaneous deflection at SLS:

$$E_{cm} = 32700 \text{ N/mm}^2$$

$$I_g = \frac{b \cdot h^3}{12} = \frac{1000 \cdot 200^3}{12} = 6.67 \cdot 10^8 \text{ N/mm}^2$$

Column Strip AB (Figure 12)

$$\chi_1 = \frac{-34 \cdot 10^6}{32700 \cdot 6.67 \cdot 10^8} = -1.56 \cdot 10^{-6}\text{mm}^{-1}$$

$\chi_2 = 4.50 \cdot 10^{-6}\text{mm}^{-1}$; assessed by means of nonlinear sectional analysis

$$\chi_3 = \frac{-69 \cdot 10^6}{32700 \cdot 6.67 \cdot 10^8} = -3.17 \cdot 10^{-6}\text{mm}^{-1}$$

$$\delta_{AB} = \frac{5700^2}{96} \cdot (-1.56 \cdot 10^{-6} + 10 \cdot 4.50 \cdot 10^{-6} - 3.17 \cdot 10^{-6}) = 13.62 \text{ mm}$$

Column Strip CD (Figure 12)

$$\chi_1 = \frac{-36 \cdot 10^6}{32700 \cdot 6.67 \cdot 10^8} = -1.65 \cdot 10^{-6}\text{mm}^{-1}$$

$\chi_2 = 5.26 \cdot 10^{-6}\ \text{mm}^{-1}$; assessed by means of nonlinear sectional analysis

$$\chi_3 = \frac{-73 \cdot 10^6}{32700 \cdot 6.67 \cdot 10^8} = -3.35 \cdot 10^{-6}\text{mm}^{-1}$$

$$\delta_{CD} = \frac{5700^2}{96} \cdot (-1.65 \cdot 10^{-6} + 10 \cdot 5.26 \cdot 10^{-6} - 3.35 \cdot 10^{-6}) = 16.11 \text{ mm}$$

Middle Strip EF (Figure 12)

$$\chi_1 = \frac{0 \cdot 10^6}{32700 \cdot 6.67 \cdot 10^8} = 0\ \text{mm}^{-1}$$

$\chi_2 = 1.47 \cdot 10^{-6}\text{mm}^{-1}$; assessed by means of nonlinear sectional analysis

$$\chi_3 = \frac{-25 \cdot 10^6}{32700 \cdot 6.67 \cdot 10^8} = -1.14 \cdot 10^{-6}\text{mm}^{-1}$$

$$\delta_{EF} = \frac{6000^2}{96} \cdot (0 + 10 \cdot 1.47 \cdot 10^{-6} - 1.14 \cdot 10^{-6}) = 5.08 \text{ mm}$$

Total deflection

$$\delta_{tot} = \frac{13.62 + 16.11}{2} + 5.08 = \mathbf{20.0\ mm}$$

The studied HRC alternative evidenced sufficient ductility in accordance with MC 2010 [19], considering that $5 \cdot \delta_{SLS} = 16$ mm (section 4.2).

Taking into account a significant number of aspects covered by the proposed approach, the Figure A1 is aimed at presenting the structured sequence of the required steps to carry out the design procedure of FRC/HRC column-supported flat slabs in terms of flexural behaviour, cracking control, and instantaneous deformations. Each transitional step to perform the analysis is complemented by the reference to the certain information of the manuscript, facilitating the identification of the latter for more comprehensive study of the theoretical base.

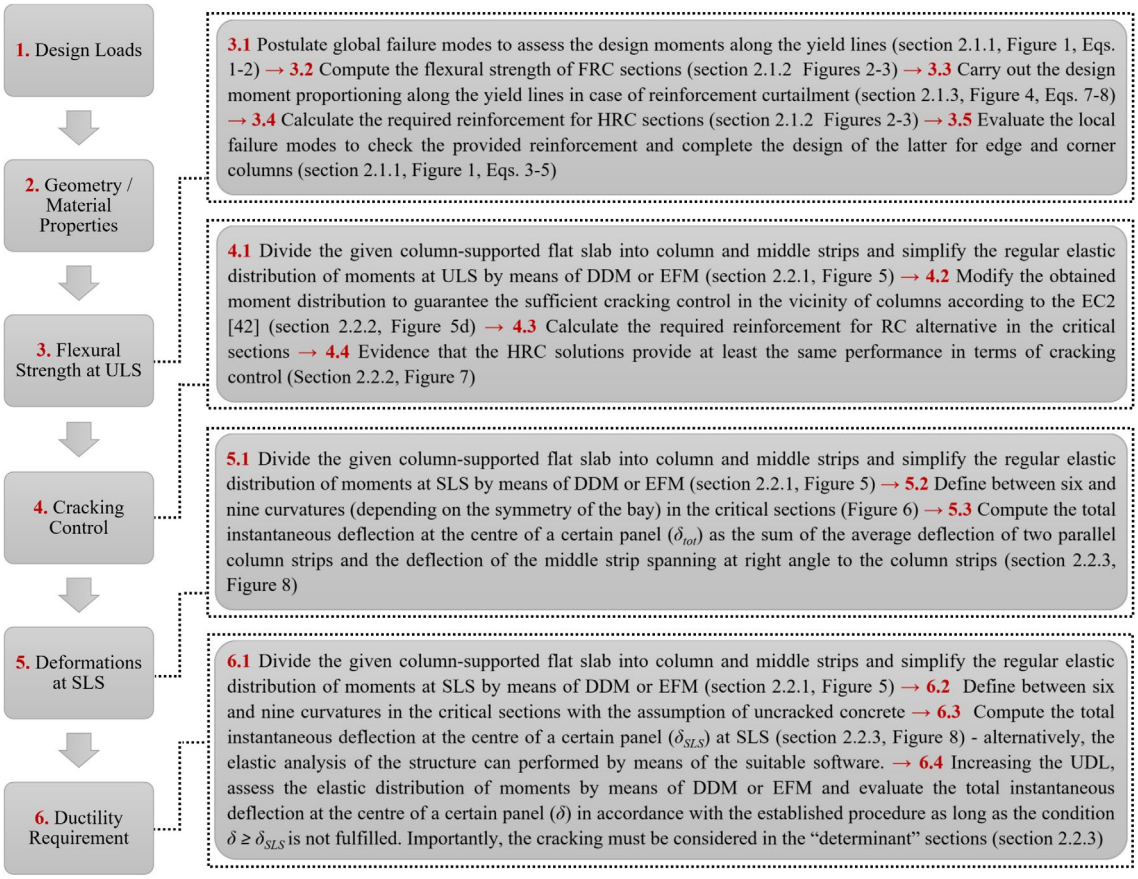

Fig. A1 Flowchart of the algorithm of the proposed method

ACKNOWLEDGMENTS

This research has been possible owe to the economic funds provided by the SAES project (BIA2016-78742-C2-1-R) of Spanish Ministerio de Economía, Industria y Competitividad. The first author, personally, thanks the Department of Enterprise and Education of Catalan Government for providing support through the PhD Industrial Fellowship (2018 DI 77) in collaboration with Smart Engineering Ltd. (UPC's Spin-Off).

REFERENCES

[1] Blanco A, Pujadas P, de la Fuente A, Cavalaro SHP, Aguado A. Influence of the type of fiber on the structural response and design of FRC slabs. J Struct Eng (United States) 2016;142:1–11. https://doi.org/10.1061/(ASCE)ST.1943-541X.0001515.

[2] di Prisco M, Colombo M, Pourzarabi A. Biaxial bending of SFRC slabs: Is conventional reinforcement necessary? Mater Struct Constr 2019;52:1–15. https://doi.org/10.1617/s11527-018-1302-0.

[3] Fall D, Shu J, Rempling R, Lundgren K, Zandi K. Two-way slabs: Experimental investigation of load redistributions in steel fibre reinforced concrete. 2014. https://doi.org/10.1016/j.engstruct.2014.08.033.

[4] Pujadas P, Blanco A, Cavalaro S, Aguado A. Plastic fibres as the only reinforcement for flat suspended slabs: Experimental investigation and numerical simulation. Constr Build Mater 2014;57:92–104. https://doi.org/10.1016/j.conbuildmat.2014.01.082.

[5] Michels J, Waldmann D, Maas S, Zürbes A. Steel fibers as only reinforcement for flat slab construction - Experimental investigation and design. Constr Build Mater 2012;26:145–55. https://doi.org/10.1016/j.conbuildmat.2011.06.004.

[6] Facconi L, Minelli F, Plizzari G. Steel fiber reinforced self-compacting concrete thin slabs – Experimental study and verification against Model Code 2010 provisions. Eng Struct 2016;122:226–37. https://doi.org/10.1016/j.engstruct.2016.04.030.

[7] Falkner H. STEEL FIBRE AND POLYMERE CONCRETE BASICS , MODEL CODE 2007 AND APPLICATIONS 2007:381–400.

[8] Aidarov S, Mena F, de la Fuente A. Structural response of a fibre reinforced concrete pile-supported flat slab: full-scale test. Eng Struct 2021;239. https://doi.org/10.1016/J.ENGSTRUCT.2021.112292.

[9] Barros J, Salehian H, Pires M, Gonçalves D. Design and testing elevated steel fibre reinforced self-compacting concrete slabs. Fibre Reinf Concr 2012:1–12.

[10] Destrée X, Mandl J. Steel fibre only reinforced concrete in free suspended elevated slabs: Case studies, design assisted by testing route, comparison to the latest SFRC standard documents. Tailor Made Concr Struct 2008:437–43.

[11] Gossla U. Development of SFRC Free Suspended Elevated Flat Slabs. Aachen: 2005.

[12] Hedebratt J, Silfwerbrand J. Full-scale test of a pile supported steel fibre concrete slab. Mater Struct Constr 2014;47:647–66. https://doi.org/10.1617/s11527-013-0086-5.

[13] Parmentier B, Itterbeeck P Van, Skowron A. The flexural behaviour of SFRC flat slabs : the Limelette full- scale experiments for supporting design model codes. Proc. FRC, 2014.

[14] Maturana Orellana A. Estudio teórico-experimental de la aplicabilidad del hormigón reforzado con fibras de acero a losas de forjado multidireccionales. 2013. https://doi.org/10.1174/021435502753511268.

[15] Mandl J. Flat Slabs Made of Steel Fiber Reinforced Concrete (SFRC). CPI Worldw., 2008.

[16] Karv C. Shear and punching resistance of steel fibre reinforced concrete slabs. Aalto University, 2017.

[17] Salehian H, Barros JAO. Prediction of the load carrying capacity of elevated steel fibre reinforced concrete slabs. Compos Struct 2017;170:169–91. https://doi.org/10.1016/j.compstruct.2017.03.002.

[18] Ministerio de Fomento. Instrucción de Hormigón Estructural (EHE-08). 2008. https://doi.org/10.1017/CBO9781107415324.004.

[19] fib. fib Model Code for Concrete Structures 2010. 2010.

[20] Italian National Research Council. CNR. CNR-DT 204 /2006 Guide for the Design and Construction of Fiber-Reinforced Concrete Structures. Rome: 2006.

[21] German Society for Concrete and Construction Technology. DBV. Guide to Good Practice "Steel Fibre Concrete." Berlin: 2001.

[22] RILEM TC 162-TDF. Recommendations of RILEM TC 162-TDF: Test and design methods for steel fibre reinforced concrete: bending test. Mater Struct 2002;35:579–82. https://doi.org/10.1617/14007.

[23] ACI Committee 544. Report on Design and Construction of Steel Fiber-Reinforced Concrete Elevated Slabs. 2004.

[24] di Prisco M, Martinelli P, Dozio D. The structural redistribution coefficient KRd: a numerical approach to its evaluation. Struct Concr 2016;17:390–407. https://doi.org/10.1002/suco.201500118.

[25] Maturana A, Canales J, Orbe A, Cuadrado J. Análisis plástico y Ensayos de Losas multidireccionales de HRFA. Inf La Construcción 2014;66:e031. https://doi.org/10.3989/ic.13.021.

[26] Choi KK, Reda Taha MM, Park HG, Maji AK. Punching shear strength of interior concrete slab-column connections reinforced with steel fibers. Cem Concr Compos 2007;29:409–20. https://doi.org/10.1016/j.cemconcomp.2006.12.003.

[27] Gouveia ND, Fernandes NAG, Faria DMV, Ramos AMP, Lúcio VJG. SFRC flat slabs punching behaviour - Experimental research. Compos Part B Eng 2014;63:161–71. https://doi.org/10.1016/j.compositesb.2014.04.005.

[28] Higashiyama H, Ota A, Mizukoshi M. Design Equation for Punching Shear Capacity of SFRC Slabs. Int J Concr Struct Mater 2011;5:35–42. https://doi.org/10.4334/ijcsm.2011.5.1.035.

[29] Ju H, Cheon NR, Lee DH, Oh JY, Hwang JH, Kim KS. Consideration on punching shear strength of steel-fiber-reinforced concrete slabs. Adv Mech Eng 2015;7:1–12. https://doi.org/10.1177/1687814015584251.

[30] Kueres D, Polak MA, Hegger J. Two-parameter kinematic theory for punching shear in steel fiber reinforced concrete slabs. Eng Struct 2020;205:110086. https://doi.org/10.1016/j.engstruct.2019.110086.

[31] Maya LF, Fernández Ruiz M, Muttoni A, Foster SJ. Punching shear strength of steel fibre reinforced concrete slabs. Eng Struct 2012;40:83–94. https://doi.org/10.1016/j.engstruct.2012.02.009.

[32] Nguyen-Minh L, Rovňák M, Tran-Quoc T, Nguyen-Kim K. Punching shear resistance of steel fiber reinforced concrete flat slabs. Procedia Eng 2011;14:1830–7. https://doi.org/10.1016/j.proeng.2011.07.230.

[33] Yang JM, Yoon YS, Cook WD, Mitchell D. Punching shear behavior of two-way slabs reinforced with high-strength steel. ACI Struct J 2010;107:468–75. https://doi.org/10.14359/51663820.

[34] Barros JAO, Moraes Neto BN, Melo GSSA, Frazão CMV. Assessment of the effectiveness of steel fibre reinforcement for the punching resistance of flat slabs by experimental research and design approach. Compos Part B Eng 2015;78:8–25. https://doi.org/10.1016/j.compositesb.2015.03.050.

[35] Tan KH, Venkateshwaran A. Punching shear in steel fiber-reinforced concrete slabs with or without traditional reinforcement. ACI Struct J 2019;116:107–18. https://doi.org/10.14359/51713291.

[36] Gödde L, Mark P. Numerical simulation of the structural behaviour of SFRC slabs with or without rebar and prestressing. Mater Struct Constr 2015;48:1689–701. https://doi.org/10.1617/s11527-014-0265-z.

[37] Teixeira MDE, Barros JAO, Cunha VMCF, Moraes-Neto BN, Ventura-Gouveia A. Numerical simulation of the punching shear behaviour of self-compacting fibre reinforced flat slabs. Constr Build Mater 2015;74:25–36. https://doi.org/10.1016/j.conbuildmat.2014.10.003.

[38] Soranakom C, Mobasher B. Numerical simulation of FRC round panel tests and full-scale elevated slabs. ACI Spec Publ 2007;248:31–40.

[39] Salehian H, Barros JAO. Assessment of the performance of steel fibre reinforced self-compacting concrete in elevated slabs. Cem Concr Compos 2015;55:268–80. https://doi.org/10.1016/j.cemconcomp.2014.09.016.

[40] Nogales A, de la Fuente A. Numerical-aided flexural-based design of fibre reinforced concrete column-supported flat slabs. Eng Struct 2021;232:1–24. https://doi.org/10.1016/j.engstruct.2020.111745.

[41] Facconi L, Plizzari G, Minelli F. Elevated slabs made of hybrid reinforced concrete: Proposal of a new design approach in flexure. Struct Concr 2019;20:52–67. https://doi.org/10.1002/suco.201700278.

[42] Gödde L, Mark P. Numerical simulation of the structural behaviour of SFRC slabs with or without rebar and prestressing. Mater Struct Constr 2015;48:1689–701. https://doi.org/10.1617/s11527-014-0265-z.

[43] EN 1992-1-1. Eurocode 2: Design of concrete structures: General rules and rules for buildings. Brussels: CEN; 2004. https://doi.org/[Authority: The European Union Per Regulation 305/2011, Directive 98/34/EC, Directive 2004/18/EC].

[44] Johansen KW. Yield-line theory. Cement and Concrete Association; 1962.

[45] Johansen KW. Yield-line formulae for slabs. Cement and Concrete Association; 1972.

[46] Johansen KW. Brudlinieteorier. Denmark: København : Gjellerups; 1943.

[47] Kennedy G, Goodchild CH. Practical Yield Line Design. Surrey, UK: Concrete Centre; 2004.

[48] Moss RM. Approaches to the design of reinforced concrete flat slabs. Construction Research Communications Limited by permission of Building Research Establishment; 2001.

[49] Gesund H, Dikshit OP. Yield line analysis of the punching problem at slab/column intersections. Am Concr Institute, ACI Spec Publ 1971;SP-030:177–201.

[50] CEN. EN 14651. Test method for metallic fibre concrete. Measuring the flexural tensile strength (limit of proportionality (LOP), residual). 2007.

[51] ACI Committee 544. Guide for Design with Fiber-Reinforced Concrete. Farmington Hills, MI, USA: 2018.

[52] di Prisco M, Martinelli P, Parmentier B. On the reliability of the design approach for FRC structures according to fib Model Code 2010: the case of elevated slabs. Struct Concr 2016;17:588–602. https://doi.org/10.1002/suco.201500151.

[53] Colombo M, Martinelli P, di Prisco M. On the evaluation of the structural redistribution factor in FRC design: a yield line approach. Mater Struct 2017;50:1–18. https://doi.org/10.1617/s11527-016-0969-3.

[54] Leporace-Guimil B, Mudadu A, Conforti A, Plizzari GA. Influence of fiber orientation and structural-integrity reinforcement on the flexural behavior of elevated slabs. Eng Struct 2022;252:113583. https://doi.org/10.1016/j.engstruct.2021.113583.

[55] Conforti A, Cuenca E, Zerbino R, Plizzari GA. Influence of fiber orientation on the behavior of fiber reinforced concrete slabs. Struct Concr 2021;22:1831–44. https://doi.org/10.1002/suco.202000612.

[56] Blanco A, Pujadas P, Fuente A De, Cavalaro SHP, Aguado A. Assessment of the fibre orientation factor in SFRC slabs. Compos PART B 2015;68:343–54. https://doi.org/10.1016/j.compositesb.2014.09.001.

[57] Laranjeira F, Aguado A, Molins C, Grünewald S, Walraven J, Cavalaro S. Framework to predict the orientation of fibers in FRC: A novel philosophy. Cem Concr Res 2012;42:752–68. https://doi.org/10.1016/j.cemconres.2012.02.013.

[58] Joint ACI-ASCE Committee 421. Guide to Design of Reinforced Two-Way Slab Systems. Farmington Hills, MI, USA: 2015.

[59] Montoya J, Meseguer Á, Morán F, Arroyo J. Hormigón Armado. 2011.

[60] Jofriet JC. Flexural Cracking of Concrete Flat Plates. J Am Concr Inst 1973;70:805–9. https://doi.org/10.14359/7139.

[61] Brotchie JF, Russel JJ. Flat Plate Structures I. Elastic-Plastic Analysis. Am Concr Inst 1964:959–96.

[62] ACI. Control of Cracking in Concrete Structures, ACI Manual of Concrete Practice. ACI Comm 224 2008:224.2R-1–12.

[63] ACI. 318-14 - Building Code Requirements for Structural Concrete and Commentary. 2014.

[64] Nawy E. Crack Control in Reinforced Concrete Structures. ACI J Proc 1968;65:825–36. https://doi.org/10.14359/7515.

[65] Orenstein G, Nawy E. Crack Width Control in Reinforced Concrete Two-Way Slabs Subjected To a Uniformly Distributed Load. Am Concr Inst-J 1970;67:57–61. https://doi.org/10.14359/7259.

[66] The Concrete Society. Technical Report No. 64. Guide to the design and construction of reinforced concrete flat slabs. Camberley, UK: 2007.

[67] Blanco A, Pujadas P, de la Fuente A, Cavalaro S, Aguado A. Application of constitutive models in European codes to RC-FRC. Constr Build Mater 2013;40:246–59. https://doi.org/10.1016/j.conbuildmat.2012.09.096.

[68] Pujadas P, Blanco A, de la Fuente A, Aguado A. Cracking behavior of FRC slabs with traditional reinforcement. Mater Struct Constr 2012;45:707–25. https://doi.org/10.1617/s11527-011-9791-0.

[69] Tiberti G, Minelli F, Plizzari G. Cracking behavior in reinforced concrete members with steel fibers: A comprehensive experimental study. Cem Concr Res 2015;68:24–34. https://doi.org/10.1016/j.cemconres.2014.10.011.

[70] Groli G, Caldentey AP. Improving cracking behaviour with recycled steel fibres targeting specific applications – analysis according to fib Model Code 2010. Struct Concr 2017;18:29–39. https://doi.org/10.1002/suco.201500170.

[71] Tošić N, Pecić N, Poliotti M, Marí A, Torres L, Dragaš J. Extension of the ζ-method for calculating deflections of two-way slabs based on linear elastic finite element analysis. Struct Concr 2021.

[72] The Concrete Society. Technical Report No. 58. Deflections in Concrete Slabs and Beams. Camberley, UK: Concrete Society; 2005.

[73] Ghali A. Prediction of deflections of two-way floor systems. ACI Struct J 1989;86:551–62. https://doi.org/10.14359/3283.

[74] Beeby AW. A radical redesign of the in-situ concrete frame process, Task 4: Early striking of formwork and forces in backprops. London: 2000.

[75] Chang K-Y, Hwang S-J. Practical estimation of Two-Way Slab Deflections 1996;122:150–9.

[76] Kripanarayanan KM, Branson DE. Short-Time Deflections of Flat Plates, Flat Slabs, and Two-Way Slabs. J Am Concr Inst 1976;73:686–90. https://doi.org/10.14359/11107.

[77] Nilson AH, Walters DB. Deflection of Two-Way Floor Systems By the Equivalent Frame Method. J Am Concr Inst 1975;72:210–8. https://doi.org/10.14359/11132.

[78] Timoshenko S, Woinowsky-Krieger S. Theory of plates and shells. McGraw-Hill; 1959.

[79] Tošić N, Aidarov S, de la Fuente A. Systematic Review on the Creep of Fiber-Reinforced Concrete. Materials (Basel) 2020;13:5098. https://doi.org/10.3390/ma13225098.

[80] Ghali A, Favre R, Elbadry M. Concrete Structures. Stesses and Deformation - Third Edition. vol. 4. 1999.

[81] Galeote E, Blanco A, de la Fuente A. Design-oriented approach to determine FRC constitutive law parameters considering the size effect. Compos Struct 2020;239:112036. https://doi.org/10.1016/j.compstruct.2020.112036.

[82] Gobierno de España. Código Técnico de la Edificación (CTE) Documento básico: Seguridad estructural. Apartado de "Acciones en la Edificación" 2009.

[83] Mena F, Aidarov S, de la Fuente A. Hormigones autocompactantes reforzados con fibras para aplicaciones con alta responsabilidad estructural. Campaña experimental en laboratorio. III Congr. Consult. Estructuras, 2019, p. 1–10.

[84] Galeote E, Blanco A, Cavalaro SHP, de la Fuente A. Correlation between the Barcelona test and the bending test in fibre reinforced concrete. Constr Build Mater 2017;152:529–38. https://doi.org/10.1016/j.conbuildmat.2017.07.028.

[85] Cavalaro SHP, Aguado A. Intrinsic scatter of FRC: an alternative philosophy to estimate characteristic values. Mater Struct Constr 2015;48:3537–55. https://doi.org/10.1617/s11527-014-0420-6.

[86] EN 1992-2. Eurocode 2: Design of concrete structures: Concrete bridges: Design and detailing rules. 2005.

[87] CSI. SAP2000 Integrated Software for Structural Analysis and Design 2021.

[88] Cervenka V. SIMULATING A RESPONSE. Concr Eng Int 2000;4:45–9.

[89] Červenka V, Jendele L, Červenka J. ATENA Program Documentation: Part 1. Theory. Prague: 2011.

[90] Cervenka V. Global safety formats in fib Model Code 2010 for design of concrete structures. 11th Int Probabilistic Work 2013:31–40.

2.3. JOURNAL PAPER III. COST-ORIENTED ANALYSIS OF FIBRE REINFORCED CONCRETE COLUMN-SUPPORTED FLAT SLABS CONSTRUCTION

Published in Journal of Building Engineering (2022).

Stanislav Aidarov [a, b, *], Ana Nadaždi [c], Evgeniy Pugach [d], Nikola Tošić [b], Albert de la Fuente [b]

[a] Smart Engineering Ltd., UPC Spin-Off, Jordi Girona 1-3, 08034 Barcelona, Spain

[b] Civil and Environmental Engineering Department, Universitat Politècnica de Catalunya (UPC), Jordi Girona 1-3, 08034 Barcelona, Spain

[c] Faculty of Civil Engineering, University of Belgrade, Bulevar kralja Aleksandra 73, 11000 Belgrade, Serbia

[d] Department of Construction Technology and Management, Moscow State University of Civil Engineering, Yaroslavskoye Shosse 26, 129337, Moscow, Russia

* Corresponding author. Tel.: +34 633 634 207; Full Postal address: 08034, Barcelona, Jordi Girona 1; Email address: stanislav.aidarov@upc.edu ; stanislav.aydarov@smartengineeringbcn.com

Abstract

Fibre reinforced concrete (FRC) is increasingly being used in elements with high structural responsibility, the constructed FRC column-supported flat slabs (CSFSs, hereinafter) with partial or even total substitution of reinforcing steel bars being a supporting evidence for that statement. These pioneer experiences provide encouraging results with respect to resource optimization and construction time reduction without jeopardising the structural reliability. Despite such promising achievements, the use of FRC in CSFSs is still limited in the building sector. To provide an additional impulse for the use of FRC, a comprehensive comparison between FRC and traditional reinforced concrete (RC) technologies for CSFSs in terms of execution procedure and overall costs is needed. With this in mind, an industrial-oriented study was carried out with the main objective of elaborating a simplified method for the preliminary comparison of RC and FRC solutions. This method permits to assess the major amount of the required reinforcement (flexural reinforcement) followed by an evaluation of the time saving effect due to the partial or total substitution of reinforcing steel bars by fibres. For this purpose and for the sake of generalization, several databases were examined and 33 interviews with experts on *in situ* construction were conducted so that a wide range of productivity rates and other particularities could be identified. Based on the proposed method, a case study was

analysed in order to indicate the potential direct costs (materials + labour) for a number of RC and FRC solutions using data from the examined databases and conducted interviews. The results reflect an increment of direct costs for both fibre and hybrid (fibre + reinforcing steel bars, HFRC) solutions; however, these increment can be compensated by the reduction of the construction period and, as a consequence, time-dependent costs (i.e., preliminaries, equipment costs, overheads, and finance costs). The outcomes of this research are meant to prove support to designers and construction planners with regard to the suitability of using FRC for CSFSs.

Keywords: elevated slab, two-way slab, fibre reinforced concrete, hybrid reinforced concrete, construction process, cost analysis, comparative study

Nomenclature

List of symbols

A_s	area of reinforcement
b	section width
C_f	fibre content
$CMOD$	crack mouth opening displacement
d	section depth
f_c	cylinder compressive strength of concrete
f_{Ftu}	ultimate residual strength for FRC
f_L	limit of proportionality
$f_{R,i}$	residual flexural tensile strength of FRC corresponding to $CMOD_i$
f_{uf}	fibre tensile strength
f_y	yield strength of reinforcing steel in tension
h	overall depth of member
L_f	fibre length
M_E	value of applied moment
M_R	value of resistant moment
$Ø_f$	fibre diameter
q_G	permanent load
q_Q	variable load
q_S	combination of acting loads
q_{SW}	self–weight load
V_f	volume fraction of fibres
x	depth of compression zone
γ_c	partial safety factor for concrete
γ_F	partial safety factor for FRC
γ_G	partial safety factor for permanent loads
γ_Q	partial safety factor for variable loads
ε_{cu}	ultimate compressive strain in the FRC
ε_{Fu}	ultimate tensile strain in the FRC

General subscripts

m	mean value of the variable
k	characteristic value of the variable
d	design value of the variable
FRC	fibre reinforced concrete
$HFRC$	hybrid-reinforced FRC

1. INTRODUCTION

Flat slabs are amongst the most popular forms of *in situ* concrete frame construction [1]. This structural element typically constitutes 80-90% of the cost of a concrete frame [2], whereas the latter may represent about 10% of the cost of a multi-storey building [3]. Moreover, the construction of a concrete frame tends to take, in general, 50% of the overall duration of the project, this process being a governing factor of the critical path for the completion of the building [1].

Taking this into account, research is conducted in order to provide innovative solutions for concrete frame construction which may reduce both direct and time-dependent costs without jeopardising the performance of the structure at both ultimate and serviceability limit states (ULS and SLS, respectively). One of the most promising achievements is the use of fibre reinforced concrete (FRC) in two-way slabs with the purpose of substituting partially (hybrid-reinforced FRC, hereafter referred to as HFRC) or even totally, the steel bar reinforcement (reinforced concrete, RC).

In this regard, results derived from real-scale tests (Table 1) allow confirming the flexural [4–6] and punching strength [7–9], redistribution capacity [10–13], ductility [4,14,15], deformation and cracking control [5,10,16] of FRC slabs in statically indeterminate structures. The reported results prompted the implementation of this technology for the construction of a dozen buildings with further recognition of positive outcomes with respect to the optimization of resources and reduction of construction time [17–19]. A detailed cost comparison between steel fibre reinforced concrete (SFRC) and traditional solutions for a real project was reported by Orellana [17] – 12% reduction of total costs was achieved through using an HFRC flat slabs for the construction of the LKS office building in Spain.

Despite the successful experiences of FRC slab construction, the widespread use of this technology is still hindered because of a number of factors related to the general comprehension of the material's properties, design procedure, and comparative analysis of potential alternatives. In this sense, numerous research programmes were (and are) focused on the material characterization of FRC [28–32] and elaboration of design approaches [33–36] to precisely evaluate the structural response of FRC elements.

In contrast, a limited number of studies were aimed at explicitly identifying the potential of FRC column-supported flat slabs with regard to its possible economic benefits. This aspect is of paramount importance, especially, in the light of the fact that construction companies tend to compare only the material costs disregarding the manpower and time-dependent costs – variables that have strong influence on the overall comparative cost analysis.

With this in mind, a straightforward method for the preliminary comparison of the RC, HFRC, and FRC flat slab solutions was developed. This method permits to assess the major amount of the required reinforcement (flexural reinforcement) followed by an evaluation of the time saving effect due to the use of structural fibres. Several national and international construction databases were examined to determine both the cost and production rates for concrete CSFSs. Moreover, 33 experts were interviewed to (1) verify and

complement the obtained information and (2) to identify and quantify sources of deviation of the construction activities performance rates.

Implementing the elaborated method, a 30.3 × 18.3 × 0.2 m slab supported by 24 columns with square cross sections of 0.3 m was considered as case study. Four different alternatives derived from varying the amount of fibres were assessed: RC, FRC and two HFRC solutions. The material and labour costs were calculated in accordance with the examined databases – some extra costs respect to the RC traditional solution were identified for the HFRC and FRC alternatives. The results' analysis proved that a significant reduction of the construction span was achieved due to use of FRC and that the influence of the time-dependent costs could be the driver when the use of fibres as steel bar replacement is a decision to be made.

Table 1. Experimental research programmes focused on SFRC two-way slabs

Authors	Parameters of SFRC slabs				Loading Conditions	
	Type	C_f [kg/m^3]	L_{max}/h [m/m]	Steel Bars	ULS	SLS
di Prisco et al. (2019) [5]	SSLT	35	13	Yes/None		●
Blanco et al. (2016) [10]	SSLT	40	15	None		●
Leporace-Guimil et al. (2022) [20]	SSLT	50	17	None		●
Fall et al. (2014) [12]	SSLT	35	28	Yes/None		●
Facconi et al. (2016) [14]	SSLT	20/25	32	None		●
Facconi et al. (2016) [14]	SSLT	25	32	None		●
Barros et al. (2012) [21]	FSFT	90	16	Yes*		●
Salehian et al. (2012) [22]	FSFT	90	16	Yes*	●	●
Destreé et al. (2008) [23]	FSFT	45	19	No		●
Hedebratt et al. (2014) [24]	FSFT	40/80	23	Yes/None		●
Døssland (2008) [25]	FSFT	62	23	Yes/None		●
Destreé et al. (2008) [23]	FSFT	100	28	Yes*		●
Gossla (2005) [26]	FSFT	100	30	Yes*	●	●
Parmentier et al. (2014) [27]	FSFT	70	30	Yes*	●	●
Aidarov et al. (2021) [4]	FSFT	70	30	Yes*	●	●

2. METHODOLOGY

This study is subdivided into five parts as shown in Figure 1. Part I describes the framework to evaluate the viability of RC, HFRC, and FRC solutions for CSFSs. Initially, the design procedure to assess the flexural behaviour of each alternative is covered. This approach is oriented to assess the reduction of the steel bar amount owing to the contribution of fibres. Likewise, technological aspects related with the construction operations involved in the erection of the elevated slabs are described; especially, those processes that are to be modified

due to use of FRC. Finally, the economic aspects related with the construction of the residential and office buildings are identified and discussed.

Part II is focused on the examination of databases in order to explore the production rates and corresponding costs associated to the construction of column-supported flat slabs, which is mainly comprised of: (1) formwork installation, (2) reinforcement fixing, (3) concrete placement, and (4) formwork striking. For this purpose, the commercial Spanish database BEDEC [37] along with Serbian [38] and Russian [39] national databases were studied aiming at covering a representative both geographic and economic conditions. As mentioned, information on reinforcement fixing and concrete pouring productivity rates was complemented by the data reported from interviewing 33 experts on *in situ* concrete works, this permitting to establish frequency histograms for these rates.

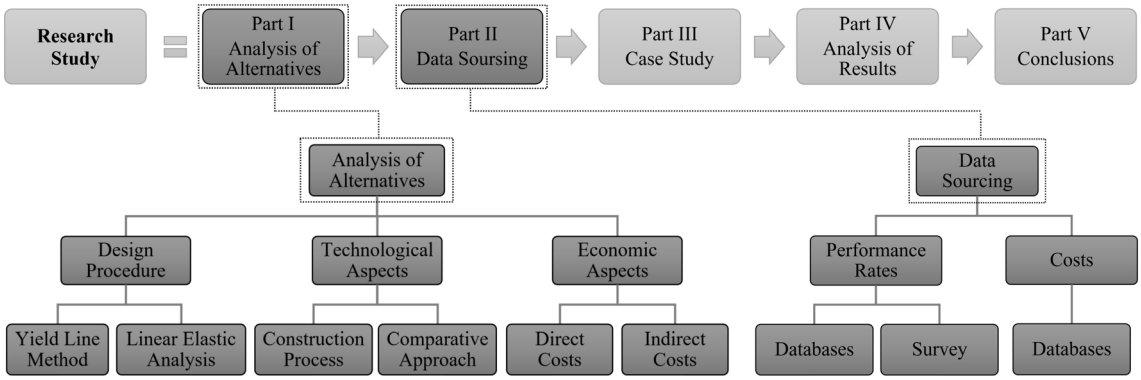

Fig. 1. Outline of the study

In Part III, a CSFS was designed considering RC, HFRC, and FRC solutions. Based on the results obtained, Part IV is focused on assessing, for each solution: (1) the required amount of traditional reinforcement, (2) the potential reduction of the construction period, and (3) material and labour costs for three different countries: Spain, Serbia, and Russia, i.e. varying the production rates and direct costs in accordance with the examined databases. Additionally, with the purpose of examining the sensitivity of the results, the reduction of the construction period along with the correspondent direct costs are computed by introducing the cumulative distribution functions of the production rates. Finally, in Part V conclusions are derived, and topics requiring further investigation identified.

3. ANALYSIS OF ALTERNATIVES

3.1. DESIGN PROCEDURE

Fibre reinforcement can substitute (even totally) traditional reinforcement at ULS as long as the material meets the following relationships: $f_{R1k}/f_{Lk} > 0.4$ and $f_{R3k}/f_{R1k} > 0.5$ [40], where f_{Lk} is the characteristic limit of proportionality and f_{R1k}, f_{R3k} are the characteristic values of the residual flexural tensile strengths at the crack mouth opening displacement (CMOD) of 0.5 mm and 2.5 mm, respectively. Once the above-mentioned conditions are fulfilled by FRC, various combinations of "fibre + steel bar" (HFRC solutions) may be suitable for providing structural reliability at both SLS and ULS for CSFSs, i.e. increasing f_R up to a magnitude beyond which steel bars are unnecessary. Depending on the geometry and load conditions, there exist solutions that lead to reductions of the steel amount (fibres with/out steel bars) per

volume of concrete [36]. These solutions, although presenting an equivalent bearing capacity, might differ in costs and construction time.

Taking into account the significant number of variables involved in the reinforcement optimization problem, a straightforward pre-design approach is proposed herein. For this purpose, the Yield Line Method (YLM) [41–43] is implemented owing to its proven capacity to simulate the failure mechanism of flat slabs. Furthermore, YLM is accepted for the design of RC slabs in national [44] and international standards [40,45] and, particularly for FRC and HFRC flat slabs, in the ACI 544 recommendations [46] and other scientific contributions [4,12,21,27].

Alternatively, linear elastic analysis (LEA) can be performed to obtain the bending moments due to the applied external loads (M_{Ed}); LEA being recommended in case of HFRC flat slabs. The design value of the resisting bending moment of the hybrid reinforced section ($M_{Rd,HFRC}$, Eq. 1) can be computed by assuming a simplified rigid-plastic model for simulating both compression and residual tension performance of FRC at ULS (Figure 2).

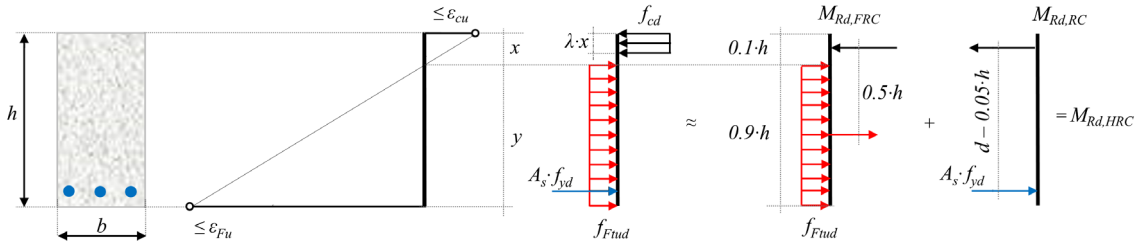

Fig. 2. Simplified sectional model to assess flexural strength of HRC

The design value of the residual tensile strength of the FRC (f_{Ftud}) can be expressed as $f_{Ftu,d} = f_{R3k}/(3\gamma_F)$, $\gamma_F = 1.50$ being the partial safety factor for FRC (compression and tension). Detailed description of the design of HFRC elevated slabs by means of LEA can be found elsewhere [36]. Thereafter, the resisting bending moment to be provided by steel rebars ($M_{Rd,RC}$, Eq. 2) can be approximated as the excess of bending moment $M_{Ed} - M_{Rd,FRC}$, where $M_{Rd,FRC}$ is the design value of the resisting bending moment due to the FRC (Eq. 3).

$$M_{Rd} = M_{Rd,FRC} + M_{Rd,RC} \quad (1)$$

$$M_{Rd,RC} = A_s \cdot f_{yd} \cdot (d - 0.05 \cdot h) \quad (2)$$

$$M_{Rd,FRC} = 0.45 \cdot f_{Ftu,d} \cdot h^2 \cdot b \quad (3)$$

Once both the mechanical performance of FRC (in terms of f_{R3k}) and fibre type is established, the fibre content (C_f) that meets this material performance should be obtained to quantify the material costs. At pre-design level, a reliable value of C_f for a specific concrete class and workability is unlikely to be known by the designer unless this gathers a large database of FRC characterization results and/or the fibre supplier provides the relevant data.

Alternatively, the designer can deduce an estimation of C_f by resorting to semi-empirical statistical correlations. For instance, Tiberti et al. [31] reported an extensive FRC flexural performance characterization on notched beams – tested under the three point bending tests (3PBTs) according to the EN 14651 [47] – comprising 528 beams with different fibre dosages and different both mechanical and geometric properties of the fibres, as well as

a variety of concrete matrices. Based on the results and a comprehensive regression analysis, the Equation 4 was proposed to estimate the mean value of f_{R3m}, where $f_{cm,cube}$ is the mean cube compressive strength of concrete (in MPa); V_f is the volume fraction of fibres; L_f / $Ø_f$ is the aspect ratio; and f_{uf} is the fibre tensile strength (in GPa). The accepted relation f_k/f_m = 0.7 might be assumed to obtain f_{R3k}.

$$f_{R3m} = \sqrt{f_{cm,cube}} \cdot 1.430 \cdot \left[V_f \cdot \left(L_f / Ø_f\right) \cdot f_{uf}\right] \quad (4)$$

3.2. TECHNOLOGICAL ASPECTS

The design of RC/HFRC/FRC solutions for CSFSs should be sensitive to the construction procedure. In this regard, the construction of elevated slabs consists of the following main activities: (1) shoring of successive floors (formwork installation), (2) reinforcement fixing, and (3) concrete pouring (Figure 3). Despite the limited number of activities, similar projects could be developed with significant differences because of multiple factors related to the working hours and shifts per day, machinery and shoring systems available, site conditions, project location, size and skills of the crew, etc. The objective of this section is to describe the general effect of partial or total substitution of traditional reinforcement by fibres on the main construction phases.

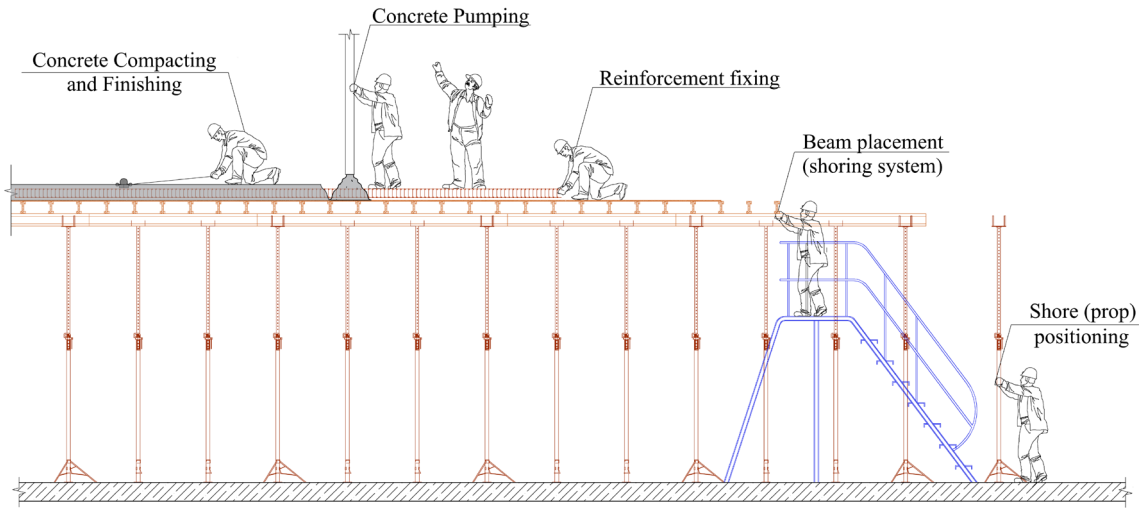

Fig. 3. Activities involved in flat slab construction (schematic representation)

Primarily, the addition of fibres to the concrete mix requires the modification of the material granular skeleton in order to provide sufficient workability. Moreover, it is recommendable to guarantee self-compactability of the composite since vibration of FRC may have a negative influence on fibre orientation and, as a consequence, bearing capacity [17,21]. Self-compactability requires the amount of cement and fine aggregates to be increased, this leading to a consequent increase of the concrete costs while a reduction of the vibration costs.

The reduction in reinforcement placement allows: (1) reducing the crew size (steel fixers) maintaining the same construction rate or (2) accelerating the erection of a storey with the same initial crew. This activity depends on the skill of the crew along with socio-economic and organizational factors. For instance, Proverbs et al. [48] reported significant differences between reinforcement fixing productivity rates in France, Germany, and UK, highlighting

that the coefficient of variation values were exceptionally high in each of the three countries (up to 90%). Christian and Hachey [49], focused their analysis on the effects of delay times on production rates in construction. The study revealed that 37% of time was non-productive for a typical concrete worker: 4% idle, 4% waiting for supervision, and 29% waiting for materials. For reinforcement fixing activities these percentages can be, to a certain extent, assumed in case of insufficient site management. Accordingly, the production rates could also have a noticeable impact on the comparative analysis of the alternatives.

The construction rate to be achieved determine the construction sequence to be implemented. This can consist of: (1) shoring/striking (SS), (2) shoring/clearing/striking (SCS), and (3) shoring/reshoring/striking (SRS) [50]. Recent studies have proven that the proper shoring system may lead to a positive effect on either rental or depreciation costs [51–53]. Additionally, for HFRC/FRC solutions, the flexural tensile strength ($f_{ct,fl}$) tends to be higher (by 30-35%) respect to that of a RC due to the concrete mix composition and, hence, the shoring time could be shortened in the former alternatives [51].

For a preliminary cost analysis, sufficient for decision-making on concrete reinforcement strategy, the productivity rates and corresponding crew sizes are the necessary data to evaluate the sequence and duration of the main activities. With these established, the portions of those activities (e.g., steel bar placing and fixing) that extend the critical path of the project should be identified and quantified. Then, by comparing the duration of the activities that drive the critical construction path of each alternative, the potential reduction of the construction period can be estimated.

3.3. ECONOMIC ASPECTS

The information generated for each alternative (RC, HFRC, and FRC) in conjunction with the estimation of required labour inputs and potential critical paths of the project permit to assess the cost-efficiency of those. For this purpose, the straightforward approach is the direct comparison of the material costs. The differences arise from the reinforcement ratio (fibres with/out steel bars) and the concrete mix. The concrete mix for HFRC/FRC, as it was discussed previously, should have a suitable workability to avoid vibration during the placement of the material. The increase of both cement and fine aggregates amount (and the use of superplasticizers) to comply with this requirement lead to an increase of compressive concrete strength (f_{ck}). Assuming that a concrete C30 (classification from the *fib* Model Code 2010 [40], f_{ck} = 30 N/mm^2) is representative for a traditional RC flat slabs for buildings (i.e. offices and residential), the modifications necessary to achieve self-compactability of FRC can lead to a SCC45 (self-compacting concrete with f_{ck} = 45 N/mm^2). A SCC45 for HFRC/FRC alternatives can be assumed representative as per preliminary analyses. Alternatively, the concrete mixtures should be elaborated for each FRC alternative in case a more accurate analysis is required.

Thereafter, the labour costs should be calculated basing on the productivity rates of the defined crews. These costs will differ for HFRC/FRC solutions because of a number of factors: (1) the use of SCC reduces the required labour input to pour the elevated slabs, (2) the quantity of the reinforcing steel bars to be fixed is also decreased, and (3) the increased construction rate may have an influence on the shoring approach of the successive floor (SS,

SCS, or SRS, see section 3.2). In case that the shoring system is to be changed/modified, the variation of rental or depreciation costs should be also considered.

Furthermore, the time-dependent costs (preliminaries, overheads, equipment costs, etc.) should be identified and quantified. Moreover, from the client's perspective, the effect of a faster construction on the finance costs and the additional profit must be taken into account. In fact, time-related costs could be an essential factor within the comparative analysis, particularly, in case of large buildings – in such projects these costs tend to outweigh additional material costs from using innovative methods [1]. Finally, the computed material, labour, and time-related costs of alternatives are to be compared to decide the most suitable solution for the project.

4. DATA SOURCING

4.1. PRODUCTIVITY RATES

The construction of a concrete frame is highly dependent on the productivity rates of the main work operations involved in the process: erection of shoring system, reinforcement fixing, and concrete placing. Hence, the comparison of RC, HFRC, and FRC alternatives demands the scheduling of the construction period in order to assess the labour and time-dependent costs. However, productivity rates might suffer from uncertainties since productivity is a complex science, affected by numerous factors including the bias of the individual planning engineer/project manager [48].

With this in mind, a comprehensive analysis was carried out in order to (1) identify the sources of productivity rates and its magnitudes, (2) facilitate the relevant data that could be used for future studies/industrial applications, and (3) analyse the case study based on the production rates that are typically considered for real construction projects. To this end, the commercial Spanish database BEDEC (ESP) [37] along with Serbian (SRB) [38] and Russian (RUS) [39] national databases were studied to identify the productivity rates of the above-mentioned construction operations. Table 2 gathers the productivity rates established by the examined databases. These documents contain different alternatives for carrying out the same construction operation and, therefore, the goal was to identify the most matching descriptions of the required activities for a proper comparison. As a result, the installation of a girder slab shoring system was selected for the presented study, whereas it was supposed that the concrete was to be pumped for any alternative of CSFSs.

Relatively similar production rates were observed in Russian and Spanish databases. In contrast, Serbian database provided significantly different values: skilled steel fixer, theoretically, requires 60% and 67% more time to carry out the same quantity of work comparing with the established productivity rates in Russian and Spanish databases, respectively. A similar tendency was observed when analysing the concrete pouring operations: a crew of ten workers requires 0.027, 0.033, and 0.160 operative-hours to place 1 m3 of conventional concrete in accordance with Spanish, Russian, and Serbian databases, respectively.

These databases tend to present the productivity rates in general terms, disregarding possible variations of site conditions, crew skill sets, and sometimes without accounting for

the essential factors that can have an influence on the overall performance, e.g. reinforcement ratio or thickness of the element under execution. With this in mind, the study of productivity rates was extended by interviewing experts for *in situ* construction from Spain, Serbia, and Russia in order to (1) verify and complement the information obtained in the relevant databases (especially, considering that the majority of these documents are rarely updated) and (2) identify and quantify deviations of productivity rates despite the fact that all respondents from each country were working in the same cities – Barcelona, Belgrade, and Moscow.

Table 2. Productivity rates of construction operations in accordance with the analysed databases

Construction Activities	Workers[1]	Productivity Rates[2]			"S.–N-S. Workers" Ratio[3]		
		ESP	SRB	RUS[4]	ESP	SRB	RUS
Installation of shoring system, [1 m2]	S. Craftsman	0.40	0.25	0.84	1:1	5:3	–
	N-S. Craftsman	0.40	0.15				
Striking of shoring system, [1 m2]	S. Craftsman	0.20	–	0.5	1:1	0:1	–
	N-S. Craftsman	0.20	0.40				
Reinforcement fixing, [1 t]	S. Steel Fixer	12.0	20.0	25.0	≈ 1:1	1:1	–
	N-S. Steel Fixer	10.0	20.0				
Concrete placing, [1 m3]	S. Concrete Worker	0.054	0.798	0.330	1:4	1:1	–
	N-S. Concrete Worker	0.216	0.798				
SCC placing, [1 m3]	S. Concrete Worker	0.043	–	0.250	1:5	–	–
	N-S. Concrete Worker	0.216	–				

[1] ESP and SRB databases distinguished the productivity rates of Skilled (S.) and Non-Skilled (N-S.) workers

[2] Productivity rates are presented in operative-hours per unit of construction activity, e.g. both S. and N-S. Craftsmen should spent 0.4 hours to install 1m^2 of shoring system in accordance with ESP database

[3] ESP and SRB databases suggest the certain relationship between the number of S. and N-S. workers in order to guarantee the optimal efficiency of a crew

[4] RUS database provides the average productivity rates, without distinguishing between S. and N-S. workers

The interviews were focused on the construction operations that are dependent on the possible alternatives of elevated slabs, i.e. reinforcement fixing and concrete placing. Moreover, the entry information was provided to every respondent before the interview in order to obtain more accurate data that may be especially representative for the construction of office and residential buildings. This information contained the description of the case study geometry (section 5.1) along with the assumption that the slab required 100 kg/m^3 of the reinforcing steel bars to ensure the suitable structural performance of the element. Basing on the mentioned entry conditions, respondents were asked to suggest the crew sizes and corresponding production rates of several construction operations: (1) concreting of the described slab, assuming that the activity is to be performed by the stationary pump with possible output up to 50 m^3/h; (2) concreting of the described slab by self-compacting mix, with the same equipment of (1); and (3) reinforcement fixing, supposing that the diameter of the reinforcing steel bars is 12 mm.

During the interviews, it was decided to focus on the productivity rates of the entire crews because, frequently, each construction operation is comprised of several sub-activities, e.g. the process of concrete placing can be divided into concrete pouring, vibrating and levelling of the material. Thus, the production rates of workers that are dedicated to pouring and vibrating the concrete will be different, although the joint effort leads to the slab concreting – the activity presented in databases with average productivity rates of skilled and non-skilled workers. Once the respondent evaluated the productivity rate of the entire crew for each activity, the average labour performance was calculated for a single person to compare the obtained value with that from database. Additionally, this approach permitted to gather information regarding the possible crew sizes, noticing that this parameter also varied from country to country in accordance with the received information.

Table 3 indicates the productivity rates for *in situ* concrete operations estimated by the interviewed experts from Spain, Serbia, and Russia. Attention should be paid to the reinforcement fixing activity, especially, considering that this construction operation is of paramount importance within the comparative analysis of RC, FRC, and HFRC alternatives. Despite the fact that the reinforcement fixing is mainly dependent on the manual labour, high coefficient of variation (CV) values can be observed: 25.8%, 36.0%, and 23.7%, according to results from the Spanish, Serbian, and Russian interviewed experts, respectively.

Table 3. Productivity rates of construction operations in accordance with the conducted interviews[1]

Construction Activities	Country	Number of Respondents	Productivity Rates[2]			CV, %	Crew Size[3]
			Least Efficient	Average	Most Efficient		
Reinforcement fixing, [1 t]	ES	11	26.2	11.7	9.81	25.8	5
	SRB	6	50.0	30.5	22.7	36.0	6
	RU	16	49.0	31.9	21.8	23.7	12
Concrete placing, [1 m^3]	ES	11	0.36	0.17	0.10	39.6	4
	SRB	6	0.44	0.25	0.20	25.5	6
	RU	16	0.29	0.20	0.14	24.5	7
SCC placing, [1 m^3]	ES	11	0.36	0.14	0.08	44.1	4
	SRB	6	0.30	0.13	0.08	43.0	5
	RU	16	0.21	0.15	0.11	20.4	5

[1] Respondents gave their informed consent to analyse the obtained results within the research study in question

[2] Productivity rates are presented in operative-hours per unit of construction activity

[3] Most likely crew size according to respondent's answers

From the results gathered in Table 3, it can be noticed the significant dispersion of the productivity rates. For instance, the reinforcement fixing productivity rate (in operative-hours per tonne) ranges from 26.2 to 9.81 (with an average of 11.7); 50.0 to 22.7 (30.5) and 49.0 to 21.8 (31.9) in Spain, Serbia and Russia, respectively. It must be highlighted that the average productivity rate for this activity in Spain is 2.6 times higher than that reported for Serbia and Russia and, hence, this could make FRC-based solutions more suitable for some

scenarios (i.e. those for which construction time is a decision-making driver) in Serbian and Russian regions.

Additionally, it is important to remark the distinctions between the performance rates that are suggested by databases and those confirmed by the respondents. For instance, in accordance with interviewed respondents from Spain, the average productivity rate of reinforcement fixing is two times higher than that reported within the Spanish database [37]. This stresses that productivity rates should be treated from a statistical perspective.

4.2. COSTS

The magnitude of the time-dependent costs are sensitive to the project conditions (i.e. project size, rental machinery, finance costs) and the importance given to the magnitude of those (or its fraction respect to the total costs) depends on each stakeholder involved into the project. In this regard, only the material and labour costs were identified in the cited databases and gathered in Table 4. Spanish and Russian databases [37,39] gather prices updated at 1st of June 2021 and the 1st of November 2021, respectively. Serbian database [38] gathers only the information related to the productivity rates and, thereby, material prices were established from an analysis of the market (November 2021). The labour costs in Serbia were derived from considering the average salaries and wages provided by the Statistical Office of the Republic of Serbia [54].

Table 4. Material and labour costs in accordance with the analysed databases

Country	Material Costs			Labour Costs			
				Concrete Workers		Steel Fixers	
	C30 [€/m3]	SCC, C45 [€/m3]	B500C [€/t]	S. Worker	N-S. Worker	S. Worker	N-S. Worker
ES	71.3	92.5	970.0	20.4	18.0	20.4	19.0
SRB[1]	56.8	80.0	780.0	5.0	3.0	5.0	3.0
RUS[2]	54.3	73.8	1002.0	3.7		4.2	

[1] Exchange rate was adopted as 1 € = 117.6 RSD (Serbian dinar)

[2] Exchange rate was adopted as 1 € = 83.0 RUB (Roubles)

Fibres to be used with structural purposes (i.e. replace steel bars) could be made of different material (metallic or synthetic) and geometry (aspect ratio, and anchorage type). As per material, steel macrofibres are those commonly used in case of slab elements expected to be cracked due to bending during service conditions. Nonetheless, synthetic macrofibres have proven to be also a suitable material for this application once certain design considerations are taken into account [11]. Hooked-end resulted to be the most efficient anchorage type for elements subjected to bending where both cracking control and bearing capacity at failure conditions are required. For the latter, tensile strength of the steel superior to 1,100 N/mm^2 is recommended in order to avoid premature failure of the fibres bridging cracks. Finally, for providing sufficient embedded length across cracks while guaranteeing a proper mixing and workability of the concrete, aspects ratios ($\lambda_f = L_f / Ø_f$) ranging between 50 and 80 are also advisable.

As per costs of the fibres, the national markets of each country were explored in order to (1) identify steel macrofibres with similar geometrical and mechanical properties and (2) determine the fibre prices at 1st of June 2021 for Spain and at 1st of November 2021 for Serbia and Russia (Table 5). Authors are aware that the presented prices (unlike the productivity rates) can face a significant variation within a relatively short period, especially considering current supply chain challenges (e.g., due to COVID-19, and logistic transport issues) and potentially rising inflation. However, this information was adopted to emphasize the current situation of the market and, more importantly, to carry out the analysis of the case study.

Table 5. Mechanical properties and prices of the selected fibres

Country	L_f [mm]	$Ø_f$ [mm]	f_{uf} [MPa]	Geometry	Price [€/t]
ES	60	0.75	1300	Hooked-end	1300
SRB	60	0.75	1300	Hooked-end	1180
RU	62	0.75	1500	Hooked-end	1200

5. CASE STUDY

5.1. GEOMETRY AND REINFORCEMENT LAYOUT

The selection of the geometry for the case study was oriented to reproduce common dimensions that could be representative for office and residential buildings. As a result, a 30.3 × 18.3 × 0.2 m^3 slab supported by 24 columns with square cross sections of 0.3 m was analysed. The uniform column grid (Figure 4) formed fifteen panels of 6.0 x 6.0 m^2 each.

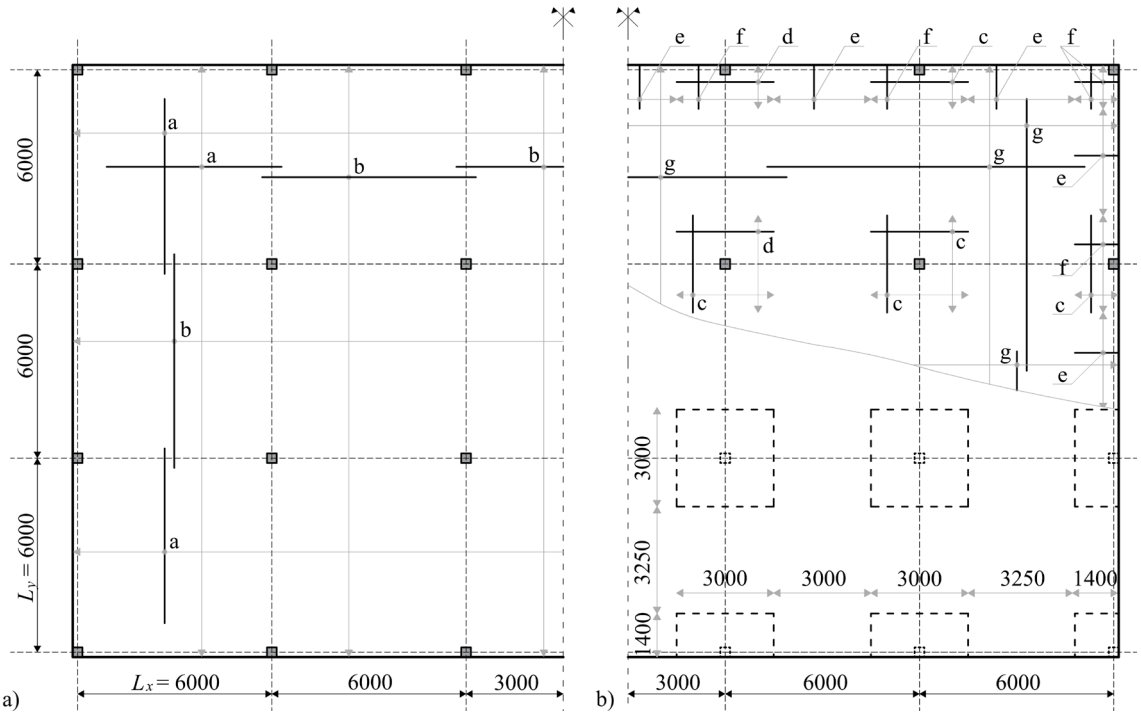

Fig. 4. Geometry of the case study along with: a) bottom reinforcement layout; b) top reinforcement layout

Additionally, Figure 4 presents the adopted reinforcement layout: the bottom reinforcement (Figure 4a) is placed across the bays whereas the specific conditions are introduced to the top reinforcement layout (Figure 4b). A continuous top mat is adopted in order to remove trip hazards before and during concrete placement [55], fulfilling the minimum required reinforcement for crack control of the slab (Clause 7.7.4.3 of the fib Model Code 2010 [40]). The rest of the top reinforcement to guarantee the adequate flexural behaviour, as per YLM, is concentrated over the columns in accordance with the following ratios: the areas of $0.5 \cdot L_x \times 0.5 \cdot L_y$, $0.5 \cdot L_{x/y} \times (0.2 \cdot L_{y/x} + \text{E.D.})$, and $(0.2 \cdot L_x + \text{E.D.}) \times (0.2 \cdot L_y + \text{E.D.})$ are respectively placed over the internal, edge, and corner columns – E.D. in the presented expressions is equal to the distance between the centreline of column to edge of the slab, i.e. edge distance. Additionally, the "U" bars were considered along the edges of the slab (reinforcing steel bars "e" and "f", Figure 4b) as it is suggested by YLM.

5.2. DESIGN ACTIONS AND MATERIAL PROPERTIES

The loads specified in the Spanish Building Code for residential buildings [56] were taken as a reference to compute the load combinations for ULS. Apart from the self-weight (q_{SW}) of 4.8 kN/m^2, a dead load (q_G) and variable load (q_Q) of 2.0 and 3.0 kN/m^2, respectively, were assumed. Load partial safety factors $\gamma_G = 1.35$ and $\gamma_Q = 1.50$ were adopted to estimate the design load at ULS: $q_{Sd} = \gamma_G \cdot (q_{SW} + q_G) + \gamma_Q \cdot q_Q = 13.7$ kN/m^2. This load was considered for the preliminary assessment of the required flexural reinforcement of each alternative (RC, FRC, and two HFRC solutions).

The RC solution was considered as reference for cost comparison purposes. The remaining three alternatives were obtained by incrementing f_{R3k} up to reaching the required q_{Sd} of 13.7 kN/m^2; this process resulting in FRC 3c, FRC 6c, and FRC 9c solutions (according to fib Model Code 2010 classification; the first number being the strength class, f_{R1k}, and c meaning that the ductility ratio f_{R3k}/f_{R1k} ranges between 0.9 and 1.1). Table 6 gathers the mechanical performance of the structural materials and the amount of fibres (C_f), in case of a FRC-based solution.

Table 6. Mechanical properties and fibre content of the considered materials

Alternative	f_{ck} [MPa]	$f_{cm,cube}$ [MPa]	f_{yk} [MPa]	f_{R3k} [MPa]	f_{R3m} [MPa]	Cf [kg/m^3][1]		
						ESP	SRB	RUS
RC	30	38	500	–	–	–	–	–
FRC 3c	45	60	500	3.4	5.8	40	40	35
FRC 6c	45	60	500	6.0	8.9	60	60	50
FRC 9c	45	60	500	9.6	12.7	85	85	75

[1] $C_f = 7850 \cdot V_f$ (see Equation 4)

The characteristic cylinder compressive strengths (f_{ck}) of 30 MPa and 45 MPa were assigned for RC and FRC solutions, respectively. The established values of f_{ck} permitted to compute $f_{cm,cube}$ according to the Clause 5.1.4 of the *fib* Model Code 2010 [40]. The characteristic yield strength of reinforcing steel in tension (f_{yk}) of 500 MPa was assumed. The mean values of f_{R3} were determined by imposing CoV of 25%, 20%, and 15% [57] for FRC 3c, FRC 6c, and FRC 9c, respectively, and considering that f_{R3} is normally distributed.

Finally, the required C_f to achieve each f_{R3m} performance was computed by means of the Equation 4 and rounded up to the nearest multiple of 5; variables presented in the Equation 4 are gathered in Table 5 (L_f, $Ø_f$, and f_{uf}) and Table 6 (f_{R3m} and $f_{cm,cube}$).

6. ANALYSIS OF ALTERNATIVES

6.1. FLEXURAL REINFORCEMENT

The case study (Figure 4) was analysed by means of YLM; the global and local collapse mechanisms were adopted allowing to compute the design bending moments along the yield lines of the studied column-supported flat slab subjected to q_{Sd} at ULS. The magnitude of these moments were calculated by means of standard formulae – the detailed description of the design procedure can be found elsewhere [13,46,58,59]. Thereafter, the amount of flexural reinforcement ($A_{s,req}$) was assessed by means of the sectional analysis (Figure 2) for each solution, varying the post-cracking residual tensile strength, i.e. FRC 3c, FRC 6c, and FRC 9c alternatives (Table 6). Nevertheless, an additional 20% of reinforcement in weight ($A_{s,disp}$) was considered to account for anchorages, splices, auxiliary reinforcement, and other purposes (i.e. adjusting to specific bar diameters).

Table 7 gathers $A_{s,disp}$, resulting in a steel bar reinforcement amount of 84.8 kg/m^3, 49.8 kg/m^3, 20.4 kg/m^3, and 0.0 kg/m^3 for RC, FRC 3c, FRC 6c, and FRC 9c alternatives, respectively. The C_f for the FRC-based solutions should be added to $A_{s,disp}$. The amount of the derived steel bar reinforcement might be slightly increased in case of FRC solutions (especially FRC 9c) by providing the structural integrity steel bars in accordance with North American Regulations [46,60]. This reinforcement should be placed in the bottom of the slab for providing continuity among columns in each direction in order to prevent local failures [61] that could lead to the collapse of the entire structure. Nevertheless, the described reinforcement will have a minor effect on the further comparative analysis and, thus, was omitted.

Table 6. Mechanical properties and fibre content of the considered materials

Reinforcement	$A_{s,req}$ [mm^2/m]				$A_{s,disp}$ [mm^2/m]			
	RC	FRC3c	FRC6c	FRC9c	RC	FRC3c	FRC6c	FRC9c
a	534	329	178	0	641	395	214	0
b	350	147	0	0	420	176	0	0
c	882	617	600	0	1058	740	720	0
d	402	161	141	0	482	193	169	0
e	267	165	89	0	320	198	107	0
f	647	439	289	0	776	527	347	0
g	232	142	0	0	278	170	0	0
Average weight of reinforcement [kg/m^3]:					84.8	49.8	20.4	0.0

6.2. CONSTRUCTION PROCESS

The construction of a concrete frame, as it was previously mentioned, can significantly differ because of multiple factors related to the working hours and shifts per day, machinery and shoring system available, site conditions, project location, size and competence of the crews, among others. Thus, a number of assumptions have to be introduced with regard to the construction process in order to assess costs and time.

In this sense, the first consists in assuming that the shoring system and the approach of its installation is the same for all alternatives; hence, time-independent costs related to this construction operation may be ignored within the comparative analysis. However, a more detailed analysis could require the evaluation of the optimum construction method of shoring the successive floors to identify and quantify variations of the rental/depreciation costs derived from construction rates and different mechanical properties of the concrete (section 3.2) – this aspect is to be further investigated in future research. The next assumptions concern the concrete placement activity – disregarding the fact that self-compacting concrete may be placed faster, it is assumed that the performance rate of this operation is mainly dependent on the concrete delivery process (by means of concrete trucks). Hence, the implementation of this type of concrete leads only to the reduction of the demanded labour input (the vibration is omitted) without affecting on the overall construction rate.

Finally, the key aspect is the potential reduction of the construction period due to partial/total substitution of steel bar reinforcement by fibres. The construction period is expected to be the determining parameter when comparing alternatives since this directly influence on the time-related costs. The assessment of the construction period requires to establish several parameters, such as (1) number of steel fixers in the crew, (2) amount of labour hours in a shift, and (3) number of shifts per a day. These parameters could be suffered from significant variations and uncertainties; alternatively, the required labour input (Figure 5) to fix the reinforcement for 1m^3 of concrete (Table 7) was computed based on the productivity rates gathered in Table 2.

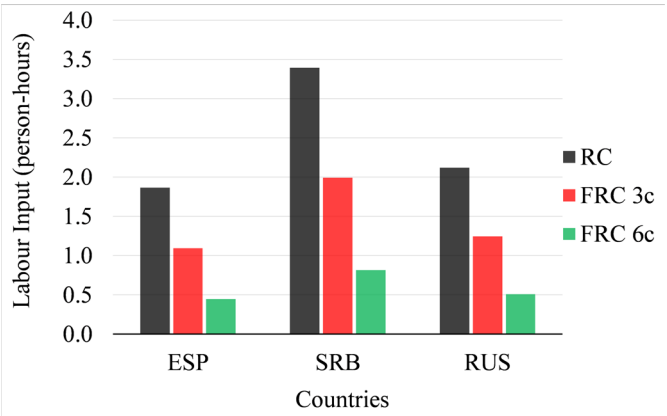

Fig. 5. Required person-hours to fix the reinforcement for 1 m^3 of concrete for each solution in accordance with the examined databases

The results presented in Figure 5 are the basis to assess the time-savings (if any) by calculating the overall volume of the slabs and, by establishing the crew size, to compute the expected duration of the reinforcement fixing. However, the portion of this activity influencing on the critical path of the project must be quantified in order to assess the

reduction of the construction period. This portion might be primarily influenced by the construction operations sequence. For instance, the reinforcement fixing process is to be entirely on the critical path in case that this activity starts once the shoring system is totally installed. In contrast, both operations may be overlapped and then only a part of the reinforcement fixing task would extend the project duration.

With this in mind, the same experts that estimated the performance rates of several construction activities (section 4.1) were asked to provide the percentage of the rebar fixing operation that would be on the critical path, taking into account the next conditions: (1) the presented slab should be poured at once, i.e. without dividing it into the pouring zones and (2) the reinforcement fixing starts as soon as the installed area of formwork permits the initiation of the process. As a result, the majority of respondents (22 out of 33 experts) indicated that at least 70% of the reinforcement would be on the critical path way. This result is in line with the previous studies, e.g. Goodchild [1] stated that generally 66% of the flexural bar fixing and 100% of shear reinforcement fixing tended to extend the duration of the construction project.

Taking into consideration that the productivity rates described in databases significantly differed from those obtained by interviewing the experts of in situ construction, the assessment of the required labour input was repeated based on the performance rates gathered in Table 3. For this purpose, the Monte Carlo method was used for assessing the cumulative probability distribution of the labour input to produce 1 m^3 of concrete for each alternative. PERT distributions were assigned to the involved variables (i.e. productivity rate of the reinforcement fixing). In this regard, the PERT distribution belongs to a family of continuous probability distributions consisting of: the minimum, the maximum, and the most likely values that a variable may take – these values were established in agreement with the conducted interviews (Table 3).

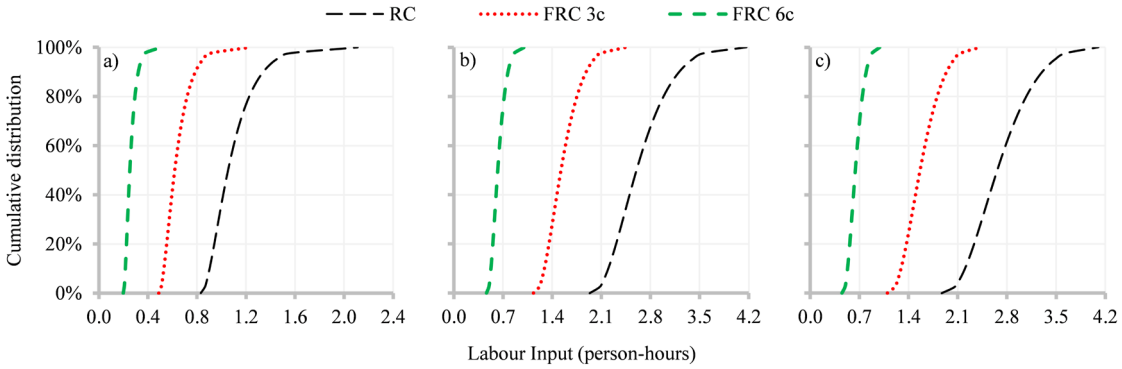

Fig. 6. Cumulative distributions for the required person-hours to fix the reinforcement for 1m^3 of concrete for each solution in accordance with the conducted interviews in different countries: a) ESP; b) SRB; c) RUS

The results of the probabilistic analysis are shown in format of cumulative distributions (Figure 6) of the demanded labour inputs to fix 84.8 kg (RC), 49.8 kg (FRC 3c), and 20.4 kg (FRC 6c) of reinforcement in 1 m^3 of concrete. These outcomes evidence that the RC solution is more susceptible to variation of the productivity rate of the reinforcement fixing, whereas FRC alternatives are more robust because of the reduction of the work amount related to this operation. This aspect may be of a paramount importance for decision-making

process of the reinforcement strategy; this being more evident when information about the potential crew size and its labour performance is unknown (or uncertain).

6.3. COST ANALYSIS

Generally, the costs can be divided into two main groups: direct costs and indirect costs. However, the composition of direct and indirect costs varies from company to company; for instance, Tan et al. [62] highlighted that contractors had different perceptions as to what were indirect costs. The same research study also concluded that indirect costs estimating involved management decisions that were highly subjective, involving qualitative information that was often vague and difficult to structure and quantify. Therefore, being acutely aware that the main purpose of this study is to (1) outline the aspects that face certain modifications due to use of FRC and (2) propose a straightforward method to identify those modifications, authors decided to concentrate the analysis of the case study on costs that comprise the material and labour expenses. The remaining costs that are also influenced by the selected alternative (preliminaries, overheads, equipment, and finance costs) are assumed as a time-dependent costs. These costs should be calculated individually for each particular project on the basis of the possible reduction on the construction period – this aspect was described in the section 3.2 and presented at the end of this section.

Both material and labour costs were computed pursuant to the explored databases. Importantly, the comparative analysis involves only the expenses that are supposed to be different between the analysed solutions – the prices of concrete, steel reinforcing bars, and fibres, as well as the wage rates of concrete workers and steel fixers, relying on the computed labour input for each alternative (Figure 5). The installation of shoring system was omitted because of the assumption that this construction operation would be identical for RC and FRC solutions. Figure 7 reveals that the use of reinforcing steel bars as a unique reinforcement brings the most economical solution in all three countries, whereas FRC 6c and FRC 9c solutions perform similarly (differences below 5%) in economic terms. These FRC alternatives, in average, result in 5.3%, 25.4%, and 7.8% cost increment respect to the RC solution in Spain, Serbia, and Russia, respectively.

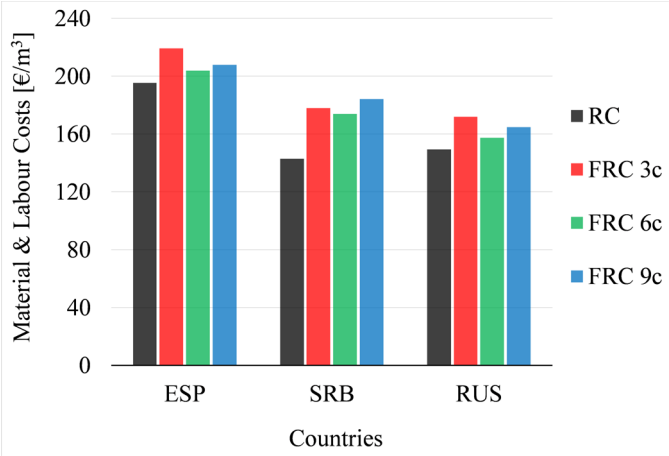

Fig. 7. Material and labour costs correspondent to the production of 1m³ of concrete for each alternative

The same cost analysis was carried out by means of a probabilistic approach, adopting as variables the productivity rates of concrete placing and reinforcement fixing. For this purpose, the PERT distributions were imposed to the above-mentioned variables, taking as a reference the experts' suggestions in respect to the labour performances (Table 3). Furthermore, the concrete placing operation was distinguished for RC and FRC solutions, i.e. the placement of conventional concrete was assumed for RC alternative, whereas the FRC was supposed to be a self-compacting material.

Results of the probabilistic analysis are shown in Figure 8. It is noticeable that the RC solution remains the most economically viable solution, although it is considerably susceptible to the variation of the performance rate – the aspect of a paramount importance for decision-making process of the reinforcement strategy. Likewise, FRC 6c and FRC 9c require similar material and labour expenses (in Russia and Spain), leading to the cost increment (in average) of 13.4%, 30.4%, and 6.5% in Spain, Serbia, and Russia, respectively.

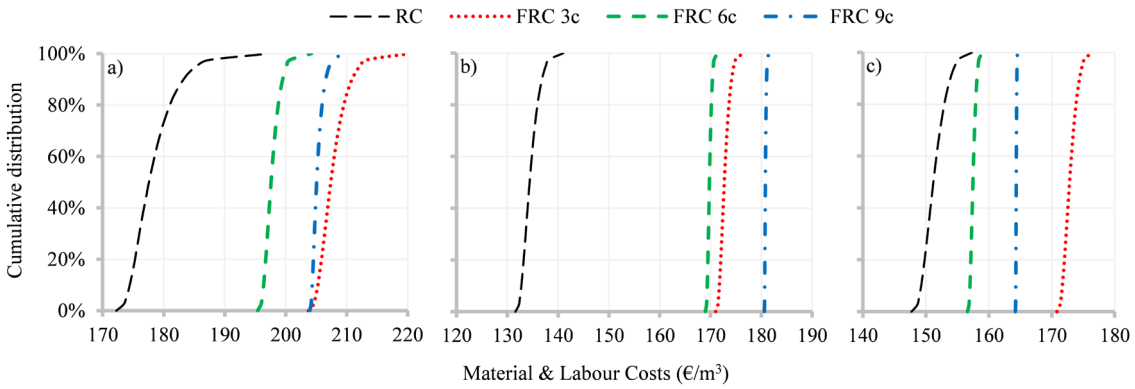

Fig. 8. Cumulative distributions for the material and labour costs correspondent to 1m³ of concrete for each alternative in accordance with the conducted interviews in different countries: a) ESP; b) SRB; c) RUS

Once the expenses concerned the material and labour are computed, the time-related costs considering the gradual decreasing of construction period should be assessed. However, the estimation of these costs that are comprised of preliminaries, general overheads, equipment costs, site overheads, finance costs and possible profit increment will differ from (1) project to project and (2) company to company. Therefore, it was decided to calculate the potential reduction of the project duration assuming that 24 consecutive floors of the case study slab were to be constructed, imposing that 70% of the reinforcement fixing would be on the critical path. It is important to mention that the time-saving effect, generally, depends linearly on the number of floors and the considerable amount of those was taken only for illustrative purposes, i.e. highlighting the potential reduction of the construction period that could be achieved by using FRC solutions in case of relatively high number of floors to be constructed.

The assumptions made to determine the number of days required to fix the reinforcement for 24 floors were: (1) 8 labour hours per day and (2) the crew sizes of steel fixers were taken in accordance with the conducted interviews (Table 3), i.e. 5, 6, and 12 workers in Spain, Serbia, and Russia, respectively. As a result, Figure 9 presents the required days to place and fix the steel bar reinforcement for a 24-storey building with the slab

geometry (and bearing capacity) of the case study in accordance with the databases and conducted interviews (considering average magnitudes of the productivity rates).

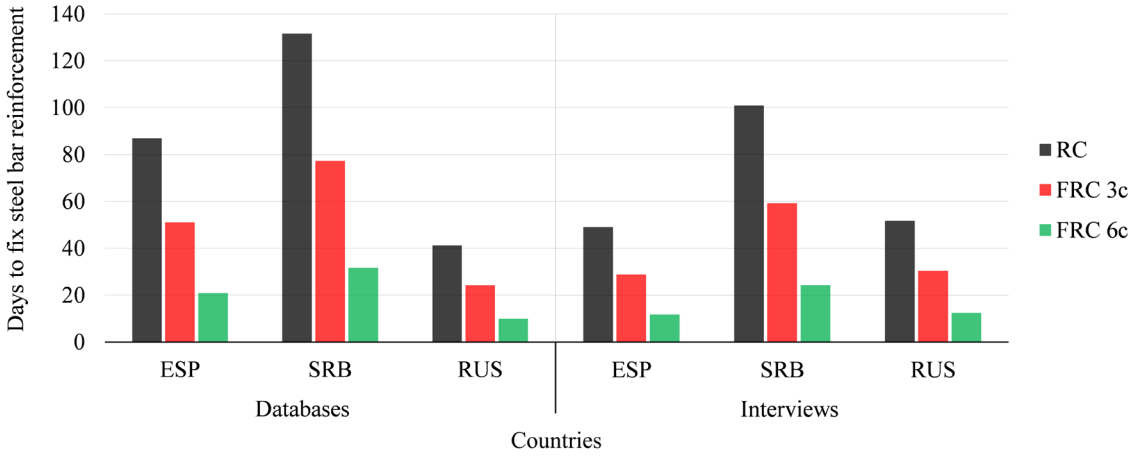

Fig. 9. Required days to fix the steel bar reinforcement that is on the critical path of the project for 24 floors of the given slab

With this preliminary assessment of the time required for placing/fixing the reinforcement for each alternative, the last step in a real project would be to answer: does the shorter duration of this phase cover the additional costs related to the implementation of FRC/HFRC instead of traditional solution? This question would be also followed by: if so, what solution is the most viable in terms of technological aspects and overall costs, i.e. FRC 3c, FRC 6c or FRC 9c? These questions must be answered by taking into consideration all factors related to the specific project (also cracking and deformability service limit states). Nonetheless, being aware that these questions are determining in the decision-making process, future research work is to be focused on the analysis of specific projects in order to provide a database that comprises the description of the residential and/or office buildings with a detailed calculation of time-dependent costs. This information, along with that presented in this paper, will serve as practical tool for the viability assessment of RC, HFRC, and FRC alternatives for the construction of column-supported flat slabs.

7. CONCLUSIONS

In this paper, a simplified practical approach to evaluate the viability of HFRC/FRC column-supported flat slabs is proposed. Four alternatives (RC, two HFRC, and FRC) for a given slab geometry and bearing capacity were analysed. Additionally, Spanish, Serbian, and Russian databases were examined to determine the material costs along with the productivity and wage rates that correspond to the construction of in situ concrete elevated slabs. Finally, 33 experts on *in situ* building construction were interviewed to quantify the labour performances of reinforcement fixing and concrete placement based on their experience from the real practice. As a result, the following conclusions can be drawn:

- The productivity rate of the reinforcement fixing, this being an essential operation involved in the construction of elevated *in situ* concrete flat slabs, has a high coefficient of variation in accordance with the conducted interviews: 25.8%, 36.0%, and 23.7% in Spain, Serbia, and Russia, respectively. The difference of the performance rates is even more significant between the countries. This factor is of

paramount importance and should be taken into account within the analysis of different alternatives.

- HFRC and FRC solutions are less sensitive to variations of the production rates of the construction operations involved in the erection process of the *in situ* column-supported concrete flat slabs. This observation highlights that the use of FRC/HFRC flat slabs ease the overall scheduling of the construction project.

- The material expenses along with the labour costs (neglecting the equipment costs) tend to be higher in case of HFRC and FRC alternatives. However, the case study showed that certain FRC solutions may lead to minor increment of these costs: FRC 6c and FRC 9c alternatives increased the above mentioned costs (in average) by 5.3% and 7.8% in agreement with Spanish and Russian databases, respectively.

- The partial or total substitution of reinforcing steel bars by fibres can lead to reductions of the construction time and, as a consequence, time-dependent costs. Basing on the production rates suggested by experts, the case study (a 24-storey building with stablished geometry and load conditions, and other assumption described within the manuscript) could lead to the reduction of the project period by 49, 52, and 101 days in Spain, Russia, and Serbia, respectively.

Even though the conducted research study proved the potential of the use of FRC in column-supported flat slab in terms of economic benefits, certain aspects are still to be studied. In this regard, the effect of the increased construction rate on the method of shoring the successive floors along with the analysis of the optimum reinforcement layout for hybrid solutions are among the topics that should be investigated. Furthermore, the industrial-oriented study that involves the analysis of specific projects in order to provide a database that comprises the description of the residential and/or office buildings with a detailed calculation of time-dependent costs can complement the presented investigation. Finally, the social and environmental aspects should be also introduced to the analysis of the potential alternatives in order to provide the more comprehensive study.

It should be remarked that the costs for the alternatives analysed might face significant modifications due to potential variation of market prices of the studied materials (e.g. steel macrofibres, reinforcing steel bars). Nonetheless, the conclusions drawn herein can still be valid if these costs' variations affect globally (and/or these variations tend to be uniform).

ACKNOWLEDGMENTS

This study was financially supported by the Spanish Ministry of Science and Innovation under the scope of project CREEF (PID2019-108978RB-C32). The first author, personally, thanks the Department of Enterprise and Education of Catalan Government for providing support through the PhD Industrial Fellowship (2018 DI 77) in collaboration with Smart Engineering Ltd. (UPC's Spin-Off).

REFERENCES

[1] Goodchild CH. Rationalisation of flat slab reinforcement. Research Focus; 2001.

[2] The Concrete Society. Technical Report No. 58. Deflections in Concrete Slabs and Beams. Camberley, UK: Concrete Society; 2005.

[3] The Concrete Society. Technical Report No. 64. Guide to the design and construction of reinforced concrete flat slabs. Camberley, UK: 2007.

[4] Aidarov S, Mena F, de la Fuente A. Structural response of a fibre reinforced concrete pile-supported flat slab: full-scale test. Eng Struct 2021;239. https://doi.org/10.1016/J.ENGSTRUCT.2021.112292.

[5] di Prisco M, Colombo M, Pourzarabi A. Biaxial bending of SFRC slabs: Is conventional reinforcement necessary? Mater Struct Constr 2019;52:1–15. https://doi.org/10.1617/s11527-018-1302-0.

[6] Blanco A, Pujadas P, Fuente A De, Cavalaro SHP, Aguado A. Assessment of the fibre orientation factor in SFRC slabs. Compos PART B 2015;68:343–54. https://doi.org/10.1016/j.compositesb.2014.09.001.

[7] Barros JAO, Moraes Neto BN, Melo GSSA, Frazão CMV. Assessment of the effectiveness of steel fibre reinforcement for the punching resistance of flat slabs by experimental research and design approach. Compos Part B Eng 2015;78:8–25. https://doi.org/10.1016/j.compositesb.2015.03.050.

[8] Gouveia ND, Fernandes NAG, Faria DMV, Ramos AMP, Lúcio VJG. SFRC flat slabs punching behaviour - Experimental research. Compos Part B Eng 2014;63:161–71. https://doi.org/10.1016/j.compositesb.2014.04.005.

[9] Cheng M-Y, Parra-Montesinos G. Evaluation of Steel Fiber Reinforcement for Punching Shear Resistance in Slab-Column Connections— Part I: Monotonically Increased Load 1991:166–85.

[10] Blanco A, Pujadas P, de la Fuente A, Cavalaro SHP, Aguado A. Influence of the type of fiber on the structural response and design of FRC slabs. J Struct Eng (United States) 2016;142:1–11. https://doi.org/10.1061/(ASCE)ST.1943-541X.0001515.

[11] Pujadas P, Blanco A, Cavalaro S, Aguado A. Plastic fibres as the only reinforcement for flat suspended slabs: Experimental investigation and numerical simulation. Constr Build Mater 2014;57:92–104. https://doi.org/10.1016/j.conbuildmat.2014.01.082.

[12] Fall D, Shu J, Rempling R, Lundgren K, Zandi K. Two-way slabs: Experimental investigation of load redistributions in steel fibre reinforced concrete. 2014. https://doi.org/10.1016/j.engstruct.2014.08.033.

[13] di Prisco M, Martinelli P, Parmentier B. On the reliability of the design approach for FRC structures according to fib Model Code 2010: the case of elevated slabs. Struct Concr 2016;17:588–602. https://doi.org/10.1002/suco.201500151.

[14] Facconi L, Minelli F, Plizzari G. Steel fiber reinforced self-compacting concrete thin slabs – Experimental study and verification against Model Code 2010 provisions. Eng Struct 2016;122:226–37. https://doi.org/10.1016/j.engstruct.2016.04.030.

[15] Michels J, Waldmann D, Maas S, Zürbes A. Steel fibers as only reinforcement for flat slab construction - Experimental investigation and design. Constr Build Mater 2012;26:145–55. https://doi.org/10.1016/j.conbuildmat.2011.06.004.

[16] Pujadas P, Blanco A, de la Fuente A, Aguado A. Cracking behavior of FRC slabs with traditional reinforcement. Mater Struct Constr 2012;45:707–25. https://doi.org/10.1617/s11527-011-9791-0.

[17] Maturana Orellana A. Estudio teórico-experimental de la aplicabilidad del hormigón reforzado con fibras de acero a losas de forjado multidireccionales. 2013. https://doi.org/10.1174/021435502753511268.

[18] Mandl J. Flat Slabs Made of Steel Fiber Reinforced Concrete (SFRC). CPI Worldw., 2008.

[19] Karv C. Shear and punching resistance of steel fibre reinforced concrete slabs. Aalto University, 2017.

[20] Leporace-guimil B, Mudadu A, Conforti A, Plizzari GA. Influence of fiber orientation and structural-integrity reinforcement on the flexural behavior of elevated slabs. Eng Struct 2022;252:113583. https://doi.org/10.1016/j.engstruct.2021.113583.

[21] Barros J, Salehian H, Pires M, Gonçalves D. Design and testing elevated steel fibre reinforced self-compacting concrete slabs. Fibre Reinf Concr 2012:1–12.

[22] Salehian H, Barros JAO. Assessment of the performance of steel fibre reinforced self-compacting concrete in elevated slabs. Cem Concr Compos 2015;55:268–80. https://doi.org/10.1016/j.cemconcomp.2014.09.016.

[23] Destrée X, Mandl J. Steel fibre only reinforced concrete in free suspended elevated slabs: Case studies, design assisted by testing route, comparison to the latest SFRC standard documents. Tailor Made Concr Struct 2008:437–43.

[24] Hedebratt J, Silfwerbrand J. Full-scale test of a pile supported steel fibre concrete slab. Mater Struct Constr 2014;47:647–66. https://doi.org/10.1617/s11527-013-0086-5.

[25] Døssland ÅL. Fibre Reinforcement in Load Carrying Concrete Structures. 2008.

[26] Gossla U. Development of SFRC Free Suspended Elevated Flat Slabs. Aachen: 2005.

[27] Parmentier B, Itterbeeck P Van, Skowron A. The flexural behaviour of SFRC flat slabs : the Limelette full- scale experiments for supporting design model codes. Proc. FRC, 2014.

[28] Aidarov S, Mena F, de la Fuente A. Self-compacting Steel Fibre Reinforced Concrete: Material Characterization and Real Scale Test up to Failure of a Pile Supported Flat Slab. RILEM-fib Int. Symp. Fibre Reinf. Concr., Springer, Cham; 2021, p. 702–13. https://doi.org/https://doi.org/10.1007/978-3-030-83719-8_60.

[29] Alberti MG, Enfedaque A, Gálvez JC. The effect of fibres in the rheology of self-compacting concrete. Constr Build Mater 2019;219:144–53. https://doi.org/10.1016/j.conbuildmat.2019.05.173.

[30] Cavalaro SHP, Aguado A. Intrinsic scatter of FRC: an alternative philosophy to estimate characteristic values. Mater Struct Constr 2015;48:3537–55. https://doi.org/10.1617/s11527-014-0420-6.

[31] Tiberti G, Germano F, Mudadu A, Plizzari GA. An overview of the flexural post-cracking behavior of steel fiber reinforced concrete. Struct Concr 2017:1–24. https://doi.org/10.1002/suco.201700068.

[32] Parmentier B, De Grove E, Vandewalle L, Van Rickstal F. Dispersion of the mechanical properties of FRC investigated by different bending tests. Proc Int FIB Symp 2008 - Tailor Made Concr Struct New Solut Our Soc 2008:123. https://doi.org/10.1201/9781439828410.ch84.

[33] di Prisco M, Plizzari G, Vandewalle L. Fibre reinforced concrete: New design perspectives. Mater Struct Constr 2009;42:1261–81. https://doi.org/10.1617/s11527-009-9529-4.

[34] Facconi L, Minelli F. Verification of structural elements made of FRC only: A critical discussion and proposal of a novel analytical method. Eng Struct 2017;131:530–41. https://doi.org/10.1016/j.engstruct.2016.10.034.

[35] Minelli F, Plizzari G. Derivation of a simplified stress-crack width law for Fiber Reinforced Concrete through a revised round panel test. Cem Concr Compos 2015;58:95–104. https://doi.org/10.1016/j.cemconcomp.2015.01.005.

[36] Facconi L, Plizzari G, Minelli F. Elevated slabs made of hybrid reinforced concrete: Proposal of a new design approach in flexure. Struct Concr 2019;20:52–67. https://doi.org/10.1002/suco.201700278.

[37] Instituto de Tecnología de la Construcción de Cataluña – ITeC, editor. BEDEC - Banco Construcción. 2016.

[38] Mijatović R, editor. Normativi i standardi rada u građevinarstvu. Visokogradnja. Knjiga 2, 12 izdanje. Belgrade: Građevinska knjiga; 2008.

[39] Комитет города Москвы по ценовой политике в строительстве и государственной экспертизе проектов, editor. База сметных нормативов ТСН-2001. Moscow: 2006.

[40] fib. fib Model Code for Concrete Structures 2010. 2010.

[41] Johansen KW. Yield-line formulae for slabs. Cement and Concrete Association; 1972.

[42] Johansen KW. Yield-line theory. Cement and Concrete Association; 1962.

[43] Kennedy G, Goodchild CH. Practical Yield Line Design. Surrey, UK: Concrete Centre; 2004.

[44] Ministerio de Fomento. Instrucción de Hormigón Estructural (EHE-08). 2008. https://doi.org/10.1017/CBO9781107415324.004.

[45] EN 1992-1-1. Eurocode 2: Design of concrete structures: General rules and rules for buildings. Brussels: CEN; 2004. https://doi.org/[Authority: The European Union Per Regulation 305/2011, Directive 98/34/EC, Directive 2004/18/EC].

[46] ACI Committee 544. Report on Design and Construction of Steel Fiber-Reinforced Concrete Elevated Slabs. 2004.

[47] CEN. EN 14651. Test method for metallic fibre concrete. Measuring the flexural tensile strength (limit of proportionality (LOP), residual). 2007.

[48] Proverbs DG, Holt GD, Olomolaiye PO. A comparative evaluation of reinforcement fixing productivity rates amongst French, German and UK construction contractors. Eng Constr Archit Manag 1998;5:350–8. https://doi.org/10.1108/eb021088.

[49] Christian J, Hachey D. Effects of Delay Times on Production Rates in Construction. J Constr Eng Manag 1995;121:20–6. https://doi.org/10.1061/(asce)0733-9364(1995)121:1(20).

[50] Buitrago M, Moragues JJ, Calderón PA, Adam JM. Structural failures in cast-in-place RC building structures under construction. Handb. Mater. Fail. Anal. with case Stud. from Constr. Ind., Mathew Deans; 2018. https://doi.org/10.1016/B978-0-08-101928-3.00008-2.

[51] Buitrago M, Adam JM, Alvarado YA, Moragues JJ, Gasch I, Calderón PA. Designing construction processes in buildings by heuristic optimization. Eng Struct 2016;111:1–10. https://doi.org/10.1016/j.engstruct.2015.12.009.

[52] Buitrago M, Adam JM, Moragues JJ, Calderón PA. Load transmission between slabs and shores during the construction of RC building structures – A review. Eng Struct 2018;173:951–9. https://doi.org/10.1016/j.engstruct.2018.07.046.

[53] Alvarado Y, Gasch I, Calderón PA. Study of technical and economical alternatives of a shoring and striking process during the construction of a building with reinforced concrete slab floors. Ing Constr 2016;31:139–46.

[54] Statistical Office of the Republic of Serbia n.d. https://data.stat.gov.rs/Home/Result/2403040508?languageCode=en-US.

[55] Institution of Structural Engineers/Concrete Society. Standard method of detailing structural concrete: a manual for best practice. Third Edit. London: 2006.

[56] Gobierno de España. Código Técnico de la Edificación (CTE) Documento básico: Seguridad estructural. Apartado de “Acciones en la Edificación” 2009.

[57] Nogales A, de la Fuente A. Numerical-aided flexural-based design of fibre reinforced concrete column-supported flat slabs. Eng Struct 2021;232:1–24. https://doi.org/10.1016/j.engstruct.2020.111745.

[58] Aidarov S, Sutera L, Valerio M, de la Fuente A. Elevated Steel Fibre Reinforced Concrete Slabs and the Hybrid Alternative: Design Approach and Parametric Study at Ultimate Limit State. RILEM Bookseries 2022;36:504–13.

[59] Colombo M, Martinelli P, di Prisco M. On the evaluation of the structural redistribution factor in FRC design: a yield line approach. Mater Struct 2017;50:1–18. https://doi.org/10.1617/s11527-016-0969-3.

[60] Canadian Standards Association. Design of Concrete Structures CSA A23.3-04.

[61] Mitchell D, Cook WD. Preventing Progressive Collapse of Slab Structures. J Struct Eng 1984;110:1513–32. https://doi.org/10.1061/(ASCE)0733-9445(1984)110:7(1513).

[62] Tah JHM, Thorpe A, McCaffer R. A survey of indirect cost estimating in practice. Constr Manag Econ 1994;12:31–6. https://doi.org/10.1080/01446199400000004.

3. CONCLUSIONS AND FUTURE PERSPECTIVES

The main purpose of this chapter is to discuss the relevance and limitations of the main contributions derived from the thesis. Additionally, opinions on future research lines are integrated in the discussion.

Contents

3.1. GENERAL CONCLUSIONS

Currently, the construction of FRC column-supported flat slabs for office and residential buildings is one of the most attractive and challenging fields of FRC application. This is, in part, owe to the large reinforcing demands that result from considering the required structural reliability to be achieved. The lack of previous experiences (experimental results and/or already constructed buildings), design-oriented recommendations, and economic analyses are also among the factors that are hindering the widespread use of this technology. With this in mind, this thesis presents a comprehensive analysis of the topic in order to provide guidance for designers and practitioners, based on experimental results, numerical simulations, and techno-economic analysis.

For this purpose, a real-scale FRC column-supported flat slab was constructed. In contrast to the previous experiences, a fibre content was considerably reduced (volume fraction 0.9%) and the studied element was tested under different magnitudes of the uniformly distributed load for the sake of more detailed analysis. *The observations made during the experimental programme evidenced the suitable structural response in terms of cracking control, deflections, and overall bearing capacity* – the achieved results can serve as a reference for future construction projects and scientific contributions.

Thereafter, a simplified method to assess flexural capacity, instantaneous deflections, ductility requirements in bending, and crack-width governing parameters was developed. *The results derived from the study were validated by means of nonlinear analysis, proving the accuracy and precision of the proposed method.* This outcome should complement the relevant design-oriented recommendations that are mainly focused on the behaviour of FRC/HFRC flat slabs at ultimate conditions (flexural and punching strength).

Finally, a straightforward cost-oriented approach for the preliminary comparison of the RC, HFRC, and FRC flat slab solutions was elaborated. The developed assessment tool allows considering the governing material-structural and economic parameters. *As a result of a study case, the analysis highlighted some extra direct costs for the HFRC and FRC alternatives. However, FRC solutions led to a reduction of the construction span and, as a consequence, time-dependent costs – essential factor that must be taken into account within the comparative analysis.* The information presented in this industrial-oriented study is meant to be an illustrative example to project managers and construction planners with regard to the suitability of using FRC for column-supported flat slabs.

3.2. SPECIFIC CONCLUSIONS

In response to the specific objectives discussed in Chapter 1, the specific conclusions are listed below, grouped within three blocks addressed in this thesis:

BLOCK 1: REAL-SCALE TESTING OF FRC CSFS

- A SFRC with f_{R1m} = 7.2 MPa and f_{R3m} = 7.7 MPa (resulting in a 3e and 7c strength classes considering characteristic and mean values, respectively) proved to be sufficient to guarantee a suitable structural response for loads representative of residential buildings in a column-supported slab with a span-to-depth ratio of 30.

- A load increase from the characteristic load combination (q_k = 9.8 kN/m^2) to 16.0 kN/m^2 led to an increment of deflections of 31 mm, without evidencing signs of failure; this proving both the moment redistribution capacity and the ductility of the system.
- The performance in terms of cracking and deflections resulted to be acceptable even when the structural system was subjected to loads 13% greater than the quasi-permanent load combination ($q_{k,\psi 2}$ = 7.7 kN/m^2) for residential buildings.
- The results derived from performing the inductive test (non-destructive test oriented to characterize distribution and amount of steel fibres) on drilled cores confirmed that a 76.8% were favourably oriented along the slab in-plane axis.
- The analytical solution provided a suitable prediction (overestimation of 11%) of the failure load respect to the UDL applied (16 kN/m^2). It is important to remark that the failure was not reached during the load test and, therefore, the difference could have been even minor.
- The numerical prediction led to overestimation (53%) in terms of bearing capacity of the tested SFRC flat slab. Caution is required when designing this structural typology by means of FE packages, and the proper constitutive equations and material partial safety factors must be taken into account.

BLOCK 2: DESIGN OF FRC CSFS

- The Yield Line Method permits to evaluate the overall flexural capacity of the HRC flat slabs with a possibility of distributing moments while accounting for the presence of FRC and HRC sections along the same yield line. Based on nonlinear analyses, the analytical approach provides a reliable results in terms of overall bearing capacity in flexure in case of the given structure subjected to uniformly distributed loads (UDL).
- The proposed approach, based on the crossing beam analogy along with indirect control of cracking for RC flat slabs, proved to be promising for dealing with the design at both SLS (crack width control and instantaneous deflection control).
- Additionally, the proposed method permits to check the ductility requirements for bending ($\delta_{peak} \geq 5 \cdot \delta_{SLS}$) by evaluating the expected deflections at ULS.

BLOCK 3: COST-ORIENTED ANALYSIS OF FRC CSFS CONSTRUCTION

- The productivity rate of the reinforcement fixing, this being an essential operation involved in the construction of elevated *in situ* concrete flat slabs, has a high coefficient of variation in accordance with the conducted interviews: 25.8%, 36.0%, and 23.7% in Spain, Serbia, and Russia, respectively. The difference of the performance rates is even more significant between the countries. This factor is of paramount importance and should be taken into account within the analysis of different alternatives.
- HFRC and FRC solutions are less sensitive to variations of the production rates of the construction operations involved in the erection process of the *in situ* column-

supported concrete flat slabs. This observation highlights that the use of FRC/HFRC flat slabs ease the overall scheduling of the construction project.

- The material costs along with the labour costs (neglecting the equipment costs) tend to be higher in case of HFRC and FRC alternatives. However, the case study showed that certain FRC solutions may lead to minor increment of these costs: FRC 6c and FRC 9c alternatives increased the above mentioned costs (in average) by 5.3% and 7.8% in agreement with Spanish and Russian databases, respectively.
- The partial or total substitution of reinforcing steel bars by fibres can lead to reductions of the construction time and, as a consequence, time-dependent costs. Basing on the production rates suggested by experts, the case study (a 24-storey building with stablished geometry and load conditions, and other assumption described within the manuscript) could lead to the reduction of the project period by 49, 52, and 101 days in Spain, Russia, and Serbia, respectively.

3.3. FUTURE PERSPECTIVES

Despite the contributions reported in the previous section, further research on the topics covered in this doctoral thesis is still required. Taking this into account, several suggestions are provided below, being divided into three blocks:

BLOCK 1: REAL-SCALE TESTING OF FRC CSFS

- Investigate the suitable casting and curing procedures for practical and systematic concrete production.
- Analyse time-dependent deformations for larger periods than those considered in the presented study.
- Study the structural response of hybrid solutions in order to identify the best “fibre + reinforcing steel bars” configurations for the given geometry and boundary conditions.
- Increase the current databases related to fibre distribution and orientation in the FRC slabs – the aspects of paramount importance for further design procedures.

BLOCK 2: DESIGN OF FRC CSFS

- Propose the method to adjust the current constitutive models (derived from 3PBT) in order to accurately predict the behaviour of FRC two-way slabs by means of analytical and/or numerical approaches. This method could possibly take into account the orientation and/or redistribution factors.
- Develop and validate the simplified method for estimation of the long-term behaviour of FRC/HFRC slabs.
- Carry out the parametric analyses, varying geometry, reinforcement layout, and load conditions in order to complement the study of the structural response of FRC/HFRC slabs.

BLOCK 3: COST-ORIENTED ANALYSIS OF FRC CSFS CONSTRUCTION

- Study the effect of the increased construction rate of FRC slabs on the method of shoring of the successive floors.
- Analyse the essential aspects related to the construction procedure, such as: FRC placement, quality control protocol, and placement of the construction joints.
- Provide a simplified approach to estimate the time-dependent costs based on the analysis of already constructed residential and/or office buildings.

ANNEX: COMPLEMENTARY PUBLICATIONS

This annex reproduces the published journal paper and research contributions that complement the results derived in the thesis. Each manuscript follows its own numbering of sections, figures, equations and references.

Contents

RESEARCH CONTRIBUTION I: SELF-COMPACTING STEEL FIBRE REINFORCED CONCRETE: MATERIAL CHARACTERIZATION AND REAL SCALE TEST UP TO FAILURE OF A PILE SUPPORTED FLAT SLAB

Published in: Concrete Structures: Fibre Reinforced Concrete: Improvements and Innovations II. X RILEM-fib International Symposium on Fibre Reinforced Concrete (BEFIB) 2021

Stanislav Aidarov [a, b, *], Francisco Mena [b], Albert de la Fuente [b]

[a] Smart Engineering Ltd., UPC Spin-Off, Jordi Girona 1-3, 08034 Barcelona, Spain

[b] Civil and Environmental Engineering Department, Universitat Politècnica de Catalunya (UPC), Jordi Girona 1-3, 08034 Barcelona, Spain

* Corresponding author. Tel.: +34 633 634 207; Full Postal address: 08034, Barcelona, Jordi Girona 1; Email address: stanislav.aidarov@upc.edu ; stanislav.aydarov@smartengineeringbcn.com

Abstract

Steel Fibre Reinforced Concrete (SFRC) is increasingly being used in the construction industry providing structural, technological and economic benefits. However, this relatively new material has not demonstrated its full potential due to presence of certain aspects related to both concrete mix and structural design that should be further investigated. Specifically, pile-supported flat slabs is an interesting field of application of the SFRC; however, there are still aspects needing attention and solutions in order to make this structural application more attractive from both economic and technical points of view, these being (among others): the effect of new types of fibres on material properties and more insight regarding the structural capacity at both serviceability and ultimate limit state. Complementing the existing knowledge in aforementioned areas might lead to considerable expansion of SFRC application in elements with high structural responsibility. To this end, an extensive experimental program was carried out within the industrial-oriented project eFIB that contained characterization of 15 concrete mixes with different fibre types and its content (up to 120 kg/m^3) and construction of 10 × 12 meters SFRC flat slab. This prototype was loaded in different stages with permanent and life-loads in order to study both cracking and time deformation responses; the structure was eventually led to failure. The results of the described research are presented and discussed herein.

Keywords: fibre reinforced concrete, real scale test, flat slab, two-way slab, numerical simulation.

1. INTRODUCTION

The use of Steel Fibre Reinforced Concrete (SFRC) in the elements with different structural responsibility is already an attractive alternative for the solutions in which, not long ago, the traditional reinforcement was treated as axiomatic. Addition of steel fibres to the cement-based composites demonstrates the remarkable results in terms of residual tensile strength, crack resistance, durability and fatigue [1–4] what allows to apply this technological material in pavements, precast elements and elevated flat slabs [5–8].

The latter could be named as one the most complex challenges for the aforementioned material due to occurrence of relatively high stresses within the service life-span of the structure. Despite the existence of already executed elevated SFRC flat slabs which have highlighted the technological, economic and environmental positive outcomes, this approach is still of concern to most of engineers due to certain aspects that require further study, such as: maintenance of structural integrity under ultimate loading conditions; the effect of long-term loads in terms of deformation and cracking; potential reduction of fibre content to make the solution more competitive in comparison with those traditional (ex., reinforced concrete with steel bars) and the established criteria of quality control (material and structure). These aspects are among the first to be analysed in order to confirm the technical feasibility of the partial (or even total) substitution of traditional reinforcement in pile supported slabs.

In this context, the industrial-oriented project eFIB (financially supported by Spanish Ministry of Economy, Industry and Competitiveness; reference: RTC-2016-5263-5) was carried out with the aim to increase the knowledge base in the above-described aspects. In turn, the purpose of the research contribution is to report the results obtained from the characterization of SFRC mixes with different fibre type/content and real-scale testing of a SFRC elevated flat slab.

2. CHARACTERIZATION OF SFRC

2.1. DEVELOPMENT OF SFRC MIXES

Development and posterior characterization of produced SFRC mixes was divided into three phases in accordance with Figure 1. The first phase was concentrated on the study of the properties in fresh and hardened states of six different concrete mixes, in which, two types of fibres were used, varying its content from 60 to 120 kg/m^3 with interval of 30 kg/m^3.

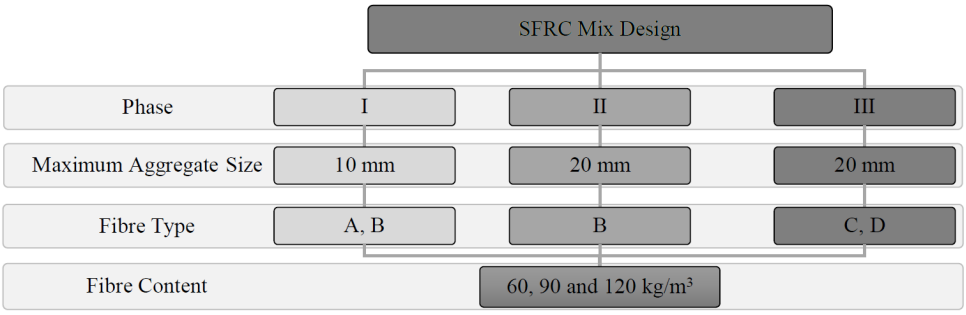

Fig. 1. Phases of SFRCs characterization

The influence of maximum aggregate size on the rheological and mechanical properties of the material was the main goal of the second phase. Fibre B was selected for this phase due to better performance of the latter during the first part of the study. SFRC mixes with modified granular skeleton and same range of fibre contents (60, 90 and 120 kg/m^3) demonstrated the similar performance in terms of studied properties with respect to previously obtained results. Therefore, the concrete composition of the material with maximum aggregate size of 20 mm was maintained for the characterization of concrete mixes reinforced by fibres C y D – third part of the analysis. The examination of fifteen SFRCs considering four fibre types and three different contents was carried out; the important details to be pointed out are: (1) fibres with the tensile strength ranging from 1500 to 2300 N/mm^2 and with the different type of anchorages were taken into consideration (Table 1) and (2) the principal variables of the concrete granular skeleton did not face any significant modifications for the sake of comparability (Table 2).

Table 1. Properties of studied fibres

Fibre	A	B	C	D
f_{uf} [Mpa]	1800	1900	1500	2300
Length [mm]	50±3	60±3	60	60
Diameter [mm]	1	0.9	0.9	0.9
Aspect Ratio	50	67	65	65
Geometrical Form	Hooked-end			

Table 2. Granular skeleton (in kg/m^3)

Material	Dosage
Cement	425
Filler	25
Water	200
Fine Aggregate	1325
Coarse Aggregate	400

2.2. ANALYSIS OF SFRC PROPERTIES IN THE FRESH STATE

Owe to the type of application, self-compactability was found to be convenient. Therefore, each concrete mix was tested for required slump flow in accordance with the Spanish Code on Structural Concrete (EHE-08) [9]. The obtained results demonstrated possible development of the self-compacting concrete mixes even with fibre content of 120 kg/m^3; information on the achieved slump flow values is depicted in Figure 2. The coding X(Y)-Z, where X, Y and Z being respectively the fibre type, maximum aggregate size and fibre amount was established for referring to each SFRC mix.

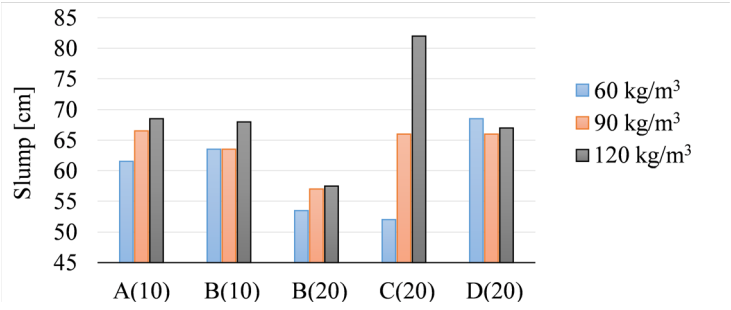

Fig. 2. Slump flows of studied SFRCs.

Minimum permitted slump flow for concrete to be considered as self-compacting per EHE-08 is equal to 55 cm. Figure 2 shows that only 2 out of 15 SFRCs did not reach this value. However, these mixes contained only 60 kg/m^3, therefore, most likely a slight lack of

superplasticizer was the cause of insufficient flowability. Furthermore, the effect of maximum aggregate size increment on compactability of SFRCs could be appreciated on the example of mixes B (10) and B (20); the reduction of slump flows was equal to 10, 7 and 10 cm for the identical fibre contents of 60, 90 and 120 kg/m^3, respectively.

Apart from slump-flow testing [10], the estimation of density and air content of fresh concrete was carried out [11,12]. Density ranged between 2.16 and 2.40 g/cm^3 – common values for self-compacting concretes, whereas the obtained values of air contents were comprised between 3.0 and 11.0 % (Figure 3). Analysing the results presented in Figure 3, it was decided to disregard the performance of SFRC B(20)-60 in hardened state due to high value of air content which might be caused by anomalous effect of one of the applied additives.

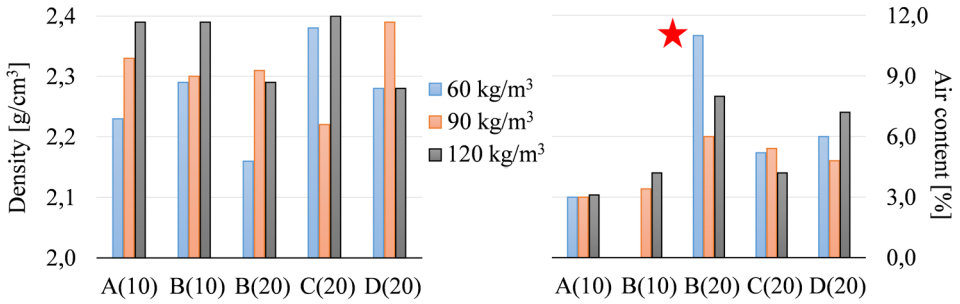

Fig. 3. Density and air content in fresh SFRCs.

2.3. ANALYSIS OF SFRC PROPERTIES IN THE HARDENED STATE

2.3.1. Compressive strength and Young Modulus

Compressive strength of produced SFRCs was evaluated through testing 6 cast cylinders for each mix [13]; three of those were analysed at 7 days and the remaining – at 28 days. Mean values of the compressive strength at 7 days ($f_{cm,7}$) were ranged between 38.3 and 52.8 MPa, whilst the performance at 28 days varied from 50.2 to 67.9 MPa (Figure 4). The ratios $f_{cm,7}$ to $f_{cm,28}$ of studied materials were within the range of 0.67 to 0.80 – expected values for normal/high strength concretes.

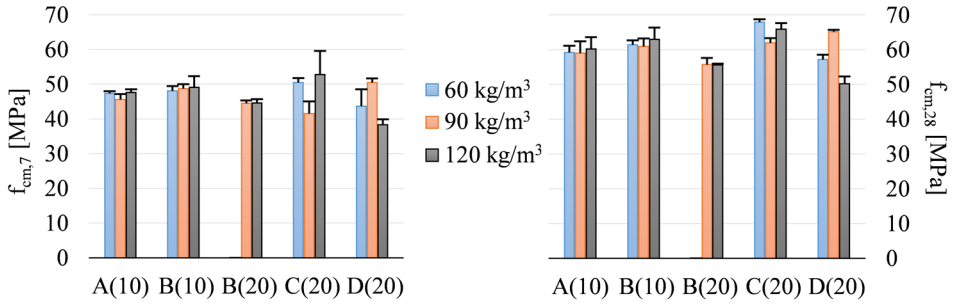

Fig. 4. Mean values of $f_{cm,7}$ and $f_{cm,28}$ with corresponding standard deviations.

The results depicted in Figure 4 are in line with the previous works which highlighted the absence of any significant influence of the fibre content on compressive strength of the concrete; this parameter mainly depends on the material matrix, i.e. amount of the cement paste and granular skeleton [14,15]. Considering the above stated, the modification of maximum aggregate size could have had an effect on the studied mechanical properties.

However, the amount of coarse aggregate was not significant in the concrete dosages throughout the experimental programme (Table 2) due to established workability requirements. Therefore, the difference in compressive strength of the studied SFRCs can possibly be explained by the variation of moisture content of aggregates and environmental conditions which, along with the incorporated additives, had an impact on the air content in the elaborated concrete mixes.

The Young Modulus was comprised between 30.0 and 38.1 GPa – found to be sufficient for providing stiffness to the slab. However, the presence of considerable amount of fine aggregates in the designed dosages resulted in lower values of Young Modulus in comparison with those suggested by RILEM TC 162-TDF [16] for SFRCs (black line, Figure 5). In fact, the obtained results better met the prediction of EHE-08 for conventional concrete (blue line, Figure 5). This observation acknowledges the certain reduction of Modulus of Elasticity due to requirement of increased binder content in order to provide the self-compactability of the material in question [17].

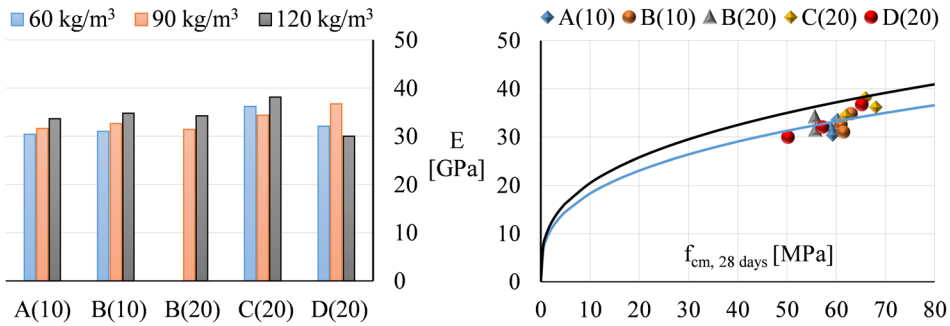

Fig. 5. Young Modulus of SFRCs.

2.3.2. Residual Tensile Strength

Measurements of residual tensile strength were carried out for each SFRC in accordance with EN 14651 [18]. Under a simply-supported three point bending configuration on the notched prisms, the limit of proportionality (f_{LOP}) and flexural residual strengths (f_R) corresponding to certain values of crack mouth opening displacement (CMOD = 0.5, 1.5, 2.5 and 3.5 mm) were found (Table 3).

Mean values of f_{R1} ranged between 4.0 and 14.0 MPa, whereas f_{R3} presented values from 4.2 to 14.3 MPa. These results complied with the minimum established requirements to substitute conventional reinforcement at ultimate limit state according to the *fib* Model Code 2010 [17]: $f_{R1k}/f_{LOPk} > 0.4$ and $f_{R3k}/f_{R1k} > 0.5$.

3. REAL SCALE TESTING OF SFRC FLAT SLAB

3.1. PREVIOUS EXPERIENCES AND CONSTRUCTION OF SFRC PROTOTYPE

The selection of a suitable fibre type and amount for the design and construction of a SFRC flat slab was preceded by the study of already existing cases (Table 4). The concrete mix with fibre content of 100 kg/m^3 was predominantly used in those cases with significant span to depth ratio (L_{max}/d), in which the so called Anti-Progressive Collapse reinforcement (APC)

was also included. This reinforcement should be placed in the bottom of the slab in alignment with columns in both directions and this is intended to be capable of providing post-failure resistance of the structural element [19].

Table 3. Post-cracking residual strengths (in MPa) and fib MC-2010 classification

SFRC	$f_{LOP,m}$ (CV)	$f_{LOP,k}$	$f_{R1,m}$ (CV)	$f_{R1,k}$	$f_{R3,m}$ (CV)	$f_{R3,k}$	Class
A(10)-60	3.6 (7.8)	3.2	3.9 (13.0)	3.1	4.4 (22.7)	2.8	3b
A(10)-90	4.1 (14.1)	3.1	6.4 (29.1)	3.3	6.1 (22.7)	3.9	3d
A(10)-120	5.0 (14.6)	3.8	8.0 (26.5)	4.5	6.6 (19.7)	4.4	4c
B(10)-60	4.7 (11.4)	3.8	7.5 (25.6)	4.4	7.7 (27.5)	4.3	4c
B(10)-90	5.4 (14.6)	4.1	11.4 (19.0)	7.84	10.4 (13.7)	8.07	7c
B(10)-120	5.6 (12.3)	4.5	12.1 (6.2)	10.9	11.3 (21.3)	7.73	10a
B(20)-60	4.6 (11.3)	3.8	6.8 (23.8)	4.2	7.1 (15.6)	5.3	4d
B(20)-90	5.52 (17.0)	4.0	10.5 (25.6)	6.1	9.0 (29.7)	4.6	6b
B(20)-120	6.3 (7.9)	5.4	11.7 (12.1)	9.4	10.8 (17.3)	7.8	9b
C(20)-60	4.7 (2.2)	4.9	7.3 (14.9)	5.5	7.1 (16.6)	5.2	5c
C(20)-90	5.2 (6.6)	4.8	9.6 (15.6)	7.2	9.8 (15.3)	7.3	7c
C(20)-120	6.6 (14.1)	5.1	14.0 (12.9)	11.0	14.3 (15.3)	10.7	11c
D(20)-60	4.2 (12.4)	3.4	6.6 (25.9)	3.8	7.44 (11.5)	6.0	3e
D(20)-90	4.8 (9.0)	4.1	10.0 (12.9)	7.9	10.4 (11.7)	8.4	7c
D(20)-120	5.9 (20.6)	9.1	13.7 (20.6)	9.1	13.9 (29.2)	7.2	9b

Analysing the collected information, it was decided to execute the SFRC pile supported flat slab with span to depth ratio of 30 (the upper limit of those already constructed, see Table 3), consisting of 4 panels of 5 × 6 m^2 each with a slab thickness of 0.2 m supported onto 0.25 m-square cross-section reinforced concrete columns, see Figure 6. Residential building loads according to the Spanish Code (self-weight of 4.8 kN/m^2, dead-load of 2.0 kN/m^2 and 3.0 kN/m^2 of live-load) were considered. Additionally, following the recommendations of Canadian Standards, the APC reinforcement was installed.

Table 4. Previous experiences of SFRC flat slabs

Fibre Type		C_f	L_{max}/h	Traditional	Building /	Country
Length [mm]	Diam. [mm]	[kg/m^3]	[m/m]	Reinforcement	Prototype	
50	1,3	100	30	Yes [1]	Prototype	Luxembourg
37	0,5	90	16	Yes [1]	Prototype	Portugal
50	1,3	100	28	Yes [1]	Prototype	Estonia
-	-	100	24	Yes [1]	Building	Lithuania
50	1,3	100	27	Yes [2]	Building	Spain

NB: Yes [1] – only presence of APC bars; Yes [2] – presence of APC bars + traditional reinforcement in the areas with particularly high stresses

Based on the established parameters of geometry and loads, the design of SFRC prototype was carried out by means of yield line method [20,21] and non-linear numerical analysis [22]. The report provided by ACI [23] was used for the analytical solution, whereas numerical simulations were performed through the software "ABAQUS" applying different constitutive models in accordance with RILEM [16] and *fib* Model Code [17].

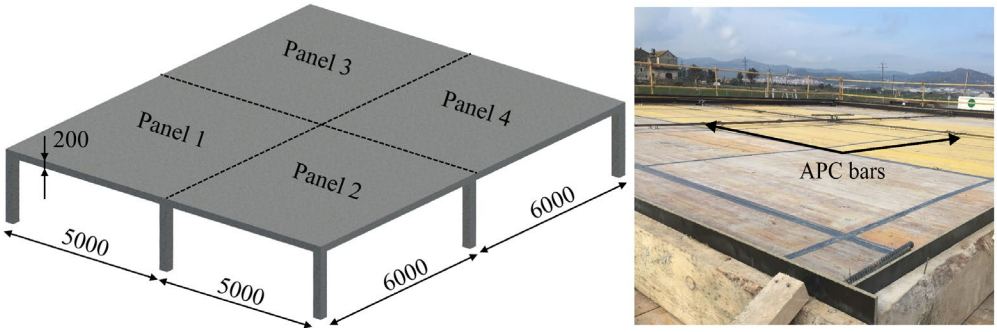

Fig. 6. Geometry of the prototype and installed APC bars

Design output along with the obtained information of studied SFRCs (fibre content – residual tensile strength relationship) permitted to reduce fibre content in the selected concrete mix by 30% in comparison with previous experiences (Table 3), providing the required mechanical properties. Applying the established material, SFRC pile supported flat slab was constructed and, during the execution, the appropriate workability was pointed out: no fibre-balling was detected and the rheological properties of the material did not differ significantly with those achieved throughout experimental program (Figure 7)

Fig. 7. a) SFRC pumping b) SFRC flat slab in the fresh state

After the construction and during the curing period, the effect of climatic conditions (very low temperatures in Barcelona, including snow) coupled with autogenous shrinkage of concrete was observed – these phenomena led to appearance of certain cracking of upper surface of the slab. However, the observed cracks were controlled by presence of fibres and had no influence on the structural capacity of the SFRC element. The evaluation of shrinkage cracks was followed by formwork removal and installation of prisms in the centres of each field of the SFRC slab in order to monitor the produced deflections during the loading process that is described below.

3.2. LOADING OF SFRC PROTOTYPE

Main objective of the loading process was to evaluate the response of the structure in terms of cracking and deformations under long-term loads of considerable magnitudes. For this purpose, the load was provided by means of concrete cubes of 0.5 × 0.5 × 0.6 m (≈350

kg each). It is worth noticing that the structure was loaded gradually, dividing the whole process into four steps. This approach permitted the identification and measurement of both instantaneous and long-term deflections for different values of uniformly distributed loads (Figure 8)

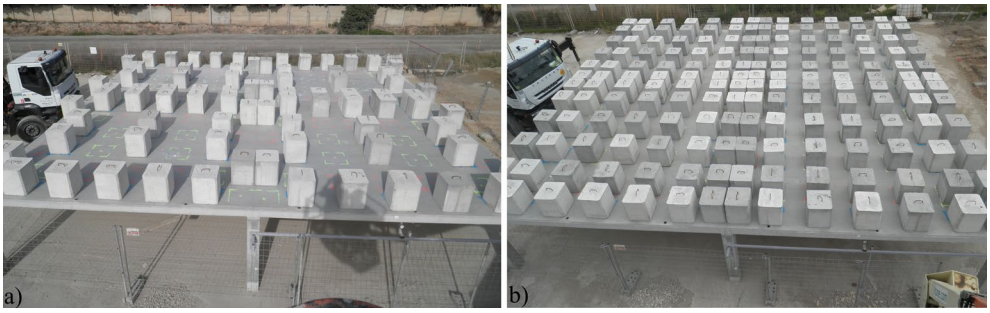

Fig. 8. a) Second phase of loading; b) Fourth phase of loading

Time-spans between loading phases depended on the response of the structure, i.e. the next phase could only be started when there was no any increment of deflection within the certain time period. Crack patterns on the bottom surface of the slab were measured during the whole loading process. The fourth phase, the total load (self-weight included) was equal to 9.8 kN/m^2 (which includes both the permanent and variable loads).

After a stabilization process (which took place within 4.5 months), a loading tests was performed in order to bring to failure the structure. To this end, water tanks were placed onto the slab, according to different distributions, and these were filled in phases of 0.1 m (1.0 kN/m^2 per phase). Firstly, panels 1 and 2 of the prototype (Figure 9a) were loaded up to reaching a total equivalent load of 14.0 kN/m^2 (as reference, design load being q_d = 1.35·(4.8+2.0) + 1.50·3.0 = 13.7 kN/m^2). However, SFRC prototype showed barely no increase of cracking respect the fourth phase and still potential deformation capacity, so the loading process continued until reaching a load of 16.0 kN/m^2. Even at this load level, no loss of integrity or deflections that would have led to predict an imminent failure were observed, so the slab was left fully-loaded until the next day. The following morning, the increment of deflection was equal to 10 mm and still no signs of failure; hence, the structure proved to have a significant strength and ductility capacity.

Fig. 9. SFRC flab under ultimate loading conditions: a) loading of the first half of the slab; b) loading of the rest of the slab

The last load step consisted in transportation of water tanks on the other part of the slab (panels 3 and 4) with posterior repetition of the test (Figure 9b). Those panels were also

loaded up to 16.0 and 14.5 kN/m^2, respectively, despite the already damaged half of the structure.

The deflections of the structure were monitored by means of prisms and topography. These were measured before and after every load step to quantify the instantaneous component. The time-dependent component of the deflections (owe to creep, shrinkage and temperature variations) was measured 3 days per week. The results derived from the measurements during four phases proved the homogeneity of the material resistant properties and the proper position of the loads as the total deflections measured in the mid-span of the four bays showed no significant differences (see Figure 10). In this sense, blue, green, orange and red cubes correspond to the I, II, III and IV loading stage (cumulative), respectively.

The same structural response was observed under the ultimate loading conditions: the deformation difference of first and second panels was equal to 2 mm under the load of 16.0 kN/m^2. Even when the water tanks were emptied and some reduction of the deflections was detected, the mentioned difference kept being in the same range – it reduced to 1 mm.

An analysis of the cracking patterns at different stages of the load was carried out in parallel with the evaluation of produced deformations of the structure. The obtained information was aligned with the expected patterns derived from both the numerical analyses and the Johansen theory (for similar load and support configurations) [7,22].

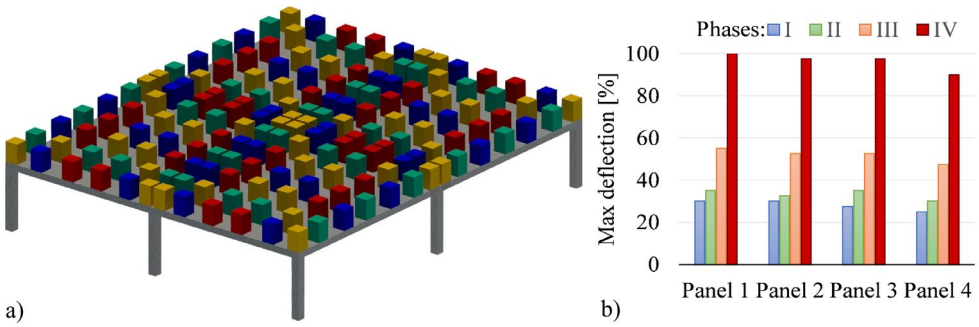

Fig. 10. Measured deflections of SFRC slab

4. CONCLUSIONS

An extensive experimental programme on characterizing concrete mixes with various fibre contents and a full-scale test of a SFRC pile supported flat slab was conducted. Suitable workability of self-compacting concrete even with fibre content of 120 kg/m^3 was observed, this providing a remarkable residual tensile strength of the material that allowed producing a SFRC flat slab of 30 in aspect ratio and 0.2 m thickness, with a 30% of fibre amount reduction respect to the existing experiences. More detailed conclusions which may be derived based on the results and analysis presented below:

- The examined materials demonstrated flexural hardening behaviour, fulfilling the established requirements to permit the substitution (also partial) of conventional reinforcement according to the *fib* Model Code 2010.
- The 7c strength FRC class (considering mean values), according to the classification of the *fib* Mode Code 2010, proved that the traditional steel bars can be replaced by

fibres providing a suitable structural response for loads representative of residential buildings in a column-supported slab with a span to depth ratio of 30.

- The tested prototype presented a greater bearing capacity than that asked for residential buildings according to the Spanish standards demonstrating no loss of integrity even under the load of 16 kN/m^2.

ACKNOWLEDGMENTS

The authors wish to express their gratitude to the Spanish Ministry of Economy and Competitiveness for the financial support in the scope of the project eFIB (reference: RTC-2016-5236-5) which was carried out along with SACYR Ingeniería e Infraestruturas. The first author also thanks the Department of Enterprise and Education of Catalan Government for providing support through the PhD Industrial Fellowship (2018 DI 77) in collaboration with Smart Engineering Ltd.

REFERENCES

[1] Blanco A, Pujadas P, de la Fuente A, Cavalaro S H P and Aguado A 2016 Influence of the type of fiber on the structural response and design of FRC slabs J. Struct. Eng. (United States) 142 1–11

[2] Barros J A O, Taheri M and Salehian H 2015 A model to simulate the moment-rotation and crack width of FRC members reinforced with longitudinal bars Eng. Struct. 100 43–56

[3] Carlesso D M, de la Fuente A and Cavalaro S H P 2019 Fatigue of cracked high performance fiber reinforced concrete subjected to bending Constr. Build. Mater. 220 444–55

[4] Vasanelli E, Micelli F, Aiello M A and Plizzari G 2014 Crack width prediction of FRC beams in short and long term bending condition Mater. Struct. Constr. 47 39–54

[5] de la Fuente A, Pujadas P, Blanco A and Aguado A 2012 Experiences in Barcelona with the use of fibres in segmental linings Tunn. Undergr. Sp. Technol. 27 60–71

[6] Belletti B, Cerioni R, Meda A and Plizzari G 2008 Design Aspects on Steel Fiber-Reinforced Concrete Pavements J. Mater. Civ. Eng. 1561 1–2

[7] Aidarov S, Mena Sebastiá F and de la Fuente A 2021 Structural response of a fibre reinforced concrete pile-supported flat slab: full-scale test Eng. Struct.

[8] Destrée X and Mandl J 2008 Steel fibre only reinforced concrete in free suspended elevated slabs: Case studies, design assisted by testing route, comparison to the latest SFRC standard documents Tailor Made Concr. Struct. 437–43

[9] Ministerio de Fomento 2008 Instrucción de Hormigón Estructural (EHE-08)

[10] CEN 2019 EN 12350-8:2019. Testing fresh concrete. Self-compacting concrete. Slump-flow test

[11] CEN 2019 EN 12350-6:2019. Testing fresh concrete. Density

[12] CEN 2019 EN 12350-7:2019. Testing fresh concrete. Air content. Pressure methods

[13] CEN 2019 EN 12390-3:2019. Testing hardened concrete. Compressive strength of test specimens

[14] König G and Kützing L 1999 Modelling the increase of ductility of HPC under compressive forces - a fracture mechanical approach (Mainz: RILEM Publications) pp 251–60

[15] Sato Y, Van Mier J G M and Walraven J C 2000 Fifth RILEM Symposium on Fibre-Reinforced Concretes (FRC) : Lyon, France, 13-15 September, 2000 Fifth Int. RILEM Symposium (RILEM Publications) pp 791–800

[16] RILEM TC162-TDF 2003 RILEM TC162-TDF: Test and design methods for steel fibre reinforced concrete. Final Recomendation Mater. Struct. 36 560–7

[17] fib 2010 fib Model Code for Concrete Structures 2010

[18] CEN 2007 EN 14651:2007. Test method for metallic fibre concrete. Measuring the flexural tensile strength (limit of proportionality (LOP), residual).

[19] Mitchell D and Cook W D 1984 Preventing Progressive Collapse of Slab Structures J. Struct. Eng. 110 1513–32

[20] Johansen K W 1962 Yield-line theory (Cement and Concrete Association)

[21] Johansen K W 1972 Yield-line formulae for slabs (Cement and Concrete Association)

[22] Nogales A and de la Fuente A 2021 Numerical-aided flexural-based design of fibre reinforced concrete column-supported flat slabs Eng. Struct. 232 1–24

[23] ACI Committee 544. and American Concrete Institute. 2015 Report on the Design and Construction of Steel Fiber-Reinforced Concrete Elevated Slabs (American Concrete Institute)

JOURNAL PAPER: SYSTEMATIC REVIEW ON THE CREEP OF FIBER-REINFORCED CONCRETE

Published in Materials 13.22 (2020).

Nikola Tošić *, Stanislav Aidarov and Albert de la Fuente

Civil and Environmental Engineering Department, Universitat Politècnica de Catalunya, Jordi Girona 1–3, 08034 Barcelona, Spain

* Corresponding author: Nikola Tošić; Email address: nikola.tosic@upc.edu

Abstract

Fiber-reinforced concrete (FRC) is increasingly used in structural applications owing to its benefits in terms of toughness, durability, ductility, construction cost and time. However, research on the creep behavior of FRC has not kept pace with other areas such as short-term properties. Therefore, this study aims to present a comprehensive and critical review of literature on the creep properties and behavior of FRC with recommendations for future research. A transparent literature search and filtering methodology were used to identify studies regarding creep on the single fiber level, FRC material level, and level of structural behavior of FRC members. Both experimental and theoretical research are analyzed. The results of the review show that, at the single fiber level, pull-out creep should be considered for steel fiber-reinforced concrete, whereas fiber creep can be a governing design parameter in the case of polymeric fiber reinforced concrete subjected to permanent tensile stresses incompatible with the mechanical time-dependent performance of the fiber. On the material level of FRC, a wide variety of test parameters still hinders the formulation of comprehensive constitutive models that allow proper consideration of the creep in the design of FRC elements. Although significant research remains to be carried out, the experience gained so far confirms that both steel and polymeric fibers can be used as concrete reinforcement provided certain limitations in terms of structural applications are imposed. Finally, by providing recommendations for future research, this study aims to contribute to code development and industry uptake of structural FRC applications.

Keywords: steel fiber reinforced concrete; polymeric fiber reinforced concrete; polymeric fiber; steel fiber; beam; crack; deflection; creep; shrinkage; modeling

1. INTRODUCTION

In recent decades, one of the most promising types of concrete, for both structural and non-structural applications has become fiber-reinforced concrete (FRC), i.e., concrete produced with steel or polymeric fibers which can bring tangible technical and economic benefits [1]. Studies using multi-criteria decision making methods, considering social, economic and environmental sustainability, have also shown that FRC can be more sustainable than reinforced concrete (RC) for different infrastructure applications, for which the use of fibers is technically viable (as unique reinforcement or in combination with traditional steel rebars) [2–4]. Considering the immense quantities of concrete produced globally, i.e., more than 25 billion tons annually [5], such advances towards more sustainable solutions are crucial.

In developed countries, more than 50% of total concrete produced is used in structural applications [6]. Therefore, FRC has been tested increasingly as a solution for partially or even completely replacing reinforcement for applications such as ground-supported slabs [7–9], pavements [10,11], roads, tunnel linings [12–18], pipe sewer lines [19,20], and flat slabs [21–25], which means that it is increasingly used in elements exposed to bending, resisting gravitational, long-term loads. Owing to extensive research over past years, structural design of FRC has been incorporated into several design codes, such as the *fib* Model Code 2010, ACI 318, Italian and the Spanish Code [26]. Nonetheless, research has so far focused mostly on short-term material and structural properties and this has left some FRC design aspects still in the early stages of research. One such aspect is the time-dependent behavior, and particularly, creep of FRC.

Even without considering the effects of fibers, the quantification of the mechanical behavior of RC structures is complex due to effects such as shrinkage, creep, and cracking [27]. FRC introduces further complexities, especially considering that FRC itself may be produced with different types of fiber such as steel fibers (steel fiber-reinforced concrete, SFRC) or polymeric fibers (polymeric fiber reinforced concrete, PFRC) that can exhibit different mechanical properties. In general, among the aspects to be considered, is the progressive creep or damage of the fiber-matrix interface and the debonding and pull-out of the fibers [26] as well as the susceptibility of fiber filaments to tensile creep, in the case of certain polymeric fibers [28] when subjected to stress levels incompatible with material properties.

When these effects are combined with creep and shrinkage of the concrete, FRC members may be subjected to increasing crack widths and, consequently, potential loss of serviceability, durability and, eventually, mechanical performance. In this regard, crack width is a governing parameter in steel-based reinforcements for concrete and extensive experimental programs have found that chloride-induced corrosion [29,30] and embrittlement [31] mechanisms are crack width sensitive. These phenomena are unexpected when polymer-based materials are used as concrete reinforcements. However, polymeric fiber creep in cracked-sections may lead to loss of mechanical capacity if these are subjected to permanent tensile stresses of magnitudes incompatible with the time-dependent mechanical properties of the fibers, tensile creep of cracked-sections also being a crack width-sensitive phenomenon. This drawback can be solved through the use of hybrid solutions (fibers and steel reinforcing bars, “hybrid-FRC”) [26].

Thus, it is evident that creep of cracked FRC elements has clear design and structural implications and should be carefully considered. Although there exist some general provisions and recommendations (rather limitative and restrictive due to the lack of consistent research), it is still necessary to derive reliable design and calculation methods for serviceability limit state (SLS) analysis of cracked FRC structures subjected to long-term bending.

While previous studies have focused only on a single fiber type or single level (fiber, material, structure), a systematic review of existing literature on the response of FRC and hybrid-FRC subjected to creep is necessary from a comprehensive and bottom-up perspective. For this purpose, this paper presents a critical assessment of published studies collected through a methodical literature search. Hence, the aim of the study is to provide insight into the main influencing parameters of FRC creep, methods for experimental characterization as well as theoretical formulation of FRC time-dependent behavior. In Section 2, details about the literature search are presented in terms of databases used, search terms and justification of publication screening. In Section 3, research on the material level is presented, from studies on the creep behavior of individual fibers and fiber material (steel and polymeric macrofibers) to long-term studies on the level of concrete specimens. In Section 4, existing research on the structural level is presented (full-scale tests on FRC and hybrid-FRC elements under long-term bending) as well as existing analytical SLS design proposals. Each section ends with a synthesis of the presented knowledge, a critical assessment of literature, and guidelines for future research. Finally, Section 5 summarizes the entire study with a concise overview and recommendations for future work that can lead to a consistent and comprehensive SLS design methodology for FRC structures.

2. METHODOLOGY

The first step in the study was a systematic literature search. For this purpose, journal and conference articles dealing with the creep behavior of SFRC and PFRC, on material and structural levels, were considered. For the literature search, the online databases of Scopus [32] and Web of Science [33] were used, complemented with personal archives compiled previously.

The following search terms were used for Article Titles in Scopus and Web of Science:

1. “fib** reinforced concrete” AND “long-term”
2. “fib** reinforced concrete” AND “time-dependent”
3. “fib** reinforced concrete” AND “creep”
4. “synthetic” AND “fib**” AND “creep”
5. “polypropylene” AND “fib**” AND “creep”

The syntax “fib**” was used to cover both British and American English spelling (fibre vs. fiber). Search terms 1–3 were used to find research at the concrete specimen and structural member level, whereas search terms 4–5 were used to find on research on the single

fiber or fiber material level (focusing on "synthetic/polymeric" fibers as these are more prone to undergo creep and polypropylene fibers as the most widely used among this type of fiber).

The initial search yielded a total of 250 studies: 125 on Scopus, 83 on Web of Science and 42 from the personal archive of the researchers. The next step was the removal of duplicate studies which led to the removal of 90 studies, leaving a total of 160 distinct journal and conference articles.

The remaining articles were screened for language (only studies in English were retained) and topic (only studies on concrete and time-dependent behavior were retained—studies on, e.g., asphalts, fiber composites and durability were excluded). This led to the removal of 69 studies, leaving 91 studies in the database.

Finally, through the institutional access available to the researchers, 19 studies could not be accessed. Therefore, the final number of studies considered in the review was 72. These studies were divided into three groups: (1) fiber level, (2) concrete level, and (3) structural level. When dividing the studies according to their content, certain studies were categorized into more than one group. Therefore, the 70 studies were divided into (overlapping) groups of 10, 43, and 23 studies for groups (1), (2), and (3), respectively, summarized in Table 1.

Table 1. Summary of systematic literature search.

Topic/Group	No. of Studies/References
Total no. of studies	72; [26,28,34–103]
Fiber level	10; [28,34–42]
Concrete level	43; [28,37,43–83]
Structural level	23; [26,44,45,84–103]

Any systematic review introduces a certain bias. Herein, the bias consists in several factors. First, the selection of studies only in English potentially excludes a body of knowledge in other languages. However, considering that the large majority of studies indexed in Scopus and Web of Science are in English, this bias is considered not significant. Second, only journal and conference articles are considered, and documents such as reports and theses are excluded. This bias can also be considered negligible as the number of these documents is not large, and, e.g., doctoral theses are typically accompanied by journal publications of the same content. Finally, a certain bias is introduced by the databases themselves; however, as the most renowned and accepted databases, Scopus and Web of Science were considered appropriate.

3. RESEARCH ON THE MATERIAL LEVEL

3.1. CREEP BEHAVIOR OF FIBERS AND FIBER-CONCRETE BOND

As a multi-level phenomenon, the creep behavior of FRC is also influenced by the behavior of the fibers themselves as well as their bond with the concrete matrix. Gettu et al. [28] identify creep of individual fibers or filaments and the progressive creep of the fiber–concrete interface as significant factors that can lead to crack width increase, as well as durability and serviceability issues in cracked FRC elements under sustained loading. However, a

fundamental difference exists between steel fibers and polymeric fibers. In the case of PFRC, the creep of individual fibers is the dominant effect in PFRC; whereas in SFRC, the pull-out creep becomes the dominant phenomenon at the material level, as steel fibers do not undergo any considerable creep at normal temperatures [28].

3.1.1. Creep Behavior of Individual Fibers or Filaments

Unlike steel fibers, which undergo negligible creep at room temperature, polymeric fibers can experience creep, particularly at elevated temperatures. This behavior is caused by their viscoelasticity; particularly, more crystalline and cross-linked polymers are less susceptible to creep [28]. In cracked FRC sections, the creep of polymeric fibers, most notably polypropylene, will lead to an increase of crack width which will in turn cause relaxation in the fibers leading to a decreased bridging effect and further crack width increases [28].

Studies on the creep behavior of polypropylene fibers date back to the 1960s and the works of Hadley and Ward [40]. These authors were among the first to perform creep and recovery tests on polypropylene filaments and propose mathematical formulations for the entire range of behaviors exhibited by polypropylene [40]. Hadley and Ward [40] found that the relationship between creep compliance (function describing the relation between total strain and stress) and stress for six fiber monofilaments—produced in different ways such as drawing and spinning—generally consists of four regions assessed qualitatively: (1) a region at low stresses in which specific creep (creep strain divided by stress) is independent of stress and linear viscoelastic behavior is observed, (2) a region at higher stresses in which specific creep develops parabolically relative to stress; this is followed by (3) a region in which specific creep is linearly related to stress, and finally, (4) a region at very high stresses, in which specific creep is once more independent of stress. Similar behavior was confirmed also by other authors [41].

Already by 1980, Takaku [42] had studied creep failure of isotactic polypropylene fibers and found it to be highly dependent on temperature (temperatures between 40 °C and 130 °C were used). More recently, Liu et al. [34] studied the creep behavior of four types of polypropylene under combined effects of temperature, ultraviolet light, and tensile stress. The authors of study [34] tested polypropylene formed into dumbbell-shaped tensile bars 150 × 10 × 4 mm—this is an important limitation to extrapolating the results of this study to polypropylene fibers used in FRC which are produced by a stretching process. The creep tests were performed under a stress lower than the polypropylene yield strength (27–36 MPa for the polypropylene tested in the study). Different temperatures were used (−30 °C to 70 °C), different loads (500–2400 N) and different ultraviolet (UV) light intensities applied for 12 h (300 and 600 μW/cm^2); and the time to failure was measured. As for the variables chosen in this study, it should be noted that when using fibers in FRC, due to the process of their addition directly in the concrete mix and subsequent embedding in the matrix, ultraviolet radiation is expected to have a negligible effect. Liu et al. [34] found that changes in temperature had the most significant effect on the creep rate of polypropylene. As an example, for sample PP1 under a load of 500 N, at 50 °C there was no creep failure; at 60 °C creep failure occurred after 18,000 s and at 70 °C after 1800 s. The effect of temperature was explained by the increase of the free volume of polypropylene and the subsequent weakening of intermolecular forces. At the same time, under a constant temperature, increasing load led

to an increase of the creep rate. For example, when sample PP1 was at a temperature of 23 °C and a load of 800 N, no creep failure occurred; however, increasing the load to 900 N led to creep failure after 13,000 s and increasing the load to 1000 N led to creep failure after 2000 s. The effect of stress was explained by the decrease of the barrier for bond dissociation that enables the movement of molecular chains. The most important finding by the authors of study [34] is that of a critical failure strain, ε_{crit}, that varied depending on temperature but was not affected by tensile stress or ultraviolet light irradiation [34], Figure 1. At room temperature (23 °C), ε_{crit} varied between 12% and 17% for the different polypropylene types and increased/decreased with increasing/decreasing temperature.

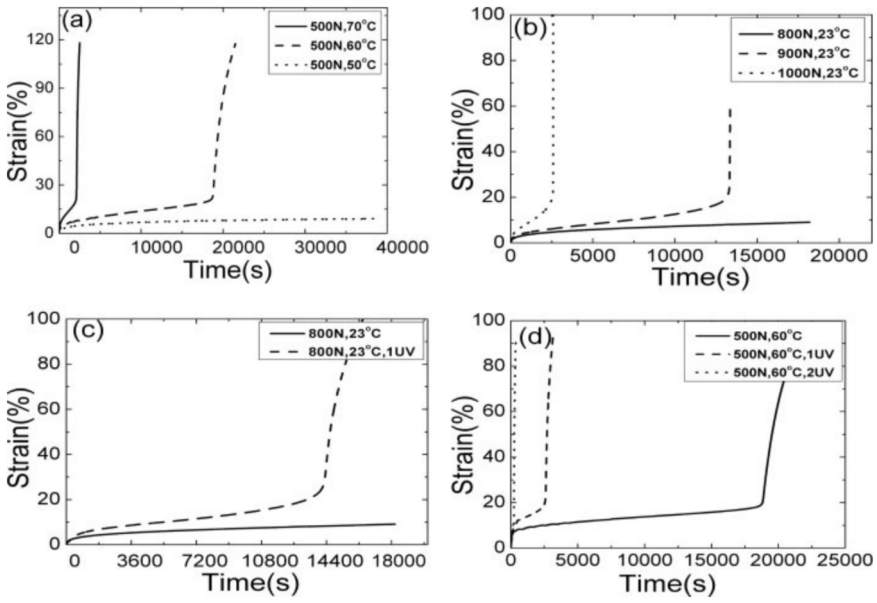

Fig. 1. Values of ε_{crit} for polypropylene sample PP1 under different aging conditions (authorized reprint from [34]): effect of varying stress and UV intensity under (a) 23°C, (b) 60°C, (c) 0°C and (d) –30°C.

Fouda et al. [39] tested the influence of temperature on creep deformation of polypropylene fibers based on optical measurements (interferometry). Undrawn polypropylene fibers were subjected to a constant load for up to 230 min under temperatures of 23 °C, 30 °C, and 40 °C. These authors found that the creep rate (increment of creep over an increment of time) firstly decreased with increasing strain (primary creep) and then remained constant (secondary creep). Nonetheless, up to 5 min, the creep behavior seemed to be independent of temperature. Fouda et al. [39] were able to successfully match the observed behavior to a model consisting of a series connection of a two-component Kelvin chain:

$$J(t) = \frac{1}{E_1} \cdot \left(1 - e^{-t/\tau_1}\right) + \frac{1}{E_2} \cdot \left(1 - e^{-t/\tau_2}\right) \quad (1)$$

where $J(t)$ is the compliance function at time t, E_1 and E_2 are the spring moduli, and τ_1 and τ_2 are the retardation times of the Kelvin models 1 and 2, respectively. Finally, these authors also found that fiber yield stress and modulus of elasticity decreased with increasing temperature, whereas the fiber yield strain increased with increasing temperature [39]. It should be noted for this study as well that undrawn fibers were used, i.e., fibers not produced in the same way as those intended for application in FRC. Therefore, a potentially different

behavior of drawn polypropylene fibers could be expected, thus warranting further investigations into this topic.

Vrijdaghs et al. [35] tested two types of polypropylene macrofibers for uniaxial tensile creep. A total of 26 samples (14 of fiber A and 12 of fiber B) were tested at a temperature of 20 °C and relative humidity (RH) of 60%. Five different load levels were considered, from 22% to 63% of the fiber strength. The time to failure and strain at failure were recorded. The authors [35] found that all samples underwent failure in the secondary creep phase. The time to failure ranged from several hours for samples loaded to 63% of fiber strength to several months for fibers loaded to 22% of their strength. The strains at failure were significant (40–100%) and the creep coefficients (ratios of creep strain to instantaneous strain) were generally larger than 10. However, these results only describe the behavior of polypropylene alone, i.e., the observed behavior is not expected to be replicable at the structural level once fiber–matrix interaction comes into play as well as the presence of steel reinforcement in structural members.

3.1.2. Pull-Out Behavior of Fibers

Whereas in the case of polymeric fiber reinforced concrete (PFRC) temperature has an effect mostly through single fiber or filament creep, in the case of SFRC the effect of temperature is mostly exerted through changes in the fiber–concrete bond [28]. This process consists of debonding and frictional pull-out, as shown in Figure 2. As for PFRC, particularly polypropylene fiber reinforced concrete (PPFRC), the Poisson's ratio (v) of polypropylene (0.40–0.45) causes significant lateral contraction of the fibers facilitating debonding [28].

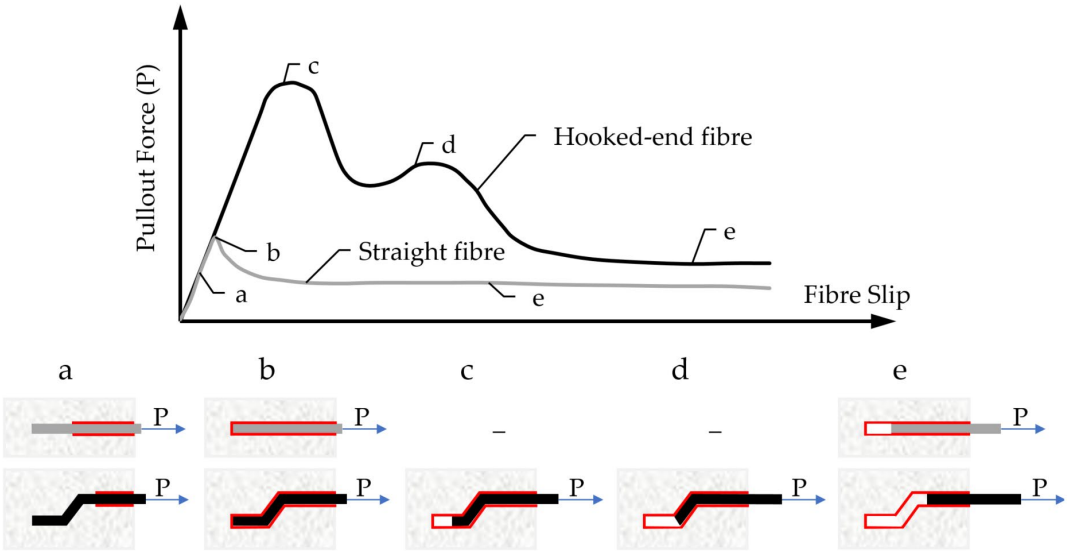

Fig. 2. Example of debonding and fiber pull-out of straight and hooked-ended fibers (adapted from [28]). (a) Partial debonding, (b) Full debonding, (c) Plastic deformation of fiber hook (1), (d) Plastic deformation of fiber hook (2) and (e) pull-out.

Vrijdaghs et al. [36] performed creep pull-out tests on two types of polypropylene macrofibers for which fiber creep was assessed previously [35]. These authors used a test setup in which a single fiber was embedded over varying lengths (10–30 mm) in a concrete cylinder while the other end of the fiber was clamped between steel plates over a length of 65 mm with 20 mm of free length. Then, the fibers were tested under a temperature of 20 °C and

relative humidity (RH) of 60% under loads corresponding to 25–75% of the pull-out strength obtained in short-term tests (P_{max}). It was found that all specimens loaded above 40% of P_{max} failed within 60 days due to complete fiber pull-out. The authors of study [36] calculated the initial debonded length of the fibers of l_{db} = 14.4 mm consisting of 3–4 mm within the concrete (4–5 times the fiber diameter) and ~10 mm in the clamps. Over this length, the creep of the fiber itself was considered [35]. Once these results were superimposed on the long-term pull-out results, it was found that there is an excess of creep deformation above the single fiber creep. The authors concluded that this was due to the progressive debonding caused by time-dependent Poisson contraction of the fiber [36].

Pull-out creep tests on PFRC specimens were also performed by Babafemi et al. [38] who tested three types of polymeric macrofibers embedded in 50 mm cubes and loaded to 50% of the pull-out strength for 30 days, Figure 3. These authors found a significant effect of fiber type with one fiber failing after 22 days, whereas the pull-out displacement of the other two fiber types gradually decreased. X-ray computed tomography images of the samples were taken and it was found that immediately after loading, an initial debonding occurs and the instantaneous axial displacement is actually a consequence of the elongation of the fiber over the debonded length, and not of pull-out. Over time, the dominant effect becomes fiber creep over the debonded length which leads to Poisson contraction, loss of friction and subsequent pull-out.

A similar study to that of Vrijdaghs et al. [36] was performed by Nieuwoudt et al. [37], but on SFRC using hooked-end steel fibers. Among other properties, the authors performed single fiber pull-out creep tests on single steel fibers embedded in 100 mm cubes. In these tests, the variables were load level, fiber orientation angle, fiber mechanical anchorage, and fiber pre-slipping. The tests were performed for 240–250 days. It was found that increasing the load level led to increasing pull-out. The results for different fiber orientation angles did not show a clear trend. As for mechanical anchorage, the more kinks the steel fiber had, the higher was the pull-out creep—this was ostensibly due to the fact that specimens with steel fibers with more kinks were actually loaded to higher absolute loads, and thus, caused higher creep, as well as the fact that more concrete is in the zone around the kinks, exposed to localized sustained compressive loading leading to higher creep.

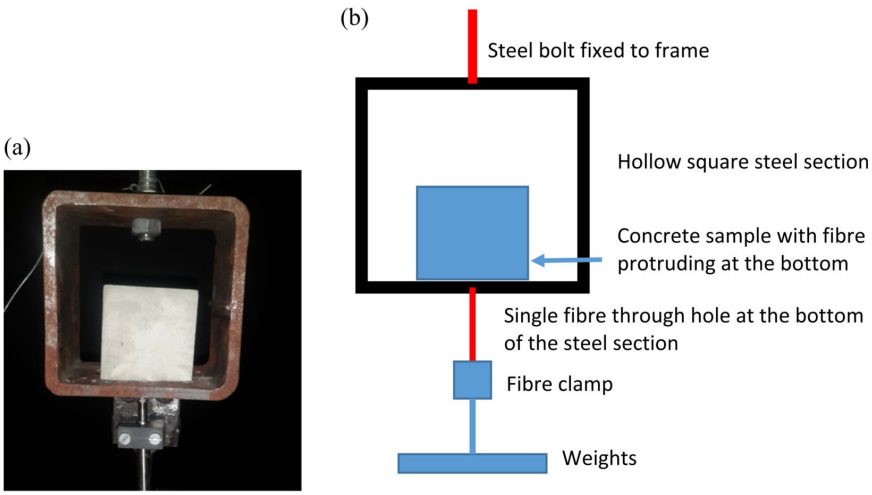

Fig. 3. Sample placed in position on steel section for the pull-out creep test (b) diagram of the setup [38].

3.1.3. Summary of the Results on the Creep Behavior of Fibers and Fiber–Concrete Bond

The studies that were analyzed reveal important conclusions at the material level. In terms of individual fiber creep—beside the fact that it is negligible for steel fibers—the creep of polymeric, particularly polypropylene fibers needs to be taken into account under certain circumstances. All studies point to a clear influence of temperature on polypropylene creep behavior, as well as the existence of a critical failure strain that is temperature-dependent, but load-independent [34]. Furthermore, it is important that studies have confirmed the applicability of Kelvin chain models for describing polypropylene creep behavior [39]. What remains to be formulated is a temperature dependency of the series Kelvin chain model.

At the level of fiber–concrete bond, several pull-out tests with important conclusions were presented. In the case of SFRC, fiber shape (number of kinks in hooked-end fibers) was shown to cause an important effect through complex stress localizations around the kinks leading to potentially higher pull-out creep [37]. In PFRC, the creep of individual fibers needs to be superimposed on the pull-out creep that seems to be of secondary importance in this case [38]. A potential way forward in this area is the proposal of time-dependent and temperature dependent Kelvin chain models that would consider only pull-out creep in the case of SFRC and combined effects of individual fiber creep and pull-out creep in the case of PFRC.

3.2. CREEP BEHAVIOR OF FIBER-REINFORCED CONCRETE (FRC)

So far, the largest number of research studies on the creep behavior of FRC was performed on the material level of specimens in long-term compression, tension, and bending. However, these tests are time-consuming and with a large number of influencing factors, this challenging proper execution. Even though the number of performed tests is significant, almost all of them have been performed with different parameters, from the type of FRC, to the type of test, applied load, duration, or type of measurements recorded. This poses significant challenges in interpreting the results, synthesizing conclusions, and proposing constitutive models.

In terms of tensile creep of FRC—which is of primary interest in this paper—a typical test procedure is shown in Figure 4. Whether the test is uniaxial tension or bending, the specimen is first pre-cracked to a pre-defined crack-opening (point B) for which the residual strength f_R is determined. This pre-crack width is usually within the range of 0.2–0.5 mm but this can vary significantly. Further, the average crack opening is mostly used as a quantification of the crack opening [75]. Subsequently, the specimen is unloaded (B-C) and moved to the long-term testing frame. This is important to note, since the specimen typically is tested in different machines for short-term and long-term characterization. This can entail a change in boundary conditions and undesired influences [75].

As pre-cracking is normally performed at low crack opening rates, creep deformations develop during this stage as well. Part of this deformation is recovered in the unloaded state (C-D). Afterwards, the specimen is reloaded to a fraction of the residual stress measured during pre-cracking (D-E/E'/E''), $\sigma_c = \alpha \cdot f_R$, where α is the so-called "creep load ratio," typically chosen in the range of 30–70%; nonetheless, its proper justification is very important. The reloading time t_L should be as short as possible, in order to limit the

interference of instantaneous and delayed deformations [75]. During the long-term tests, deformations increase at a constant load (E-F/E'-F'/E''-F''). At the end of the long-term test (if failure did not occur), the specimen is unloaded (F/F'/F''-G) and part of the long-term deformation is recovered (G-H). Finally, the specimen might be reloaded to failure in a final short term test (H-I-J).

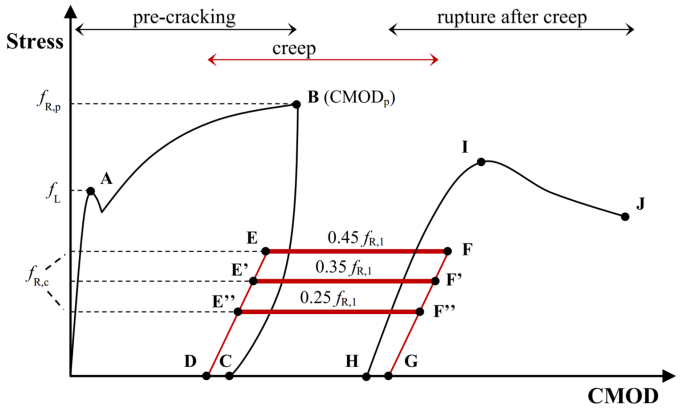

Fig. 4. Main stages of the cracked fiber-reinforced concrete (FRC) creep test methodology [56].

In the following subsections, studies on compressive creep and shrinkage of FRC and tensile creep in uniaxial tension and bending are summarized and existing analytical and numerical models are presented with an identification of existing knowledge gaps and recommendations for future research.

3.2.1. Effect of Fibers on Compressive Creep and Shrinkage of FRC

Although shrinkage and compressive creep are important phenomena, they have been often overlooked in research on FRC. The benefits of fiber reinforcement in terms of reducing plastic shrinkage are well-known and acknowledged [104] and can be significant—for example, Pešić et al. [54] report 70–80% of plastic shrinkage reduction with moderate amounts of steel and plastic fibers (0.40–1.25%). However, tests on drying shrinkage and creep are less numerous.

The ACI Committee 544 report on FRC [105] suggests that the addition of less than 1% of steel fibers (80 kg/m^3) does not induce an effect on compressive creep. Nonetheless, the results of individual researchers can differ. For example, Nakov et al. [52] tested C30/37 concretes with 0, 30, and 60 kg/m^3 of steel fibers in compression for 400 days, exposed to a compressive stress of 7.5 MPa (stress-to-strength ratio of approximately 0.2). These authors found creep to decrease with increasing steel fiber content. After fitting the analytical B3 creep prediction model [106] to their experimental results and extrapolating to 100 years, the creep coefficient was reduced by 11.1% and 17.8% for SFRC with 30 and 60 kg/m^3 of steel fibers, respectively, relative to the ordinary Portland cement concrete (OPC). Similarly, Chern and Young [62] also found that the inclusion of up to 2% of steel fibers reduces both creep and shrinkage with increasing fiber volume V_f. Additionally, Chern and Young [62] noted that the effect of fibers increased over time, i.e., the differences between SFRC and OPC increased over time due to more activation of fibers as the concrete underwent creep. In a study on high-performance FRC, Afroughsabet and Teng [58] tested FRC with only steel fibers and with a mix of two different steel fibers and a mix of two different steel fibers and

polyvinyl alcohol fibers. These authors found that the addition of fibers decreased creep and shrinkage and that adding mixes of fibers was beneficial to the reduction of deformation.

Contrary to these results, Błyszko [60] tested SFRC and OPC and found a significant increase in compressive creep when adding steel fibers. However, it should be noted that the test lasted only around 15 days and the concretes were exposed to high compressive stresses equal to 40% and 85% of their compressive strength. In this case, even the 40% load level can be considered to fall under non-linear creep conditions where significant microcracking is present in the concrete, this potentially affecting the fiber bond and causing damage to the matrix. Since such high compressive stresses are unlikely to occur under typical service conditions of FRC structural applications, they can be considered of less significance for design implications.

Overall, the question of FRC compressive creep and shrinkage is empirical and its resolution depends on significantly more tests being performed. Such results could then be included in existing creep and shrinkage databases, such as the NU-ITI [107], and existing models such as the *fib* Model Code 2010 [108] and B4 [109] could be adapted for FRC. Until then, considering expected stress levels in FRC structural applications and typical fiber contents, effects of fibers on creep and shrinkage could be disregarded.

3.2.2. FRC Long-Term Uniaxial Tension Tests

Theoretically, long-term uniaxial tension tests should be a preferable choice for testing the tensile creep of FRC. However, performing them carries significant challenges in equipment and measurement design such as the requirement for relatively large samples and the possible occurrence of secondary moments causing stress redistribution [75]. Therefore, such studies are less numerous than long-term bending tests and practical experience is quite limited. A typical long-term uniaxial tension test setup is shown in Figure 5.

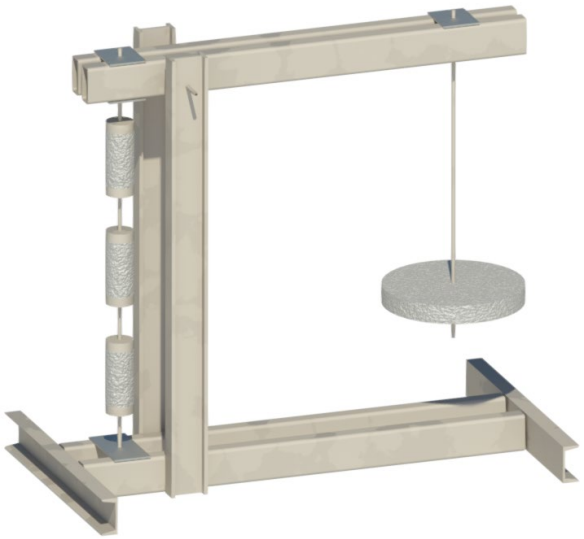

Fig. 5. Experimental setup for long-term uniaxial tension tests (adapted from [75]).

An overview of the setup and parameters of long-term uniaxial tension tests is provided in Table 2. Two of the studies tested SFRC with hooked-end steel fibers and two studies tested PPFRC. The fiber volume is relatively uniform as are specimen type, climate

conditions, test duration, and fiber aspect ratio. There is a somewhat larger variation in the pre-crack width selected for the test with an average close to 0.4–0.5 mm. Finally, load level was also widely varied in the test. Notably, all studies except that by Zhao et al. [49] defined the load level as a percentage of the residual strength f_R at the selected pre-crack width. However, Zhao et al. [49] defined it as the percentage of maximum pre-cracking load P_{max}. Zhao et al. [49] and Nieuwoudt et al. [37] explicitly state that shrinkage was also measured and taken into account in the analysis.

Table 2. Summary of parameters in long-term uniaxial tension tests.

Ref.	FRC Type	Fiber Aspect Ratio	V_f	Specimens [1] (mm)	Pre-Crack Width (mm)	Load Level [2]	Climate (T & RH) [3]	Time (Days)
[37]	SFRC	67	0.5%	100/100/500	0.40–0.75	30–85%	–	240
[49]	SFRC	65	1.0%	Ø100/300	0.05; 0.20	30% [2]	20 °C, 60%	100
[50]	PPFRC	50	1.0%	Ø100/300	0.20	30–45%	20 °C, 60%	180
[79]	PPFRC	50	1.0%	100/100/500	0.50	30–70%	23 °C, 65%	240

[1] All specimens were notched; [2] Relative to maximum pre-cracking load; [3] Temperature and relative humidity

A summary of the results is shown in Table 3 where f_{max} is the maximum pre-cracking stress, f_{R1} and f_{R3} are residual strengths at crack widths of 0.5 and 2.5 mm, respectively, and ϕ_w is the crack width creep coefficient defined as the ratio of the increase in crack width over time w_{creep} divided by the initial crack width after loading in the creep test w_{init}. However, it should be noted that at time t in the long-term test, the total crack width w_{tot} is composed of the following:

$$w_{\mathrm{tot}} = w_{\mathrm{irr}} + w_{\mathrm{inst}} + w_{\mathrm{creep}} + \delta_{sh} \quad (2)$$

$$\varphi_{\mathrm{w}} = w_{\mathrm{creep}}/w_{\mathrm{inst}} \quad (3)$$

where w_{irr} is the irrecoverable crack opening upon unloading in the short-term tests and δ_{sh} is the shrinkage of the specimen.

Table 3. Summary of long-term uniaxial tension test results.

Ref.	f_{max} (MPa)	f_{R1} (MPa)	f_{R3} (MPa)	ϕ_w
[37]	3.65	1.76	2.13	0.87–2.10
[49]	6.84; 8.00	6.59; 7.50	6.02; 6.81	0.95–2.10 [1] ~0.8–4.0 [2]
[50]	3.70	1.78	2.05	<1.00 [3] ~9 [4]
[79]	~3.00	~0.80	~1.00	–

[1] At pre-crack 0.05 mm; [2] At pre-crack 0.20 mm; [3] At load level 30%; [4] At load level 45%

The results in Table 3 reveal several interesting outcomes. Firstly, in the case of SFRC, the crack width creep coefficient is similar to the concrete creep coefficient in tension. Since in the case of SFRC there is no creep of the fibers, the only creep in tension comes from the fiber-concrete bond. This is actually a complex superposition of compressive and tensile

concrete creep. Since tensile creep of concrete is in the same order of magnitude as compressive creep, with studies claiming it has either similar [110] or 50–100% greater values [111], this explanation seems plausible.

However, for PPFRC the situation is quite different. For the study by Babafemi and Boshoff [79] ϕ_w values could not be extracted. The authors of that study note that there was no crack width stabilization even for specimens loaded to 30% of pre-cracking residual strength, whereas specimens loaded to 60% and 70% failed within 10 and 1 days, respectively. In the case of Vrijdaghs et al. [50], specimens loaded to 30% exhibited very low crack width increases that did not surpass initial crack width values even after 180 days. However, when loaded to 45% of the residual strength, very large ϕ_w values were recorded and initial crack widths were surpassed within hours. These results point to the special importance of controlling for individual fiber creep in the case of PFRC.

3.2.3. Long-Term Bending Tests

The majority of long-term tests on FRC on the material level were performed in the form of long-term bending tests on prismatic specimens. Such tests typically employ a lever system in order to maintain a constant load, and generally, several stacked specimens are used, Figure 6. The use of stacked specimens means that not all of them are exposed to the same load; however, considering the scatter of FRC residual strength, this can typically be overcome by careful arrangement of the specimens [75]. In the vast majority of cases, four-point bending is used; however, this means that the long-term test configuration differs from the typical short-term characterization (e.g., using the EN 14651 three-point bending test [112]).

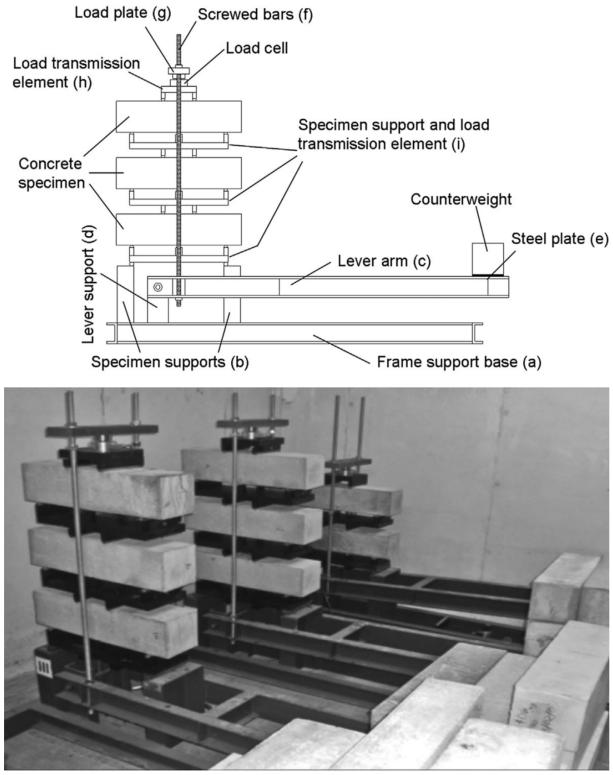

Fig. 6. Experimental setup for long-term bending tests [55].

Unlike uniaxial tension tests in which the crack width, i.e., crack opening displacement (COD), is directly measured, in bending tests, the measured deformation is usually the crack mouth opening displacement (CMOD), crack tip opening displacement (CTOD) or the mid-span deflection. The results are then reported in terms of creep coefficient representing the ratio of the creep and initial deformation components. It should be kept in mind that the measured deformation is affected by the tensile creep of fibers and the fiber–concrete bond as well as the compressive creep of concrete in the compressed zone and shrinkage. Since the crack can propagate significantly in the cracked section (e.g., up to 100 mm in a 150 mm high cross section [28]), the compressive stress in the cracked zone can become high and cause nonlinear creep and microcracking. Hence, the use of "creep coefficients" obtained directly from bending tests without compensating for compressive creep and shrinkage should be done with caution [28].

An overview of the setup and parameters of long-term bending tests is provided in Table 4. The table reveals that there is a wide variety of parameter choices in the majority of the tests performed so far. Importantly, SFRC and PFRC are relatively equally represented with several studies performing comparative research on their long-term behavior. Furthermore, the majority of the tests are four-point bending tests, although Zerbino et al. [78] demonstrated that the use of three-point bending in long-term tests would not significantly alter the nature of the obtained results. As in uniaxial bending tests, the creep load is selected as a percentage (typically 50%) of the residual strength at the selected pre-crack width (typically 0.5 mm); nonetheless, both the pre-crack widths and load levels can vary significantly. It is important to keep in mind that, from the point of view of SLS design, even the pre-cracking widths of 0.5 mm exceed typically allowed crack widths: for example, the Eurocode 2 crack width limit for RC members under the quasi-permanent combination is 0.3 mm for the majority of ambient exposure classes [113].

As for the results, comparing and analyzing them quantitatively is more difficult than in the case of uniaxial tension tests. Namely, creep coefficients are sometimes reported in terms of CMOD, sometimes in terms of deflections. Additionally, the creep coefficient is sometimes defined based on the initial crack width after loading in the creep test (i.e., compensating for the irrecoverable crack width w_{irr}) and other times in terms of the initial crack width related to the origin ($w_{irr} + w_{inst}$) (Figure 4). Finally, shrinkage is not always taken into account, whereas the effect of compressive creep is almost never discussed. Therefore, only a qualitative discussion of the results is meaningful. Generally, as in the case of uniaxial tension tests, the creep of SFRC is not drastic, specimens never experience tertiary creep or failure and creep coefficients are commensurable to those in compression [56,57,71,80]. As for results on PFRC, as in earlier described studies, the deformations tended to strongly depend on temperature. For example, Buratti and Mazzotti [83] tested PFRC under increasing temperature from 20 °C to 50 °C which had a major effect on their behavior, increasing deformation and even leading to failure. Kurtz and Balaguru [47] compared polypropylene and nylon FRC pre-cracked to 0.75 mm. The authors of study [47] found that the "maximum infinitely sustainable stress" (i.e., stress that did not lead to creep failure) was 24.9% for PPFRC and 38.3% for nylon FRC.

Table 4. Summary of parameters in long-term bending tests.

Ref.	FRC Type	Fiber Aspect Ratio	V_f	Specimens (mm) and Test Type	Pre-Crack Width (mm)	Load Level	Climate (T and RH)	Time (Days)
[47]	PFRC	-	~0.1%	100/100/350 Cantilever	0.75	22–88%	-	Until failure
[48]	PPFRC	50	1.0%	100/100/500 4-point	0.20	30–50%	23 °C; 65%	240
[53]	SFRC	-	0.5%	50–150/150/600 4-point	0.50	60%	23 °C	110
[55]	SFRC	45-80	0.5%; 0.9%	150/150/600 4-point	0.50	60%; 80%	-	90
[56]	SFRC	50	1.25%	150/150/600 4-point	0.05-0.50	25–45%	22 °C	180
[57]	SFRC	50	0.50%	150/150/600 4-point	0.2-3.5	64–156% [1]	16–23 °C; 22–64%	630
[63]	SFRC	44	1.0%; 2.0%	50/50/650 3-point	-	20% [1]	23 °C	120
[65]	SFRC	65	1.90%	40/80/1200 4-point	n/a [2]	50% [2]	-	150
[70]	SFRC; PPFRC	44; 83	0.50%	150/150/600 4-point	0.25; 1.50; 2.50	40–70%	-	90
[71]	SFRC; PPFRC	50-160	0.50%	150/150/600 4-point	0.50	70%	20 °C; 60%	90
[78]	SFRC; PPFRC	40-100	0.40%	150/150/600 4- & 3-point	0.50	50–70%	21 °C	290
[80]	SFRC; PFRC	-	~0.40%	100/100/500 4-point	1.75	50%; 60%	21 °C [3]	3200
[83]	PFRC	40-100	0.3–0.8%	300/120/2000 3-point	0.20	50%	20–50 °C	90

[1] Relative to maximum pre-cracking load; [2] Pre-cracking test stopped after fist cracking; [3] Aluminium-sealed

Nonetheless, as stated above, the generally adopted pre-crack widths in these studies exceed common code limitations [113] and, therefore, the "maximum infinitely sustainable stresses" are most likely higher at crack widths corresponding to code limits (0.2–0.4 mm), probably approaching 60% of residual strength at those crack widths. In terms of other parameters, Zerbino et al. [53] found that varying beam width did not significantly affect results, at least for SFRC, but increasing width did reduce variability. Zerbino et al. [53] also did not find any effect of creep deformation on ultimate strength.

One parameter that was identified as potentially having explanatory power was the crack opening rate COR [56,71,78]:

$$COR^{i-j} = \left(CMOD_{\mathrm{ct}}^{j} - CMOD_{\mathrm{ct}}^{i}\right)/\left(t_j - t_i\right) \quad (4)$$

where $COR^{i\text{-}j}$ is the crack opening rate in time increment i–j, $CMOD_{\mathrm{ct}}^{i}$ and $CMOD_{\mathrm{ct}}^{j}$ are total crack opening at times t_i and t_j, respectively. COR tends to stabilize after a few weeks; hence, measurements should be performed for at least 90 days [71]. However, much more work is needed in this direction in order to define conformance and acceptance criteria in terms of COR.

Nonetheless, the variability of parameters in tests and the variability of FRC long-term properties have made it difficult to identify clear influences of certain parameters. For example, Llano-Torre et al. [68] performed a quantitative analysis of literature on long-term uniaxial and bending tests of SFRC, PFRC and glass fiber FRC. These authors analyzed two crack width creep coefficients at 90 days: one related to the origin (taking into account $w_{\mathrm{irr}} + w_{\mathrm{init}}$), ϕ_{o} and another taking into account only w_{init} (as the one in Table 3), ϕ_{c}. Analyzing the relationship between these creep coefficients and applied load level (IFa)—expressed as a percentage of residual strength at pre-cracking (0.5 mm)—a very large scatter was found, obscuring any clear trend and effect of load level (which should be theoretically considered a primary factor).

3.2.4. Modeling the Creep Behavior of FRC

The fact that there is a wide variety of tests, test parameters, and reported results on the long-term behavior of FRC has impeded the proposal of general analytical models. So far, most of the work has been restrained to numerical models of long-term uniaxial tension or bending tests on FRC, typically validated only on a smaller number of experimental results [48,76].

Vrijdaghs et al. [76] modeled own uniaxial tension tests on PFRC notched cylinders using a two-phase finite element model. The authors used a MATLAB algorithm for random placing of fibers in a DIANA model [76]. The numerical models consisted of 3D solid elements modeling concrete, embedded reinforcement elements, bond-slip reinforcement elements and beam elements modeling the fibers, Figure 7.

Using this model, Vrijdaghs et al. [76] find a good qualitative description of the experimental behavior, even though instantaneous crack widths are overestimated, probably due to instantaneous load application in the model versus the gradual application in the experiment. Most importantly, these authors found that stresses in the 90% of the fibers crossing the crack were under 10–15% of fiber strength (the specimens were loaded to 30–

45% of the residual strength at a pre-crack width of 0.2 mm). The most loaded fibers were under stresses only 20–30% of their strength. Over time, stress redistributed from the most loaded to the less loaded fibers. The simulations were continued up to 50 years, finding no structural failures. The results point to long-term behavior in PFRC being a serviceability limit state problem rather than an ultimate limit state problem [76].

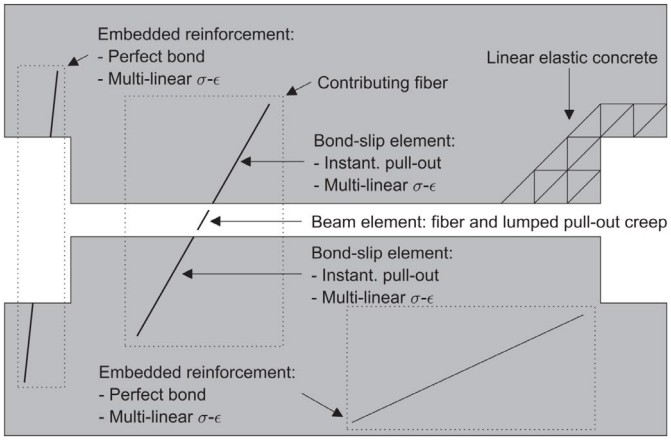

Fig. 7. Overview of the finite element model and different element types [76].

Babafemi and Boshoff [48] also performed numerical modeling in DIANA; however, in this case on long-term bending tests on PFRC. The authors used a mono-phase model, i.e., only concrete, assigning viscoelastic properties only to elements in tension. The long-term behavior of PFRC was modeled using a Kelvin chain of four elements. The authors of study [48] achieved a fair degree of accuracy in modeling time-dependent crack opening. However, it should be noted that concrete compressive creep—with a potentially significant effect in bending tests—was not taken into account.

Considering the results of these two studies, there seems to be a way forward in further investigating viscoelastic constitutive models for numerical analyses of the creep behavior of FRC. However, it remains imperative to include factors such as compressive creep and shrinkage, as well as to find a way to appropriately combine different fiber "positions" in the element (e.g., fully embedded or bridging a crack).

3.2.5. Summary of the Results on the Creep Behavior of FRC

From the analyses of material-level results on long-term testing of SFRC and PFRC specimens it can be seen that the relatively large number of results is yet to be systematically synthesized into analytical models. The large variation in test parameters and reported results is currently one barrier. Furthermore, there is still a lack of fully comprehensive testing that would in one experimental program contain shrinkage tests, compression creep tests and tension tests (uniaxial, bending or both). The results of numerical simulations provide encouraging results that viscoelastic constitutive models so far used for OPC will be applicable to FRC once proper calibration against experimental results is performed.

4. RESEARCH ON THE STRUCTURAL LEVEL

4.1. LONG-TERM TESTS ON FULL-SCALE FRC MEMBERS

As with other properties of concrete, the long-term behavior of FRC observed on the material level cannot be directly extrapolated to structural behavior. Therefore, full scale long-term tests on FRC members are necessary. However, executing such tests is a challenge due to the large numbers of parameters involved, their time-consuming nature, and significant economic cost. Nonetheless, several researchers have performed such tests on beams and pipes (Figures 8 and 9), with a summary of their main parameters given in Table 5.

Fig. 8. Experimental setup for testing FRC beams (authorized reprint from [98]).

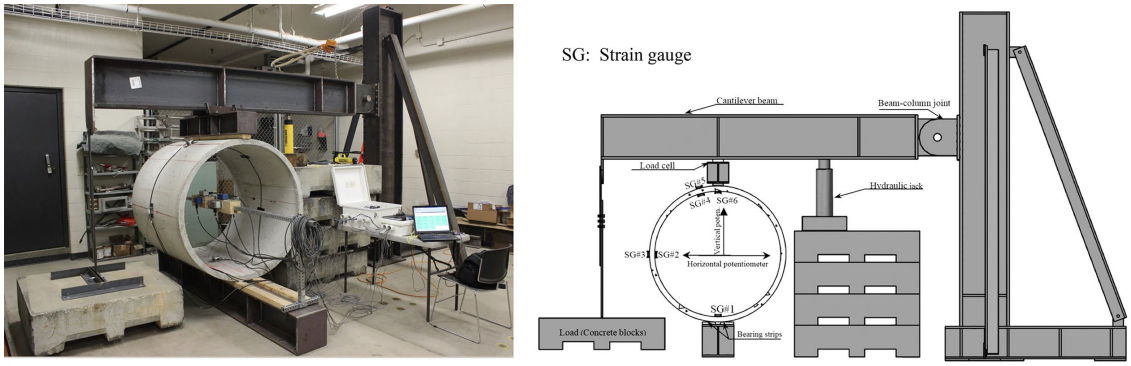

(a) (b)

Fig. 9. (a) Photograph and (b) schematic diagram of the long-term test setup [94].

While there are not enough results for analyzing in detail the effect of certain parameters, several important general conclusions can be drawn. First, it can be seen that material-level behavior does not translate to structural behavior, particularly in the case of PFRC members without steel reinforcement in the studies by Park et al. [93] and Attiogbe et al. [96]—the tested pipes did not exhibit drastic increases of vertical displacements, nor creep failure, rather, a very minor effect of pre-cracking on the long-term vertical displacements was found (both for buried and unburied pipes). Secondly, in the case of R-SFRC members, the steel fibers always decreased deflections and crack widths. For example, Tan et al. [100] found that after 10 years, deflections of R-SFRC beams with 2% of steel fibers were 36% smaller than the deflections of RC beams. Nakov et al. [101] saw decreases in total deflections after one year of 18% and 25% for R-SFRC with 0.8% and 1.6% of steel fibers, respectively,

relative to RC. In the study by Aslani et al. [95] deflections always decreased with the addition of fibers (~0.5%). Adding only steel fibers was the most effective, followed by mixing steel and polypropylene fibers in equal volumes, whereas adding polypropylene fibers decreased deflections only slightly; nonetheless, all beams experienced deflection stabilization after 240 days. At the same time, results for crack widths are not conclusive for R-SFRC, although generally crack widths tend to be reduced relative to RC.

Table 5. Summary of parameters in long-term uniaxial tension tests.

Ref.	Concrete Type	ρ [1]	V_f	Member (mm)	Load Level [2]	Time (days)	Main Results
[88]	RC; R-SFRC [3]	0.45%; 1.25%	0.75%; 1.5%	100/150/3000 beams	0.60	180	Deflections decrease with increasing V_f up to 0.75%, then remain ~ constant
[93]	RC; PPFRC	-	0.40%; 0.80%	Ø600; Ø900 pipes	– [4]	180	Larger change of vertical displacements for PPFRC but stabilization over time; crack widths continued to increase
[94]	R-PPFRC	0.20%	1.0%	Ø1200 pipes	0.40	120	Deflection increase over 5 days then stabilization; crack widths continued to increase
[95]	RC; R-SFRC; R-PPFRC [5]; R-MFRC [6]	0.85%	~0.5% [7]	400/161/3500 beams	0.30–0.50	240	Deflections decrease in order of RC, R-PPFRC, R-MFRC, R-SFRC
[96]	PPFRC	-	–	Ø600; Ø900 pipes	– [8]	417	Pre-cracking had a minor effect on the increase of pipe vertical deflection
[97]	RC; R-SFRC; R-PPFRC	0.9%	0.6% [9]; 0.9% [10]	250/250/3000 beams	0.50	300	Presence of fibers decreases cracks
[100]	RC; R-SFRC	1.5%	0–2%	100/125/2000 beams	0.50	365	Deflections decrease with increasing V_f
[101]	RC; R-SFRC	0.37%	0.8%; 1.6%	150/280/3000 beams	0.40–0.45	365	Deflections decrease with increasing V_f; no clear trends for crack widths

[1] Longitudinal reinforcement ratio; [2] relative to ultimate load; [3] reinforced SFRC member; [4] pipes were pre-cracked then buried under load corresponding to cracking load; [5] reinforced PPFRC member; [6] reinforced mixed FRC (mix of steel and polypropylene fibers); [7] only steel, only polypropylene, or steel + polypropylene 1:1 volume ratio; [8] pipes were tested at "service load" either uncracked or pre-cracked at "ultimate load; [9] steel fiber content; [10] polypropylene fiber content.

It should be noted that the majority of the "hybrid-FRC" members (i.e., members with fibers and steel reinforcement) had relatively large reinforcement ratios. It is possible that long-term deflection and crack development will be more critical for members containing

fibers and minimum steel reinforcement; therefore, this is something that should be determined in future research. Nonetheless, it can be safely claimed that creep failure of FRC elements in the presence of minimum steel reinforcement is not to be expected.

4.2. SERVICEABILITY LIMIT STATE (SLS) DESIGN OF FRC

Plizzari and Serna [26] specify two types of FRC structural applications: "enhancing crack behavior which is particularly important at SLS and also for durability requirements" and "replacing all or part of the conventional reinforcement for structural capacity at Ultimate Limit States (ULS)" [26].

In practice and in cases where cracking is expected under service conditions, hybrid-FRC members are most likely to be used (with fibers and steel reinforcement). Whether fibers are added only for enhancing SLS behavior or whether steel reinforcement is partially replaced, in order to assess deflections and crack widths, the creep behavior of FRC needs to be considered.

Because of the significant uncertainties still related with FRC in general, and its creep behavior in particular, codes tend to apply strict limitations on its properties when it is to be used as a structural material. For example, the *fib* Model Code 2010 [108] requires a minimum "performance class" of "1.0 a" when FRC residual strength is required for equilibrium conditions (complete or even partial reinforcement substitution): the minimum values of f_{R1k} and f_{R3k} (characteristic residual strengths obtained in the EN 14,651 [112] test at a CMOD of 0.5 and 2.5 mm, respectively) are 1.0, and 0.5 MPa, respectively. Furthermore, f_{R1k} must be greater than $0.4 \cdot f_{Lk}$, where f_{Lk} is the characteristic limit of proportionality as defined by EN 14651 [112]) and f_{R3k} must be greater than $0.5 \cdot f_{R1k}$. In terms of ductility, the *fib* Model Code 2010 [108] also requires one of the following conditions to be satisfied:

$$\delta_u \geq 20 \cdot \delta_{SLS} \quad (5)$$

$$\delta_{peak} \geq 5 \cdot \delta_{SLS} \quad (6)$$

where δ_u is the ultimate displacement of the structure or member, δ_{peak} is the displacement at peak load, and δ_{SLS} is the displacement under service conditions. In reality, these conditions are very strict, and usually either preclude the use of FRC without reinforcement or require flexural hardening of the structural element [26].

However, besides these general recommendations, there is not much guidance in the *fib* Model Code 2010 [108], or other codes (for example the Spanish EHE-08 [114], in terms of providing specific models or expressions for incorporating creep behavior of FRC into structural analysis and design. Even though certain research in this direction has been conducted and some models have been put forward, currently this area remains the one that is most open to advances.

One of the earliest works in this area was done by Tan et al. [98,99] and continued by Tan and Saha [100]. The authors formulated an adjustment of the ACI 318 Building Code [115] procedure for deflection control making it applicable to SFRC beams, mostly based on own experimental results. The ACI 318 model is based on calculating deflections using an effective moment of inertia (interpolated between the uncracked and fully cracked states).

Instantaneous deflections are multiplied by a factor to take into account creep, whereas deflections due to shrinkage are calculated from the induced curvature. In terms of SFRC adjustments, the proposed method provides an expression for the moment of inertia of a cracked section, considering the contribution of fibers through a ratio of the moduli of elasticity of steel fibers and concrete and the equivalent areas of fibers in the compressed and tensile zone. At the level of deflections, the multiplicator for creep effects is adjusted by an empirical formula based only on the volume of steel fibers V_f. These authors also propose obtaining SFRC crack widths by adjusting those calculated for RC members through a linear relation dependent also on the fiber volume V_f. Relatively good agreement of model predictions with results of 10-year beam measurements was found [100]. Since the method was developed on own experimental results, there is room for improvement and generalization of the method by including properties such as tensile creep of FRC.

So far, most work on SLS constitutive modeling and design of SFRC has been undertaken in a sequence of papers by Amin and Gilbert [44,84], Amin et al. [102,103], and Watts et al. [86,87]. The authors started by developing a model for the tension stiffening effect in R-SFRC [102] and then succeeded in applying the model in the calculation of instantaneous crack widths [84] and instantaneous and time-dependent deflections [87,103].

Amin et al. [102] proposed an extension of the so-called tension chord model (TCM) to R-SFRC to model the tension stiffening effect, also explicitly accounting for shrinkage. A general scheme of the model is reproduced in Figure 10, where λ is a factor between 0 and 1, f_{ct} is the concrete tensile strength, s_r is the crack spacing, w is the crack width, σ_f is the stress in steel fibers crossing a crack, $\sigma_{c,avg}$ is the average tension-stiffening stress, $\sigma_{s,cr}$ is the steel reinforcement stress in the cracked section, $\sigma_{s,avg}$ is the average stress in steel reinforcement, and τ_b is the bond stress.

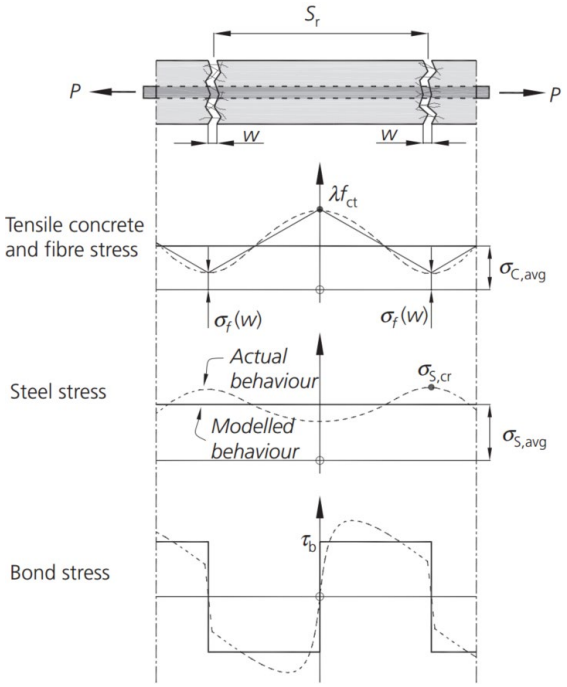

Fig. 10. Tension chord including the effect of steel fibers and reinforcing bar (authorized reprint from [102]).

The proposed model allowed these authors to define tension stiffening stresses for minimum and maximum crack spacing scenarios. The results were verified against own experimental results as well as those previously published in literature [102].

Subsequently, Amin et al. [103] applied the TCM model for R-SFRC to calculating instantaneous deflections of members in bending. They built on the model originally proposed by Kenel et al. [116]. In this model, deflections are not calculating by interpolating between deflections calculated for the uncracked and fully cracked states—as is done in the *fib* Model Code 2010 approach [108]—but rather by calculating the deflection of a fully cracked member and reducing it by tension stiffening contributions:

$$a = a_1 - \Delta a_0 - \Delta a_1 \quad (7)$$

where a is the total deflection, a_1 is the deflection of the member that would be obtained assuming it is fully cracked over its entire length, and Δa_0 and Δa_1 are the stiffening effects of uncracked and cracked regions of the member, respectively. The stiffening effects are due to a "curvature offset" $\Delta\chi$ for which the Amin et al. [103] propose a formulation for R-SFRC (based on their TCM model), as well as a method of calculating cracked sectional properties, similar to the method applied by Tan et al. [98]. The method was successfully verified using available experimental data. Watts et al. [87] further applied this model to time-dependent deflections of R-SFRC members. The model is based on Equation (7) and the previous study by Amin et al. [103], expanded by accounting for the increases in curvature over time due to creep (only compressive creep is considered) and shrinkage. A comparison with available test data showed good results. Finally, based on the same TCM model Amin and Gilbert [84] proposed an iterative procedure for instantaneous crack width calculation.

It can be seen that, although current codes still do not incorporate provisions for time-dependent analysis of FRC, progress is being made. The TCM model developed by Amin et al. [102] is a significant way forward. What still remains is the adaptation of the model to PFRC on the tension chord level, as well as the incorporation of time-dependent polymeric fiber properties into long-term deflection predictions. This can potentially be done by modifying sectional properties as is achieved by the effective modulus method and the compressive creep coefficient.

4.3. SUMMARY OF THE RESULTS ON STRUCTURAL LEVEL TESTING AND MODELING OF FRC CREEP BEHAVIOR

The previous sections have shown that research on the creep behavior of FRC exists on the structural level, both in terms of experimental and theoretical work. However, the body of literature is still insufficient for design and practical purposes and more work is needed until it is mature enough to translate into design codes and wider practical applications by industry.

In terms of experimental research, work should be focused on hybrid-FRC but also on cases with reinforcement ratios close to the minimum; particularly, more experiments are needed on R-PFRC. Furthermore, the current experiments do not provide a clear link between long-term bending or uniaxial tension tests on the material and structural level, i.e., available results on the material level (e.g., crack width creep coefficients) are not applicable to structural tests. In terms of theoretical work, the broadening of current models (whether

existing ACI or *fib* Model Code approaches or TCM models) to R-PFRC is still lacking. Current results from numerical simulations are reason for optimism that with more comprehensive testing, formulation, validation, and calibration of theoretical models through numerical parametric studies will be possible.

5. CONCLUSIONS

In this study, a systematic and critical literature review on the creep behavior of FRC and FRC structural members has been presented. The study covered research on the single fiber level, material level of FRC, and structural level of FRC and hybrid-FRC members, including experimental and theoretical works.

The methodology employed for literature search and filtering is transparently presented and potential biases (only literature in English and journal and conference articles are considered) are discussed. This, notwithstanding the review performed herein, offers several important conclusions from the current state of the art as well as clear recommendations for future research.

On the single fiber level, single fiber creep tests results allow concluding that SFRC might be susceptible to pull-out creep, whilst PFRC is susceptible also to fiber creep provided fibers are subjected to permanent tensile stresses of magnitudes incompatible with the temperature and time-dependent mechanical properties of each type of polymeric fibers. Series Kelvin chain models can describe the creep behavior of both SFRC and PFRC but research is still needed to propose a unified model applicable to both FRC types.

On the FRC material level, there is still a large variety in the ranges of parameter values used in long-term uniaxial tension and bending tests. Future tests should include long-term uniaxial tension or bending tests coupled with shrinkage and compressive creep tests. Then, Kelvin chain models could be applied to the results of such tests to propose a temperature and load-dependent constitutive models that could further be validated using numerical analyses.

Finally, structural-level research has shown promising results in terms of hybrid-FRC performance, both SFRC and PFRC, since long-term increases of deflections and crack widths of hybrid FRC solutions are lower than for traditional RC solutions. Existing theoretical work has forged a way to consider the contribution of fibers in deflection and crack width calculations. Nonetheless, work on SFRC can be expanded to cover PFRC as well. Future research should focus on hybrid-FRC with low reinforcement ratios and PFRC solutions. However, all experiments should be as comprehensive as possible: accompanied by shrinkage, compression, and tensile creep tests so that material-level results could be directly applied to modeling structural behavior. Finally, it should be noted that use of hybrid FRC solutions (both steel and polymeric) with steel reinforcement converts FRC creep to a solvable serviceability-related problem, while at the same time bringing tangible and objective technical and economic benefits.

In conclusion, FRC subjected to creep (especially in the cracked state) is an interesting and dynamic area that has seen significant advances over the past decades but still

offers room for improvement, all with the aim of reaching a consensus that will enable code development and industry uptake of structural FRC applications.

ACKNOWLEDGMENTS

This study has received funding from the European Union's Horizon 2020 research and innovation programme under the Marie Sklodowska-Curie grant agreement No 836270 and from BASF. This support is gratefully acknowledged. Any opinions, findings, conclusions, and/or recommendations in the paper are those of the authors and do not necessarily represent the views of the individuals or organizations acknowledged.

REFERENCES.

[1] di Prisco, M.; Plizzari, G.; Vandewalle, L. Fibre reinforced concrete: New design perspectives. Mater. Struct. 2009, 42, 1261–1281, doi:10.1617/s11527-009-9529-4.

[2] FIB Bulletin 83. In Precast Tunnel Segments in Fibre-Reinforced Concrete; International Federation for Structural Concrete (fib): Lausanne, Switzerland, 2018.

[3] de la Fuente, A.; Blanco, A.; Armengou, J.; Aguado, A. Sustainability based-approach to determine the concrete type and reinforcement configuration of TBM tunnels linings. Case study: Extension line to Barcelona Airport T1. Tunn. Undergr. Sp. Technol. 2017, 61, 179–188, doi:10.1016/j.tust.2016.10.008.

[4] de La Fuente, A.; Casanovas-Rubio, M.D.M.; Pons, O.; Armengou, J. Sustainability of Column-Supported RC Slabs: Fiber Reinforcement as an Alternative. J. Constr. Eng. Manag. 2019, 145, 1–12, doi:10.1061/(ASCE)CO.1943-7862.0001667.

[5] WBCSD The Cement Sustainability Initiative. World Bus. Counc. Sustain. Dev. 2017, 41.

[6] Scrivener, K.L.; Vanderley, J.M.; Gartner, E.M. Eco-Efficient Cements: Potential, Economically Viable Solutions for a Low-CO2, Cement Based Materials Industry; UN Environment: Paris, France, 2016.

[7] Roesler, J.R.; Altoubat, S.A.; Lange, D.A.; Rieder, K.A.; Ulreich, G.R. Effect of synthetic fibers on structural behavior of concrete slabs-on-ground. ACI Mater. J. 2006, 103, 3–10, doi:10.14359/15121.

[8] Meda, A.; Plizzari, G.A.; Riva, P. Fracture behavior of SFRC slabs on grade. Mater. Struct. Constr. 2004, 37, 405–411, doi:10.1617/14093.

[9] Alani, A.M.; Beckett, D. Mechanical properties of a large scale synthetic fibre reinforced concrete ground slab. Constr. Build. Mater. 2013, 41, 335–344, doi:10.1016/j.conbuildmat.2012.11.043.

[10] Meda, A.; Plizzari, G.A. New design approach for steel fiber-reinforced concrete slabs-on-ground based on fracture mechanics. ACI Struct. J. 2004, 101, 298–303, doi:10.14359/13089.

[11] Chen, S. Steel fiber concrete slabs on ground: A structural matter. ACI Struct. J. 2007, 104, 373–375.

[12] Caratelli, A.; Meda, A.; Rinaldi, Z.; Romualdi, P. Structural behaviour of precast tunnel segments in fiber reinforced concrete. Tunn. Undergr. Sp. Technol. 2011, 26, 284–291, doi:10.1016/j.tust.2010.10.003.

[13] Chiaia, B.; Fantilli, A.P.; Vallini, P. Evaluation of minimum reinforcement ratio in FRC members and application to tunnel linings. Mater. Struct. Constr. 2007, 40, 593–604, doi:10.1617/s11527-006-9166-0.

[14] Chiaia, B.; Fantilli, A.P.; Vallini, P. Combining fiber-reinforced concrete with traditional reinforcement in tunnel linings. Eng. Struct. 2009, 31, 1600–1606, doi:10.1016/j.engstruct.2009.02.037.

[15] de la Fuente, A.; Pujadas, P.; Blanco, A.; Aguado, A. Experiences in Barcelona with the use of fibres in segmental linings. Tunn. Undergr. Sp. Technol. 2012, 27, 60–71, doi:10.1016/j.tust.2011.07.001.

[16] Jamshidi Avanaki, M.; Hoseini, A.; Vahdani, S.; de Santos, C.; de la Fuente, A. Seismic fragility curves for vulnerability assessment of steel fiber reinforced concrete segmental tunnel linings. Tunn. Undergr. Sp. Technol. 2018, 78, 259–274, doi:10.1016/j.tust.2018.04.032.

[17] Plizzari, G.A.; Tiberti, G. Steel fibers as reinforcement for precast tunnel segments. Tunn. Undergr. Sp. Technol. 2006, 21, 438–439, doi:10.1016/j.tust.2005.12.079.

[18] Meda, A.; Rinaldi, Z.; Caratelli, A.; Cignitti, F. Experimental investigation on precast tunnel segments under TBM thrust action. Eng. Struct. 2016, 119, 174–185, doi:10.1016/j.engstruct.2016.03.049.

[19] de La Fuente, A.; Escariz, R.C.; De Figueiredo, A.D.; Aguado, A. Design of macro-synthetic fibre reinforced concrete pipes. Constr. Build. Mater. 2013, 43, 523–532, doi:10.1016/j.conbuildmat.2013.02.036.

[20] de La Fuente, A.; Escariz, R.C.; De Figueiredo, A.D.; Molins, C.; Aguado, A. A new design method for steel fibre reinforced concrete pipes. Constr. Build. Mater. 2012, 30, 547–555, doi:10.1016/j.conbuildmat.2011.12.015.

[21] Massicotte, B. High performance fibre reinforced concrete for structural applications. In Proceedings of the 3rd FRC International Workshop Fibre Reinforced Concrete: From Design to Structural Applications, Desenzano, Lake Garda, Italy, 27–30 June 2018.

[22] Aidarov, S.; de la Fuente, A.; Mena, F.; Ángel, S. Campaña experimental de un forjado de hormigón reforzado con fibras a escala real. In Proceedings of the ACE; Fundació Privada Institut d'Estudis Estructurals: Barcelona, Spain, 2019; pp. 1–10.

[23] Destrée, X.; Mandl, J. Steel fibre only reinforced concrete in free suspended elevated slabs: Case studies, design assisted by testing route, comparison to the latest SFRC standard documents. In Proceedings of the Proceedings of the International FIB Symposium 2008 - Tailor Made Concrete Structures: New Solutions for our Society, Amsterdam, The Netherlands, 19–21 May 2008; pp. 437–443.

[24] Gossla, U. Development of SFRC Free Suspended Elevated Flat Slabs; Aachen University of Applied Sciences: Aachen, Germany, 2005.

[25] Parmentier, B.; Van Itterbeeck, P.; Skowron, A. The Behaviour of SFRC Flat Slabs: The Limelette Full-Scale Experiments to Support Design Model Codes; ACI Special Publication; American Concrete Institute: Farmington Hills, MI, USA, 2014.

[26] Plizzari, G.; Serna, P. Structural effects of FRC creep. Mater. Struct. Constr. 2018, 51, 1–11, doi:10.1617/s11527-018-1290-0.

[27] Ghali, A.; Favre, R.; Eldbadry, M. Concrete Structures. Stresses and Deformation; Taylor & Francis: New York, NY, USA, 2002; ISBN 0203987527.

[28] Gettu, R.; Zerbino, R.; Jose, S. Factors Influencing Creep of Cracked Fibre Reinforced Concrete: What We Think We Know & What We Do Not Know. In Proceedings of the Creep Behaviour in Cracked Sections of Fibre Reinforced Concrete; Serna, P., Llano-Tore, A., Cavalaro, S.H.P., Eds.; Springer: Berlin/Heidelberg, Germany, 2017; pp. 3–12.

[29] Berrocal, C.G.; Löfgren, I.; Lundgren, K. The effect of fibres on steel bar corrosion and flexural behaviour of corroded RC beams. Eng. Struct. 2018, 163, 409–425, doi:10.1016/j.engstruct.2018.02.068.

[30] Vieira, M.D.M. Assessment of Chloride Corrosion in Steel Fibre Reinforced Cementitious Composites. Ph.D. Thesis, Universitat Politècnica de Catalunya, Barcelona, Spain, 2018.

[31] Bernard, E.S. Changes in long-term performance of fibre reinforced shotcrete due to corrosion and embrittlement. Tunn. Undergr. Sp. Technol. 2020, 98, 103335, doi:10.1016/j.tust.2020.103335.

[32] Science Direct Scopus. Available online: https://www.scopus.com/home.uri (accessed on 28 July 2020).

[33] Clarivate Analytics Web of Science. Available online: www.webofknowledge.com (accessed on 28 July 2020).

[34] Liu, X.; Huang, Y.; Deng, C.; Wang, X.; Tong, W.; Liu, Y.; Huang, J.; Yang, Q.; Liao, X.; Li, G. Study on the Creep Behavior of Polypropylene. Polym. Eng. Sci. 2009, 49, 1375–1382, doi:10.1002/pen.

[35] Vrijdaghs, R.; di Prisco, M.; Vandewalle, L. Creep Deformations of Structural Polymeric Macrofibers. In Proceedings of the Creep Behaviour in Cracked Sections of Fibre Reinforced Concrete; Serna, P., Llano-Tore, A., Cavalaro, S.H.P., Eds.; Springer: Valencia, Spain, 2017; pp. 53–62.

[36] Vrijdaghs, R.; di Prisco, M.; Vandewalle, L. Short-term and creep pull-out behavior of polypropylene macrofibers at varying embedded lengths and angles from a concrete matrix. Constr. Build. Mater. 2017, 147, 858–864, doi:10.1016/j.conbuildmat.2017.05.005.

[37] Nieuwoudt, P.D.; Babafemi, A.J.; Boshoff, W.P. The response of cracked steel fibre reinforced concrete under various sustained stress levels on both the macro and single fibre level. Constr. Build. Mater. 2017, 156, 828–843, doi:10.1016/j.conbuildmat.2017.09.022.

[38] Babafemi, A.J.; du Plessis, A.; Boshoff, W.P. Pull-out creep mechanism of synthetic macro fibres under a sustained load. Constr. Build. Mater. 2018, 174, 466–473, doi:10.1016/j.conbuildmat.2018.04.148.

[39] Fouda, I.M.; El-Farahaty, K.A.; Seisa, E.A. Interferometric Study of Creep Deformation and Some Structural Properties of Polypropylene Fiber at Three Different Temperatures. J. Appl. Polym. Sci. 2008, 110, 761–768, doi:10.1002/app.

[40] Hadley, D.W.; Ward, I.M. Non-linear creep and recovery behaviour of polypropylene fibres. J. Mech. Physcs Solids 1965, 13, 397–411.

[41] Sabuncuoglu, B.; Acar, M.; Silberschmidt, V.V. Analysis of creep behavior of polypropylene fibers. Appl. Mech. Mater. 2011, 70, 410–415, doi:10.4028/www.scientific.net/AMM.70.410.

[42] Takaku, A. Effect of temperature on creep fracture of polypropylene fibers. J. Appl. Polym. Sci. 1980, 25, 1861–1866, doi:10.1002/app.1981.070261105.

[43] Pujadas, P.; Blanco, A.; Cavalaro, S.H.P.; De La Fuente, A.; Aguado, A. Flexural Post-cracking Creep Behaviour of Macro-synthetic and Steel Fiber Reinforced Concrete. In Proceedings of the Creep Behaviour in Cracked Sections of Fibre Reinforced Concrete; Serna, P., Llano-Tore, A., Cavalaro, S.H.P., Eds.; Springer: Valencia, Spain, 2017; pp. 77–87.

[44] Amin, A.; Gilbert, R.I. Steel fiber-reinforced concrete beams—Part I: Material characterization and in-service behavior. ACI Struct. J. 2019, 116, 101–111, doi:10.14359/51713288.

[45] Amin, A.; Ian Gilbert, R. Steel fiber-reinforced concrete beams—Part II: Strength, ductility, and design. ACI Struct. J. 2019, 116, 113–123, doi:10.14359/51713289.

[46] Kusterle, W. Viscous material behavior of solids- creep of polymer fiber reinforced concrete. In Proceedings of the 5th Central European Congress on Concrete Engineering, Baden, Germany, 24–25 September 2009; pp. 95–99.

[47] Kurtz, S.; Balaguru, P. Postcrack creep of polymeric fiber-reinforced concrete in flexure. Cem. Concr. Res. 2000, 30, 183–190, doi:10.1016/S0008-8846(99)00228-8.

[48] Babafemi, A.J.; Boshoff, W.P. Testing and modelling the creep of cracked macro-synthetic fibre reinforced concrete (MSFRC) under flexural loading. Mater. Struct. Constr. 2016, 49, 4389–4400, doi:10.1617/s11527-016-0795-7.

[49] Zhao, G.; di Prisco, M.; Vandewalle, L. Experimental investigation on uniaxial tensile creep behavior of cracked steel fiber reinforced concrete. Mater. Struct. Constr. 2015, 48, 3173–3185, doi:10.1617/s11527-014-0389-1.

[50] Vrijdaghs, R.; di Prisco, M.; Vandewalle, L. Uniaxial tensile creep of a cracked polypropylene fiber reinforced concrete. Mater. Struct. 2018, 51, 1–12, doi:10.1617/s11527-017-1132-5.

[51] Noushini, A.; Castel, A.; Gilbert, R.I. Creep and shrinkage of synthetic fibre-reinforced geopolymer concrete. Mag. Concr. Res. 2019, 71, 1070–1082, doi.org/10.1680/jmacr.18.00053.

[52] Nakov, D.; Markovski, G.; Arangjelovski, T.; Mark, P. Experimental and analytical analysis of creep of steel fibre reinforced concrete. Period. Polytech. Civ. Eng. 2018, doi:10.3311/PPci.11184.

[53] Zerbino, R.; Giaccio, G.; Monetti, D.; Torrijos, M. Effect of Beam Width on the Creep Behaviour of Cracked Fibre Reinforced Concrete. In Proceedings of the Creep Behaviour in Cracked Sections of Fibre Reinforced Concrete; Serna, P., Llano-Tore, A., Cavalaro, S.H.P., Eds.; Springer: Valencia, Spain, 2017; pp. 169–178.

[54] Pešić, N.; Živanović, S.; Garcia, R.; Papastergiou, P. Mechanical properties of concrete reinforced with recycled HDPE plastic fibres. Constr. Build. Mater. 2016, 115, 362–370, doi:10.1016/j.conbuildmat.2016.04.050.

[55] García-Taengua, E.; Arango, S.; Martí-Vargas, J.R.; Serna, P. Flexural creep of steel fiber reinforced concrete in the cracked state. Constr. Build. Mater. 2014, 65, 321–329, doi:10.1016/j.conbuildmat.2014.04.139.

[56] Monetti, D.H.; Llano-Torre, A.; Torrijos, M.C.; Giaccio, G.; Zerbino, R.; Martí-Vargas, J.R.; Serna, P. Long-term behavior of cracked fiber reinforced concrete under service conditions. Constr. Build. Mater. 2019, 196, 649–658, doi:10.1016/j.conbuildmat.2018.10.230.

[57] Zerbino, R.L.; Barragán, B.E. Long-term behavior of cracked steel fiber-reinforced concrete beams under sustained loading. ACI Mater. J. 2012, 109, 215–224, doi:10.14359/51683708.

[58] Afroughsabet, V.; Teng, S. Experiments on drying shrinkage and creep of high performance hybrid-fiber-reinforced concrete. Cem. Concr. Compos. 2020, 106, 103481, doi:10.1016/j.cemconcomp.2019.103481.

[59] Babafemi, A.J.; Boshoff, W.P. Time-dependent behaviour of pre-cracked polypropylene fibre reinforced concrete (PFRC) under sustained loading. Res. Appl. Struct. Eng. Mech. Comput. 2013, 1593–1598, doi:10.1201/b15963-286.

[60] Błyszko, J. Comparative Analysis of Creep in Standard and Fibre Reinforced Concretes under different Load Conditions. Procedia Eng. 2017, 193, 478–485, doi:10.1016/j.proeng.2017.06.240.

[61] Teixeira Buttignol, T.E.; Colombo, M.; di Prisco, M. Long-term aging effects on tensile characterization of steel fibre reinforced concrete. Struct. Concr. 2016, 17, 1082–1093, doi:10.1002/suco.201500149.

[62] Chern, J.C.; Young, C.H. Compressive creep and shrinkage of steel fibre reinforced concrete. Int. J. Cem. Compos. Light. Concr. 1989, 11, 205–214, doi:10.1016/0262-5075(89)90100-0.

[63] Chern, J.C.; Young, C.H. Pickett effect and creep in flexure of steel-fiber reinforced concrete. J. Chinese Inst. Eng. Trans. Chinese Inst. Eng. 1992, 15, 695–702, doi:10.1080/02533839.1992.9677464.

[64] Babafemi, A.J.; Boshoff, W.P. Macro-Synthetic Fibre Reinforced Concrete: Creep and Creep Mechanisms. In Proceedings of the Creep Behaviour in Cracked Sections of Fibre Reinforced Concrete; Serna, P., Llano-Tore, A., Cavalaro, S.H.P., Eds.; Springer: Valencia, Spain, 2017; pp. 179–191.

[65] Galeote, E.; Blanco, A.; de la Fuente, A.; Cavalaro, S.H.P. Creep Behaviour of Cracked High Performance Fibre Reinforced Concrete Beams Under Flexural Load. In

Proceedings of the Creep Behaviour in Cracked Sections of Fibre Reinforced Concrete; Springer: Berlin/Heidelberg, Germany, 2017; pp. 111–123.

[66] Kohoutkova, A.; Vodička, J.; Kristek, V. Creep and Shrinkage of Fibre-Reinforced Concrete and a Guide for Modeling. In Proceedings of the CONCREEP 10; ASCE: Reston, VI, USA, 2015; pp. 707–713.

[67] Marangon, E.; Toledo Filho, R.D.; Fairbairn, E.M.R. Basic Creep under Compression and Direct Tension Loads of Self-compacting-steel Fibers Reinforced Concrete BT—RILEM HPFRCC6 High Performance Fiber Reinforced Cement Composites 6. RILEM HPFRCC6 High Perform. Fiber Reinf. Cem. Compos. 6 2012, 2, 171–178.

[68] Llano-Torre, A.; García-Taengua, E.; Martí-Vargas, J.R.; Serna, P. Compilation and study of a database of tests and results on flexural creep behavior of fibre reinforced concrete specimens. Concr. - Innov. Des. fib Symp. Proc. 2015, 253–254.

[69] Nürnbergerová, T.; Babál, B. Long-term behaviour of plain and steel fibre reinforced concrete rings. Mater. Struct. 1992, 25, 412–416, doi:10.1007/BF02472257.

[70] Pujadas, P.; Blanco, A.; Cavalaro, S.; de la Fuente, A.; Aguado, A. The need to consider flexural post-cracking creep behavior of macro-synthetic fiber reinforced concrete. Constr. Build. Mater. 2017, 149, 790–800, doi:10.1016/j.conbuildmat.2017.05.166.

[71] Serna, P.; Martí-Vargas, J.R.; Bossio, M.E.; Zerbino, R. Creep and residual properties of cracked macro-synthetic fibre reinforced concretes. Mag. Concr. Res. 2016, 68, 197–207, doi:10.1680/macr.15.00111.

[72] Sturm, A.B.; Visintin, P.; Oehlers, D.J.; Seracino, R. Time-Dependent Tension-Stiffening Mechanics of Fiber-Reinforced and Ultra-High-Performance Fiber-Reinforced Concrete. J. Struct. Eng. 2018, 144, 1–14, doi:10.1061/(ASCE)ST.1943-541X.0002107.

[73] Sprince, A.; Korjakins, A.; Pakrastinsh, L. Time-Dependent Behavior of High Performance Fiber-Reinforced Concrete; Trans Tech Publications Ltd.: Bäch, Switzerland, 2013; Volume 705, pp. 75–80, doi:10.4028/www.scientific.net/AMR.705.75.

[74] Vrijdaghs, R.; Verstrynge, E.; Vandewalle, L.; di Prisco, M. A two-phased and multi-scale finite element analysis of the tensile creep behavior of polypropylene fiber reinforced concrete. Comput. Model. Concr. Struct. - Proc. Conf. Comput. Model. Concr. Concr. Struct. EURO-C 2018 2018, 857–866, doi:10.1201/9781315182964-100.

[75] Buratti, N.; Mazzotti, C. Creep Testing Methodologies and Results Interpretation. In Proceedings of the Creep Behaviour in Cracked Sections of Fibre Reinforced Concrete; Serna, P., Llano-Tore, A., Cavalaro, S.H.P., Eds.; Springer: Valencia, Spain, 2017; pp. 13–25.

[76] Vrijdaghs, R.; di Prisco, M.; Vandewalle, L. Creep of polymeric fiber reinforced concrete: A numerical model with discrete fiber treatment. Comput. Struct. 2020, 233, 106233, doi:10.1016/j.compstruc.2020.106233.

[77] Vrijdaghs, R.; di Prisco, M.; Vandewalle, L. A Numerical Model for the Creep of Fiber Reinforced Concrete. In Proceedings of the High Tech Concrete: Where Technology and Engineering Meet; International Federation for Structural Concrete (fib): Maastricht, The Netherlands, 2017; pp. 366–373.

[78] Zerbino, R.; Monetti, D.H.; Giaccio, G. Creep behaviour of cracked steel and macro-synthetic fibre reinforced concrete. Mater. Struct. Constr. 2016, 49, 3397–3410, doi:10.1617/s11527-015-0727-y.

[79] Babafemi, A.J.; Boshoff, W.P. Tensile creep of macro-synthetic fibre reinforced concrete (MSFRC) under uni-axial tensile loading. Cem. Concr. Compos. 2015, 55, 62–69, doi:10.1016/j.cemconcomp.2014.08.002.

[80] Kusterle, W. Flexural Creep Tests on Beams - 8 Years of Experience with Steel and Synthetic Fibres. In Proceedings of the Creep Behaviour in Cracked Sections of Fibre Reinforced Concrete; Serna, P., Llano-Tore, A., Cavalaro, S.H.P., Eds.; Springer: Valencia, Spain, 2017; pp. 27–39.

[81] Van Bergen, S.; Pouillon, S.; Vitt, G. Experiences from 14 Years of Creep Testing of Steel and Polymer Fiber Reinforced Concrete. In Proceedings of the Creep Behaviour in Cracked Sections of Fibre Reinforced Concrete; Serna, P., Llano-Tore, A., Cavalaro, S.H.P., Eds.; Springer: Valencia, Spain, 2017; pp. 41–52.

[82] Arango, S.E.; Serna, P.; Martí-Vargas, J.R.; García-Taengua, E. A Test Method to Characterize Flexural Creep Behaviour of Pre-cracked FRC Specimens. Exp. Mech. 2012, 52, 1067–1078, doi:10.1007/s11340-011-9556-2.

[83] Buratti, N.; Mazzotti, C. Experimental tests on the effect of temperature on the long-term behaviour of macrosynthetic Fibre Reinforced Concretes. Constr. Build. Mater. 2015, 95, 133–142, doi:10.1016/j.conbuildmat.2015.07.073.

[84] Amin, A.; Gilbert, R.I. Instantaneous crack width calculation for steel fiber-reinforced concrete flexural members. ACI Struct. J. 2018, 115, 535–543, doi:10.14359/51701116.

[85] Raymond, A.; Gilbert, I.; Bernard, C.E.S. Time-dependent Analysis of Macro-synthetic FRC Sections with Bar Reinforcement. 2015.

[86] Watts, M.J.; Amin, A.; Gilbert, R.I.; Kaufmann, W. Behavior of fiber reinforced concrete members under sustained axial/flexural load. Struct. Concr. 2019, 1–17, doi:10.1002/suco.201900227.

[87] Watts, M.J.; Amin, A.; Gilbert, R.I.; Kaufmann, W.; Minelli, F. Simplified prediction of the time dependent deflection of SFRC flexural members. Mater. Struct. Constr. 2020, 53, doi:10.1617/s11527-020-01479-8.

[88] Ashour, S.A.; Mahmood, K.; Wafa, F.F. Long-term deflection of high-strength fiber reinforced concrete beams. Struct. Eng. Mech. 1999, 8, 531–546.

[89] Ezeldin, A.S.; Shiah, T.W. Analytical immediate and long-term deflections of fiber-reinforced concrete beams. J. Struct. Eng. 1995, 121, 727–738, doi:10.1061/(ASCE)0733-9445(1995)121:4(727).

[90] Habel, K.; Denarié, E.; Brühwiler, E. Time dependent behavior of elements combining ultra-high performance fiber reinforced concretes (UHPFRC) and reinforced concrete. Mater. Struct. Constr. 2006, 39, 557–569, doi:10.1617/s11527-005-9045-0.

[91] Kaminski, M.; Bywalski, C. Influence of creep deformations on value of long term deflections of steel fiber-reinforced concrete beams. In Proceedings of the 8th International Conference on Creep, Shrinkage and Durability of Concrete and Concrete Structures, Ise-

Shima, Japan, 30 September–2 October 2008; Volume 1, pp. 729–734, doi:10.1201/9780203882955.ch97.

[92] Neutov, S.; Sydorchuk, M.; Surianinov, M. Experimental studies of reinforced concrete and fiber-reinforced concrete beams with short-term and long-term loads. Mater. Sci. Forum 2019, 968 MSF, 227–233, doi:10.4028/www.scientific.net/MSF.968.227.

[93] Park, Y.; Abolmaali, A.; Attiogbe, E.; Lee, S.H. Time-dependent behavior of synthetic fiber-reinforced concrete pipes under long-term sustained loading. Transp. Res. Rec. 2014, 71–79, doi:10.3141/2407-07.

[94] Al Rikabi, F.T.; Sargand, S.M.; Khoury, I.; Kurdziel, J. A new test method for evaluating the long-term performance of fiber-reinforced concrete pipes. Adv. Struct. Eng. 2020, 23, 1336–1349, doi:10.1177/1369433219894243.

[95] Aslani, F.; Nejadi, S.; Samali, B. Long-term flexural cracking control of reinforced self-compacting concrete one way slabs with and without fibres. Comput. Concr. 2014, 14, 419–444, doi:10.12989/cac.2014.14.4.419.

[96] Attiogbe, E.; Abolmaali, A.; Park, Y. Polypropylene fiber-reinforced concrete pipes under sustained loading. In Proceedings of the 9th RILEM International Symposium on Fiber Reinforced Concrete - BEFIB 2016, Vancouver, BC, Canada, 19–21 September, 2016; pp. 1128–1138.

[97] Vasanelli, E.; Micelli, F.; Aiello, M.A.; Plizzari, G. Long term behavior of FRC flexural beams under sustained load. Eng. Struct. 2013, 56, 1858–1867, doi:10.1016/j.engstruct.2013.07.035.

[98] Tan, K.H.; Paramasivam, P.; Tan, K.C. Instantaneous and long-term deflections of steel fiber reinforced concrete beams. ACI Struct. J. 1994, 91, 384–393.

[99] Tan, K.H.; Paramasivam, P.; Tan, K.C. Creep and shrinkage deflections of RC beams with steel fibers. J. Mater. Civ. Eng. 1994, 6, 474–494.

[100] Tan, K.H.; Saha, M.K. Ten-year study on steel fiber-reinforced concrete beams under sustained loads. ACI Struct. J. 2005, 102, 472–480.

[101] Nakov, D.; Markovski, G.; Arangjelovski, T.; Mark, P. Creeping effect of SFRC elements under specific type of long term loading. In RILEM Bookseries; Springer: Dordrecht, The Netherlands, 2017.

[102] Amin, A.; Foster, S.J.; Watts, M. Modelling the tension stiffening effect in SFR-RC. Mag. Concr. Res. 2016, 68, 339–352, doi:10.1680/macr.15.00188.

[103] Amin, A.; Foster, S.J.; Kaufmann, W. Instantaneous deflection calculation for steel fibre reinforced concrete one way members. Eng. Struct. 2017, 131, 438–445, doi:10.1016/j.engstruct.2016.10.041.

[104] Banthia, N.; Gupta, R. Influence of polypropylene fiber geometry on plastic shrinkage cracking in concrete. Cem. Concr. Res. 2006, 36, 1263–1267, doi:10.1016/j.cemconres.2006.01.010.

[105] ACI Committee 544. Report on Fiber Reinforced Concrete;: ACI: Farmington Hills, MI, USA, 2002.

[106] Bažant, Z.P.; Baweja, S. Creep and shrinkage prediction model for analysis and design of concrete structures - model B3. Mater. Struct. 1995, 28, 357–365.

[107] Bažant, Z.P.; Li, G.H. NU-ITI database on concrete creep and shrinkage. Available online: http://iti.northwestern.edu/publications/bazant/index.html (accessed on 14 January 2017).

[108] FIB. fib Model Code for Concrete Structures 2010; International Federation for Structural Concrete (fib): Lausanne, Switzerland, 2013; ISBN 9783433604090.

[109] Bažant, Z.P.; Hubler, M.H.; Wendner, R. RILEM draft recommendation: TC-242-MDC multi-decade creep and shrinkage of concrete: Material model and structural analysis. Mater. Struct. 2015, 48, 753–770, doi:10.1617/s11527-014-0485-2.

[110] Gilbert, R.I.; Ranzi, G. Time-Dependent Behaviour of Conrete Structures; Spon Press: New York, NY, USA, 2011.

[111] Neville, A.M. Properties of Concrete; Pearson Education Ltd.: Harlow, UK, 1995.

[112] EN 14651 Test method for metallic fibred concrete — Measuring the flexural tensile strength (limit of proportionality (LOP), residual). Br. Stand. Inst. 2005, doi:9780580610523.

[113] Eurocode 2: Design of Concrete Structures - Part 1-1: General Rules and Rules for Buildings; EN 1992-1-1; CEN: Brussels, Belgium, 2004; ISBN 978 0 580 62664 7.

[114] EHE. Instrucción de Hormigón Estructural (EHE-08); EHE: Madrid, Spain, 2008.

[115] ACI 318-14. Building Code Requirements for Structural Concrete (ACI 318-14) and Commentary; ACI: Farmington Hills, MI, USA, 2014.

[116] Kenel, A.; Nellen, P.; Frank, A.; Marti, P. Reinforcing steel strains measured by Bragg grating sensors. J. Mater. Civ. Eng. 2005, 17, 423–431, doi:10.1061/(ASCE)0899-1561(2005)17:4(423).

RESEARCH CONTRIBUTION II: STEEL FIBRE REINFORCED CONCRETE TWO-WAY SLAB: EVALUATION OF STRUCTURAL RESPONSE UNDER UNIFORMLY DISTRIBUTED LOAD

Published in: Concrete Structures: New Trends for Eco-Efficiency and Performance. Proceedings of the fib Symposium 2021 held online from Lisbon, Portugal.

Stanislav Aidarov [a, b, *], Nikola Tošić [b], Albert de la Fuente [b]

[a] Smart Engineering Ltd., UPC Spin-Off, Jordi Girona 1-3, 08034 Barcelona, Spain

[b] Civil and Environmental Engineering Department, Universitat Politècnica de Catalunya (UPC), Jordi Girona 1-3, 08034 Barcelona, Spain

* Corresponding author. Tel.: +34 633 634 207; Full Postal address: 08034, Barcelona, Jordi Girona 1; Email address: stanislav.aidarov@upc.edu ; stanislav.aydarov@smartengineeringbcn.com

Abstract

The continuous study of the mechanical properties of fibre reinforced concrete (FRC) along with development of new fibre types and enhanced concrete mixes demonstrated adequate bearing capacity of the material and its possible application even in elements with significant structural responsibility, such as two-way slabs with span to depth ratios up to 30. However, FRC technology is still limited in this type of structures because of certain aspects, mainly related to design procedures that require further study. Therefore, the feasibility of using constitutive models derived from three-point bending tests on notched beams to assess the behaviour of statically indeterminate horizontal structural elements is among the questions that shall be analysed in detail. With this in mind, a full-scale FRC pile-supported flat slab was constructed and gradually loaded until failure by means of uniformly distributed load. The obtained results highlighted the significant redistribution capacity and ductile response of the tested element. Additionally, based on the characterization of the applied material, constitutive models were developed in accordance with the *fib* Model Code 2010 and both analytical and numerical predictions were carried out. The estimated behaviour of the FRC flat slab by means of the yield line method and nonlinear simulation was compared with the experimental result and a good agreement with the latter can be pointed out in case of the analytical prediction, whereas the numerical simulation tended to overestimate the bearing capacity of the studied structure. However, further investigations are still required in order to suitably predict the structural response of FRC two-way slabs subjected to different boundary conditions and load types.

Keywords: fibre reinforced concrete, real scale test, flat slab, two-way slab, numerical simulation.

1. INTRODUCTION

In recent decades, one of the most challenging research lines in the field of concrete technology has become fibre reinforced concrete (FRC) and its possible application for both structural and non-structural purposes. In the early stages, FRC had been primarily considered as a potential alternative to traditional solutions (concrete reinforced with steel bars) in elements which were subjected to relatively low bending moments during transient and service situations and/or those whose consequence of failure are minor. The most representative examples of the FRC application for this type of elements are slabs on grade [1–3], precast tunnel segments [4–7], reinforced retaining walls [8], and sewerage pipes [9].

In fact, the use of FRC in the above presented elements is still prevalent. However, the continuous research related to (1) enhancement of concrete mixes, (2) implementation of new fibre types, and (3) progress in terms of design procedures permitted to start implementing this material in elements with higher structural responsibility, such as FRC flat slabs for residential/office buildings. Firstly, several full-scale tests [10–12] demonstrated that the presence of relatively high fibre contents (volume fraction up to 1.3%) in the concrete mix was capable of providing considerable flexural and punching strength. The promising outcome of these tests inspired confidence in the structural capacities of the material and, as a result, the technology was also applied in real projects. The Ditton Nams shopping mall (Latvia), the Triangle office building (Estonia), the Rocca Al-Mare office tower (Estonia), and the LKS office building (Spain) were constructed with almost total substitution of the traditional reinforcement by structural macro-fibres.

This substitution had a positive effect on construction speed, which, in turn, led to significant economic savings. For instance, the nine-week time-saving effect along with the reduction of the required machinery were highlighted during the construction of 16-floor Rocca Al-Mare office tower, whereas the 12% reduction of total costs (comparing with the initially considered solution with steel reinforcing bars) was denoted in case of the LKS office building [13]. The latter was further studied using multi-criteria decision making method and the enhancement of overall sustainability performance of the chosen technological approach was pointed out [14] – an aspect of paramount importance considering the immense quantities of globally produced concrete.

Despite the achieved results, the use of FRC for two-way slabs is still far from being a common solution for residential/office buildings and, the cause of which lies in a number of constraining factors which are mainly related to design procedures. Although recent studies demonstrated the significant redistribution capacity of the material [15–17] along with possible enhancements in terms of ductility [6], cracking control [18] and deformations [19,20], practitioners have certain concerns regarding the structural response of FRC in both ultimate and serviceability limit states (ULS and SLS, respectively). Especially, these concerns are addressed to FRC two-way elements considering the fact that the majority of the current codes and guidelines [21-23] suggest to derive the constitutive models in tension for FRC by means of a three-point bending test on a notched beam in accordance with EN 14651 [24] which, in turn, can lead to inaccurate evaluation of FRC behaviour in statically indeterminate structures.

Taking the above stated into account, an extensive experimental program was carried out which was comprised of three main parts: (1) characterization of 15 self-compacting steel fibre reinforced concrete (SFRC) mixes with different fibre contents and type; (2) construction of SFRC slabs of different dimensions maintaining the same slenderness; (3) testing these slabs under various boundary and load conditions in order to assess the behaviour of structures in terms of cracking, produced deformations and ultimate bearing capacity. This paper focuses on the construction of a four-panel SFRC flat slab and its testing under uniformly distributed load (UDL).

Additionally, the rigid plastic and multilinear constitutive models were computed in accordance with the *fib* Model Code 2010 [21] and both analytical and numerical estimation of the ultimate UDL was provided. The yield line method along with the rigid plastic model were considered for the analytical approach, whereas the multilinear constitutive equation was used to simulate the testing procedure by means of finite element software ATENA 5.7.0 [25]. The calculated predictions were compared with the experimental outcome and the obtained results demonstrated a significant accuracy in case of the analytical prediction, whereas the numerical simulation overestimated the bearing capacity of the studied two-way SFRC element – this phenomenon was already depicted in several works [26,27] and, therefore, requires further studies in order to suitably evaluate the structural response of the FRC two-way slabs by means of multilinear constitutive models.

2. EXPERIMENTAL INVESTIGATION

2.1. TESTED SFRC FLAT SLAB PROTOTYPE

Selecting the geometry for SFRC flat slab prototype, the main goal was to reproduce the common dimensions of slab panels that could be used in residential and office buildings. As a result, an SFRC slab formed by four panels of 6.0 × 5.0 m each was constructed, resulting in a 12.0 × 10.0 × 0.2 m SFRC slab supported by nine columns with square cross-section of 0.25 m. Additionally, the anti-progressive collapse reinforcement (APC) was installed (Figure 1b) in accordance with North American Standards [28,29]; although the APC reinforcement is the reinforcement to prevent local failures and has a minor effect on overall bearing capacity of the tested SFRC slab. The chosen geometry provided the span-to depth ratio of 30 which, to the best of the authors' knowledge, corresponded to the upper limit of those already constructed (Table 1). Figure 1 presents the geometry of the superstructure along with certain phases of the construction process.

2.2. MATERIAL PROPERTIES

The self-compacting SFRC with a steel fibre content of 70 kg/m^3 (volume fraction 0.9%) was used for the construction of the prototype in question – the lower limit reported in the scientific literature related to the erection and testing of full-scale SFRC two-way slabs of this slenderness (Table 1). After the material characterization of 15 concrete mixes with different fibre types/contents [37], it was decided to use a fibre of a high tensile strength (2300 MPa), with a double hooked-end shape and an aspect ratio of 65. Additionally, close attention was paid to the mix elaboration in order to guarantee sufficient workability of the material

and, as a consequence, avoid concrete vibration. The details of the used concrete mix are gathered in Table 2.

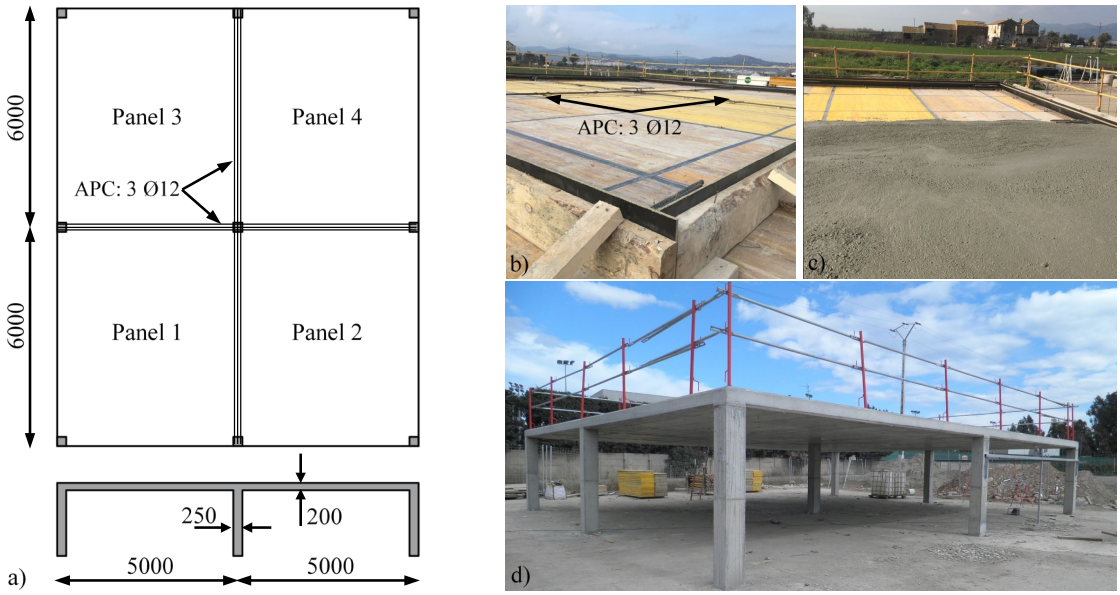

Fig. 1. a) Geometry of SRFC flat slab; b) Installed formwork; c) SFRC pumping; d) SFRC flat slab after formwork striking

Table 1. Cases of SFRC application in two-way slabs

Reference	Type	C_f [kg/m^3]	$L_{max/h}$ [m/m]	Steel bars	l_f / $Ø_f$ / R_m - type
(Barros et al. 2012) (Salehian and Barros 2015)	FSFT	90	16	Yes*	37/0.5/1100 – SHE
(Destrée and Mandl 2008)	FSFT	45	19	No	50/1.3/850 – C
(Hedebratt and Silfwerbrand 2014)	FSFT	40/80	23	Yes/No	60/0.9/1160 – SHE
(Døssland 2008)	FSFT	62	23	Yes/No	60/0.9/1000 – SHE
(Destrée and Mandl 2008)	FSFT	100	28	Yes*	50/1.3/850 – C
(Benoit Parmentier and Itterbeeck 2015)	FSFT	70	30	Yes*	60/1.0/1450 – SHE
(Gossla 2005)	FSFT	100	30	Yes*	50/1.3/900 – C
(Ošlejs 2008)	RB	100	24	Yes*	50/1.3/900 – C
(Maturana et al. 2014)	RB	100	27	Yes	50/1.3/900 – C
Present study	FSFT	70	30	Yes*	60/0.9/2300 - DHE

NB: C_f – fibre content; L_{max} – maximum span; h – depth of the slab; l_f – fibre length in mm; $Ø_f$ – fibre diameter in mm; R_m – fibre tensile strength in MPa; FSFT – full scale field test; RB – real building; DHE – double hooked-end; SHE – single hooked end; C – crimped; Yes* – only presence of anti-progressive collapse [36] steel bars.

The construction of the SFRC flat slab prototype required four concrete trucks and each of the batches was tested to assess the properties of the material. Mean values at 28 days for the modulus of elasticity (E_{cm}), compressive strength (f_{cm}), and residual flexural strengths ($f_{Rm,i}$) were evaluated in accordance with standards EN 12390-13 [38], EN 12390-3 [39], and EN 14651 [24], respectively. Three specimens per batch were tested in order to estimate the

magnitudes of E_{cm} and f_{cm}, whereas four 150 × 150 × 600 mm notched prisms were tested for $f_{Rm,i}$. However, taking into account that the bearing capacity of the entire structure is to be computed, the overall mechanical properties were considered in this study and presented in Table 3 and partially in Figure 2.

Table 2. Concrete mixture

Cement CEM II/A-L 45,2R (kg/m^3)	425
Coarse aggregate 10/20 (kg/m^3)	250
Coarse aggregate 4/10 (kg/m^3)	150
Fine aggregate 0/4 (kg/m^3)	725
Fine aggregate 0/2 (kg/m^3)	600
Limestone filler (kg/m^3)	25
Water-cement ratio	0.47
Additives (% on cement content)	2.77
Steel fibres (kg/m^3)	70

Table 3. Concrete mixture

Property	Batches 1-4	
	Average (MPa)	CV (%)
E_{cm}	26310	4.9
f_c	42.9	7.8
f_{LOP}	4.4	12.4
f_{R1}	7.2	35.3
f_{R2}	8.1	26.0
f_{R3}	7.7	24.7
f_{R4}	7.3	22.7

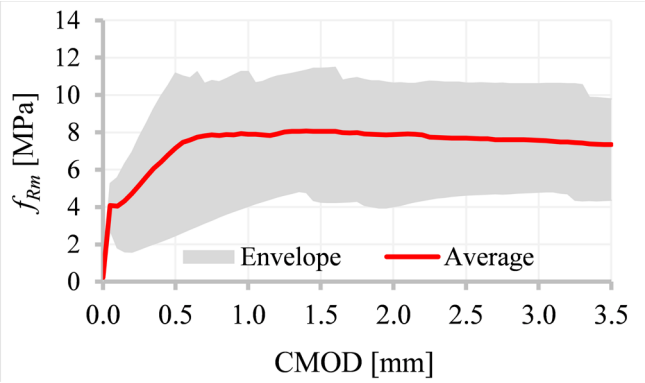

Fig. 2. f_{Rm} – CMOD curve of applied SFRC

Figure 2, additionally, demonstrates higher scatter of f_R in comparison with the expected values, especially for the given fibre content [40,41]. This phenomenon affected significantly on the magnitudes of the characteristic values of residual tensile strengths what, in turn, would have had a significant influence on the construction procedure / quality control if the material had been used for the real building. Therefore, the necessity of a rigorous control of FRC elaboration in order to keep the properties of the material in line with those obtained in the laboratory should be pointed out; the main factors to achieve the sufficient homogeneity are related to the mixing procedure [42], transportation [13], and pouring approach [22].

2.3. TEST SETUP AT ULS

The Spanish Building Code for residential buildings [43] was taken as a reference in order to establish the magnitude of the UDL at ULS; apart from the self-weight (q_{SW} = 4.8 kN/m^2), a dead load (q_G) and variable load (q_Q) of respectively 2.0 and 3.0 kN/m^2 were adopted. Additionally, the load partial safety factors γ_G = 1.35 and γ_Q = 1.5 were considered in order to evaluate the design load $q_{SD} = \gamma_G \cdot (q_{SW} + q_G) + \gamma_Q \cdot q_Q$ = 13.7 kN/m^2.

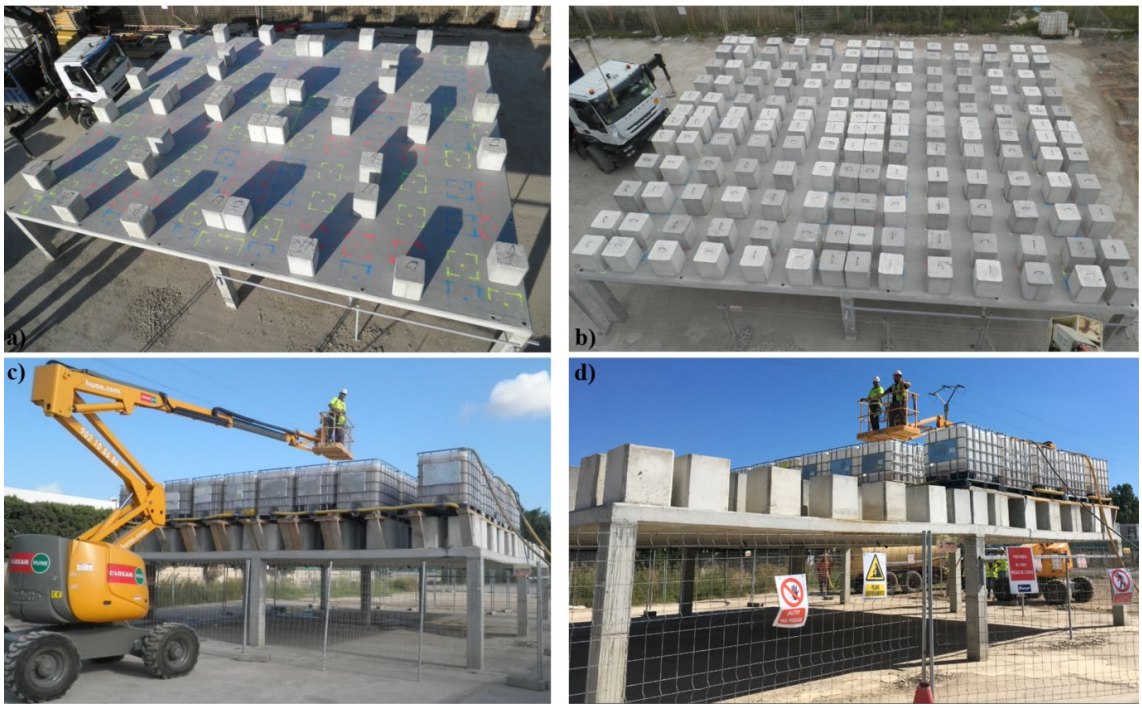

Fig. 3. a-b) Different phases of loading by means of concrete cubes; c-d) Simulation of ULS condition

The load was applied gradually – at first stages, the load increments were provided by means of 0.5 × 0.5 × 0.6 m concrete cubes (≈ 350 kg each). In total, the concrete cubes simulated a UDL of 9.8 kN/m^2 (Figure 3a-b). Gradual loading also provided the possibility of evaluating the behaviour of the SFRC flat slab under SLS conditions, which is out the scope of this paper; the obtained results can be found in the work by [44]. Furthermore, the water tanks were placed onto the first half of the slab to achieve the required ultimate loading (Figure 3c). In fact, this configuration permitted to increase the load up to 16 kN/m^2. Each panel was loaded increasing the water level by steps of 300 mm (2 kN/m^2 per step); the rate of filling was controlled by the inspection of deformations by means of installed prisms and

topography, i.e. further increment of water level could only be permitted in case of stability of the structure in terms of produced displacements under the increased load. Once the first half of the slab was tested, the water tanks were shifted on the other side of the structure (Figure 3d) with the following repetition of the loading procedure.

2.4. EXPERIMENTAL RESULTS

The evaluation of the structural response under ULS started with the loading of the panel 1 up to 14.0 kN/m^2. The SFRC slab demonstrated sufficient structural integrity under this load magnitude and, therefore, the loading process continued until reaching the load of 16.0 kN/m^2 – the maximum possible UDL for the established test configuration. Subsequently, the panel 2 was loaded up to 16.0 kN/m^2 and the structure showed no signs of pre-failure damage.

Taking into consideration that further load increments were restricted by the test setup, the water tanks were emptied and shifted to other half of the SFRC slab (Figure 3d). Thus, the procedure was repeated: panel 3 was loaded up to 16.0 kN/m^2 based on the previously obtained results despite the fact that panels 1 and 2 were already damaged. Finally, the load of 14.5 kN/m^2 was reached during the loading of the panel 4. Further testing of this panel was stopped owing to the presence of significant shear cracks around the corner column, although the studied SFRC slab maintained its structural integrity.

3. PREDICTION OF THE ULTIMATE LOAD

3.1. ANALYTICAL PREDICTION

Previous experiences [10,22] along with the presented case demonstrated that the punching failure is unlikely to occur in the relatively slender structures (span-to-depth ratio up to 30) under UDL. Therefore, the flexural strength assessment of the applied material was required to evaluate the bearing potential of the studied SFRC flat slab. Currently, the majority of codes [21,22,45] suggest the simplified rigid plastic model for the analytical estimation of the ULS response of FRC in tension which is identified by a value of f_{Ftu}.

This value only depends on the characteristic residual tensile strength at the crack mouth opening displacement (CMOD) of 2.5 mm (f_{R3}) in accordance with EN 14651 [24] and can be calculated as $f_{Ftu} = f_{R3} / 3$; the obtained analytical prediction results are to be compared with the experimental outcome and, therefore, the mean values should be considered and the safety coefficients are to be omitted throughout the process. Using the sectional model to compute the flexural strength of the FRC (Figure 4) and the previously obtained mechanical properties of the latter (Table 3), resisting moment of the material in question results to be 48.4 kNm/m for the theoretically established depth of the real-scale FRC slab (h = 200 mm).

Furthermore, the ultimate load should be calculated based on the resisting moment. For this purpose, generally, the Yield-Line Method is suggested as an analytical tool to estimate flexural capacity of FRC two-way slabs [29] by establishing the “applied load – produced moment” ratio which, in turn, depends on the boundary conditions and type of loading. In case of pile-supported flat slabs with a uniform column grid, this ratio can be computed by means of already developed formulae. Taking this into account, the aforementioned ratio can be assessed by means of Equation 1:

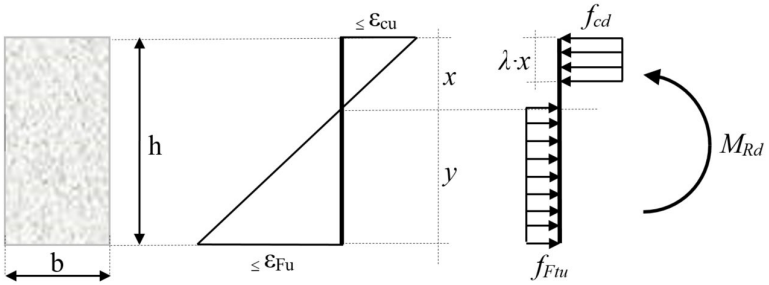

Fig. 4. Sectional model to evaluate flexural strength of FRC

$$M_P^+ = \frac{UDL \cdot L_r^2}{2 \cdot (\sqrt{(1 + \oslash_h)} + 1)^2} \quad (1)$$

The ratio of negative to positive flexural capacities of the prototype cross sections ($\oslash_h$) is to be considered as 1.0 for the sake of simplicity, i.e. considering that the material is perfectly homogenous; although this assumption could be controversial in terms of real fibre distribution along the depth of a SFRC element – several works pointed out the tendency for an increase of fibre percentage from the top to the bottom of SFRC slab [30,44]. The distance of 5.65 m between the negative yield line and the slab edge (L_r) for the established geometry of the slab was adopted according to the produced crack pattern; hence, the magnitude of the ultimate UDL is 17.7 kN/m^2 – 10.6% above the experimentally obtained magnitude of UDL. However, the structure eventually was not led to failure and, therefore, the difference between real response and the analytical prediction could have been lower if the test setup had permitted further increment of the load.

3.2. NUMERICAL PREDICTION

3.2.1. Model description

The finite element software ATENA 5.7.0 [25] was used to model the previously described testing procedure. Special attention was given to the modelling of the tensile behaviour of concrete. For this purpose, the multilinear constitutive diagram was adopted in accordance with the *fib* MC 2010 [21] and the material properties (Table 3); apart from the tensile strength of concrete (f_{ct}), this diagram is mainly defined by the residual tensile strengths f_{R1} and f_{R3} at CMOD of 0.5 mm and 2.5 mm (3-4), respectively (Figure 5a). It is important to note that the characteristic length (l_{cs}) which is required to estimate the corresponding strain values of strain (5-6) depends on the selected mesh and can be adopted as the cubic root of the finite element volume in case of solid elements, i.e. $l_{cs} = (V_e)^{1/3}$ [46]

$$f_{ct} = 0.3 \cdot f_{ck}^{2/3} \quad (1)$$

$$f_{Fts} = 0.45 \cdot f_{R1} \quad (2)$$

$$f_{Ftu} = 0.5 \cdot f_{R3} - 0.2 \cdot f_{R1} \quad (3)$$

$$\varepsilon_{SLS} = CMOD_1 / l_{cs} \quad (4)$$

$$\varepsilon_{ULS} = w_u / l_{cs} \quad (5)$$

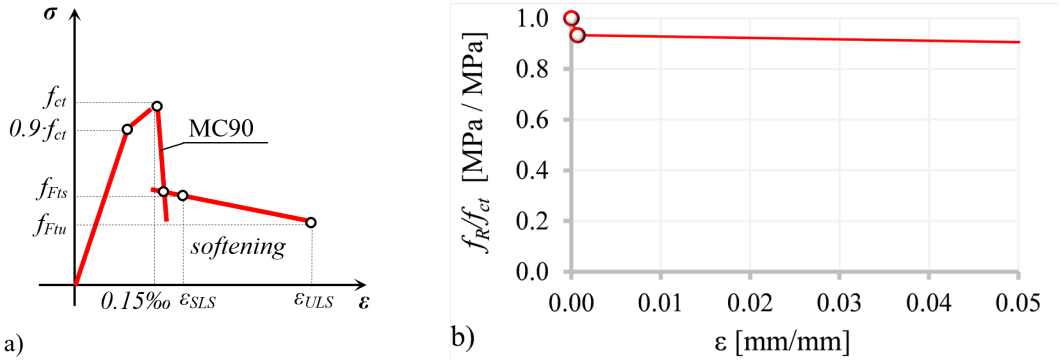

Fig. 5. a) Constitutive diagram in tension for FRC according to the fib MC 2010; b) Introduction of the computed constitutive model to ATENA (l_{cs} = 50 mm)

Taking into account the symmetry of the tested element (Figure 1a), only a quarter of the slab was modelled to favour the efficiency of the analysis. Additionally, almost the entire structure was modelled by means of 3D shell elements considering that the latter are subjected principally to bending stresses; only the zones of support-slab connections were presented by solid 3D elements, although the previous studies demonstrated that the punching failure was unlikely to occur in this type of structure/loading (Figure 6). As a result, a total of 3461 hexahedral elements were required to model the studied SFRC slab.

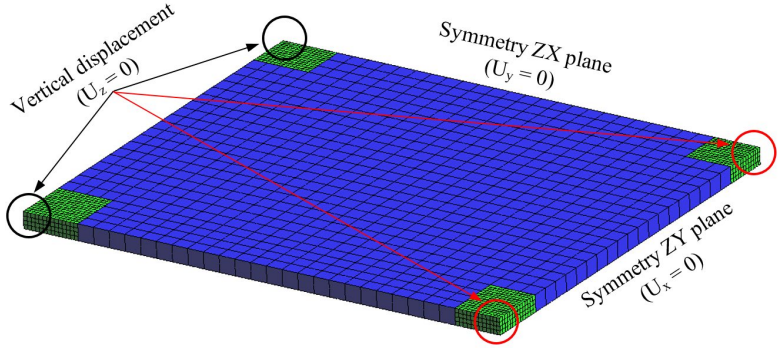

Fig. 6. Considered finite element model

Finally, it is important to remark that the restriction of the vertical displacements near the corner and edge columns (highlighted in black in Figure 6) led to a local failure and, thus, provided inaccurate results in terms of the overall bearing capacity of the structure. Taking this phenomenon into account, the tensile pre- and post-cracking strengths of these solid regions were enhanced in order to comply with the experimentally obtained cracking pattern and potential failure mode.

3.2.2. Numerical results

The simulation of the test procedure provided a numerical UDL – δ curve, where δ is the deflection of the panel centre. The main objective of this simulation was to evaluate the maximum magnitude of UDL in order to compare the latter with both experimental outcome and analytical prediction. As a result, the UDL which led to a loss of structural integrity (further load increment produced excessive deformations) was equal to 24.5 kN/m^2, which is 53.1% higher than the experimentally obtained value.

Furthermore, numerically computed magnitudes of UDL considerably exceeded the analytical prediction – the difference of 38.4% was achieved. Although 16 kN/m^2 should not be treated as the ultimate load since the structure was not led to collapse, the numerical prediction led to certain overestimation in terms of bearing capacity of the tested SFRC flat slab, taking into account the produced damage during the testing along with the fact that the significant cracking was observed during the loading of the fourth panel.

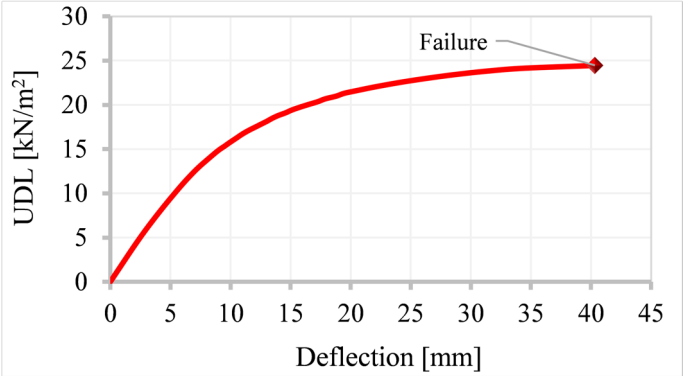

Fig. 7. Numerical load – deflection relationship for the studied SFRC slab

4. CONCLUSIONS

In this paper, results of an extensive experimental programme on a full-scale SFRC flat slab was presented. The constructed SFRC flat slab was subjected to gradually increasing uniformly distributed load (UDL) up to reaching 16 kN/m^2. Furthermore, analytical and numerical predictions of the bearing capacity were carried out using Yield Line Theory and finite element software. The following conclusions may be derived based on the obtained results:

- An SFRC with mean value of f_{R1} = 7.2 MPa and f_{R3} = 7.7 MPa provided structural integrity during the whole loading process. For the target load UDL = 14 kN/m^2 (target load for residential/office buildings), the structure proved to guarantee sufficient ductility and bending moment redistribution capacity.
- The analytical solution provided a suitable prediction (overestimation of 11%) of the failure load respect to the UDL applied (16 kN/m^2). It is important to remark that the failure was not achieved during the load test and, therefore, the difference could have been even minor.
- The numerical prediction led to certain overestimation (53%) in terms of bearing capacity of the tested SFRC flat slab. Caution is required when designing this structural typology by means of FE packages, and the proper constitutive equations and material partial safety factors must be taken into account.

ACKNOWLEDGMENTS

The authors wish to express their gratitude to the Spanish Ministry of Economy, Industry and Competitiveness (MINECO) for the financial support in the scope of the project eFIB (reference: RTC-2016-5263-5) which was carried out along with SACYR Ingeniería e

Infraestructura. The authors also appreciate valuable input of Francisco Mena into the manuscript. The first author, personally, thanks the Department of Enterprise and Education of Catalan Government for providing support through the PhD Industrial Fellowship (2018 DI 77) in collaboration with Smart Engineering Ltd. (UPC's Spin-Off).

REFERENCES

[1] Alani AM, Beckett D. Mechanical properties of a large scale synthetic fibre reinforced concrete ground slab. Constr Build Mater 2013;41:335–44. https://doi.org/10.1016/j.conbuildmat.2012.11.043.

[2] Belletti B, Cerioni R, Meda A, Plizzari G. Design Aspects on Steel Fiber-Reinforced Concrete Pavements 2009;20:599–607. https://doi.org/10.1061/(ASCE)0899-1561(2008)20.

[3] Meda A, Plizzari GA, Riva P. Fracture behavior of SFRC slabs on grade. Mater Struct Constr 2004;37:405–11. https://doi.org/10.1617/14093.

[4] Jamshidi M, Hoseini A, Vahdani S, Santos C De, De A. Seismic fragility curves for vulnerability assessment of steel fiber reinforced concrete segmental tunnel linings. Tunn Undergr Sp Technol 2018;78:259–74. https://doi.org/10.1016/j.tust.2018.04.032.

[5] de la Fuente A, Pujadas P, Blanco A, Aguado A. Experiences in Barcelona with the use of fibres in segmental linings. Tunn Undergr Sp Technol 2012;27:60–71. https://doi.org/10.1016/j.tust.2011.07.001.

[6] Liao L, de la Fuente A, Cavalaro S, Aguado A. Design of FRC tunnel segments considering the ductility requirements of the Model Code 2010. Tunn Undergr Sp Technol Inc Trenchless Technol Res 2015;47:200–10. https://doi.org/10.1016/j.tust.2015.01.006.

[7] Chiaia B, Fantilli AP, Vallini P. Combining fiber-reinforced concrete with traditional reinforcement in tunnel linings. Eng Struct 2009;31:1600–6. https://doi.org/10.1016/j.engstruct.2009.02.037.

[8] de la Fuente A, Aguado A, Molins C, Armengou J. Innovations on components and testing for precast panels to be used in reinforced earth retaining walls. Constr Build Mater 2011;25:2198–205. https://doi.org/10.1016/j.conbuildmat.2010.11.003.

[9] de la Fuente A, Escariz RC, de Figueiredo AD, Aguado A. Design of macro-synthetic fibre reinforced concrete pipes. Constr Build Mater 2013;43:523–32. https://doi.org/10.1016/j.conbuildmat.2013.02.036.

[10] Gossla U. Development of SFRC Free Suspended Elevated Flat Slabs. Aachen: 2005.

[11] Destrée X, Mandl J. Steel fibre only reinforced concrete in free suspended elevated slabs: Case studies, design assisted by testing route, comparison to the latest SFRC standard documents. Tailor Made Concr Struct 2008:437–43.

[12] Parmentier B, Itterbeeck P Van, Skowron A. The flexural behaviour of SFRC flat slabs : the Limelette full- scale experiments for supporting design model codes. Proc. FRC, 2014.

[13] Maturana Orellana A. Estudio teórico-experimental de la aplicabilidad del hormigón reforzado con fibras de acero a losas de forjado multidireccionales. 2013. https://doi.org/10.1174/021435502753511268.

[14] de la Fuente A, Casanovas-Rubio MDM, Pons O, Armengou J. Sustainability of Column-Supported RC Slabs: Fiber Reinforcement as an Alternative. J Constr Eng Manag 2019;145:1–12. https://doi.org/10.1061/(ASCE)CO.1943-7862.0001667.

[15] Colombo M, Martinelli P, di Prisco M. On the evaluation of the structural redistribution factor in FRC design: a yield line approach. Mater Struct 2017;50:1–18. https://doi.org/10.1617/s11527-016-0969-3.

[16] di Prisco M, Martinelli P, Dozio D. The structural redistribution coefficient KRd: a numerical approach to its evaluation. Struct Concr 2016;17:390–407. https://doi.org/10.1002/suco.201500118.

[17] Fall D, Shu J, Rempling R, Lundgren K, Zandi K. Two-way slabs : Experimental investigation of load redistributions in steel fibre reinforced concrete. Eng Struct 2014;80:61–74. https://doi.org/10.1016/j.engstruct.2014.08.033.

[18] Groli G, Caldentey AP. Improving cracking behaviour with recycled steel fibres targeting specific applications – analysis according to fib Model Code 2010. Struct Concr 2017;18:29–39. https://doi.org/10.1002/suco.201500170.

[19] Tošić N, Aidarov S, de la Fuente A. Systematic Review on the Creep of Fiber-Reinforced Concrete. Materials (Basel) 2020;13:5098. https://doi.org/10.3390/ma13225098.

[20] Tan KH, Paramasivam P, Tan KC. Instantaneous and long-term deflections of steel fiber reinforced concrete beams. ACI Struct J 1994;91:384–93.

[21] fib. fib Model Code for Concrete Structures 2010. 2010.

[22] Ministerio de Fomento. Instrucción de Hormigón Estructural (EHE-08). 2008. https://doi.org/10.1017/CBO9781107415324.004.

[23] RILEM TC 162-TDF. Recommendations of RILEM TC 162-TDF: Test and design methods for steel fibre reinforced concrete: bending test. Mater Struct 2002;35:579–82. https://doi.org/10.1617/14007.

[24] CEN. EN 14651. Test method for metallic fibre concrete. Measuring the flexural tensile strength (limit of proportionality (LOP), residual). 2007.

[25] Cervenka V. SIMULATING A RESPONSE. Concr Eng Int 2000;4:45–9.

[26] Blanco A, Pujadas P, de la Fuente A, Cavalaro SHP, Aguado A. Influence of the type of fiber on the structural response and design of FRC slabs. J Struct Eng (United States) 2016;142:1–11. https://doi.org/10.1061/(ASCE)ST.1943-541X.0001515.

[27] Pujadas P, Blanco A, Cavalaro S, Aguado A. Plastic fibres as the only reinforcement for flat suspended slabs: Experimental investigation and numerical simulation. Constr Build Mater 2014;57:92–104. https://doi.org/10.1016/j.conbuildmat.2014.01.082.

[28] Canadian Standards Association. Design of Concrete Structures CSA A23.3-04. 2004.

[29] ACI Committee 544. Report on Design and Construction of Steel Fiber-Reinforced Concrete Elevated Slabs. 2004.

[30] Barros J, Salehian H, Pires M, Gonçalves D. Design and testing elevated steel fibre reinforced self-compacting concrete slabs. Fibre Reinf Concr 2012:1–12.

[31] Salehian H, Barros JAO. Assessment of the performance of steel fibre reinforced self-compacting concrete in elevated slabs. Cem Concr Compos 2015;55:268–80. https://doi.org/10.1016/j.cemconcomp.2014.09.016.

[32] Hedebratt J, Silfwerbrand J. Full-scale test of a pile supported steel fibre concrete slab. Mater Struct Constr 2014;47:647–66. https://doi.org/10.1617/s11527-013-0086-5.

[33] Døssland ÅL. Fibre Reinforcement in Load Carrying Concrete Structures. 2008.

[34] Ošlejs J. New Frontiers for Steel Concrete. Concr Int 2008;3:45–50.

[35] Maturana A, Canales J, Orbe A, Cuadrado J. Análisis plástico y Ensayos de Losas multidireccionales de HRFA. Inf La Construcción 2014;66:e031. https://doi.org/10.3989/ic.13.021.

[36] Mitchell D, Cook WD. Preventing Progressive Collapse of Slab Structures. J Struct Eng 1984;110:1513–32. https://doi.org/10.1061/(ASCE)0733-9445(1984)110:7(1513).

[37] Aidarov S, Mena F, de la Fuente A. Caracterización de las propiedades en estado fresco y endurecido de hormigones autocompactantes reforzados con altas cuantías de macrofibras metálicas. VIII Congr. la Asoc. Española Ing. Estructural, 2021, p. 1–9.

[38] CEN. EN 12390-13:2013. Testing hardened concrete. Determination of secant modulus of elasticity in compression. 2013.

[39] CEN. EN 12390-3:2019. Testing hardened concrete. Compressive strength of test specimens. 2019.

[40] Molins C, Aguado A, Saludes S. Double punch test to control the energy dissipation in tension of FRC (Barcelona test). Mater Struct 2009;42:415–25. https://doi.org/10.1617/s11527-008-9391-9.

[41] Parmentier B, De Grove E, Vandewalle L, Van Rickstal F. Dispersion of the mechanical properties of FRC investigated by different bending tests. Proc Int FIB Symp 2008 - Tailor Made Concr Struct New Solut Our Soc 2008:123. https://doi.org/10.1201/9781439828410.ch84.

[42] Grunewald S. Performance-based design of self-compacting fibre reinforced concrete. 2004.

[43] Gobierno de España. Código Técnico de la Edificación (CTE) Documento básico: Seguridad estructural. Apartado de “Acciones en la Edificación” 2009.

[44] Aidarov S, Mena F, de la Fuente A. Structural response of a fibre reinforced concrete pile-supported flat slab: full-scale test. Eng Struct 2021;239. https://doi.org/10.1016/J.ENGSTRUCT.2021.112292.

[45] Italian National Research Council CNR. CNR-DT 204 /2006 Guide for the Design and Construction of Fiber-Reinforced Concrete Structures. Rome: Consiglio Nazionale Delle Ricerche; 2006.

[46] fib Committee. Fib 83 Precast tunnel segments in fibre-reinforced concrete. 2017.